

**Feather Keratin Derived Sustainable Biosorbents for Adsorption of Heavy
Metal Ions from Water**

by

Muhammad Zubair

A thesis submitted in partial fulfillment of the requirements for the degree of

Doctor of Philosophy

in

Bioresource Technology

Department of Agricultural, Food and Nutritional Science
University of Alberta

© Muhammad Zubair, 2023

ABSTRACT

Water is the epicenter of sustainability and has an essential part of the existence and development of the ecosystem and socioeconomic pillars. However, one in every three humans does not have access to clean drinking water around the globe and heavy metal ions pollution is the major contributor. This study aimed to develop keratin derived biosorbents for the removal of heavy metals from contaminated water.

Poultry feathers, an underutilized poultry industry by-product with high keratin protein contents, can be used as a sustainable biomass for biosorbents production to clean heavy metals contaminated water. However, keratin itself has a low biosorption efficiency for heavy metals, which can be improved by exposing the active sites of the feather keratin through effective modifications. This research focused on the synthesis of biosorbents from chicken feathers keratin (CFK), i.e., the extraction and nanomodification of keratin with graphene oxide (GO), nanochitosan (NC) and surface modified graphene oxide (SMGO) to transform into biosorbents for water remediation from heavy metals.

In the first study, a facile method was used to synthesize keratin derived biosorbents using water dispersed graphene oxide. To develop the biosorbents, feathers were washed with anti-bacterial soap, dried at 50 °C and defatted with hexane followed by the dissolution of keratin with a mixture of urea, tris-base and sodium sulfite. The keratin was modified using different ratios of graphene oxide (1, 3 and 5%) to enhance its biosorption efficiency. The nanomodification of keratin was carried out by cross-linking with the graphene oxide predominantly via an esterification reaction. The nanomodified biosorbents were then tested against a synthetic wastewater solution containing 600 μgL^{-1} of 8 trace metals, i.e., Ni^{II} , Co^{II} , Pb^{II} , Cd^{II} , Zn^{II} , As^{III} , Se^{VI} and Cr^{VI} . The 10 ml solution of multi-metals was amended with 0.1g of each prepared

biosorbents and incubated for 24 hours, followed by centrifugation and analyzed using inductively coupled plasma-mass spectrometer (ICP-MS). Among synthesized biosorbents CFK modified with GO (1%) exhibited ≥ 99.04 and ≥ 99.11 and $\geq 97.84\%$ removal efficiency for Ni^{II} , Se^{VI} , and As^{III} , respectively

In the second study, the biosorbents were prepared by first unraveling and then cross-linking keratin with NC. The nanomodifications were carried out using different concentrations of NC (1, 3 and 5%) in the keratin solution. The mixtures were treated at $75\text{ }^{\circ}\text{C}$ overnight which predominantly promoted the formation of ester bonds between the hydroxyl groups of nanochitosan and the carboxylic groups of the keratin biopolymer. The ICP-MS results indicated that CFK modified with NC (3%) showed better removal efficiency than CFK containing 1 and 5% nanochitosan. CFK having 3% NC had removal efficiencies of ≥ 98.80 , ≥ 98.44 , $\geq 92.96\%$ for Se^{VI} , As^{III} and Pb^{II} , respectively.

In the third study, graphene oxide was modified first with acryl amide to introduce the acrylic groups on the graphene oxide surface. Introducing acrylic groups on the graphene oxide facilitates the grafting or graft copolymerization with keratin biopolymer. GO was modified with acryl amide under alkaline conditions using N, N'-dicyclohexylcarbodiimide and hydroxy benzotriazole as coupling agent. The surface modified GO was then graft-copolymerized with the keratin in the presence of potassium persulfate and sodium thiosulfate as radical initiators. The successful grafting of SMGO onto the CFK resulted in better metal cations removal efficiencies than oxyanions i.e. ≥ 99.21 , ≥ 99.03 and $\geq 96.34\%$ for Pb^{II} , Cd^{II} and Co^{II} , respectively

Overall, this research study has demonstrated that modification of feather keratin with GO, NC and SMGO effectively improves its biosorption efficiency for removing multiple trace metal ions from synthetic wastewater in a single treatment. Among synthesized biosorbents CFK-GO, CFK-NC, CFK-SMGO derived biosorbents exhibited biosorption of metals upto 99, 98 and 99%, respectively. Furthermore, insights into the biosorption mechanism revealed that the electrostatic interaction, chelation and complexation primarily contributed to the removal of multiple heavy metal ions from synthetic wastewater in a single treatment. The chemical/physical interaction of the protein biopolymers with the nanoparticles led to the improved surface functionalities of the keratin with substantial morphological changes, uncovering surface functional groups which enhanced the biosorption efficiency of keratin for heavy metals. Moreover, environmentally friendly keratin derived biosorbents will help treat industrially contaminated water and minimize poultry feather related environmental pollution.

PREFACE

Chapter one provides an introduction, literature review and objectives of the thesis. This chapter will be submitted in a peer review journal with some modifications as a review article.

Chapter two of this thesis describes all the experimental methods, procedures and instrumentations used to achieve the objectives which are mentioned in the chapters 3,4 and 5.

Chapter three of this thesis has been published by Zubair, M., Roopesh, MS., Ullah, A (2022). “Nano-Modified Feather Keratin Derived Green and Sustainable Biosorbents for the Remediation of Heavy Metals from Synthetic Wastewater.” *Chemosphere*, 308, 136339. I performed all laboratory analyses, data interpretation and writing of the manuscript. Dr. Ullah and Dr. MS Roopesh contributed to conceptualization, manuscript review and editing.

Chapter four of this thesis is under "pending revisions" in the *International Journal of Biological Macromolecules* by Zubair, M, Roopesh, MS., Ullah, A (2022) “Chemically Cross-linked Keratin and Nanochitosan Based Biosorbents for Heavy Metals Remediation.” I performed all laboratory analyses, data interpretation and writing of the manuscript. Dr. Aman Ullah and Dr. MS Roopesh contributed to conceptualization, manuscript review and editing.

Chapter five of this thesis has been prepared as a manuscript for submission to peer-reviewed journal: Zubair, M., Roopesh, MS., Ullah, A. “Green Nanoengineered Keratin Derived Biosorbents with Acryl Amide Modified Graphene Oxide for Heavy Metal Ions Removal from Synthetic Wastewater.” I performed all laboratory analyses, data interpretation and writing of the manuscript. Dr. Aman Ullah and Dr. MS Roopesh contributed to conceptualization, manuscript review and editing. This chapter will be submitted in a peer review journal for publication.

Chapter six of the thesis presents the summary and future recommendations for this research study.

DEDICATION

Dedicated to my Beloved Family

ACKNOWLEDGEMENTS

There are many people who encouraged and supported me throughout my work, for which I am forever grateful. First and foremost, I would like to express my sincere gratitude to my supervisor Dr. Aman Ullah for offering me this opportunity to pursue my doctoral degree and for his devoted time and efforts throughout my degree. I am deeply grateful to my co-supervisor Dr. M.S. Roopesh for his invaluable motivation and academic support. I would like to extend my gratitude to my committee member Dr. Tariq Siddique throughout my program, especially in crafting the candidacy report.

I am indebted to my mother and Late Father, whose encouragement takes me to complete my doctoral degree. I would like to thank my wife during my Ph.D., especially during the pandemic when I went on a leave of absence. I also want to thank my brother and sisters. I am so blessed to have them always by my side. I will not be able to accomplish this without their love and support.

Last but not least, Dr. Ishtiaq Ahmad Khan, without his support and mentorship, I won't be able to complete this milestone.

TABLE OF CONTENTS

ABSTRACT	ii
PREFACE	v
DEDICATION	vi
ACKNOWLEDGEMENTS	vii
LIST OF TABLES	xii
LIST OF FIGURES	xiii
LIST OF ABBREVIATIONS	xvi
CHAPTER 1: Introduction and Literature Review	1
1.1. Introduction.....	1
1.2. Heavy metals contamination	4
1.3. Adsorption	6
1.3.1. Bio-derived adsorbents.....	8
1.3.2. Proteins derived bio-adsorbents.....	9
1.3.2.1. Soy proteins	9
1.3.2.2. Gelatin	10
1.3.2.3. Zein proteins	11
1.3.2.4. Natural silk protein.....	12
1.3.2.5. Albumen protein	12
1.3.3. Keratin biopolymer as a bio-adsorbent	13
1.3.4. Chemical modification of keratin	22
1.3.4.1. Graphene oxide (GO)	23
1.3.4.2. Nanochitosan (NC).....	24
1.4. Research Objectives, Questions and Hypotheses	26
1.5. References.....	30
CHAPTER 2: Experimental Methods and Data Analysis	38
2.1. Chemicals and Materials.....	38
2.2. Proximate Analysis of Chicken Feathers.....	38

2.2.1. Moisture content analysis.....	38
2.2.2 Determination of total fat contents	39
2.2.3. Determination of ash contents	39
2.2.4. Determination of proteins contents.....	39
2.3. Pre-treatment and Dissolution of Chicken Feathers	40
2.4. Preparation of Chicken Feathers Keratin-Graphene Oxide Derived Biosorbents	41
2.4.1. Preparation of graphene oxide (GO).....	41
2.4.2. Preparation of chicken feather keratin-graphene oxide derived biosorbents	42
2.5. Preparation of Chicken Feathers Keratin-Nanochitosan Derived Biosorbents.....	43
2.5.1. Preparation of nanochitosan	43
2.5.2. Preparation of keratin-nanochitosan based biosorbents.....	43
2.6. Preparation of Chicken Feathers Keratin-Nanochitosan Derived Biosorbents.....	44
2.6.1. Surface modification of graphene oxide	44
2.6.2. Preparation of keratin/ surface modified graphene oxide derived biosorbent.....	45
2.7. Instrumentation.....	45
2.7.1 ATR-FTIR analysis.....	45
2.7.2. X-ray photoelectron spectroscopy	46
2.7.3. X-ray diffraction analysis.....	46
2.7.4. Scanning and transmission electron microscopies (SEM and TEM) analysis	46
2.7.5. Thermal behaviour studies	47
2.7.6. Surface area and pore size distribution analysis	47
2.7.7. Dynamic light scattering (DLS).....	48
2.7.8. Inductively coupled plasma mass spectrometry (ICP-MS).....	48
2.8. Statistical Analysis.....	49
2.9. References.....	51
CHAPTER 3: Nano-Modified Feather Keratin Derived Green and Sustainable Biosorbents for the Remediation of Heavy Metals from Synthetic Wastewater	52
3.1. Introduction.....	52
3.3. Results & Discussions.....	56
3.3.1. Characterization of graphene oxide	57
3.3.1.1. Structural analysis.....	57

3.3.1.2. Crystallinity analysis.....	58
3.3.1.3. Thermal properties analysis.....	59
3.3.2. Structural analysis of biosorbents	60
3.3.3. Thermal behavior of biosorbents	68
3.3.4. Morphology and internal structure.....	71
3.3.5. Surface area and pore size determination.....	74
3.3.6. Biosorption performance.....	78
3.3.7. Mechanistic insights of biosorption.....	83
3.4. Conclusions.....	90
3.5. References.....	92
CHAPTER 4: Green Biosorbents Prepared from Chemically Cross-link Keratin Biopolymer using Nanochitosan for Heavy Metals Remediation from Water	95
4.1. Introduction.....	95
4.2. Experimental strategy	97
4.3. Results & Discussions.....	99
4.3.1. Characterization of nanochitosan	99
4.3.1.1. Structural analysis.....	99
4.3.1.2. Crystallinity analysis.....	100
4.3.2. Structure characterization of the biosorbents	101
4.3.3. Surface characterization of the biosorbents.....	106
4.3.4. Thermal stability and phase behavior of the biosorbents.....	110
4.3.5. Biosorption performance and mechanism.....	112
4.4. Conclusions.....	122
4.5. References.....	124
CHAPTER 5: Green Nanoengineered Keratin Derived Biosorbents with Acryl Amide Modified Graphene Oxide for Heavy Metal Ions Removal from Synthetic Wastewater ...	127
5.1. Introduction.....	127
5.2. Experimental strategy	129
5.3. Results & Discussions.....	131
5.3.1. Structural analysis.....	131
5.3.2. Surface morphology and internal structure	135

5.3.3. Thermal properties	140
5.3.4. Biosorption Performance.....	145
5.4. Conclusions.....	150
5.5. References.....	151
CHAPTER 6: Summary and Future Perspectives.....	154
6.1. References.....	159
Bibliography.....	160
Appendices:	175
Appendix-I: Cumulative surface area, pore volume, micropore pore volume and V-t surface area of the CFK and biosorbents	175
Appendix-II: Metals biosorption efficiency (%) of dissolved CFK.....	175
Appendix-III: Metals biosorption efficiency of CFK-GO (0.5%)	175
Appendix-IV: Cumulative surface area of (a) CFK (b) CFK-GO (1%) (c) CFK-GO (3%) (d) CFK-GO (5%) as determined by non-linear DFT	176
Appendix-V: Scanning electron microscopy images of chicken feather keratin after biosorption	176
Appendix-VI: Transmission electron microscopy images of SMGO (a & b) and CFK-SMGO (c).....	178
Appendix-VII: Graphical representation of the CFK-GO derived biosorbents.....	178
Appendix-VIII: Determination of chicken feathers keratin molecular weight.....	179
Appendix-IX: Comparison of biosorption performance of biosorbents for metal ions among study I, II and III	180
Appendix-X: Comparison of biosorption performance of biosorbents within study I, II and III.....	181
Appendix-XI: Dynamic light scattering (DLS) results of NC	184
Appendix-XII: Permission for figure 1.1.....	186
Appendix-XIII: References.....	187

LIST OF TABLES

CHAPTER 1

Table 1.1: WHO and USEPA standards.....	4
Table 1.2: Sources of industries for heavy metals	5
Table 1.3: Benefits and drawbacks of heavy metals polluted water treatment techniques	7
Table 1.4: Protein based bio-adsorbents for heavy metal ions removal from polluted water	11
Table 1.5.: Keratin amino acids, their pKa values and isoelectric points (pI)	15
Table 1.6: Keratin derived bio-adsorbents for heavy metal removal from polluted water	20

CHAPTER 2

Table 2.1: Initial concentration of trace metals before biosorption	49
---	----

CHAPTER 3

Table 3.1: Proximate analysis of the chicken feathers.....	57
Table 3.2: % Crystallinity of chicken feather keratin and derived biosorbents	68
Table 3.3: BET and NLDFT results.....	75

CHAPTER 4

Table 4.1: % Crystallinity of chicken feather keratin and CFK-NC biosorbents.....	105
Table 4.2: BET surface area of the biosorbents.....	118

CHAPTER 5

Table 5.1: % Crystallinity of CFK and CFK-SMGO biosorbent	135
---	-----

LIST OF FIGURES

CHAPTER 1

Figure 1.1: Total heavy metal concentrations (mg/L^{-1}) of global rivers and lakes from 1970-2010 (Zhou et al., 2020) (Reproduced with the permission of Elsevier).....	3
Figure 1.2: Secondary structures of keratin protein (a) alpha helix and ((b) beta pleated sheet ...	14
Figure 1.3: Polypeptide backbone representing keratin's inter- and intra- molecular bonding (strength and stability).....	18
Figure 1.4: Structure of graphene oxide.....	23
Figure 1.5: Potential interaction b/w keratin proteins and graphene oxide.....	24
Figure 1.6. Structure of nanochitosan	25
Figure 1.7: Potential interactions b/w keratin proteins and nanochitosan.....	25

CHAPTER 2

Figures 2.1: Workflow for chicken feather keratin-graphene oxide derived biosorbents.....	42
Figures 2.2: Workflow for chicken feather keratin-nanochitosan derived biosorbents.....	44

CHAPTER 3

Figure 3.1:ATR-FTIR of graphite and graphene oxide	58
Figure 3.2 : XRD patterns of graphite and graphene oxide.....	59
Figure 3.3: TGA of graphite and graphene oxide	60
Figure 3.4: ATR-FTIR of graphene oxide, chicken feather keratin (CFK), CFK-GO (1%), CFK-GO (3%) and CFK-GO (5%)	61
Figure 3.5: Amide I region 2 nd derivative of chicken feather keratin (CFK), CFK-GO (1%), CFK-GO (3%) and CFK-GO (5%)	63
Figure 3.6: Amide II region of chicken feather keratin (CFK), CFK-GO (1%), CFK-GO (3%) and CFK-GO (5%)	65
Figure 3.7: High Resolution Carbon 1s spectra of chicken feather keratin (CFK), CFK-GO (1%), CFK-GO (3%) and CFK-GO (5%)	66
Figure 3.8: XRD patterns of GO, chicken feather keratin (CFK), CFK-GO (1%), CFK-GO (3%) and CFK-GO (5%)	67
Figure 3.9: (a) TGA & (b) DTG curves GO, chicken feather keratin (CFK), CFK-GO (1%), CFK-GO (3%) and CFK-GO (5%)	69
Figure 3.10: DSC heat flow signals GO, chicken feather keratin (CFK), CFK-GO (1%), CFK-GO (3%) and CFK-GO (5%)	71
Figure 3.11: SEM images of (a) chicken feather keratin (CFK), (b) CFK-GO (1%), (c) CFK-GO (3%) and (d) CFK-GO (5%)	73
Figure 3.12: TEM micrographs of (a) graphene oxide (b) chicken feather keratin (CFK), (c) CFK-GO (1%), (d) CFK-GO (3%) and (e) CFK-GO (5%).....	74

Figure 3.13: Pore size distribution (PSD) of (a) CFK (b) CFK-GO (1%) (c) CFK-GO (3%) (d) CFK-GO (5%) using non-linear density functional theory method (NLDFT).....	76
Figure 3.14: Pore volume calculated from nitrogen uptake at the given relative pressure (a) CFK (b) CFK-GO (1%) (c) CFK-GO (3%) (d) CFK-GO (5%) using multipoint BET	77
Figure 3.15: Biosorption efficiency of chicken feather keratin (CFK), graphene oxide (GO), CFK-GO (1%), CFK-GO (3%) and CFK-GO (5%) for metal cations (Ni, Cd, Pd, Zn, Co) 81	
Figure 3.16: Biosorption efficiency of chicken feather keratin (CFK), graphene oxide (GO), CFK-GO (1%), CFK-GO (3%) and CFK-GO (5%) for oxyanions (Cr, As, Se).....	82
Figure 3.17: SEM images of (a-d) chicken feather keratin (CFK) and (e-h) biosorbents after biosorption	85
Figure 3.18: TGA curves of (a) chicken feather keratin (CFK) before biosorption (red) and after biosorption (black) (b) chicken feather keratin derived biosorbent before biosorption (red) and after biosorption (black).....	86
Figure 3.19: XRD patterns of (a) chicken feather keratin (CFK) before biosorption (red) and after biosorption (black) (b) chicken feather keratin derived biosorbent before biosorption (red) and after biosorption (black).....	87
Figure 3.20: ATR-FTIR of (a) chicken feather keratin (CFK) before biosorption (red) and after biosorption (black) (b) chicken feather keratin derived biosorbent before biosorption (red) and after biosorption (black).....	88
Figure 3.21: XPS N1s spectra of the (a) chicken feathers keratin and (b) biosorbent before and after biosorption	90

CHAPTER 4

Figure 4.1: ATR-FTIR of chitosan and nanochitosan.....	100
Figure 4.2: XRD patterns of chitosan and nanochitosan.....	101
Figure 4.3: ATR- FTIR signals of neat chicken feather keratin and prepared keratin biosorbents.	103
Figure 4.4: XPS peaks of neat chicken feather keratin and prepared keratin biosorbents.....	104
Figure 4.5: XRD patterns of neat chicken feather keratin and prepared keratin biosorbents.	106
Figure 4.6: SEM images of (a, b) neat chicken feather keratin (c, d) CFK-NC (1%) (e,f) CFK-NC (3%) (g, h) CFK-NC (5%).....	108
Figure 4.7: TEM images of chicken feather keratin (CFK), NC, CFK-NC (1%), CFK-NC (3%) and CFK-NC (5%).....	109
Figure 4.8: TGA curves of chicken feather keratin (CFK), NC, CFK-NC (1%), CFK-NC (3%) and CFK-NC (5%).....	111
Figure 4.9: DSC curves of chicken feather keratin (CFK), NC, CFK-NC (1%), CFK-NC (3%) and CFK-NC (5%).....	112
Figure 4.10: Biosorption performance of the keratin-nanochitosan derived biosorbents for anionic species (As, Se, Cr).....	114
Figure 4.11: Biosorption performance of the keratin-nanochitosan derived biosorbents for cations species ((Ni, Co, Pb, Cd, Zn).....	116

Figure 4.12: Pore size distribution of (a) chicken feather keratin (CFK) (b) CFK contains 1% nanochitosan (c) CFK contains 3% nanochitosan (d) CFK contains 5% nanochitosan using non-linear density functional theory method (NLDFT)	117
Figure 4.13: SEM images of biosorbent after biosorption from metal-contaminated water.....	119
Figure 4.14: Structural elucidation of biosorbent to determine the biosorption mechanism with (a) XRD (b) TGA (c) ATR- FTIR (d) XPS	121
Figure 4.15: Plausible mechanism of metal ions removal from the keratin derived biosorbents	122

CHAPTER 5

Figure 5.1: ATR-FTIR spectra of GO, AA and SMGO.....	131
Figure 5.2: ATR-FTIR (a) and XPS spectra of CFK and CFK-SMGO biosorbent.....	133
Figure 5.3: XRD patterns of GO and SMGO	134
Figure 5.4: XRD patterns of CFK, SMGO and CFK-SMGO biosorbents.....	135
Figure 5.5: SEM images of (a-b) GO (c-d) SMGO (e-f) CFK (g-l) CFK-SMGO biosorbent	138
Figure 5.6: TEM images of GO, SMGO) CFK and CFK-SMGO derived biosorbent	139
Figure 5.7: Thermo-gravimetric analysis (TGA) of GO and SMGO	140
Figure 5.8: DTG of GO and SMGO	141
Figure 5.9: TGA curves of CFK, SMGO and CFK-SMGO derived biosorbent.....	142
Figure 5.10: DTG curves of CFK, (SMGO), CFK-SMGO derived biosorbent	143
Figure 5.11: DSC curves of GO and SMGO	144
Figure 5.12: DSC curves of CFK, SMGO and CFK-SMGO derived biosorbent.....	145
Figure 5.13: Biosorption performance of the CFK, SMGO, CFK-SMGO for anionic species (As, Se, Cr).....	147
Figure 5.14: Biosorption performance of the CFK, SMGO, CFK-SMGO for cationic species ((Ni, Co, Pb, Cd, Zn)	149

LIST OF ABBREVIATIONS

AA: Acryl amide	SMGO: Surface modified graphene oxide
AOAC: Association of official agricultural chemists	TEM: Transmission electron microscopy
ATR-FTIR: Attenuated total reflectance - Fourier transform infrared spectroscopy	TGA: Thermal gravimetric analysis
BET: Brunauer Emmett Teller	UNO: United Nations Organisation
CFK: Chicken feather keratin	USEPA: United States Environmental Protection Agency
DLS: Dynamic light scattering	WHO: World Health Organization
DMF: Dimethyl formamide	XPS: X-ray photoelectron spectroscopy
FK: Feather keratin	XRD: X-ray diffraction
DSC: Differential scanning calorimetry	
DTG: Differential thermogravimetric analysis	
GO: Graphene oxide	
HoBt: Hydroxy benzotriazole	
ICP-MS: Inductively coupled plasma- mass spectrometry	
pI: Isoelectric point	
NC: Nanochitosan	
NLDFT: Non-local density functional theory	
DCC: N, N'-dicyclohexylcarbodiimide	
POSS: (Polyhedral Oligomeric Silsesquioxanes)	
SEM: Scanning electron microscopy	

CHAPTER 1: Introduction and Literature Review

1.1. Introduction

Environmental pollution has become one of the major threats on the planet earth due to rapid urbanization, ever-increasing energy needs and substantial growth in industrial activities to maintain the luxurious life of humans, particularly in the last 2-3 decades (Siddiqua et al., 2022). The world is facing inadequate access to clean drinking water, especially in countries with limited resources, which is expected to be more dreadful in the coming years (Zubair & Ullah, 2021). However, a clean environment, including water, is one of the fundamental requirements for life and an essential element in building sustainable societies. The protection of the quality of water is critical in creating a benign environment to sustain ecological balance (Hoekstra, 2015; Parker & Brown, 2003).

According to the United Nations Office for Sustainable Development, more than 40 percent of the global population is facing a dearth of fresh water, which is expected to worsen in the coming years. By 2050, severe chronic and recurring lack of clean water can leave one in every four people in those areas. Around the globe, at least 1.8 billion people use fecally contaminated drinking water. The global water crisis will become worse in the near future and a shortfall of around 40 percent in freshwater resources is projected in 2030 (UNO, 2020).

Around the globe, human activities are significant contributors to aggravating water scarcity by polluting natural water resources. The strict wastewater quality standards and ever-increasing contaminants have got much attention in developed nations to the existing water treatment methods and distribution systems (Siddiqua et al., 2022). Implementing essential water treatment technologies is challenging, particularly in the developing world, where suitable infrastructure is not present for water treatment. Besides, climatic changes result in the uneven

distribution of clean drinking water, destabilize the supply, and drive the communities to consume water from unconventional sources such as saline water, polluted fresh water, industrial wastewater, seawater, and stormwater (Shannon et al., 2010; Zubair et al., 2020).

Presently, the irrigation and agriculture sectors are the primary users of the world's freshwater, with a share of about 70%. While in some regions of the world, its share is more than 95% of the total water supply (Mateo-Sagasta et al., 2015; Sato et al., 2013). Therefore, the agricultural share of water has been shifting steadily to non-agricultural sectors and polluting the freshwater bodies. Competition can be seen in the allocation of fresh water in water stress areas, especially among the public, manufacturing and farming sectors (Wichelns et al., 2015).

The volume of generated wastewater has been tremendously growing due to rapid industrialization to fulfill human needs (S. Wang et al., 2018). Discharging wastewater from oil and gas, mining, agriculture, and food industries pollutes the freshwater bodies. According to the United Nations Organisation (UNO), around 80% of industrial wastewater is discharged into freshwater streams without adequate treatment (Sato et al., 2013).

In a study conducted by Zhou and coworkers, 12 heavy metal ions (Cd, Pb, Cr, Hg, Zn, Cu, Ni, Al, Fe, Mn, As, and Co) were monitored for their concentration in surface water bodies, i.e., 168 rivers and 71 lakes, from 1972 to 2017 across five continents (Zhou et al., 2020). The study concluded that metal ions concentrations were beyond the World Health Organization (WHO) and United States Environmental Protection Agency (USEPA) standards in the developing countries of Africa, Asia, and South America. Mining and manufacturing, fertilizer and pesticide use, rock weathering, and waste discharge were the four primary sources responsible for most of South America's heavy metal pollution in the river and lake water.

Fig. 1.1 reveals a tremendous increase in the mean concentrations of heavy metal ions in water bodies from the 1970s to the 2010s. The concentration of all heavy metals is above the threshold limits defined by the WHO and USEPA standards (**Table 1.1**), especially in countries with limited resources across Africa, Asia and South America. Additionally, the rising demand for clean water in expanding cities, for sustainable agriculture purposes, and to enhance energy generation in industrial development urge high quality treated effluents.

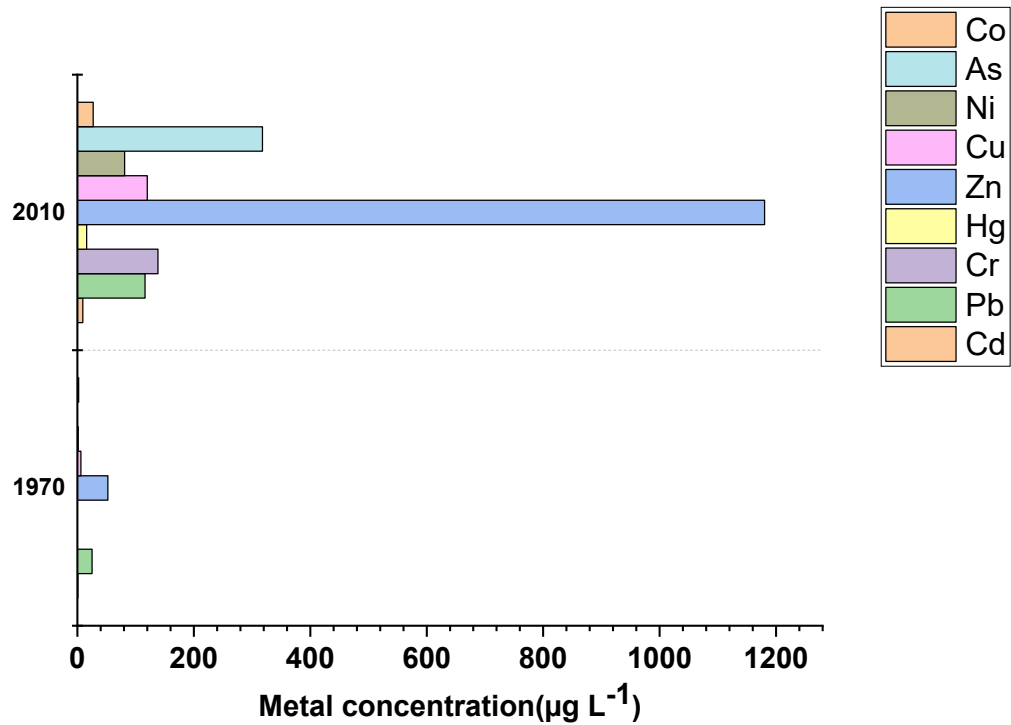


Figure 1.1: Total heavy metal concentrations (mg/L^{-1}) of global rivers and lakes from 1970-2010 (Zhou et al., 2020) (Reproduced with the permission of Elsevier).

Table 1.1: WHO and USEPA standards

<i>Metals</i>	<i>Maximum Permissible Limit (mg/L)</i>	
	WHO	EPA
<i>As</i>	0.01	0.05
<i>Cd</i>	0.003	0.005
<i>Cr</i>	0.05	0.05 for Cr (V1) 0.1 for Cr (III)
<i>Cu</i>	1.0	0.25
<i>Ni</i>	-----	0.2
<i>Hg</i>	0.01	0.05
<i>Pb</i>	0.01	0.10
<i>Zn</i>	3.0	1.0

1.2. Heavy metals contamination

There is no specific definition of heavy metal; however, based on the literature, it can be described as any naturally occurring element (metal/metalloid) with a density of 3.5-7.0 g/cm³ and toxic at a certain low concentration (Fei & Hu, 2022; Zaimie et al., 2021). Heavy metal pollution has received much interest due to its potential toxic and non-biodegradable nature. Primarily, they can enrich our food chain and ultimately accumulate in the organs of living organisms (Järup, 2003; Morais et al., 2012). Because of the hazardous nature of heavy metal ions, they are studied intensively, including zinc (Zn), cadmium (Cd), selenium (Se), chromium (Cr), cobalt (Co), copper (Cu), iron (Fe), lead (Pb), mercury (Hg), nickel (Ni), silver (Ag), arsenic (As) and manganese (Mn) (Babel & Kurniawan, 2004; Bashir et al., 2019). Heavy metal ions enter the environment through numerous sources, including chemical industries, farming, power and metallurgic plants, and mining, as shown in **Table 1.2**. There are multiple ways of heavy metal exposure to humans and animals, i.e., through inhalation, skin, food, and direct intake through drinking water. When the accumulation of heavy metals beyond the tolerance range can cause tissue and organs damage,

developing various symptoms such as dizziness, diarrhea, headache, insomnia, vomiting, amnesia and even damage to the heart, brain and kidneys and different types of cancer (**Table 1.2**) (Ali et al., 2019; Babel & Kurniawan, 2005; Duruibe, 2007; Liu et al., 2020). The level of heavy metals in drinking water is monitored under the guidelines of the WHO and USEPA to address these issues.

Table 1.2: Sources of industries for heavy metals

<i>Heavy Metals</i>	<i>Sources</i>	<i>Harmful Effects</i>
<i>Arsenic</i>	Mining, metal smelting, fossil fuel burning	Carcinogenic, skin damage, cardiorenal and gastrointestinal effects
<i>Cadmium</i>	Metal processing, battery recycling and power plants, combustion or cigarette smoke	Harmful effects on bones, liver, lungs, heart, and kidneys of human being
<i>Chromium</i>	Steel and textile industries	Kidney circulation, lung cancer, dermatitis
<i>Copper</i>	Mining, metal smelting	Weakness, lung cancer, abdominal pain, diarrhea, liver toxicity, weakness
<i>Cobalt</i>	Metallurgy mining, tanning, electroplating, paints, nuclear power plants	Diarrhea, paralyzed hypotension, pulmonary
<i>Mercury</i>	Paints, pesticides, fertilizers, pulp/paper, oil and gas refining, rubber industry, batteries and pharmaceuticals	Degradation of nervous, digestive, and immune systems, mental retardation, lungs and kidneys failure, skin and eyes problems, damage to gastrointestinal tracts
<i>Nickel</i>	Electrochemical industry, silver refineries, stainless steel manufacturing, zinc base casting and storage battery industries	Phyto-toxic, improper renal functioning, damage to DNA, Eczema and respiratory cancer
<i>Selenium</i>	Mining, refineries, agricultural run-off	Dermatological effects (hair and nail loss) cause hepatotoxicity and gastrointestinal disturbances

<i>Lead</i>	Mining, paints, smelting, batteries, mining, steel and automobile,	Damage central nervous system, improper kidney and liver functioning, high blood pressure, memory problems, cardiovascular effects and hypertension in adults
<i>Zinc</i>	Insecticides, paints, pharmaceuticals, cosmetics, galvanizing and pigments	Impaired growth, abdominal pain, bloody urine, phytotoxicity, liver and kidney failures, Anemia

1.3. Adsorption

Various conventional methods have been developed for the heavy metal contaminant's removal, including adsorption, membrane filtration, sedimentation or flocculation, chemical precipitation, ion exchange, electrochemical etc. (Chai et al., 2021; Subramaniam et al., 2019; Yang et al., 2018). Nevertheless, these decontamination methods for heavy metal removal have several drawbacks, which are listed in **Table 1.3**. Among these processes, adsorption is considered a sustainable alternative due to its unique attributes such as cost-effectiveness, abundant availability, use of simple processing, recycling and regeneration, higher metal uptake over a range of pH and capacity to eliminate metals in their complex forms (Al-Khaldi et al., 2015). Numerous adsorbents are being used for the removal of toxic heavy metals either from inorganic carbon sources such as activated carbon, carbon nanotubes, boron nitride nanosheets, silica gel, activated alumina, zeolites (Duan et al., 2020; Sharma & Naushad, 2020) or bio-based adsorbents such as modified cellulose, chitosan, starch, proteins and bio-waste (Carlos et al., 2013; Mahdavian & Mirrahimi, 2010; Zhu et al., 2021). covalent/metal-organic frameworks (Esrafilie et al., 2018; Gendy et al., 2021; Jiang et al., 2019). Recently, microplastics, carbon nitride, graphene, graphene oxide and magnetite are also being investigated for the water remediation (Elgamal et al., 2023; Qamar et al., 2023; Xu et al., 2018).

Among adsorbents, bio-derived adsorbents are preferable in heavy metal water remediation because of their better sorption capacity, and economical and eco-friendly nature. The cost and adsorption capacity are the most significant factors as these vary depending on the processing method and availability of the raw materials to develop adsorbing materials. Several bio-wastes such as vegetables, fruit peels, agricultural by-products, and plants and tree leaves are found abundantly (Bilal et al., 2021; Jayaraj et al., 2019). Thus, proper utilization of bio-wastes can address the issue of pollution and keep the ecosystem clean and green.

Table 1.3: Benefits and drawbacks of heavy metals polluted water treatment techniques

<i>Techniques</i>	<i>Benefits</i>	<i>Drawbacks</i>
<i>Ion exchange</i>	<ul style="list-style-type: none"> • High selectivity 	<ul style="list-style-type: none"> • Low capacity • Large sludge • pH-sensitive • Beads fouling
<i>Chemical precipitation</i>	<ul style="list-style-type: none"> • Low cost • Simple operation 	<ul style="list-style-type: none"> • Toxic sludge disposal • Low capacity • Ineffective for low trace ions • Required oxidation
<i>Membrane separation</i>	<ul style="list-style-type: none"> • High efficiency • High selectivity 	<ul style="list-style-type: none"> • Complex/no regeneration • High operational cost • Limited flowrate • Rapid membrane fouling • High energy needs
<i>Electro-chemical remediation</i>	<ul style="list-style-type: none"> • High efficiency • High selectivity 	<ul style="list-style-type: none"> • Complex/no regeneration • High operational cost
<i>Sedimentation and flocculation</i>	<ul style="list-style-type: none"> • High selectivity 	<ul style="list-style-type: none"> • Low capacity • Toxic sludge disposal • Poor As removal
<i>Adsorption</i>	<ul style="list-style-type: none"> • Greater capacity 	<ul style="list-style-type: none"> • Non-selectivity

- Wide pH range
- Low cost
- Simple operation
- Variety of target pollutants
- Loss of adsorbent during regeneration

Bio-adsorption is a novel method where a simple or chemically transformed adsorbent can be developed from available bio-waste materials like chicken feathers, stem, tea bags, husks, stems, leaves, hair, hooves, wool, peels, and branches. Extensive investigations have been conducted to synthesize low-cost and efficient bio-waste derived innovative adsorbents for eliminating heavy metal ions from the polluted water (Bilal et al., 2021; Kumari et al., 2018; Lohri et al., 2017). The most prominent benefit of bio-adsorption process is its suitability to remove heavy metal ions even if they are present in low concentrations unlike other techniques, which means bio-adsorption achieves better removal efficiency even at low pollutant concentrations (Demirbas, 2008; González et al., 2017)

1.3.1. Bio-derived adsorbents

Various bio-adsorbents from renewable, green, and sustainable carbon waste resources including bio-wastes such as cashew nutshell (Nuithitikul et al., 2020; SenthilKumar et al., 2011), banana peels (Li et al., 2016; Negroiu et al., 2021; Vilardi et al., 2018) orange peels (Naik et al., 2022; Wang et al., 2022) rice husk (Naik et al., 2022), sugar cane bagasse (Homagai et al., 2010; Oliveira et al., 2019), eggshells and eggshell membrane (Khaskheli et al., 2021; Park et al., 2007) and cow hooves (Osasona et al., 2013) have been studied for water remediation from heavy metals. The efficiency of bio- adsorption has been investigated in several studies for the removal of heavy metal ions from the aqueous media. Yet, many issues need to be resolved to exploit these bio-based adsorbents at the industrial level.

1.3.2. Proteins derived bio-adsorbents

The protein derived bio- adsorbents have received significant interest due to their exceptional characteristics, i.e., natural availability, biodegradable nature, eco-friendliness and the presence of multiple functional groups on the surface and side chains (Saha, Zubair, et al., 2019; Zubair et al., 2020; Zubair & Ullah, 2021). Protein derived adsorbents have been developed from keratin, gelatin, zein, soy, silk, and albumin proteins for heavy metal remediation (**Table 1.4**). The presence of reactive groups such as amino, hydroxyl, thiol, and guanidino in the protein structures makes them perfect raw materials that can be easily transformed into the desired properties for removing heavy metal ions from polluted water.

1.3.2.1. Soy proteins

Soy proteins are one of the most used proteins due to their unique structure, that can be easily converted into bio-adsorbing material for water remediation. Liu et al. (2013) prepared the hollow microspheres of soy proteins, and assessed their performance for the di-cations which include Zn (II), Ni (II), Cd (II), Cu (II), Pb (II) and metal anion Cr (III) at 70 °C (Liu et al., 2013). They concluded that Zn (II) adsorption capacity (254.95 mg/g) was higher than Cd (II) and Cr (III), attributed to the low energy barrier. Overall, the performance of the adsorbing material is better than the other natural polymeric adsorbents. In another study by the same group, soy protein isolate (SPI) was modified with polyethyleneimine (PEI) for the bio-adsorption of Cu (II) from the aqueous media. The result showed that PEI (50%) had better Cu (II) ions selectivity when co-existing with other metal cations (Cd, Pb and Zn (II)), and its adsorption capacity (33.5 to 136.2 mg/L) was increased tremendously (Liu et al., 2017). A third study reported by the Liu et al. (2016) SPI based bio-adsorbent was prepared by conjugation onto the deacetylated konjac glucomannan matrix. A comparative bio-adsorption performance revealed that conjugated SPI showed 5 times

(62.50 mg/g as compared to 12.23 mg/g) better sorption for the Cu^{2+} from an aqueous solution which can be achieved in 30 min. The better bio-adsorption capacity of conjugated soy protein isolates is ascribed to the strong Cu^{2+} ion chelation with the protein on deacetylated konjac glucomannan matrix (Liu et al., 2016).

1.3.2.2. Gelatin

Gelatin is also a good candidate for developing bio-adsorbent to remove heavy metal ions from polluted water. In a study done by Zhou et al. (2017), biochar was synthesized from bio-waste, i.e., chestnut shell and further treated with magnetic gelatin to remove As (V) from industrial wastewater. The results indicated that the addition of gelatin enhanced the biochar's surface area, which improved the arsenic bio-adsorption (Zhou et al., 2017). Abdellatif et al. (2022) prepared gelatin based gel by crosslinking with a different concentration of poly(amidoamine) hyperbranched and tested for the bio-adsorption of Cr (VI) and Cd (II). The synthesized gels showed bio-adsorption capacity (upto 98%) of 142.0 and 125.0 mg/g for Cd (II) and Cr (VI) ions, respectively. The study demonstrates that crosslinking favoured the bio-adsorption by providing more binding sites with various energies (Abdellatif et al., 2022). A study reported by Wojciechowska and coworkers (2022), gelatin was treated with organomodified silicone containing epoxy group to develop bio-adsorbents for the removal of metal cations i.e., Cu (II), Cd (II) and Pb (II) from the aqueous solutions. The results showed that the highest bio-adsorption was observed for Pb (II) ions. However, the adsorption capacity for hybrid monoliths was 3.75, 1.76 and 1.5 mg/g for Pb (II) Cd (II) and Cu (II) ions, respectively. Most importantly, desorption of metal ions for hybrid monoliths stable in aqueous media went up to 70% (Wojciechowska et al., 2022). Gelatin derived composites were prepared with hydroxyapatite/alginate for the remediation of Pb^{2+} and Cd^{2+} from the aqueous media. The removal sorption capacity of the composite was assessed to be 616 and 388 mg/g for lead and cadmium ions, respectively. The

study indicated that one metal ion adsorption was hindered by the presence of other metal ions within the aqueous medium (Sangeetha et al., 2018). In another study, gelatin based bio-adsorbent was used for the bio-adsorption of Cr (III) – Cr (VI). The results showed that gelatin had excellent sorption capacity for Cr (III) – Cr(VI) ($97.5\text{--}102.0 \pm 2.5\text{--}4.0\%$) (Mahmoud & Mohamed, 2014).

Table 1.4: Protein based bio-adsorbents for heavy metal ions removal from polluted water

Protein based Bio-adsorbents	Heavy Metals Removed	Initial Metal Concentration	Adsorption Efficiencies	References
Manganese dioxide/gelatin composites	Pb (II)	10 ppm	83-100%	(X. Wang et al., 2018)
Gelatin aerogels	Cr (IV)	25-200 ppm	98 %	(Abdellatif et al., 2022)
Gelatin bentonite composite	Pb (II)	58 ppm	73.7 %	(Pal et al., 2017)
Gelatin based nanocomposite	Cd (II) Cu (II)	200 ppm	86.1 %, 96.4 %	(Nematidil & Sadeghi, 2019)
Soy sauce residue biochar	Pb (II)	100 ppm	93.1 %	(Xu et al., 2019)
Iron loaded zein beads	As (V)	1 ppm	92.5 %	(Thanawatpo ontawee et al., 2016)
Zein/nylon-6 nanofiber membrane	Cr (VI)	1-5 ppm	87 %	(Ansari et al., 2022)
Zein nanoribbons	Pb (II)	100-200 ppm	86 %	(Wen et al., 2016)
polyethyleneimine (PEI) and zein as hydrophilic channel	Cu (II)	1000-4000 ppm	99 %	(Zhao & Liu, 2019)
Zein micro/nanofibrous membranes	Pb (II) Cd (II)	1000 ppm	94 %, 85 %	(Teng et al., 2022)

1.3.2.3. Zein proteins

Zein proteins have been used for water remediation due their good removal efficiency of pollutants from contaminated water and environmental friendly nature (Jia et al., 2020; Xu et al., 2013) Ni et al. (2018) prepared zein proteins derived superhydrogels for the removal of heavy

metal, such as copper ions. The zein proteins were hydrolyzed and modified by the graft copolymerization of acrylic acid monomers. The study concluded that hydrogel exhibited excellent copper ion removal due to its good chelation ability with the metal ion at pH 4.5 and bio-adsorption reached 208 mg/g. This bio-adsorption performance is ascribed to the presence of functional groups on polyacrylic acid and hydrolyzed zein protein (Ni et al., 2018). In another study, zein nanoribbons were used for the removal of Pb (II) from the contaminated water. Nanoribbons were produced using modified coaxial electrospinning process. Adsorption studies showed Pb (II) sorption capacity was up to 82.3% after 5 cycles with a maximum Pb (II) bio-adsorption of 89.37 mg/g (Wen et al., 2016). Zein biopolymer has been used to bio-adsorption chromium Cr (VI) from the aqueous solution. The study indicated that zein derived nanofibers removed Cr (VI) upto 87% with a concentration of 4.73 mg/g at ambient temperature. This better bio-adsorption capacity is ascribed to the presence of secondary amide, carbonyl, and hydroxyl groups present in the zein derived nanofibers (Ansari et al., 2022).

1.3.2.4. Natural silk protein

Silk protein is also studied for the heavy metal ion removal from contaminated water. Koley and coworkers developed sericin-mediated innumerable hierarchical hybrid flowers to remove Pb (II), Cd (II) and Hg (II) (Koley et al., 2016). The natural silk hybrid materials have a large surface area and functional groups on the surface which may contribute to better bio-adsorption capacity of metals from the aqueous media.

1.3.2.5. Albumen protein

Albumin protein was also used for the remediation of heavy metals from polluted water. Albumin proteins were used to fabricate the cobalt ferrite embedded nitrogen doped carbon nanocomposite for the bio-adsorption of Cd (II). The sorption capacity of 245.09 mg/g was observed for Cd (II) (Ahamad, Naushad, Al-Maswari, et al., 2019). The same group modified the

magnetic resin with egg albumen-formaldehyde and used it to remove Cd (II) from aqueous solution. The maximum adsorption capacity of 149.3 mg/g was observed for Cd (II), which was enhanced with the rise in the temperature (Ahamad, Naushad, Eldesoky, et al., 2019).

1.3.3. Keratin biopolymer as a bio-adsorbent

Amongst protein biopolymers, keratin is the most favourable choice to be used as bio-adsorbents for wastewater remediation (**Table 1.6**). Keratin is the most abundant fibrous structural protein (scleroproteins) along with collagen found in animals. The primary sources of keratin are horns, feathers, nails, hooves, claws and hair (Shah et al., 2019; Sharma & Gupta, 2016). The distinguishable characteristic of keratin from other fibrous proteins (myofibrillar, elastin, collagen) is their greater cysteine contents. Keratin proteins are in fibrous form due to the long chains of polypeptide chains and fibres cross-linking with the help of cysteine disulphide bonds and forming its basic macromolecular structure (McKittrick et al., 2012; B. Wang et al., 2016). These chains form α - (helices) or β -conformation (pleated sheets) by twisting/bending or side-by-side bond formation. So, keratins can be categorized into α - and β - keratins; however, β -keratin is more rigid than the α -keratin. The alpha keratin form is mainly present in mammals and is the main content of hair, stratum corneum, hooves, wool and horns (Chilakamarry et al., 2021; Saha, Arshad, et al., 2019).

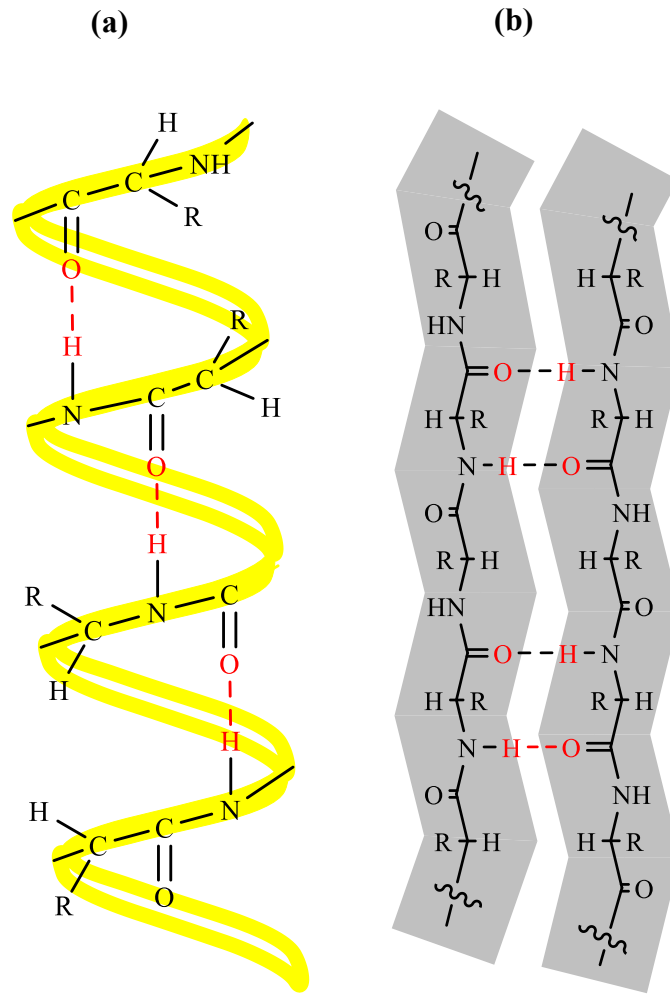


Figure 1.2: Secondary structures of keratin protein (a) alpha helix and (b) beta pleated sheet

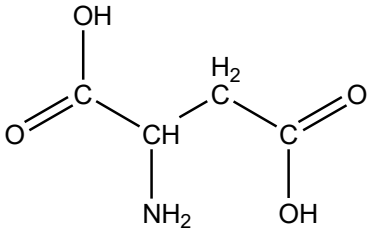
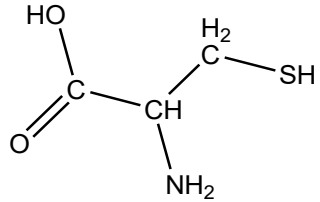
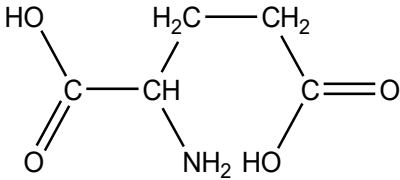
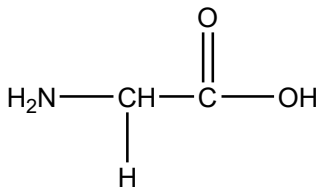
On the other hand, β -keratin is the principal constituent in avian and reptile tissues like bird feathers, claws and beaks, and claws/scales of reptiles. Studies have shown that α -keratins and β -keratins have molecular weights of approximately 40 kDa and 10-22 kDa, respectively (B. Wang et al., 2016).

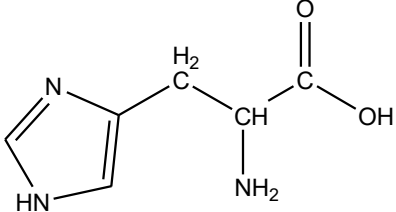
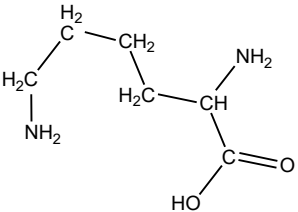
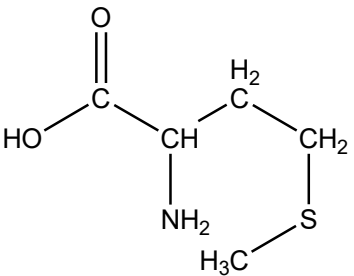
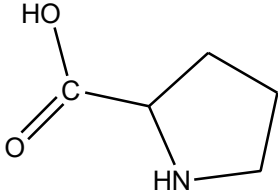
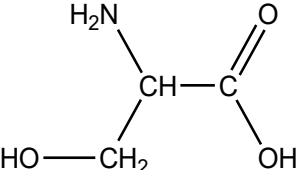
Keratins are classified as acidic/basic based on their isoelectric points (pI), where proteins are neutral (**Table 1.5**). The isoelectric point of keratin is generally altered because of protein enzymatic modification during biosynthesis. The number of ionic bonds between ammonium ion and carboxylate anion is dependent on the pH value and is higher at 4.9 pH, where the protein is

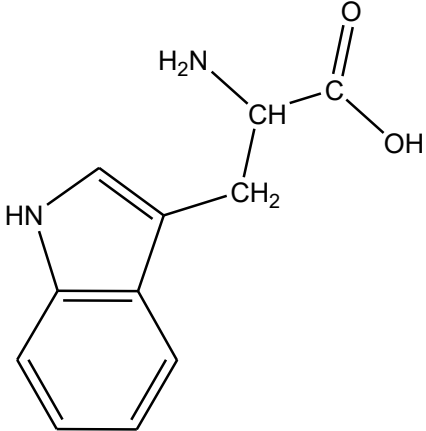
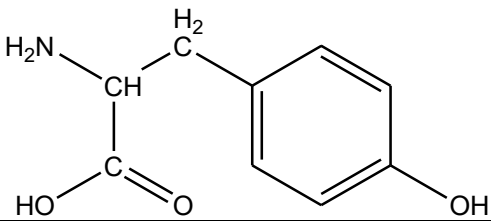
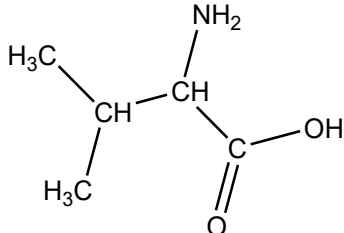
present in zwitterionic (net charge is negative) form ($\text{H}_3\text{N}^+-\text{CHR}-\text{COO}^-$) (Eichner et al., 1984; Wang et al., 2021). Both pH and zwitter ions play a significant role in protein behaviour in different environments. Generally, keratin is neutrally charged; however, ionic bonds are damaged under extreme pH (acidic or basic). The ionic bond is present between ammonium cations and carboxylic anions of the amino acids, which are deprotonated (higher pH) by the amine and protonated (lower pH) by the carboxylic (Feroz et al., 2020).

whole molecule's net charge is negative

Table 1.5.: Keratin amino acids, their pKa values and isoelectric points (pI)

Amino Acids	Structures	PKa (25 °C)			pI
		-COOH	NH ₂	Side Chain	
Aspartic Acid (Asp)		1.99	9.90	3.90	2.98
Cysteine (Cys)		1.92	10.70	8.37	5.15
Glutamic Acid (Glu)		2.10	9.47	4.07	3.08
Glycine (Gly)		2.35	9.78	-	6.06

Histidine (His)		1.80	9.33	6.04	7.64
Lysine (Lys)		2.16	9.06	10.54	9.47
Methionine (Met)		2.13	9.28	-	5.71
Proline (Pro)		1.95	10.64	-	6.30
Serine (Ser)		2.19	9.21	-	5.70
Tryptophan (Trp)		2.46	9.41	-	5.88

					
Tyrosine (Tyr)		2.20	9.21	10.46	5.63
Valine (Val)		2.29	9.74	-	6.02

Source: (Wong et al., 2012)

The α -helix and β -sheet structures of keratin proteins consist of $\sim 50\%$ protein's secondary structure, which is formed and stabilized by non-covalent interactions with hydrogen bonds. The α -helix formation is through right-handed helical structure because the tightly coiled amino acids have 3.6 residues per turn (Chilakamarry et al., 2021). The amino side chains (3-4 residues apart) are linked together, and hydrogen bonding occurs between amino and carbonyl of every fourth peptide bond to stabilize them. In comparison, the β -sheets conformation can form by the polypeptide chains which are folded back and forth (**Fig. 1.2**). As a result, twisted and pleated sheets are created and are stabilized by hydrogen bonding between backbone amino hydrogen and carbonyl oxygen atoms. Consequently, long keratin chains are compact and rod-shaped, presenting

α -conformation or stretched out into twisted or flattened β -sheets (Feughelman et al., 2003; Kreplak et al., 2004). Overall, the polypeptide backbone of the keratin structure is stabilized by inter- and intra- molecular bonding (hydrogen bonding, disulphide bonds, hydrophobic interactions and ionic bonds), which provide strength and stability to the keratin protein as shown in Fig. 1.3.

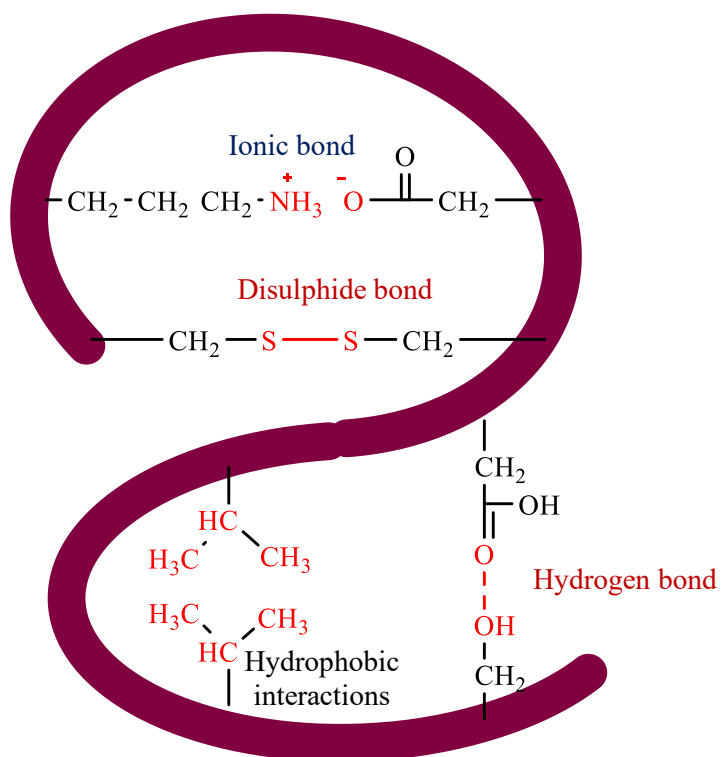


Figure 1.3: Polypeptide backbone representing keratin's inter- and intra- molecular bonding (strength and stability).

Sekimoto and coworkers investigated the wool keratin proteins to remove Pb (II) from the aqueous solution. Synthesized keratin solution was tested to remove Pb (II) ions with a concentration of 43.3 mg/g. The result exhibited that Pb- protein aggregates were formed and

removed the Pb (II) upto 95% by keratin in the colloidal solution (Sekimoto et al., 2013). In another study, chicken feather keratin was chemically modified to remove arsenic from contaminated water. The keratin biopolymers showed good biosorption capacity for arsenic (11.5×10^{-2} - 11.0×10^{-2} mg/g) from polluted water. Furthermore, study indicated that surface modified keratin was involved in monolayer and multilayer formation during the biosorption process (Khosla & Ullah, 2014). In a recent study, Chakraborty and his coworkers modified the chicken feathers using ethylene diamine and used it for the removal of Co (II), Cu (II), Fe (II) and Ni (II) metal ions from metal polluted water upto 20 mg/L concentration. The results showed the removal efficiencies of Co (II), Cu (II), Fe (II) and Ni (II) ions were 98.7%, 98.9%, 98.7% and 99% respectively (Chakraborty et al., 2020). A novel chicken feather adsorbent was reported by Kong et al. (2014), for the removal of Ni (II), Cr (VI) and Pb (II). They performed graft copolymerization was performed using poly (potassium acrylate)/polyvinyl alcohol and semi-interpenetrating polymer network (semi-IPN) super absorbent resin. The adsorbent exhibited a maximum adsorption capacity of 170.3, 78.55, and 143.2 mg /g for Ni (II), Cr (VI) and Pb (II), respectively (Kong et al., 2014; Kong et al., 2016).

Table 1.6: Keratin derived bio-adsorbents for heavy metal removal from polluted water

Keratin Derived Bio-Adsorbents	Type of Heavy Metal	Initial Metal Concentration (ppb)	Adsorption Efficiency (%)	References
Chemically modified chicken feathers	Co (II), Ni (II), Zn (II)	100	60-90	(Zahara et al., 2021)
	Cd (II)	100	87-93	
	Cu (II)	100	80-85	
	As (V)	100	87-93	
	V (V)	100	80-85	
	Cr (VI)	100	95	
Chemically modified chicken feathers	Pb (II), Ni (II), Co (II), Zn (II)	50	> 82	(Donner et al., 2019)
	V (V), Cr (VI), Se (IV)	50	68-100	
Chemically modified duck and chicken feathers	Pb (II)	100,000*	80	(H. Wang et al., 2016)
Keratin hide waste	Pb (II)	25000-150,000*	90	(Kong et al., 2014)
Wool filter coated with Bauxal	As (III)	104	34-53	(Hassan & Davies-McConchie, 2012)
Hybrid polyurethane membrane with chicken keratin (resin and fiber)	Cr (VI)	100,000*	38	(Saucedo-Rivalcoba et al., 2011)
Ionic-liquid modified bird feathers	Cr (VI)	2000-80,000*	87.7	(Sun et al., 2009b)
Keratin amino acid immobilized silica particle	Fe, Mn	50,000-100,000*	72-94	(Sayed et al., 2005)
Keratin fibers from chicken feathers	Cu (II)	2000*	62	(Kar & Misra, 2004)
	Pb (II)	2000*	100	
	Hg (II)	2000*	89.6	
Chicken feather particle treated with NaOH and dodecyl sulphate	Cu (II)	10-100	100	(Al-Asheh & Banat, 2003)
	Zn (II)	10000-100,000*	100	

* Original values were in ppm

In another study by Sun et al. (2009), chicken feathers were chemically modified using epichlorohydrin and ethylenediamine. The results indicated 90% biosorption capacity of Cr (VI) from contaminated water having concentrations between 10-80 ppm (Sun et al., 2009a). Donner and coworkers reported two chemically modified keratin biopolymers, having >82% of biosorption capacity for Pb (II), Ni (II), Co (II) and Zn (II) and 68–100% of Se (IV), V(V) and Cr (VI) from synthetic wastewater with 50 ppb concentrations of each metal (Donner et al., 2019). Zahara and coworkers recently synthesized keratin-derived adsorbents to remove the inorganic contaminants from water containing metal. They tested the adsorbents for Co (II), Ni (II), Cd (II), Cu (II), Zn (II), As (III), Cr (VI), Se (VI) and V (V) using synthetic wastewater with 100 ppb concentrations for each metal. The study concluded that synthesized biopolymers can remove 87–93% of As and Cd, 80–85% of Cu (II) and V (V), 60–90% of Co, Ni (II) and Zn (II), and 95% of Cr (VI) (Zahara et al., 2021). Mondal and coworkers developed human hair derived bio-adsorbent to remove the Cr (VI) from the aqueous solution. The bio-adsorbent exhibited good bio-adsorption capacity for Cr (VI) i.e., 9.852 mg/g and was better than the performance of the other hair derived adsorbents (Mondal & Basu, 2019).

The poultry industry similar to other sectors is also facing the issue of handling waste especially chicken feathers (Khosa et al., 2013; Tesfaye, Sithole, Ramjugernath, et al., 2017). Keratin from chicken feathers is an almost infinite source of (91% \geq) natural keratin (Teskaye, Sithole, et al., 2017a). Poultry feathers have a few applications, for example using as animal feed and fertilizer (Bhari et al., 2021; Coward-Kelly et al., 2006), while the rest are disposed of through landfills or burnt, causing environmental issues (Teskaye, Sithole, et al., 2017b). However, feather keratin is considered as a favorable choice for developing adsorbents for water remediation due to its biodegradable and biocompatible nature (Timorshina et al., 2022; Zhao et al., 2012).

1.3.4. Chemical modification of keratin

Keratin biopolymer has a robust and highly stable structure. It is insoluble in organic solvents and resistant to enzymatic degradation by proteolytic enzymes. These high mechanical and chemical resistances are attributed to the presence of high cysteine in keratin (Yamauchi & Khoda, 1997). Keratin also has an outstanding thermal resistance; however, it can be denatured at temperatures above 100 °C. So far, several methods have been used for keratin extraction including oxidation, ionic liquids, reduction, sulfitolysis, superheated hydrolysis, supercritical water and steam explosion, microwave assisted extraction, and microbial/enzymatic (Idris et al., 2013; Shavandi et al., 2017). Chicken feather keratin is rich in glycine, alanine, proline, leucine serine and valine while methionine, histidine, lysine, and tryptophan are in minor amounts (Gregg & Rogers, 1986). Most importantly, keratin consists of cysteine and cystine which give strength and stiffness to the keratin biopolymer by creating covalent bonds (sulphide and disulphide bonds) and influence the physicochemical properties. In previous studies, modified keratin either showed low biosorption efficiency or selective biosorption of metal cations or anions.

To the best of our knowledge there is no study reported so far where chicken feathers keratin protein has been used for the simultaneous removal of metals ions arsenic (As), selenium (Se), chromium (Cr) and cations including nickel (Ni), cobalt (Co), lead (Pb), cadmium (Cd) and zinc (Zn). The idea is to isolate keratin proteins from feather and further hybridize these proteins with the nanoparticles such as graphene oxide and nanochitosan to remove heavy metals from the synthetic water. These nanoparticles can interact with the keratin proteins as shown in **Fig. 1.5** and **1.7** and enhance the proteins bio-adsorption efficiency for contaminants removal from polluted water.

1.3.4.1. Graphene oxide (GO)

Graphene oxide as a water decontaminated material, is extremely thin and robust with inherent antibacterial ability, can be introduced into protein polymers to enhance their adsorption efficiency further (Zhu et al., 2010). Potential advantages of using graphene oxide include small thickness (one or several atomic layers), high mechanical strength and inherent antimicrobial activity for simultaneous removal of multiple contaminants including metals, organic and pathogens (Mkhoyan et al., 2009).

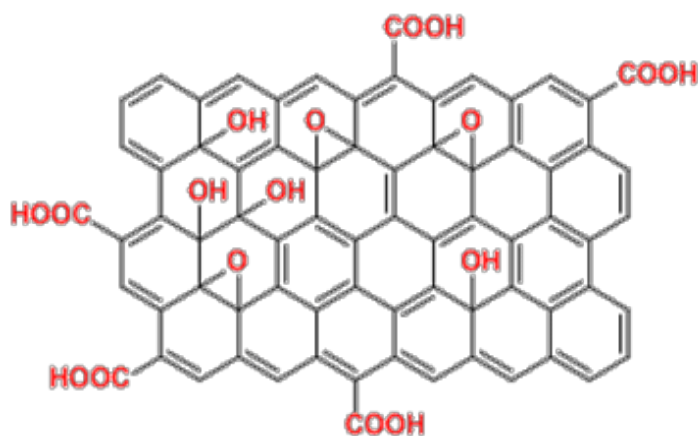


Figure 1.4: Structure of graphene oxide

Oxygenated groups in GO provide a potential advantage in water purification applications. First, the polar functional groups make it strongly hydrophilic, giving GO good dispersibility in many solvents, especially in water. Also, its chemical composition allows tunability of physicochemical properties by chemical modification (**Fig. 1.4**) (Gao, 2015; Gómez-Navarro et al., 2010). In general, the 2D nanochannels between neighboring GO sheets can be considered for passages for molecules and ions smaller than the interlayer spacing of GO sheets while hindering large species. The combination of graphene oxide with keratin proteins can improve its biosorption

efficiency by interaction with its side chains through electrostatic interaction and covalent bond formation.

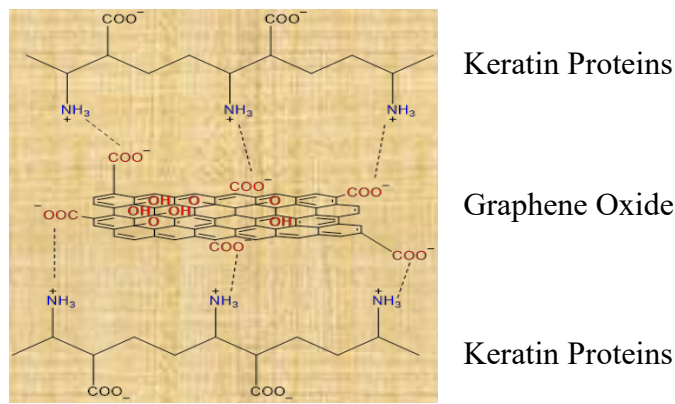


Figure 1.5: Potential interaction b/w keratin proteins and graphene oxide

1.3.4.2. Nanochitosan (NC)

Nanochitosan is polycationic in nature and contains amino and primary/secondary hydroxyl groups (**Fig. 1.6**) (Saha, Zubair, et al., 2019; Zubair et al., 2020). Nanochitosan can make electrostatic interactions with polymeric networks such as proteins to improve its removal efficiency for metals and organic dyes from the contaminated water. The presence of hydroxyl groups on the nanochitosan surface makes it an excellent candidate to interact with keratin through covalent bond formation with the side chains of the keratin. This chemical bonding can improve the removal efficiency of the keratin proteins for metal ions biosorption from contaminated water.

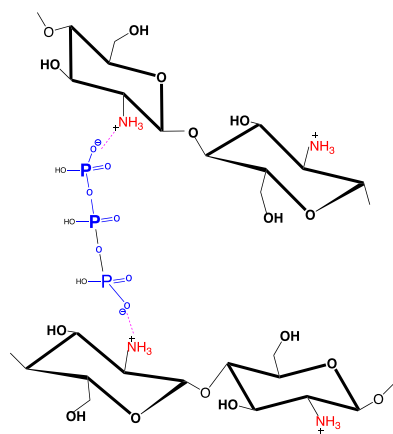


Figure 1.6. Structure of nanochitosan

It has antibacterial activity, making it a suitable candidate to be incorporated into proteins and enhance antimicrobial decontamination. Nanochitosan also shows excellent antibacterial activity compared to chitosan because of its small particle size (Hematizad et al., 2021; Mohammed et al., 2022). Bacterial cells have more affinity with chitosan nanoparticles due to their more surface area and greater affinity. The modification of keratin can be carried out using various functional groups present on its surface such as hydroxyl, thiol and carboxylic groups.

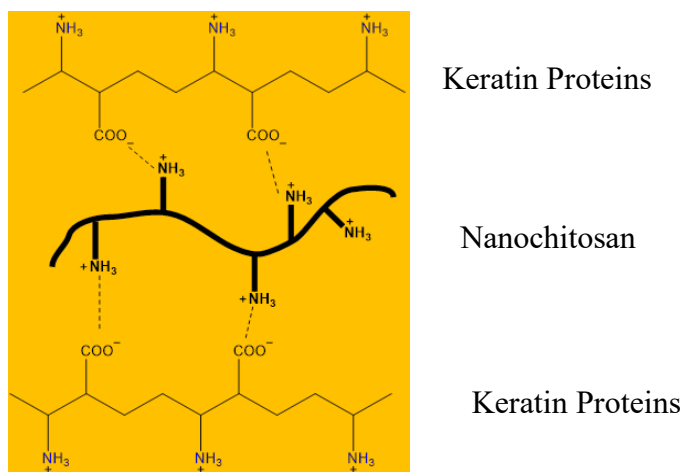


Figure 1.7: Potential interactions b/w keratin proteins and nanochitosan

The affinity of keratin towards heavy metal ions can be enhanced by surface modification or integration with nanoparticles. This work proposed the nanomodification of keratin protein by

cross-linking graphene oxide or nanochitosan to improve its biosorption efficiency for the simultaneous removal of metal cations and anions from synthetic wastewater.

1.4. Research Objectives, Questions and Hypotheses

Based on the literature review, chicken feather keratin has the potential to be transformed into biosorbents for water remediation. Nevertheless, research in keratin derived biosorbents is limited particularly in their detailed structural and surface analyses, and mechanistic phenomena during the biosorption process.

This research aims to develop green and sustainable biosorbents using keratin proteins from chicken feathers in combination with graphene oxide and nanochitosan to remove heavy metal ions from the contaminated water.

The specific objectives are:

Specific Objective I: Chicken feather keratin-graphene oxide derived biosorbents for water remediation

To expose more negative side chains of the feather keratin structures by the chemical modification with graphene oxide to remove inorganic contaminants from the synthetic wastewater.

Research Question I:

Does the chemical modification of the feather keratin structure enhance the polar and charged side chains on the surface, enhancing the removal of the inorganic contaminants from the synthetic wastewater?

Hypothesis I:

The chemical modification of chicken feathers keratin (CFK) with graphene oxide making CFK more effective for heavy metal ions removal.

Specific Objective II: Chicken feather keratin-nanochitosan derived biosorbents for water remediation

To expose more positive side chains of the feather keratin structures by the chemical modification with nanochitosan to remove inorganic contaminants from the synthetic wastewater.

Research Question II:

Does the chemical modification of feather keratin structure enhance the polar and charged side chains on the surface, enhancing the inorganic contaminants from the synthetic wastewater?

Hypothesis II:

The chemical modification of CFK with nanochitosan making CFK more effective for heavy metal ions removal.

Specific Objective III: Synthesis of biosorbent by the polymerization of surface modified graphene oxide with keratin proteins

To expose more positive side chains of the feather keratin structures by the chemical modification with surface modified graphene oxide to remove inorganic contaminants from the synthetic wastewater.

Research Question III:

Does the grafting of graphene oxide with chicken feather keratin, improve its removal efficiency for the inorganic contaminants from the synthetic wastewater?

Hypothesis III:

Surface modified graphene oxide has the acryl amide group which can be grafted to the chicken feathers keratin and makes CFK more effective towards heavy metal ions removal.

Research Approach:

To answer the research questions, the following analyses were conducted:

- a) Evaluate the structural and surface characteristics of developed chicken feather keratin (CFK) derived biosorbents after the chemical modifications with graphene oxide and nanochitosan. Various techniques including Attenuated total reflection-Fourier transform infrared spectroscopy (ATR-FTIR), X-ray photoelectron spectroscopy (XPS), X-ray diffraction (XRD), thermal gravimetric analysis (TGA), differential scanning calorimetry (DSC), scanning and transmission electron microscopy (SEM, TEM) were used for this purpose.
- b) Find out the optimized concentration for nanoparticles and study which one works best keratin proteins for biosorption purposes.
- c) Assess the biosorption capacities of the synthesized biosorbents for the metal cation (Ni^{II} , Co^{II} , Pb^{II} , Cd^{II} , Zn^{II}) and anions (Cr^{VI} , As^{III} , Se^{VI}) simultaneously from the synthetic wastewater. ICP-MS was used to determine the biosorption efficiency of each keratin derived biosorbent.
- d) Determine the underlying mechanism of biosorption of inorganic contaminants, both metal cation (Ni^{II} , Co^{II} , Pb^{II} , Cd^{II} , Zn^{II}) and anions (Cr^{VI} , As^{III} , Se^{VI}) simultaneously on the chicken feather keratin derived biosorbents from synthetic wastewater.

The core piece of this research work is to find substitute biosorbents using chicken feather keratin for heavy metal ions removal from the industrial wastewater with a potential to be applied at the industrial level. The success of this work can benefit local poultry industry farmers to address chicken feather disposal issues and provides renewable, green, sustainable raw material to industries to make eco-friendly biosorbents for water remediation.

Thesis Outline

The thesis comprises six chapters, beginning with the introduction and literature review (chapter one) that includes the recent advances and research gaps, followed by chapter two describes the experimental methods, procedures and instruments used to achieve each objective which are discussed in the chapters 3, 4 and 5. These three chapters as distinct manuscripts based on a research question, with the final chapter (Chapter six) that contains conclusions and future directions.

Chapter three describes the synthesis of chicken feather keratin derived biosorbents by chemical modification with graphene oxide and investigates their role in the simultaneous removal of metal cations and anions from synthetic wastewater. This chapter also discusses the underlying biosorption mechanism of keratin-graphene oxide derived biosorbents for metal ion removal.

Chapter four describes the chemical modification of chicken feather keratin with nanochitosan and how that affects keratin-derived biosorbents' biosorption performances. Here, biosorption mechanisms for CFK-NC are examined through various structural and surface techniques during heavy metal ion biosorption.

Chapter five describes the preparation of keratin derived biosorbent developed through surface-modified graphene oxide and later grafted onto the keratin biopolymer. This chapter also examined this biosorbent's removal efficiency for removing heavy metal ions from synthetic wastewater.

Chapter six concludes the research study with its key outcomes and future directions to further strengthen the study's applicability on an industrial scale.

1.5. References

- Abdellatif, M. M., Abdellatif, F. H. H., & Ibrahim, S. (2022). The utilization of cross-linked gelatin/PAMAM aerogels as heavy metal ions bio-adsorbents from aqueous solutions. *Polymer Bulletin*, 1-18.
- Ahamad, T., Naushad, M., Al-Maswari, B. M., & Alshehri, S. M. (2019). Fabrication of highly porous adsorbent derived from bio-based polymer metal complex for the remediation of water pollutants. *Journal of cleaner production*, 208, 1317-1326.
- Ahamad, T., Naushad, M., Eldesoky, G. E., Alqadami, A. A., & Khan, A. (2019). Synthesis and characterization of egg-albumen-formaldehyde based magnetic polymeric resin (MPR): Highly efficient adsorbent for Cd (II) ion removal from aqueous medium. *Journal of Molecular Liquids*, 286, 110951.
- Al-Asheh, S., & Banat, F. (2003). Beneficial reuse of chicken feathers in removal of heavy metals from wastewater. *Journal of cleaner production*, 11(3), 321-326.
- Al-Khaldi, F. A., Abusharkh, B., Khaled, M., Atieh, M. A., Nasser, M., Saleh, T. A., Agarwal, S., Tyagi, I., & Gupta, V. K. (2015). Adsorptive removal of cadmium (II) ions from liquid phase using acid modified carbon-based adsorbents. *Journal of Molecular Liquids*, 204, 255-263.
- Ali, H., Khan, E., & Ilahi, I. (2019). Environmental chemistry and ecotoxicology of hazardous heavy metals: environmental persistence, toxicity, and bioaccumulation. *Journal of chemistry*, 2019.
- Ansari, S., Ahmed, N., Mahar, R. B., Khatri, Z., & Khatri, M. (2022). Fabrication and characterization of electrospun zein/nylon-6 (ZN6) nanofiber membrane for hexavalent chromium removal. *Environmental Science and Pollution Research*, 29(1), 653-662.
- Babel, S., & Kurniawan, T. (2005). Various treatment technologies to remove arsenic and mercury from contaminated groundwater: an overview. *Southeast Asian Water Environment*, 1.
- Babel, S., & Kurniawan, T. A. (2004). Cr (VI) removal from synthetic wastewater using coconut shell charcoal and commercial activated carbon modified with oxidizing agents and/or chitosan. *Chemosphere*, 54(7), 951-967.
- Bashir, A., Malik, L. A., Ahad, S., Manzoor, T., Bhat, M. A., Dar, G., & Pandith, A. H. (2019). Removal of heavy metal ions from aqueous system by ion-exchange and biosorption methods. *Environmental Chemistry Letters*, 17(2), 729-754.
- Bhari, R., Kaur, M., & Sarup Singh, R. (2021). Chicken feather waste hydrolysate as a superior biofertilizer in agroindustry. *Current Microbiology*, 78(6), 2212-2230.
- Bilal, M., Ihsanullah, I., Younas, M., & Shah, M. U. H. (2021). Recent advances in applications of low-cost adsorbents for the removal of heavy metals from water: A critical review. *Separation and Purification Technology*, 278, 119510.
- Carlos, L., Einschlag, F. S. G., González, M. C., & Mártire, D. O. (2013). Applications of magnetite nanoparticles for heavy metal removal from wastewater. *Waste Water-Treatment Technologies and Recent Analytical Developments*, 3, 64-73.
- Chai, W. S., Cheun, J. Y., Kumar, P. S., Mubashir, M., Majeed, Z., Banat, F., Ho, S.-H., & Show, P. L. (2021). A review on conventional and novel materials towards heavy metal adsorption in wastewater treatment application. *Journal of Cleaner Production*, 296, 126589.

- Chakraborty, R., Asthana, A., Singh, A. K., Yadav, S., Susan, M. A. B. H., & Carabineiro, S. A. (2020). Intensified elimination of aqueous heavy metal ions using chicken feathers chemically modified by a batch method. *Journal of Molecular Liquids*, 312, 113475.
- Chilakamarry, C. R., Mahmood, S., Saffe, S. N. B. M., Arifin, M. A. B., Gupta, A., Sikkandar, M. Y., Begum, S. S., & Narasaiah, B. (2021). Extraction and application of keratin from natural resources: a review. *3 Biotech*, 11(5), 1-12.
- Coward-Kelly, G., Chang, V. S., Agbogbo, F. K., & Holtzapple, M. T. (2006). Lime treatment of keratinous materials for the generation of highly digestible animal feed: 1. Chicken feathers. *Bioresource technology*, 97(11), 1337-1343.
- Demirbas, A. (2008). Heavy metal adsorption onto agro-based waste materials: a review. *Journal of hazardous materials*, 157(2-3), 220-229.
- Donner, M. W., Arshad, M., Ullah, A., & Siddique, T. (2019). Unravelling keratin-derived biopolymers as novel biosorbents for the simultaneous removal of multiple trace metals from industrial wastewater. *Science of The Total Environment*, 647, 1539-1546.
- Duan, C., Ma, T., Wang, J., & Zhou, Y. (2020). Removal of heavy metals from aqueous solution using carbon-based adsorbents: A review. *Journal of Water Process Engineering*, 37, 101339.
- Duruibe, J. (2007). Ogwuegbu MOC Egwurugwu JN Int. *J. Phys. Sci*, 2, 112-118.
- Eichner, R., Bonitz, P., & Sun, T.-T. (1984). Classification of epidermal keratins according to their immunoreactivity, isoelectric point, and mode of expression. *The Journal of cell biology*, 98(4), 1388-1396.
- Elgamal, A. M., Abd El-Ghany, N. A., & Saad, G. R. (2023). Synthesis and characterization of hydrogel-based magnetite nanocomposite adsorbents for the potential removal of Acid Orange 10 dye and Cr (VI) ions from aqueous solution. *International Journal of Biological Macromolecules*, 227, 27-44.
- Esfarili, L., Safarifard, V., Tahmasebi, E., Esfarili, M., & Morsali, A. (2018). Functional group effect of isorecticular metal-organic frameworks on heavy metal ion adsorption. *New Journal of Chemistry*, 42(11), 8864-8873.
- Fei, Y., & Hu, Y. H. (2022). Design, synthesis, and performance of adsorbents for heavy metal removal from wastewater: a review. *Journal of Materials Chemistry A*.
- Feroz, S., Muhammad, N., Ratnayake, J., & Dias, G. (2020). Keratin-Based materials for biomedical applications. *Bioactive materials*, 5(3), 496-509.
- Feughelman, M., Lyman, D., Menefee, E., & Willis, B. (2003). The orientation of the α -helices in α -keratin fibres. *International journal of biological macromolecules*, 33(1-3), 149-152.
- Gao, W. (2015). The chemistry of graphene oxide. In *Graphene oxide* (pp. 61-95). Springer.
- Gendy, E. A., Ifthikar, J., Ali, J., Oyekunle, D. T., Elkhelifia, Z., Shahib, I. I., Khodair, A. I., & Chen, Z. (2021). Removal of heavy metals by covalent organic frameworks (COFs): A review on its mechanism and adsorption properties. *Journal of Environmental Chemical Engineering*, 9(4), 105687.
- Gómez-Navarro, C., Meyer, J. C., Sundaram, R. S., Chuvilin, A., Kurasch, S., Burghard, M., Kern, K., & Kaiser, U. (2010). Atomic structure of reduced graphene oxide. *Nano letters*, 10(4), 1144-1148.
- González, A. G., Pokrovsky, O. S., Santana-Casiano, J. M., & González-Dávila, M. (2017). Bioadsorption of heavy metals. In *Prospects and challenges in algal biotechnology* (pp. 233-255). Springer.

- Gregg, K., & Rogers, G. E. (1986). Feather keratin: composition, structure and biogenesis. In *Biology of the integument* (pp. 666-694). Springer.
- Hassan, M. M., & Davies-McConchie, J. F. (2012). Removal of arsenic and heavy metals from potable water by bauxsol immobilized onto wool fibers. *Industrial & engineering chemistry research*, *51*(28), 9634-9641.
- Hematizad, I., Khanjari, A., Basti, A. A., Karabagias, I. K., Noori, N., Ghadami, F., Gholami, F., & Teimourifard, R. (2021). In vitro antibacterial activity of gelatin-nanochitosan films incorporated with Zataria multiflora Boiss essential oil and its influence on microbial, chemical, and sensorial properties of chicken breast meat during refrigerated storage. *Food Packaging and Shelf Life*, *30*, 100751.
- Hoekstra, A. Y. (2015). The water footprint: The relation between human consumption and water use. In *The Water We Eat* (pp. 35-48). Springer.
- Homagai, P. L., Ghimire, K. N., & Inoue, K. (2010). Adsorption behavior of heavy metals onto chemically modified sugarcane bagasse. *Bioresource technology*, *101*(6), 2067-2069.
- Idris, A., Vijayaraghavan, R., Rana, U. A., Fredericks, D., Patti, A. F., & Macfarlane, D. R. (2013). Dissolution of feather keratin in ionic liquids. *Green Chemistry*, *15*(2), 525-534.
- Järup, L. (2003). Hazards of heavy metal contamination. *British medical bulletin*, *68*(1), 167-182.
- Jayaraj, K., Suriya, M., & Pius, A. (2019). Application of Bio-Waste Materials in The Green Synthesis Of Composites For Water Purification. *Advance Scientific Research*, *7*.
- Jia, X., Yang, N., Qi, X., Chen, L., & Zhao, Y. (2020). Adsorptive removal of cholesterol by biodegradable zein-graft- β -cyclodextrin film. *International Journal of Biological Macromolecules*, *155*, 293-304.
- Jiang, Y., Liu, C., & Huang, A. (2019). EDTA-functionalized covalent organic framework for the removal of heavy-metal ions. *ACS applied materials & interfaces*, *11*(35), 32186-32191.
- Kar, P., & Misra, M. (2004). Use of keratin fiber for separation of heavy metals from water. *Journal of Chemical Technology & Biotechnology: International Research in Process, Environmental & Clean Technology*, *79*(11), 1313-1319.
- Khaskheli, M. A., Abro, M. I., Chand, R., Elahi, E., Khokhar, F. M., Majidano, A. A., Aaoud, E., Hassan, E., & Rekik, N. (2021). Evaluating the effectiveness of eggshells to remove heavy metals from wastewater. *Desalination and Water Treatment*, *216*, 239-245.
- Khosa, M. A., & Ullah, A. (2014). In-situ modification, regeneration, and application of keratin biopolymer for arsenic removal. *Journal of hazardous materials*, *278*, 360-371.
- Khosa, M. A., Wu, J., & Ullah, A. (2013). Chemical modification, characterization, and application of chicken feathers as novel biosorbents. *RSC advances*, *3*(43), 20800-20810.
- Koley, P., Sakurai, M., & Aono, M. (2016). Controlled fabrication of silk protein sericin mediated hierarchical hybrid flowers and their excellent adsorption capability of heavy metal ions of Pb (II), Cd (II) and Hg (II). *ACS applied materials & interfaces*, *8*(3), 2380-2392.
- Kong, J., Yue, Q., Sun, S., Gao, B., Kan, Y., Li, Q., & Wang, Y. (2014). Adsorption of Pb (II) from aqueous solution using keratin waste–hide waste: equilibrium, kinetic and thermodynamic modeling studies. *Chemical Engineering Journal*, *241*, 393-400.
- Kong, W., Li, Q., Liu, J., Li, X., Zhao, L., Su, Y., Yue, Q., & Gao, B. (2016). Adsorption behavior and mechanism of heavy metal ions by chicken feather protein-based semi-

- interpenetrating polymer networks super absorbent resin. *RSC advances*, 6(86), 83234-83243.
- Kreplak, L., Doucet, J., Dumas, P., & Briki, F. (2004). New aspects of the α -helix to β -sheet transition in stretched hard α -keratin fibers. *Biophysical journal*, 87(1), 640-647.
- Kumari, D., Goswami, R., Kumar, M., Katakai, R., & Shim, J. (2018). Removal of Cr (VI) ions from the aqueous solution through nanoscale zero-valent iron (nZVI) Magnetite Corn Cob Silica (MCCS): a bio-waste based water purification perspective. *Groundwater for Sustainable Development*, 7, 470-476.
- Li, Y., Liu, J., Yuan, Q., Tang, H., Yu, F., & Lv, X. (2016). A green adsorbent derived from banana peel for highly effective removal of heavy metal ions from water. *RSC advances*, 6(51), 45041-45048.
- Liu, D., Li, Z., Li, W., Zhong, Z., Xu, J., Ren, J., & Ma, Z. (2013). Adsorption behavior of heavy metal ions from aqueous solution by soy protein hollow microspheres. *Industrial & engineering chemistry research*, 52(32), 11036-11044.
- Liu, F., Zou, H., Peng, J., Hu, J., Liu, H., Chen, Y., & Lu, F. (2016). Removal of copper (II) using deacetylated konjac glucomannan conjugated soy protein isolate. *International journal of biological macromolecules*, 86, 338-344.
- Liu, J., Su, D., Yao, J., Huang, Y., Shao, Z., & Chen, X. (2017). Soy protein-based polyethylenimine hydrogel and its high selectivity for copper ion removal in wastewater treatment. *Journal of Materials Chemistry A*, 5(8), 4163-4171.
- Liu, L., Liu, Q., Ma, J., Wu, H., Qu, Y., Gong, Y., Yang, S., An, Y., & Zhou, Y. (2020). Heavy metal (loid) s in the topsoil of urban parks in Beijing, China: Concentrations, potential sources, and risk assessment. *Environmental Pollution*, 260, 114083.
- Lohri, C. R., Diener, S., Zabaleta, I., Mertenat, A., & Zurbrügg, C. (2017). Treatment technologies for urban solid biowaste to create value products: a review with focus on low-and middle-income settings. *Reviews in Environmental Science and Bio/Technology*, 16(1), 81-130.
- Mahdavian, A. R., & Mirrahipi, M. A.-S. (2010). Efficient separation of heavy metal cations by anchoring polyacrylic acid on superparamagnetic magnetite nanoparticles through surface modification. *Chemical Engineering Journal*, 159(1-3), 264-271.
- Mahmoud, M. E., & Mohamed, R. H. A. (2014). Biosorption and removal of Cr (VI)–Cr (III) from water by eco-friendly gelatin biosorbent. *Journal of Environmental Chemical Engineering*, 2(1), 715-722.
- Mateo-Sagasta, J., Raschid-Sally, L., & Thebo, A. (2015). Global Wastewater and Sludge Production, Treatment and Use. In P. Drechsel, M. Qadir, & D. Wichelns (Eds.), *Wastewater: Economic Asset in an Urbanizing World* (pp. 15-38). Springer Netherlands. https://doi.org/10.1007/978-94-017-9545-6_2
- McKittrick, J., Chen, P.-Y., Bodde, S., Yang, W., Novitskaya, E., & Meyers, M. (2012). The structure, functions, and mechanical properties of keratin. *Jom*, 64(4), 449-468.
- Mkhoyan, K. A., Contryman, A. W., Silcox, J., Stewart, D. A., Eda, G., Mattevi, C., Miller, S., & Chhowalla, M. (2009). Atomic and electronic structure of graphene-oxide. *Nano letters*, 9(3), 1058-1063.
- Mohammed, A., Alobaidi, Y., & Abdullah, H. (2022). Synthesis of nanochitosan membranes from shrimp shells. *Egyptian Journal of Chemistry*.

- Mondal, N. K., & Basu, S. (2019). Potentiality of waste human hair towards removal of chromium (VI) from solution: kinetic and equilibrium studies. *Applied Water Science*, 9(3), 1-8.
- Morais, S., Costa, F. G., & Pereira, M. d. L. (2012). Heavy metals and human health. *Environmental health—emerging issues and practice*, 10(1), 227-245.
- Naik, R. L., Kumar, M. R., & Narsaiah, T. B. (2022). Removal of heavy metals (Cu & Ni) from wastewater using rice husk and orange peel as adsorbents. *Materials Today: Proceedings*.
- Negroiu, M., Țurcanu, A. A., Matei, E., Râpă, M., Covaliu, C. I., Predescu, A. M., Pantilimon, C. M., Coman, G., & Predescu, C. (2021). Novel adsorbent based on banana peel waste for removal of heavy metal ions from synthetic solutions. *Materials*, 14(14), 3946.
- Nematidil, N., & Sadeghi, M. (2019). Fabrication and characterization of a novel biosorbent and its evaluation as adsorbent for heavy metal ions. *Polymer Bulletin*, 76(10), 5103-5127.
- Ni, N., Zhang, D., & Dumont, M.-J. (2018). Synthesis and characterization of zein-based superabsorbent hydrogels and their potential as heavy metal ion chelators. *Polymer Bulletin*, 75(1), 31-45.
- Nuithitikul, K., Phromrak, R., & Saengngoen, W. (2020). Utilization of chemically treated cashew-nut shell as potential adsorbent for removal of Pb (II) ions from aqueous solution. *Scientific Reports*, 10(1), 1-14.
- Oliveira, J. A., Cunha, F. A., & Ruotolo, L. A. (2019). Synthesis of zeolite from sugarcane bagasse fly ash and its application as a low-cost adsorbent to remove heavy metals. *Journal of cleaner production*, 229, 956-963.
- Osasona, I., Ojo Adebayo, A., & Ajayi, O. O. (2013). Adsorptive Removal of Chromium (VI) from Aqueous Solution Using Cow Hooves. *Adsorptive Removal of Chromium (VI) from Aqueous Solution Using Cow Hooves.*, 2(1), 1-16.
- Pal, P., Syed, S. S., & Banat, F. (2017). Gelatin-bentonite composite as reusable adsorbent for the removal of lead from aqueous solutions: Kinetic and equilibrium studies. *Journal of Water Process Engineering*, 20, 40-50.
- Park, H. J., Jeong, S. W., Yang, J. K., Kim, B. G., & Lee, S. M. (2007). Removal of heavy metals using waste eggshell. *Journal of Environmental Sciences*, 19(12), 1436-1441.
- Parker, D. B., & Brown, M. S. (2003). Water consumption for livestock and poultry production. *Encyclopedia of Water Science, 1st Ed.; Stewart, BA, Howell, TA, Eds.*
- Qamar, M. A., Javed, M., Shahid, S., Shariq, M., Fadhali, M. M., Ali, S. K., & Khan, M. S. (2023). Synthesis and applications of graphitic carbon nitride (g-C₃N₄) based membranes for wastewater treatment: A critical review. *Heliyon*, e12685.
- Saha, S., Arshad, M., Zubair, M., & Ullah, A. (2019). Keratin as a Biopolymer. In *Keratin as a protein biopolymer* (pp. 163-185). Springer.
- Saha, S., Zubair, M., Khosa, M., Song, S., & Ullah, A. (2019). Keratin and chitosan biosorbents for wastewater treatment: a review. *Journal of Polymers and the Environment*, 27(7), 1389-1403.
- Sangeetha, K., Vidhya, G., Vasugi, G., & Girija, E. (2018). Lead and cadmium removal from single and binary metal ion solution by novel hydroxyapatite/alginate/gelatin nanocomposites. *Journal of Environmental Chemical Engineering*, 6(1), 1118-1126.
- Sato, T., Qadir, M., Yamamoto, S., Endo, T., & Zahoor, A. (2013). Global, regional, and country level need for data on wastewater generation, treatment, and use. *Agricultural Water Management*, 130, 1-13. <https://doi.org/https://doi.org/10.1016/j.agwat.2013.08.007>

- Saucedo-Rivalcoba, V., Martínez-Hernández, A., Martínez-Barrera, G., Velasco-Santos, C., Rivera-Armenta, J., & Castaño, V. (2011). Removal of hexavalent chromium from water by polyurethane–keratin hybrid membranes. *Water, Air, & Soil Pollution*, 218(1), 557-571.
- Sayed, S., Saleh, S., & Hasan, E. (2005). Removal of some polluting metals from industrial water using chicken feathers. *Desalination*, 181(1-3), 243-255.
- Sekimoto, Y., Okiharu, T., Nakajima, H., Fujii, T., Shirai, K., & Moriwaki, H. (2013). Removal of Pb (II) from water using keratin colloidal solution obtained from wool. *Environmental Science and Pollution Research*, 20(9), 6531-6538.
- SenthilKumar, P., Ramalingam, S., Sathyaselvabala, V., Kirupha, S. D., & Sivanesan, S. (2011). Removal of copper (II) ions from aqueous solution by adsorption using cashew nut shell. *Desalination*, 266(1-3), 63-71.
- Shah, A., Tyagi, S., Bharagava, R. N., Belhaj, D., Kumar, A., Saxena, G., Saratale, G. D., & Mulla, S. I. (2019). Keratin production and its applications: current and future perspective. *Keratin as a protein biopolymer*, 19-34.
- Shannon, M. A., Bohn, P. W., Elimelech, M., Georgiadis, J. G., Marinas, B. J., & Mayes, A. M. (2010). Science and technology for water purification in the coming decades. *Nanoscience and technology: a collection of reviews from nature Journals*, 337-346.
- Sharma, G., & Naushad, M. (2020). Adsorptive removal of noxious cadmium ions from aqueous medium using activated carbon/zirconium oxide composite: isotherm and kinetic modelling. *Journal of Molecular Liquids*, 310, 113025.
- Sharma, S., & Gupta, A. (2016). Sustainable management of keratin waste biomass: applications and future perspectives. *Brazilian Archives of Biology and Technology*, 59.
- Shavandi, A., Silva, T. H., Bekhit, A. A., & Bekhit, A. E.-D. A. (2017). Keratin: dissolution, extraction and biomedical application. *Biomaterials science*, 5(9), 1699-1735.
- Siddiqua, A., Hahladakis, J. N., & Al-Attiya, W. A. K. A. (2022). An overview of the environmental pollution and health effects associated with waste landfilling and open dumping. *Environmental Science and Pollution Research*.
<https://doi.org/10.1007/s11356-022-21578-z>
- Subramaniam, M. N., Goh, P. S., Lau, W. J., & Ismail, A. F. (2019). The roles of nanomaterials in conventional and emerging technologies for heavy metal removal: A state-of-the-art review. *Nanomaterials*, 9(4), 625.
- Sun, P., Liu, Z.-T., & Liu, Z.-W. (2009a). Chemically modified chicken feather as sorbent for removing toxic chromium (VI) ions. *Industrial & engineering chemistry research*, 48(14), 6882-6889.
- Sun, P., Liu, Z.-T., & Liu, Z.-W. (2009b). Particles from bird feather: A novel application of an ionic liquid and waste resource. *Journal of hazardous materials*, 170(2-3), 786-790.
- Teng, D., Xu, Y., Zhao, T., Zhang, X., Li, Y., & Zeng, Y. (2022). Zein adsorbents with micro/nanofibrous membrane structure for removal of oils, organic dyes, and heavy metal ions in aqueous solution. *Journal of hazardous materials*, 425, 128004.
- Tesfaye, T., Sithole, B., & Ramjugernath, D. (2017a). Valorisation of chicken feathers: a review on recycling and recovery route—current status and future prospects. *Clean Technologies and Environmental Policy*, 19(10), 2363-2378.
- Tesfaye, T., Sithole, B., & Ramjugernath, D. (2017b). Valorisation of chicken feathers: recycling and recovery routes. Proceedings, Sardinia,

- Tesfaye, T., Sithole, B., Ramjugernath, D., & Chunilall, V. (2017). Valorisation of chicken feathers: Characterisation of chemical properties. *Waste Management*, *68*, 626-635.
- Thanawatpootawee, S., Imyim, A., & Praphairaksit, N. (2016). Iron-loaded zein beads as a biocompatible adsorbent for arsenic (V) removal. *Journal of Industrial and Engineering Chemistry*, *43*, 127-132.
- Timorshina, S., Popova, E., & Osmolovskiy, A. (2022). Sustainable Applications of Animal Waste Proteins. *Polymers*, *14*(8), 1601.
- UNO. (2020). <https://www.un.org/sustainabledevelopment/water-and-sanitation/>
- Vilardi, G., Di Palma, L., & Verdone, N. (2018). Heavy metals adsorption by banana peels micro-powder: Equilibrium modeling by non-linear models. *Chinese Journal of Chemical Engineering*, *26*(3), 455-464.
- Wang, B., Yang, W., McKittrick, J., & Meyers, M. A. (2016). Keratin: Structure, mechanical properties, occurrence in biological organisms, and efforts at bioinspiration. *Progress in Materials Science*, *76*, 229-318.
- Wang, F., Wu, P., Shu, L., Huang, D., & Liu, H. (2022). High-efficiency adsorption of Cd (II) and Co (II) by ethylenediaminetetraacetic dianhydride-modified orange peel as a novel synthesized adsorbent. *Environmental Science and Pollution Research*, *29*(17), 25748-25758.
- Wang, H., Jin, X., & Wu, H. (2016). Adsorption and desorption properties of modified feather and feather/polypropylene melt-blown filter cartridge of lead ion (Pb²⁺). *Journal of Industrial Textiles*, *46*(3), 852-867.
- Wang, S., Li, X., Liu, Y., Zhang, C., Tan, X., Zeng, G., Song, B., & Jiang, L. (2018). Nitrogen-containing amino compounds functionalized graphene oxide: Synthesis, characterization and application for the removal of pollutants from wastewater: A review. *Journal of hazardous materials*, *342*, 177-191.
<https://doi.org/https://doi.org/10.1016/j.jhazmat.2017.06.071>
- Wang, X., Huang, K., Chen, Y., Liu, J., Chen, S., Cao, J., Mei, S., Zhou, Y., & Jing, T. (2018). Preparation of dumbbell manganese dioxide/gelatin composites and their application in the removal of lead and cadmium ions. *Journal of hazardous materials*, *350*, 46-54.
- Wang, X., Shi, Z., Zhao, Q., & Yun, Y. (2021). Study on the structure and properties of biofunctional keratin from rabbit hair. *Materials*, *14*(2), 379.
- Wen, H.-F., Yang, C., Yu, D.-G., Li, X.-Y., & Zhang, D.-F. (2016). Electrospun zein nanoribbons for treatment of lead-contained wastewater. *Chemical Engineering Journal*, *290*, 263-272.
- Wichelns, D., Drechsel, P., & Qadir, M. (2015). Wastewater: Economic Asset in an Urbanizing World. In P. Drechsel, M. Qadir, & D. Wichelns (Eds.), *Wastewater: Economic Asset in an Urbanizing World* (pp. 3-14). Springer Netherlands. https://doi.org/10.1007/978-94-017-9545-6_1
- Wojciechowska, P., Cierpiszewski, R., & Maciejewski, H. (2022). Gelatin–Siloxane Hybrid Monoliths as Novel Heavy Metal Adsorbents. *Applied Sciences*, *12*(3), 1258.
- Wong, S. S., Jameson, D. M., & Wong, S. (2012). *Chemistry of protein and nucleic acid cross-linking and conjugation*. CRC Press Boca Raton, FL, USA:.
- Xu, H., Zhang, Y., Jiang, Q., Reddy, N., & Yang, Y. (2013). Biodegradable hollow zein nanoparticles for removal of reactive dyes from wastewater. *Journal of environmental management*, *125*, 33-40.

- Xu, J., Cao, Z., Zhang, Y., Yuan, Z., Lou, Z., Xu, X., & Wang, X. (2018). A review of functionalized carbon nanotubes and graphene for heavy metal adsorption from water: Preparation, application, and mechanism. *Chemosphere*, *195*, 351-364.
- Xu, X., Zhou, C., Zhang, S., Cheng, Z., Yang, Z., Xian, J., & Yang, Y. (2019). Adsorption of Cr⁶⁺ and Pb²⁺ on soy sauce residue biochar from aqueous solution. *BioResources*, *14*(2), 4653-4669.
- Yamauchi, K., & Khoda, A. (1997). Novel proteinous microcapsules from wool keratins. *Colloids and Surfaces B: Biointerfaces*, *9*(1-2), 117-119.
- Yang, R., Li, Z., Huang, B., Luo, N., Huang, M., Wen, J., Zhang, Q., Zhai, X., & Zeng, G. (2018). Effects of Fe (III)-fulvic acid on Cu removal via adsorption versus coprecipitation. *Chemosphere*, *197*, 291-298.
- Zahara, I., Arshad, M., Naeth, M. A., Siddique, T., & Ullah, A. (2021). Feather keratin derived sorbents for the treatment of wastewater produced during energy generation processes. *Chemosphere*, *273*, 128545.
- Zaimee, M. Z. A., Sarjadi, M. S., & Rahman, M. L. (2021). Heavy metals removal from water by efficient adsorbents. *Water*, *13*(19), 2659.
- Zhao, W., Yang, R., Zhang, Y., & Wu, L. (2012). Sustainable and practical utilization of feather keratin by an innovative physicochemical pretreatment: high density steam flash-explosion. *Green Chemistry*, *14*(12), 3352-3360.
- Zhao, X., & Liu, C. (2019). Efficient removal of heavy metal ions based on the selective hydrophilic channels. *Chemical Engineering Journal*, *359*, 1644-1651.
- Zhou, Q., Yang, N., Li, Y., Ren, B., Ding, X., Bian, H., & Yao, X. (2020). Total concentrations and sources of heavy metal pollution in global river and lake water bodies from 1972 to 2017. *Global Ecology and Conservation*, *22*, e00925.
- Zhou, Z., Liu, Y.-g., Liu, S.-b., Liu, H.-y., Zeng, G.-m., Tan, X.-f., Yang, C.-p., Ding, Y., Yan, Z.-l., & Cai, X.-x. (2017). Sorption performance and mechanisms of arsenic (V) removal by magnetic gelatin-modified biochar. *Chemical Engineering Journal*, *314*, 223-231.
- Zhu, Y., He, X., Xu, J., Fu, Z., Wu, S., Ni, J., & Hu, B. (2021). Insight into efficient removal of Cr (VI) by magnetite immobilized with *Lysinibacillus* sp. JLT12: Mechanism and performance. *Chemosphere*, *262*, 127901.
- Zhu, Y., Murali, S., Cai, W., Li, X., Suk, J. W., Potts, J. R., & Ruoff, R. S. (2010). Graphene and graphene oxide: synthesis, properties, and applications. *Advanced materials*, *22*(35), 3906-3924.
- Zubair, M., Arshad, M., & Ullah, A. (2020). Chitosan-based materials for water and wastewater treatment. In *Handbook of chitin and chitosan* (pp. 773-809). Elsevier.
- Zubair, M., & Ullah, A. (2021). Biopolymers in environmental applications: industrial wastewater treatment. *Biopolymers and their industrial applications*, 331-349.

CHAPTER 2: Experimental Methods and Data Analysis

2.1. Chemicals and Materials

Broiler's white chicken feathers were supplied by Poultry Research Centre, University of Alberta and Sofina food facility in Edmonton. Graphite, sulfuric acid (H_2SO_4 , 95.098 wt.%), hydrogen peroxide (H_2O_2 30%), chitosan (50,000-190,000 Da molecular weight), 75-85% deacylated chitin, poly (D-glucosamine), sodium tripolyphosphate (TTP), acetic acid urea (99%), sodium sulfite (≥ 98), ethylenediamine tetraacetic acid (EDTA) (99%), n-hexane ($\geq 95\%$), tris-base ($\geq 99.8\%$), hydrochloric acid (HCL), zinc (Zn) sulfate heptahydrate (99%), cadmium (Cd) chloride (99.9%), chromium (Cr) oxide (99.99%), sodium meta arsenite ($\geq 99\%$), sodium selenate (95%), hydrochloric acid (HCl 35%), acryl amide ($> 99\%$), N, N'-dicyclohexylcarbodiimide (DCC), dimethyl formamide (DMF) (99.8%) and sodium thiosulfate ($\geq 99\%$) were purchased from Sigma-Aldrich and used as received. Phosphoric acid (H_3PO_4 , 85%), nickel (Ni) chloride hexahydrate (99.4%), and cobaltous (Co) sulfate heptahydrate (99.2%) were purchased from fisher scientific. While potassium permanganate (KMnO_4 , 99%) and hydroxy benzotriazole (HoBt) (97%) was purchased from Caledon and TCI America, respectively. All other reagents used were of analytical grade.

2.2. Proximate Analysis of Chicken Feathers

The moisture, protein, fat and ash contents of the chicken feathers were determined as follows.

2.2.1. Moisture content analysis

Moisture contents of raw chicken feathers were determined according to AOAC (Association of Official Agricultural Chemists) method) (William Horwitz, 2005)

$$\% \text{ Moisture contents (w/w)} = \frac{\text{Wet weight} - \text{Dry weight}}{\text{Wet weight}} \times 100$$

2.2.2 Determination of total fat contents

Lipid contents of ground raw chicken feathers was determined by Folch method (Pérez-Palacios et al., 2008). The extraction was carried out using the of 20 parts chloroform: methanol (2:1, v/v) to a part of sample. 2.5 grams of ground chicken feather were mixed with 50 ml of chloroform: methanol (2:1, v/v) followed by homogenization and centrifuged (13,000 X g) for 8 minutes and filtered. Further, 2 ml of distilled water was poured into the filtrate and the resulting mixture was shaken vigorously. The resulting bi-phasic system was centrifugated (13,000 X g) for 8 mins and the upper aqueous phase was removed. Anhydrous sodium sulphate was used to filter the lower organic phase (chloroform) and collected. Finally, lipid contents were determined gravimetrically after the evaporation of chloroform with a rotary evaporator under a vacuum.

2.2.3. Determination of ash contents

Ash contents of raw chicken feathers were determined by AOAC (William Horwitz, 2005). Chicken feathers were washed, oven dried and ground before the determination of ash contents. 2 g of chicken feathers sample was kept in a muffle furnace overnight at 550 °C. The ash contents were calculated as follows.

$$\% \text{ Ash} = \frac{\text{Weight of ash}}{\text{Weight of sample}} \times 100$$

2.2.4. Determination of proteins contents

The total protein contents of raw chicken feathers were determined by a LECO (Nitrogen/Carbon) analyzer (TruSpec®CN., MI., CA, USA.). Chicken feathers were dried and ground before the analysis.

2.2.5. Determination of chicken feather keratin molecular weight

Sodium dodecyl sulfate polyacrylamide gel electrophoresis (SDS–PAGE) performed with Bio-Rad Criterion Cell (Bio-Rad Laboratories, Inc., Canada) on a precast (10–20%) Tris–HCl gradient polyacrylamide gel. Before the electrophoresis run, each keratin protein sample was diluted in a loading buffer (Bio-Rad Laboratories, Inc., Canada). The keratin protein bands were stained using Coomassie Brilliant Blue G-250 (Alahyaribeik & Ullah, 2020). A marker of molecular weight (2 to 250 kDa) from a Bio-Rad standard low molecular weight calibration kit was used to identify the M.W. of keratin proteins.

2.3. Pre-treatment and Dissolution of Chicken Feathers

Broiler's white chicken feathers were supplied by the Poultry Research Centre, University of Alberta. First, the feathers were cleaned by several washing with anti-bacterial soap and hot water, followed by drying in a fuming hood for 4 days at room temperature. The residual moisture was removed by keeping the feathers in a ventilated oven overnight at 50 °C. The feathers were ground using Fritsch cutting Mill (Pulverisette 15, 0.25 mm, Laval Laboratory, Inc., Laval Canada) and sieved through 80 µm size mesh using laboratory brass wire mesh test sieve. Finally, lipids were removed from processed chicken feathers (50 g) with soxhlet apparatus using hexane as a solvent for 4 h. Further, the resulting ground feathers were dried and stored at room temperature for their modification into biosorbents for water purification.

Chicken feathers were dissolved using reported method with some modification (Arshad et al., 2016). The ground and sieved feathers (4 g) were taken in a round-bottomed flask containing distilled water (120 mL). In this mixture, EDTA (117 mg), tris-base (3.229 g), urea (31.8 g), and sodium sulfite (1.0 g) were added and stirred at a temperature of 90 °C for 48 h. The pH of the reaction mixture was kept at ~9.75 for protein dissolution and examined frequently during this

process. The solution was stirred for 2 days followed by sonication for 30 min to obtain the dissolved chicken feathers keratin.

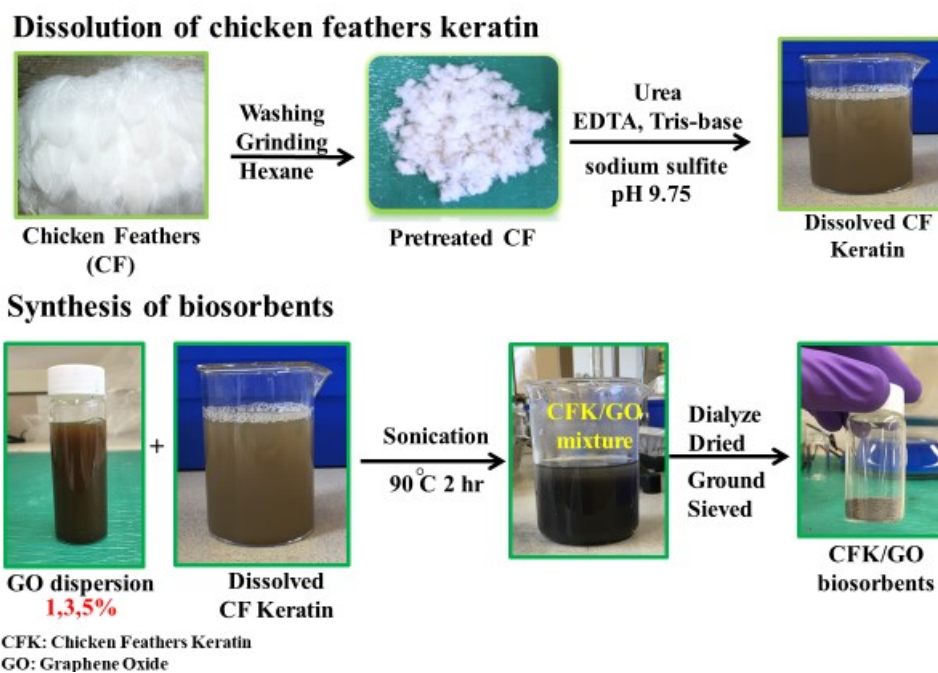
2.4. Preparation of Chicken Feathers Keratin-Graphene Oxide Derived Biosorbents

In the first study, modification of chicken feathers keratin with graphene oxide was carried out with the following procedure mentioned in 2.4.1. Firstly, graphene oxide was prepared and then introduced into the dissolved chicken feathers keratin solution. Both the graphene oxide and CFK-GO derived biosorbents are discussed in chapter three of the thesis.

2.4.1. Preparation of graphene oxide (GO)

Graphene oxide was prepared by the following procedure. A concentrated mixture of $\text{H}_2\text{SO}_4/\text{H}_3\text{PO}_4$ (100 ml: 20 ml, 5:1) was added to the graphite powder (2.5 g) with constant magnetic stirring, followed by adding potassium permanganate (12.5 g) slowly. The mixture was heated at 45 °C overnight with continuous stirring and color of the mixture was turned brown. The reaction mixture was cooled at room temperature and transferred into 300 ml ice cold water with 20 ml of H_2O_2 (30%). During the peroxide addition, bubbling and heating was observed, and the temperature of the mixture was reached up to 45 °C. The obtained yellow bright dispersion was kept at room temperature for sedimentation and neutralization (Marcano et al., 2010). The clear top layer of the graphene oxide dispersion was removed and GO was dispersed in 500 ml of HCl. The GO was washed with distilled water to eliminate acids and kept all night for freeze drying to get the solid GO.

Work Flow



Figures 2.1: Workflow for chicken feather keratin-graphene oxide derived biosorbents

2.4.2. Preparation of chicken feather keratin-graphene oxide derived biosorbents

A stock solution of graphene oxide in 45 ml of water with varying concentration of graphene oxide (1%, 3%, 5%) was prepared with the help of sonication for 30 min. Graphene oxide was added on weight percent basis into chicken feathers keratin solution with three concentrations (1%, 3% and 5%). This keratin-graphene oxide mixture was stirred for 30 min followed by 30 mins sonication. Then, keratin was precipitated at its isoelectric point (3.25–3.32) with 1M HCl solution. The precipitated modified keratin with graphene oxide were centrifuged (15 min, 5000 rpm) and washed with distilled water. The obtained chicken feathers keratin/graphene oxide biosorbent was then dried at 85 °C for 24 h in an oven, followed by grinding and sieving (mesh-80 μm) to obtain powdered biosorbent.

2.5. Preparation of Chicken Feathers Keratin-Nanochitosan Derived Biosorbents

In the second study, modification of chicken feathers keratin with nanochitosan was carried out with the procedure as mentioned in **2.5.1**. Firstly, nanochitosan was prepared and then cross-linked with the chicken feathers keratin. Both the nanochitosan and CFK-NC derived biosorbents are discussed in chapter four of the thesis.

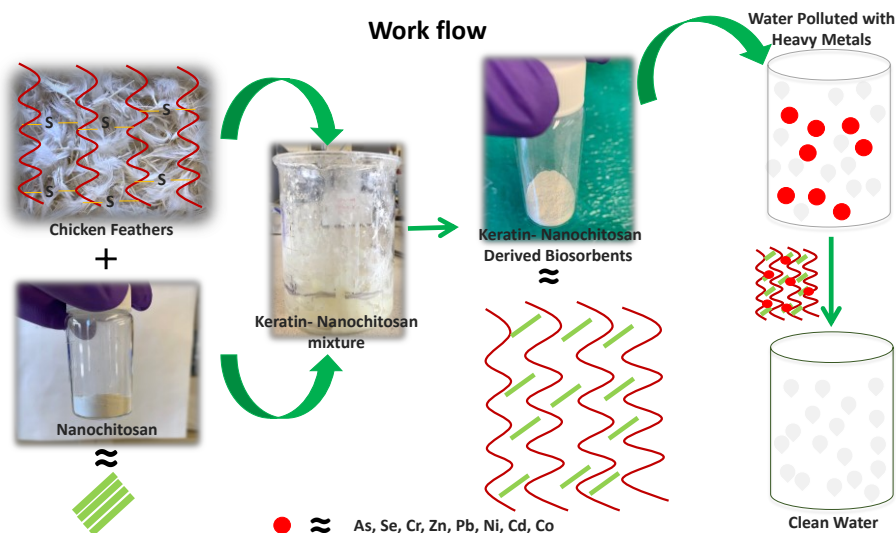
2.5.1. Preparation of nanochitosan

Chitosan nanoparticles were synthesized according to the procedure reported by Calvo et al. (Calvo et al., 1997) with some modifications based on the ionic gelation of chitosan solution with sodium tripolyphosphate (TPP) anions. 1.5 g of chitosan was first dissolved in 100 ml of 1 % acetic acid and stirred for 8 hours followed by sonication for 30 mins. 0.07 g of TPP was dissolved in a separate vial containing 70 ml distilled water. Then, the TPP solution was added dropwise to the chitosan solution until a ratio of 2:1 chitosan and TPP was achieved. This mixture was stirred for 8 hours followed by sonication for an hour and then centrifuged for 20 mins using 10,000 rpm. The supernatant was separated and nanochitosan precipitates were washed several times with distilled water and freeze-dried to obtain dry powders.

2.5.2. Preparation of keratin-nanochitosan based biosorbents

Nanochitosan particles (1%, 3%, 5%) on the weight percent basis of keratin were dispersed using a sonicator for 30 mins in 50 ml of distilled water. These dispersed nanochitosan solutions were added individually to the dissolved keratin and stirred for 30 mins, followed by 30 mins sonication. Then, the keratin-nanochitosan mixture was heated at 75 °C overnight. The mixture of modified keratin with nanochitosan was centrifuged (10 min, 3500 rpm) and washed several times with distilled water. Later, the keratin-nanochitosan biosorbents were dialyzed to remove the

unreacted materials. The chicken feathers keratin-nanochitosan derived biosorbents were then dried at 60 °C overnight in an oven. The dried biosorbents were ground and sieved through 80 µm brass mesh to obtain powdered biosorbents for further structural analysis and biosorption studies.



Figures 2.2: Workflow for chicken feather keratin-nanochitosan derived biosorbents

2.6. Preparation of Chicken Feathers Keratin-Nanochitosan Derived Biosorbents

In this study, graphene oxide was surface modified with acryl amide before grafting on the chicken feathers keratin mentioned in 2.6.1. The modification of graphene oxide with acryl amide was performed with the method mentioned below. Both the surface modified graphene oxide (SMGO) and CFK-SMGO derived biosorbents are characterized and their results are discussed in chapter five of the thesis.

2.6.1. Surface modification of graphene oxide

The acryl amide modified graphene oxide was obtained using Kumar's method with modifications (Kumar & Rani, 2015). 1 g of GO was dispersed into 100 ml of dimethyl formamide (DMF) using ultrasonication for an hour. Further, NaOH (0.9 g) was added and stirred for 60

minutes at room temperature. Subsequently, acryl amide (0.3 g) and hydroxy benzotriazole (HoBt) (8 mmol) were added to the reaction mixture, followed by the addition of N, N'-dicyclohexylcarbodiimide (DCC) (3.1 mmol) and the reaction mixture was stirred for 24 hours to complete the reaction. The surface modified graphene oxide was collected in powdered form by centrifugation and washed with DMF to eliminate the unreacted reagents. Later, water was used to remove the DMF from the product and dried at 65 °C overnight.

2.6.2. Preparation of keratin/ surface modified graphene oxide derived biosorbent

2 g of keratin was taken in a three-neck round bottom flask and 75mL of deionized water was added, followed by 6 mL of 2 M HCl to maintain the pH (~5–6) of the solution. The reaction mixture was stirred and purged for half an hour with nitrogen. Then 15 mg of potassium persulfate and 9 mg of sodium thiosulfate were poured into the reaction flask followed by 1 g acryl amide modified graphene oxide addition under inert conditions. Furthermore, the reaction mixture was stirred at 80 °C for 8 h and exposed to air for quenching. The mixture was filtered, and the product was thoroughly washed with distilled water to remove salts and the unreacted acryl amide modified graphene oxide. The product was dried at 65 °C overnight and used for metal biosorption studies.

2.7. Instrumentation

2.7.1 ATR-FTIR analysis

The changes in functional groups of the keratin proteins were assessed before and after modification with nanochitosan (NC), graphene oxide (GO), surface oxide graphene oxide (SMGO) with Bruker Optics ATR-FTIR (Esslingen, Germany). The spectrum of the neat keratin and its nanochitosan derived biosorbents were performed from 410-4000 cm^{-1} wavenumber. 16 scans of each sample were taken at 4 cm^{-1} resolution and averaged employing Bruker OPUS software 6.5 version. The instrument had a single-bound diamond ATR crystal, and the

background spectrum was performed with a clean ATR crystal before taking spectrum for each sample. To examine the spectrum's measurements and processing, Nicolet omnic software was used.

2.7.2. X-ray photoelectron spectroscopy

XPS (ULTRA spectrometer, Kratos Analytical, Manchester, U.K) was used to study the chemical bonding status of the neat and prepared biosorbents with NC, GO and SMGO. During chemical bonding analysis, monochromatic Al K α source with $h\nu = 1486.6$ eV and power of 140 W were applied while the pressure was less than 3×10^{-8} Pa in analytical chamber. The resolution of the instrument was set at 0.55 eV with a 400×700 μm analysis spot. For carbon high-resolution spectra, the analysis was performed at 20 eV and 0.1 eV step passed energy. The electron flood gun was applied for charge compensation purposes. Vision-2 software was employed to process the data and spectra were adjusted for Carbon 1s binding energy (B.E.) at 284.8 eV.

2.7.3. X-ray diffraction analysis

The X-Ray diffraction (XRD) patterns were obtained to determine the changes in crystallinity phases and % crystallinity differences between chicken feather keratin and its biosorbents using a Rigaku Ultima IV XRD unit with Cobalt radiation controlled at 38 kV and 38 mA. The samples were scanned from 5° - 40° (2θ) at a constant scanning rate of 2°min^{-1} with a 0.02 step size. Data interpretation was performed using JADE 9.6 software with the 2020 international centre for diffraction data (ICDD) database PDF 4+ and 2020-1 inorganic crystal structure databases (ICSD).

2.7.4. Scanning and transmission electron microscopies (SEM and TEM) analysis

Surface morphology and internal structural changes of the neat keratin were studied with SEM and TEM after incorporating NC, GO and SMGO. For SEM (FEI XL30, USA) analysis, the

instrument was operated at 20 kV. Neat keratin and its derived nanochitosan biosorbents were scattered onto the adhesive surface and coated with conductive gold.

TEM was employed to see the internal changes in neat keratin proteins due to its interactions developed with NC, GO and SMGO. TEM/STEM Morgagni 268 (Philips, Hillsboro, USA) instrument operated at 80 kV, equipped with Gatan Orius CCD camera. For the TEM analysis, suspension of the particles was prepared in water and a droplet of suspension was placed onto a copper-coated grid for imaging purposes.

2.7.5. Thermal behaviour studies

The thermal stability of the neat chicken feathers keratin and NC, GO and SMGO derived biosorbents was examined with a thermal analyzer (Q50, USA) instrument. Each sample was analyzed in a nitrogen atmosphere from 25-600 °C using a constant 10 °C/min heating rate.

Differential scanning calorimetry (DSC) measurements were performed to assess the biosorbents thermal behaviour with the help of 2920 Modulated DSC (TA Instrument, USA) in a nitrogen atmosphere from 25–300 °C at a constant heating rate of 5 °C per minute. The instrument was calibrated for heat flow and temperature using a sample of pure indium.

2.7.6. Surface area and pore size distribution analysis

Brunauer-Emmett-Teller (BET) analyzer was used to examine the surface area and pore size distributions of the neat chicken feather keratin and biosorbents containing NC, GO and SMGO. For the BET surface area, nitrogen adsorption/desorption isotherms were taken with liq. nitrogen at a temperature of 77 K. Specific weight of each sample was taken and outgassed for 3 hours at 70 °C under vacuum with nitrogen flow to remove the moisture from the sample before the analysis. Specific surface area was measured based on adsorption-desorption isotherms and the experimental data was processed by applying classic BET theory and non-local density functional theory model (NLDFT) method. NLDFT was further used for the determination of pore

size distributions (PSDs) and cumulative pore volume based on slit pore model. The porosity analysis particularly PSD of polymeric material is of utmost importance as it provides better insight to enhance the sorption capacity which can be measured from gas sorption isotherms at 77 K. Adsorption strength of the porous material is another factor which can be revealed using PDS as adsorption strength has inverse relationship to the pore size (Tagliavini et al., 2017). Non-local density functional theory (NLDFT) is a well-established model at molecular level for carbonaceous materials (Weber et al., 2010) and their pore size distribution. Chicken feathers keratin and its derived biosorbents pore size distribution was measured by NLDFT. Another important factor which determines sorption capacity of porous materials is pore volume. It was calculated from the total gas uptake at a given relative pressure using multipoint BET.

2.7.7. Dynamic light scattering (DLS)

The particle size of the prepared nanochitosan was determined using Malvern Zetasizer Nano-ZS, equipped with a 4.0 mW He-Ne laser which was operated at 633 nm wavelength and 173° scattering angle (Rampino et al., 2013). Nanochitosan samples were prepared at a concentration of 0.10 mg mL⁻¹ and measured in triplicate at 20 °C.

2.7.8. Inductively coupled plasma mass spectrometry (ICP-MS)

Biosorption studies were conducted with ICP-MS to assess the removal efficiencies of the developed biosorbents and compare them with the neat keratin. The biosorption performance of each sample was investigated with simulated laboratory synthetic wastewater. The contaminated water was synthesized using nano-pure water (18.2 MΩ cm; Barnstead, Thermo Scientific™). NaCl (0.02 M) and CaCl₂ (0.01 M) solutions were used to increase its ionic strength (*I*=0.05). Afterwards, this water was polluted with 8 metals up to 600 µg L⁻¹ and the pH was adjusted to 7.5 using NaOH to simulate the surface water pH. The following eight element solutions i.e., Ni^{II}, Co^{II}, Pb^{II}, Cd^{II}, Zn^{II}, As^{III}, Se^{VI} and Cr^{VI} metal(oid)s were used to test the biosorption efficiency of

the developed biosorbents. The precipitation of the metal cations and anion were also considered. Cd^{II} , Cr^{VI} , Ni^{II} , Zn^{II} and Co^{II} can be precipitated at pH of 11.0, 7, 10, 10.1 and 8.2, respectively while Pb^{II} is normally precipitated at pH between 8.0-8.5 (Kadirvelu & Namasivayam, 2000; Zainuddin et al., 2019).

In biosorption tests, 0.1 g of each keratin-nanochitosan biosorbents, neat keratin, and nanochitosan were put in the small tubes and 10 ml of laboratory simulated industrial wastewater was added to the metal (oid)s solutions. The mixture was placed on a reciprocating shaker for a day at room temperature ($\sim 20^\circ\text{C}$) to achieve the sorption process equilibrium. Later, biosorbents and metal(oid)s solutions were centrifuged while supernatants were removed and diluted for analysis using an inductively coupled plasma mass spectrometer (Perkin Elmer's Elan 6000). The results for each biosorbents performance were mentioned as the average of 3 values Each measurement was performed with blank, positive (metals contaminated water) and negative control (only biosorbent). **Table 2.1** shows the initial concentration of each metal ions in the contaminated water measured with ICP-MS.

Table 2.1: Initial concentration of trace metals before biosorption

	Co	Ni	Pb	Zn	Cd	As	Se	Cr
Initial	606.77	603.48	597.30	602.22	602.79	601.40	601.25	595.95
Concentration	(4.83)	(6.16)	(4.13)	(4.59)	(4.66)	(3.43)	(4.99)	(3.35)

Values given in parenthesis is standard deviation

2.8. Statistical Analysis

The R software 2020 was used for the sorption performance results and checked for the assumptions of homoscedasticity and normality by using Levene's and Shapiro–Wilk tests,

respectively (Team, 2019). Wherever it was necessary, the data were transformed ($\log+1$) before the analysis. We tested the influence of each biosorbent on the biosorption of each metal from the contaminated water among or within the study 1, 2 and 3 for statistical significance by ANOVA, followed by *post-hoc* pair-wise differences using Tukey's HSD test.

2.9. References

- Alahyaribeik, S., & Ullah, A. (2020). Methods of keratin extraction from poultry feathers and their effects on antioxidant activity of extracted keratin. *International Journal of Biological Macromolecules*, 148, 449-456.
- Arshad, M., Kaur, M., & Ullah, A. (2016). Green biocomposites from nanoengineered hybrid natural fiber and biopolymer. *ACS sustainable chemistry & engineering*, 4(3), 1785-1793.
- Calvo, P., Remunan-Lopez, C., Vila-Jato, J. L., & Alonso, M. (1997). Novel hydrophilic chitosan-polyethylene oxide nanoparticles as protein carriers. *Journal of applied polymer science*, 63(1), 125-132.
- Kadirvelu, K., & Namasivayam, C. (2000). Agricultural by-product as metal adsorbent: sorption of lead (II) from aqueous solution onto coirpith carbon. *Environmental technology*, 21(10), 1091-1097.
- Kumar, D., & Rani, S. (2015). Synthesis of amide functionalized graphene oxide for humidity sensing application. Proceedings of the 6th International Conference on Sensor Device Technologies and Applications (SENSORDEVICES'15),
- Marcano, D. C., Kosynkin, D. V., Berlin, J. M., Sinitskii, A., Sun, Z., Slesarev, A., Alemany, L. B., Lu, W., & Tour, J. M. (2010). Improved synthesis of graphene oxide. *ACS nano*, 4(8), 4806-4814.
- Pérez-Palacios, T., Ruiz, J., Martín, D., Muriel, E., & Antequera, T. (2008). Comparison of different methods for total lipid quantification in meat and meat products. *Food chemistry*, 110(4), 1025-1029.
- Rampino, A., Borgogna, M., Blasi, P., Bellich, B., & Cesàro, A. (2013). Chitosan nanoparticles: Preparation, size evolution and stability. *International journal of pharmaceutics*, 455(1-2), 219-228.
- Tagliavini, M., Engel, F., Weidler, P. G., Scherer, T., & Schäfer, A. I. (2017). Adsorption of steroid micropollutants on polymer-based spherical activated carbon (PBSAC). *Journal of hazardous materials*, 337, 126-137.
- Team, R. C. (2019). 2020. *R: A Language and Environment for Statistical Computing*. R Foundation for Statistical Computing, Vienna, Austria: Available at: <https://www.R-project.org/>. [Google Scholar].
- Weber, J., Schmidt, J., Thomas, A., & Böhlmann, W. (2010). Micropore analysis of polymer networks by gas sorption and ^{129}Xe NMR spectroscopy: toward a better understanding of intrinsic microporosity. *Langmuir*, 26(19), 15650-15656.
- William Horwitz, G. W. L., Jr. (2005). *Official Methods of Analysis* (18th ed.). AOAC International.
- Zainuddin, N. A., Mamat, T. A. R., Maarof, H. I., Puasa, S. W., & Yatim, S. R. M. (2019). Removal of nickel, zinc and copper from plating process industrial raw effluent via hydroxide precipitation versus sulphide precipitation. IOP Conference Series: Materials Science and Engineering,

CHAPTER 3: Nano-Modified Feather Keratin Derived Green and Sustainable Biosorbents for the Remediation of Heavy Metals from Synthetic Wastewater

3.1. Introduction

Water is one of the most precious resources on the planet earth and is the life source for all living organisms. The supply of clean water is a key to build sustainable community, environment and economy. However, scarcity of clean water is one of the most pressing challenges worldwide that is predicted to grow worse in the future as water demand continues to rise due to rapid growing world population, industrialization and greater energy needs (Shannon et al., 2010). Primarily, heavy metals discharge to water bodies has been increasing tremendously from industrial activities such as metal finishing and smelting, mining, oil and gas, paper, textile and agriculture. Arsenic alone has affected nearly 137 million people in 70 different countries. The Food and Agriculture Organization (FAO) of the United Nations estimated that annual global freshwater withdrawal is around 4000 km³ for human activities and more than 80% of the wastewater generated from this is released into the freshwater bodies without any adequate treatment. Overall, approximately 750 million people lack access to clean drinking water around the world (Motarjemi et al., 2013; Rojas & Horcajada, 2020).

Conventional techniques including reduction, co-precipitation, membrane filtration, ion exchange and adsorption are used for heavy metal removal from water. Among these methods, the adsorption is considered an effective processing method for the removal of both heavy metals and other major organic contaminants. The flexibility, high removing ability and recyclability for the adsorbent materials make adsorption widely applied treatment for water remediation. The most common adsorbents which have been used to treat wastewater include activated carbon, natural organic matter, and synthetic polymers. Activated carbon has been effective in adsorption of

organics or single type of metals under specific pH conditions but poor removal rates are observed for other target pollutants such as multi-metals. Synthetic polymers such as polyethylene terephthalate (PET), polyvinylidene difluoride (PVDF), polystyrenes, poly(ϵ -caprolactone) (PCL) and polyacrylamides (PAM) are mainly employed for the contaminants removal from the aqueous solutions (Thamer et al., 2021). These polymers are more effective in removal of organics compared to heavy metals. Secondly, they are completely non-degradable and not eco-friendly. Thus, it is pertinent to find and utilize affordable and environmentally benign materials to remove contaminants from industrial wastewaters. In this regard, natural biopolymers for the adsorption of contaminants are a sustainable and viable choice. The use of natural novel renewable carbon biomass, such as keratin (protein), for the remediation of the contaminated water can be a promising technology. Wool and hair keratin have already been used in some studies for removal of heavy metals such as chromium, cadmium, lead and copper (Badrelzaman et al., 2020; Saha, Zubair, et al., 2019; Thamer et al., 2021; Zhang et al., 2020). In recent times, our group and few other scientists (Al-Asheh et al., 2002; Gupta et al., 2006; Khosa & Ullah, 2014; Khosa et al., 2013; McGovern, 2000; Mittal, 2006; Zahara et al., 2021) also developed chicken feathers derived materials to remove heavy metal ions and organic dyes from contaminated/wastewaters owing to their greater surface area and presence of numerous reactive functional groups. The benefits of exploiting feather keratin as a biosorbent to other biopolymers are more naturally abundant and yet inexpensive bioresource (Zubair & Ullah, 2021). Chicken feathers are agricultural by-products and natural renewable bioresources of the fibrous protein, i.e., keratin. Globally, poultry industry generates around 40×10^9 kg chicken feathers every year. They have a few applications including their use as a feather meal and fertilizer, while majority of chicken feathers are either land filled or burnt and creates environmental pollution. Chicken feathers contain $\geq 90\%$ of natural keratin,

which has the potential as a biosorbent for heavy metal remediation. Protein based biosorbents are renewable and sustainable and have numerous benefits, including easy handling, excellent metal biosorption rates even at trace levels, nominal sludge production, and potential recyclability (Dodson et al., 2015; Liu & Huang, 2011; Tesfaye et al., 2017).

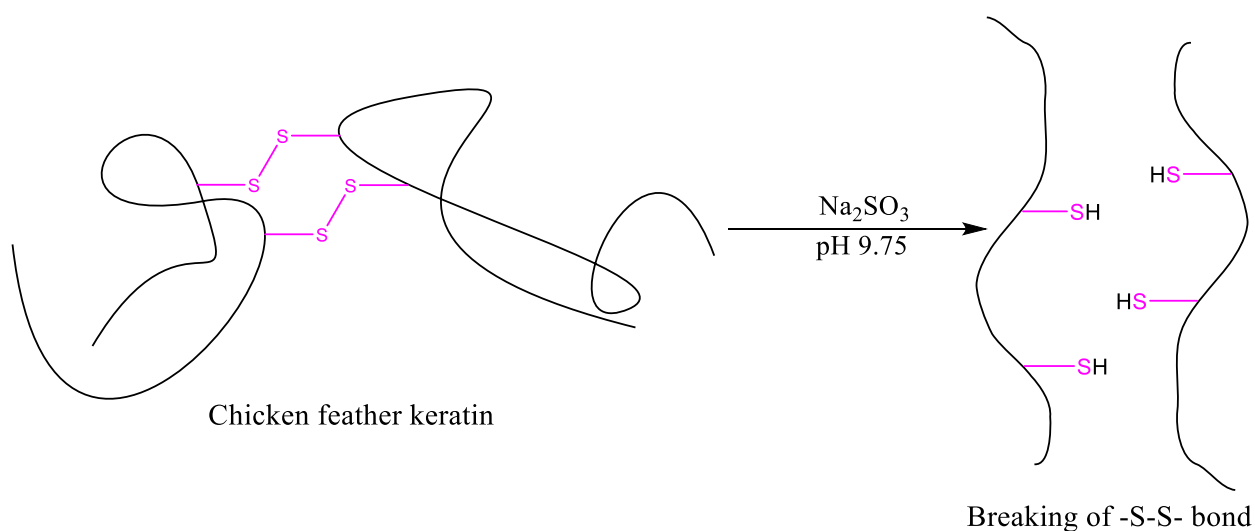
In this study, we developed a novel graphene oxide modified keratin biosorbent and investigated its potential for simultaneous removal of metal cations and oxyanions in a single treatment. The keratin biopolymer has specific side chains with unique chemical structure, bonding ability, and reactivity which determines the removal efficiency for certain contaminants (Saha, Arshad, et al., 2019). The surface affinity of the keratin towards contaminants can be enhanced by breaking cross-links in the native keratin, leading to unfolding and side chain exposure, which enhances the sorption of the pollutants. In this work, modification of keratin proteins with graphene oxide was proposed to enhance its biosorption efficiency. The graphene oxide has polar functional groups such as hydroxyl, carboxyl and epoxide (Zhu et al., 2010), which can interact with the side chains of the keratin and modify its biosorption efficiency by developing physiochemical interactions. To the best of our knowledge, no study reported so far where chicken feather keratin protein/graphene oxide has been used for the simultaneous removal of metal cations of Co, Ni, Zn, Pb and Cd and oxyanions of Cr, As and Se.

Chicken feathers keratin contains cysteine amino acid (8.83%) which oxidized to disulphide ($-S-S-$) linkage form cystine between the sulfhydryl ($-SH$) in keratin polypeptide chains. This crosslinking provides stability, strength, and stiffness to the keratin structure. However, by breaking these cross-links and modifying with nanoparticle such as graphene oxide is one of the feasible routes to increase their surface affinity for biosorption. The keratin protein has many amino acids with reactive groups such as $-SH$, $-COOH$, $-OH$, and $-NH_2$ present on

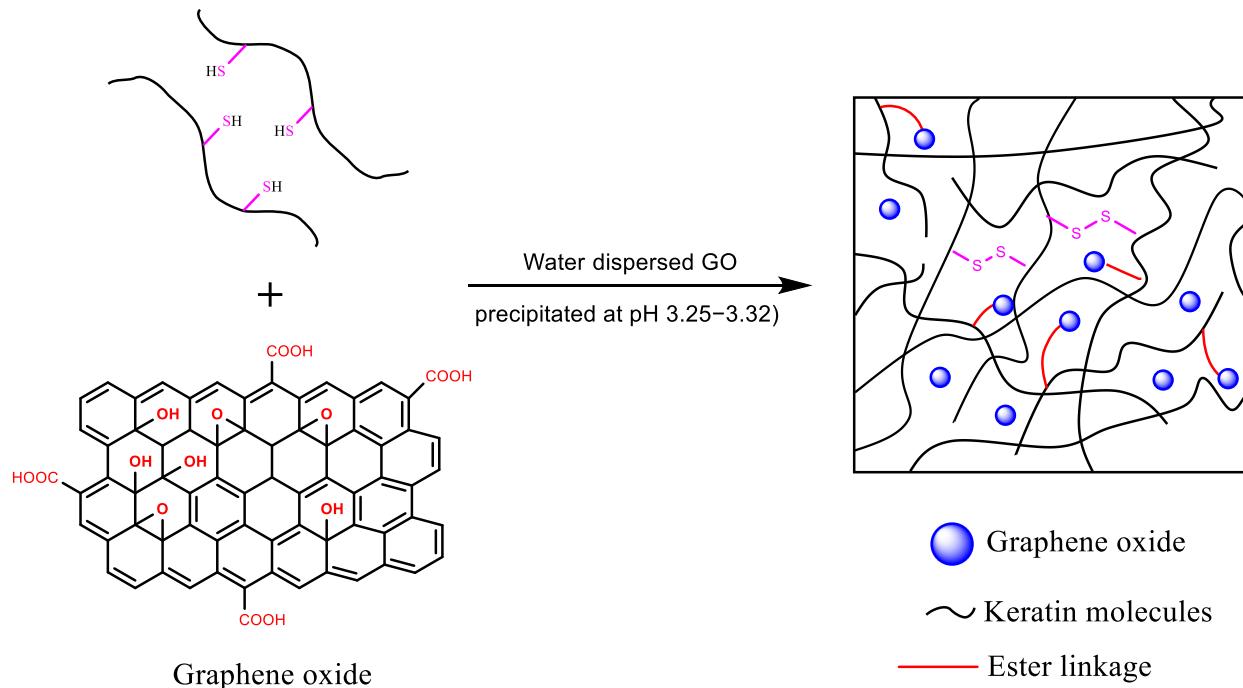
their side chains/inside the structure which can be exposed by the addition of graphene oxide to increase keratin biosorption performance. The keratin was nanomodified with graphene oxide and characterized by various techniques to study the effect of nanomodifications on its structural and biosorption properties.

In order to develop the biosorbents, disulfide crosslinks were broken down using reducing agents at 9.75 pH (slightly above pKa of SH group) shown in **Scheme 3.1. (a)**. The reduced chicken feather keratin was dissolved in the concentrated urea solution and treated with water dispersed graphene oxide followed by precipitation at its isoelectric point using hydrochloric acid as presented in **Scheme 3.1. (b)**.

(a) Dissolution of chicken feather keratin using reducing agent



(b) incorporation of graphene oxide into the keratin polymeric matrix



Scheme 3.1. Nano-modification of chicken feather keratin (CFK) with graphene oxide (GO)

3.3. Results & Discussions

Proximate analysis of the chicken feathers was performed as shown in **Table 3.1**. The results exhibited that keratin has high contents of keratin proteins (~ 94%) followed by moisture and fat contents.

Table 3.1: Proximate analysis of the chicken feathers

Quality Parameter	% (Wet basis)
Proteins	93.36±0.43
Moisture	3.94±0.21
Fats	2.23±0.03
Ash	0.38±0.02
Crude Fiber	Negligible amount

Results are presented as means ± standard deviations

3.3.1. Characterization of graphene oxide

3.3.1.1. Structural analysis

ATR-FTIR of pure graphite and graphene oxide was taken which is shown in **Fig. 3.1**. Graphite is not showing any signal in the FTIR spectrum because it doesn't contain any functional group. The graphene oxide shows typical hydroxyl peaks at around 3617, 3418, and 3166 cm^{-1} can be attributed to isolated hydroxyl groups, intercalated H_2O , and -COH within GO, respectively (Zangmeister, 2010). These peaks cannot be clearly defined due to the overlapping as shown in box. The peak at 1735 cm^{-1} is assigned to stretching vibration of C=O from carboxyl and while peak at 1614 cm^{-1} can be ascribed to in plane vibration (C=C) from unoxidized sp^2 C-C bonds of graphitic domain (El-Khodary et al., 2014). 1221 cm^{-1} due to in plane C-OH stretching vibrations (Paredes et al., 2008) while peak at 1054 cm^{-1} arises from epoxide groups (C-O-C) (Zhao et al., 2015).

ATR-FTIR of graphene oxide shows typical bands at 3350-3650 cm^{-1} , 1730 cm^{-1} , 1612 cm^{-1} , 1407 cm^{-1} , 1231 cm^{-1} which correspond to the presence of O-H, C=O stretching,

unoxidized sp^2 bonds, C=C bending vibration of OH in -COOH, and C-OH stretching, respectively (Marcano et al., 2010).

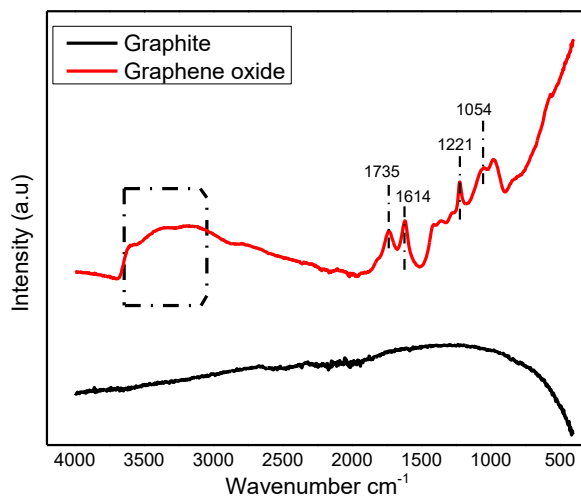


Figure 3.1:ATR-FTIR of graphite and graphene oxide

3.3.1.2. Crystallinity analysis

Fig. 3.2 shows the XRD patterns of pristine graphite and GO respectively. The crystalline peak in graphite at $2\Theta = 26.30^\circ$ corresponds to C-axis and reflections from (002) plane with interlayer spacing of 0.34 nm (El-Khodary et al., 2014). The spectra of graphite oxide (GO) showed a single and sharp diffraction peak at $2\Theta = 10.26^\circ$ ascribe to interlayer spacing of 0.83 nm, suggesting that the GO is lacking any graphite. The increase in d-value of GO is due to the increase of interlayer spacing along C-axis changes from 0.34 to 0.83 nm, due to the presence of oxygen atoms on the GO sheet (Zsirai et al., 2016). The appearance of diffraction peaks at 2Θ value of 10.8° and disappearance of 26° provides the evidence for the formation of graphene oxide sheets (GO) from graphite.

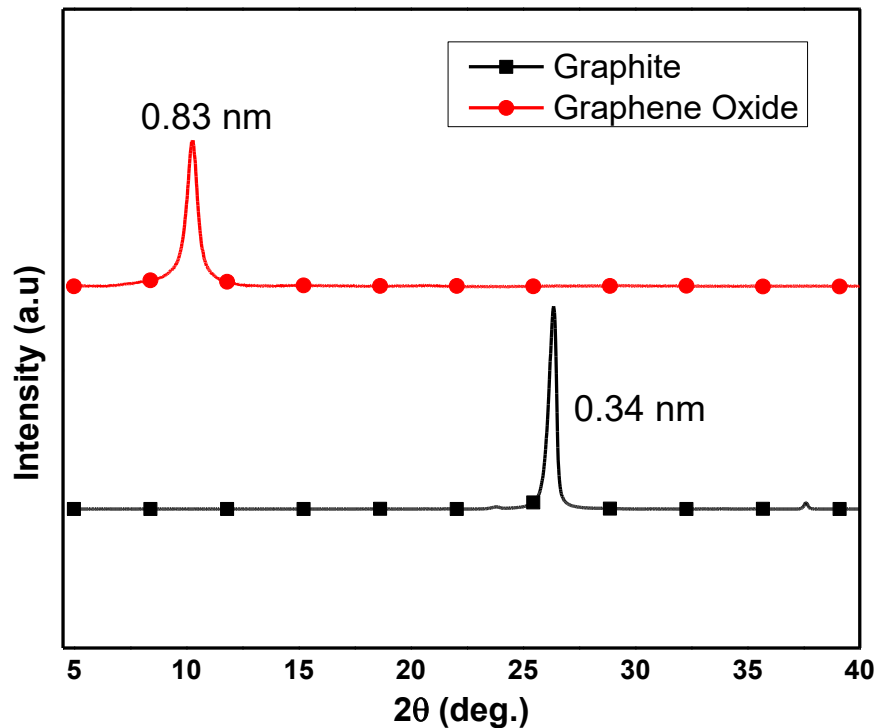


Figure 3.2 : XRD patterns of graphite and graphene oxide

3.3.1.3. Thermal properties analysis

Thermo-gravimetric analysis (TGA) of raw graphite and synthesized graphene oxide is shown in **Fig 3.3**. Graphite exhibits good stability up to 900 °C and graphite oxide (GO) is thermally unstable and loss weight in three stages. The first loss starts around 90 °C and ends around 120°C due to presence of moisture and evaporation of interstitial H₂O (Zangmeister, 2010) and the total mass was about 12%. The second stage decomposition is very sharp and is major weight loss (43%), occurred between 170–228 °C which belongs to decomposition of hydroxyl and carboxyl groups, and intercalated water release on the structure of GO. Thus, CO, CO₂ and steam released during this stage (Jeong et al., 2009; Marcano et al., 2010).

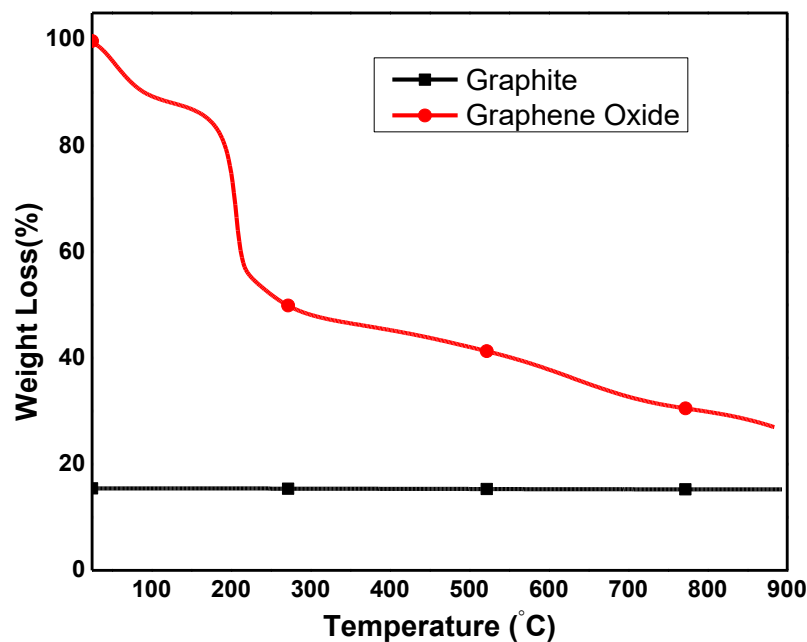


Figure 3.3: TGA of graphite and graphene oxide

As graphene oxide is highly oxidized and comprises 25–33% oxygen intercalated in a disordered cyclohexenyl matrix. The increasing of oxygen in GO to be 43% may be due to H_2O_2 , used as an oxidizing agent which increased the hydroxyl, carboxyl and carbonyl groups and other oxygen functional groups (Park et al., 2011). The third stage loss is slow and started from 350 °C up to 900 °C. This weight loss can be attributed to the decomposition of most stable oxygen functionalities such as carbonyl.

3.3.2. Structural analysis of biosorbents

The structural changes in the chicken feather keratin and biosorbents were assessed by ATR-FTIR as presented in **Fig.3.4**. It is clearly shown from the ATR-FTIR spectra of chicken feather keratin and its biosorbents have four major regions ascribed prominently to the peptide bonds (-CONH) and assigned as amide A, amide I, II and III regions. The amide regions provide

critical information related to protein conformation and backbone structure, mainly describing the protein's secondary structure i.e., α -helix and β -sheets. The first region labelled as amide A ($3282\text{-}3400\text{ cm}^{-1}$) belongs to O-H stretching and N-H stretching vibrations which are associated with the α -helix structure of the keratin proteins (Ma et al., 2016). **Fig.3.4** clearly shows that there is a significant increase in the intensity of this region in the case of graphene oxide incorporated chicken feather keratin based sorbents as compared to neat chicken feather keratin. This can be ascribed to the incorporation of graphene oxide into the keratin proteins. The presence of functional groups (-COO and -OH) on the basal planes of graphene oxide sheets establish electrostatic interaction with the polar groups of the proteins side chains, attributed to the greater number of hydrogen bonds in the chicken feather keratin derived biosorbents.

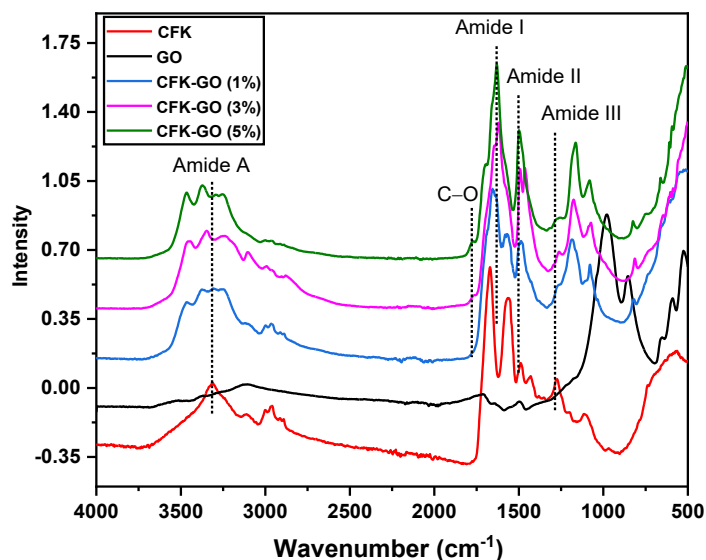


Figure 3.4: ATR-FTIR of graphene oxide, chicken feather keratin (CFK), CFK-GO (1%), CFK-GO (3%) and CFK-GO (5%)

The band at 2934 cm^{-1} is ascribed to the symmetrical CH_3 stretching vibration (Edwards et al., 1998). The strong absorption band at 1630 cm^{-1} belongs to $\text{C}=\text{O}$ stretching vibration which is directly related to the keratin proteins backbone conformation (Amide I) (Aluigi et al., 2007). In comparison, amide II band arises at 1509 cm^{-1} from in-plane N-H bending and C-N stretching vibration. However, this region shows much less sensitivity for the conformational structure of proteins than the amide I region. A weak band at 1235 cm^{-1} is recognized as amide III region that arises due to C-N stretching and N-H in plane bending with minor contribution from C-C stretching and C=O in plane bending vibration (Idris et al., 2013).

Secondary structure of proteins indicates regular repeated arrangements in the environment of neighboring amino acid residues in a polypeptide chain. It is attributed to the hydrogen bonding between the hydrogen of amide groups and carbonyl oxygens of the peptide backbone which provide secondary structures known as α -helices and β -sheets. Amide I region ($1700\text{-}1600\text{ cm}^{-1}$) typically belongs to $\text{C}=\text{O}$ stretching frequency and is determined by its spatial geometry and extent of hydrogen bonding (Aluigi et al., 2014). Nevertheless, most of the region is vague because of the extensive overlapping of the individual bands and even instrument cannot separate them. To resolve this issue, diagnostic tool i.e., second derivative is used to illustrate amide I individual band positions along with secondary structure of proteins. Since keratin protein is a complex biomolecule, overlapping of individual absorption bands resulted in broad absorption peaks. To differentiate the changes, second derivative infrared spectra were used. **Fig. 3.5** represents 2nd derivative FTIR of keratin and its derived biosorbents with varying concentration of graphene oxide (1, 3, 5%). The spectrum is represented on an offset scale for clarity. The second derivative gives direct separation of the amide I band into individual components and absorption bands. The original spectrum is revealed as negative bands in the second derivative spectrum.

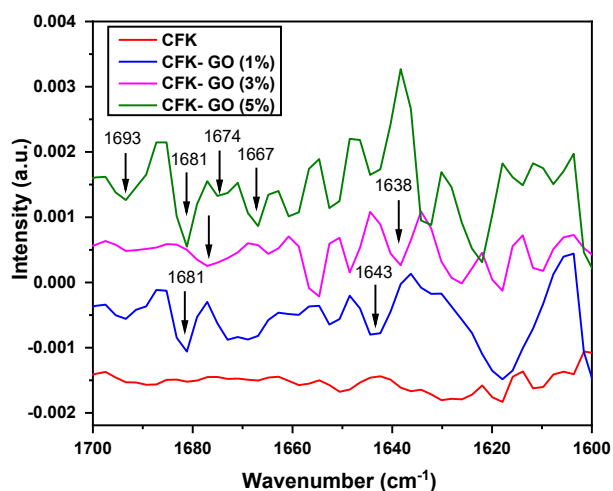


Figure 3.5: Amide I region 2nd derivative of chicken feather keratin (CFK), CFK-GO (1%), CFK-GO (3%) and CFK-GO (5%)

The most prominent individual absorption stretching bands demonstrated at 1693 and 1681 cm^{-1} can be assigned to antiparallel beta-sheet/ aggregated strands, 1667 cm^{-1} to 3_{10} - helix while 1652 cm^{-1} and 1654 cm^{-1} to α -helix of CFK-GO (3 and 5%), respectively (Ullah & Wu, 2013). The major absorption stretching bands at 1638 cm^{-1} and 1631 cm^{-1} were assigned to β -sheets structure for CFK-GO (3%) and CFK-GO (1,3%) respectively while a stretching band at 1618 cm^{-1} was attributed to the aggregated strands. Several new peaks are generated in the biosorbents. Two new peaks are observed in 2nd derivative of CFK- GO (3%) at 1648 and 1626 cm^{-1} which can be assigned to the α -helix and β -sheets, respectively. Peaks in CFK-GO (3%) at 1677 cm^{-1} while in CFK-GO (5%) at 1674 cm^{-1} corresponds to antiparallel β -sheet. Therefore, chicken feather keratin and its biosorbents possess various forms of secondary structures i.e., α -helix, β -sheets, aggregated strands and antiparallel β -sheets. However, the biosorbents mostly contain microstructures of α -helix and β -sheets as most of the new peaks are generated in these regions. These substantial changes in biosorbents suggested that the incorporation of graphene oxide provide higher number

of helices and β -sheets structures and create complex interactions with the keratin molecules (Ullah & Wu, 2013).

The chemical bonding status of the chicken feather keratin and its biosorbents was determined by high resolution Carbon 1s XPS spectra as presented in **Fig. 3.7**. The most distinctive band in ATR-FTIR spectra (**Fig. 3.4**) of biosorbents is around 1660 cm^{-1} corresponds to ester linkage. However, this band is very weak and cannot be observed in biosorbent containing 1% graphene oxide. XPS was used to confirm ester bond between the graphene oxide and chicken feather keratin. The high resolution C 1s spectra of keratin displayed three distinct peaks at 284.96, 285.94 and 288.87 eV binding energies after deconvoluting the peaks. These peaks are attributed to C-C/C-H, C-O / C-N and C = O / C-O-C bonds respectively which is consistent with the reported data (Kaur et al., 2018). However, the modified chicken feather keratin with graphene oxide exhibited an additional peak at around 289.05 eV binding energy which is not present in the neat chicken feather keratin. This peak is assigned to ester linkage (Arshad et al., 2016) confirming the modification of chicken feathers keratin with graphene oxide. This chemical bond is established between -OH group of serine amino acid present in the side chain of the keratin and carboxylic acid of the graphene oxide. Furthermore, intensities of the peaks in the biosorbents have been improved, at the same time a shift in binding energy can also be seen especially in case of C-O / C-N bonds binding energy. A peak identified at 285.94 in chicken feathers keratin has been shifted to 286.23 eV after modification with graphene oxide which confirms the changes in the substituent nature of the carbon or in its local environment.

This change in the environment is validated by the track of changes in amide II region of the ATR-FTIR spectrum (**Fig. 3.6**). The amide II region is greatly sensitive to the environment of N-H group. Generally, stronger hydrogen bonded N-H groups absorb at higher frequencies. As

compared to the chicken feather keratin, an increase in absorption intensity can be seen at 1515 cm^{-1} in case of chicken feather keratin derived biosorbents. This increase was most prominent in the case of CF- GO (5%) compared to CF- GO (3%) and CF- GO (1%) as sorbents, with maximum amount of graphene oxide (5%) could form stronger hydrogen bonds with polypeptide chains.

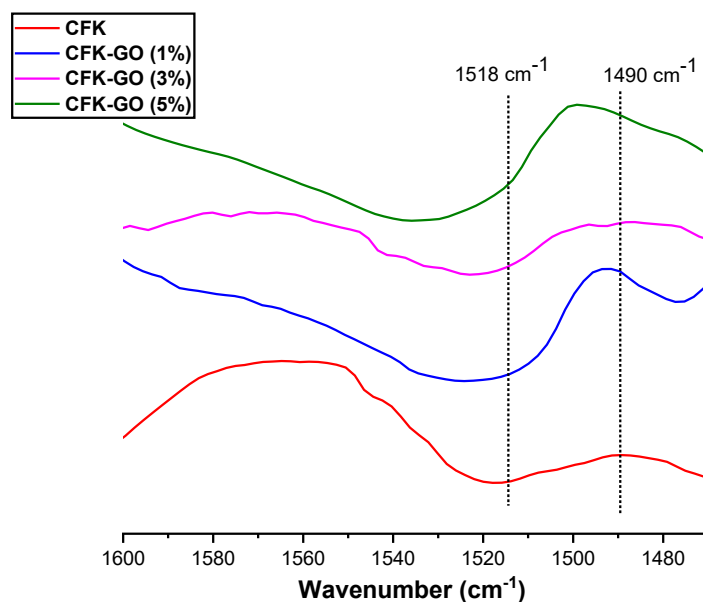


Figure 3.6: Amide II region of chicken feather keratin (CFK), CFK-GO (1%), CFK-GO (3%) and CFK-GO (5%)

As GO consists of hydroxyl and carboxyl groups which can form strong hydrogen bonds with polypeptide chains, while no such hydrogen bonding is present in neat chicken feather keratin. The variations in the absorption band in the amide II region are ascribed to the diffusion of graphene oxide sheets into the keratin chains that alters the proteins chains geometry and symmetry (Kumar & Parekh, 2020).

X- Ray diffraction (XRD) was used to determine the crystallinity patterns of the chicken feathers keratin and its sorbents as shown in **Fig. 3.8**. Chicken feather keratin had two broad peaks at about $2\theta = 9.66^\circ$ and 19.50° , corresponding to α -helix and β -sheet structure, respectively (Idris

et al., 2013; Khosa & Ullah, 2014). Whereas in derived biosorbents containing GO, these two broad peaks are shifted toward higher 2θ angle and the peak intensity of the peaks was lower than that of chicken feather keratin protein. This supports the idea of the ordering of α -helix and β -sheet structures, which resulted in higher the contents of these structures in the modified keratin chicken feathers derived biosorbents with GO.

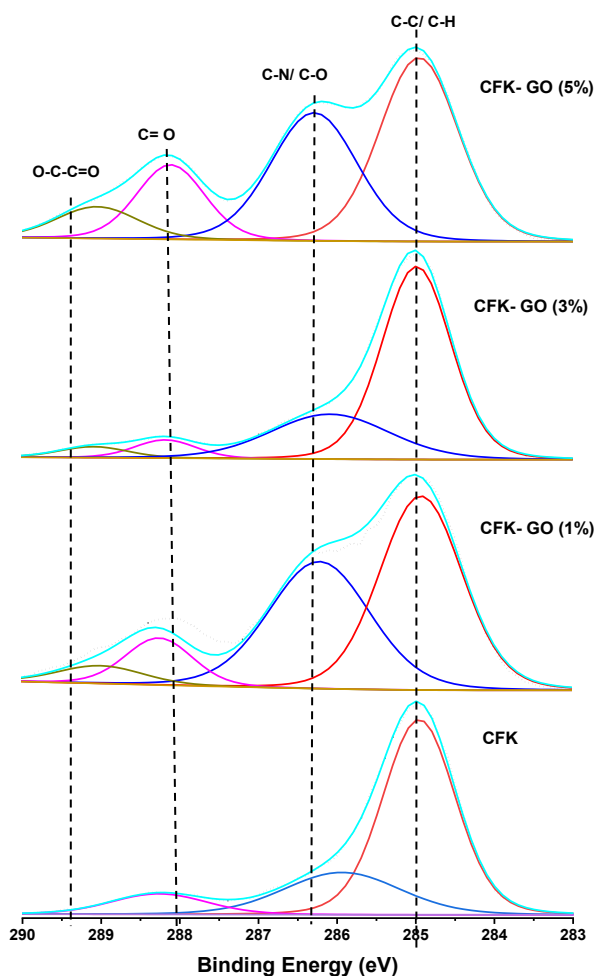


Figure 3.7: High Resolution Carbon 1s spectra of chicken feather keratin (CFK), CFK-GO (1%), CFK-GO (3%) and CFK-GO (5%)

The XRD peaks in the modified chicken feather keratin exhibited reduced intensity and a slight shift in values of 2θ for α -helix and β -sheet structures. In the case of feather keratin modified

with 5% graphene oxide, the peak belonging to the β -sheet structure split into two smaller peaks and shifted to higher 2θ values. The modification with 1% GO disrupts the α -helix and β -sheet structures more, which was evident from much-lowered intensities in comparison with 3 and 5% GO. Though, the intensity of α -helix is much lowered than β -sheet which indicated less gain of the α -helix structure after modification with 1% GO. The most evident difference in XRD pattern between CFK and derived biosorbents can be understood as new crystallinity peaks appeared between $2\theta = 27-37^\circ$ after chemical treatment with GO.

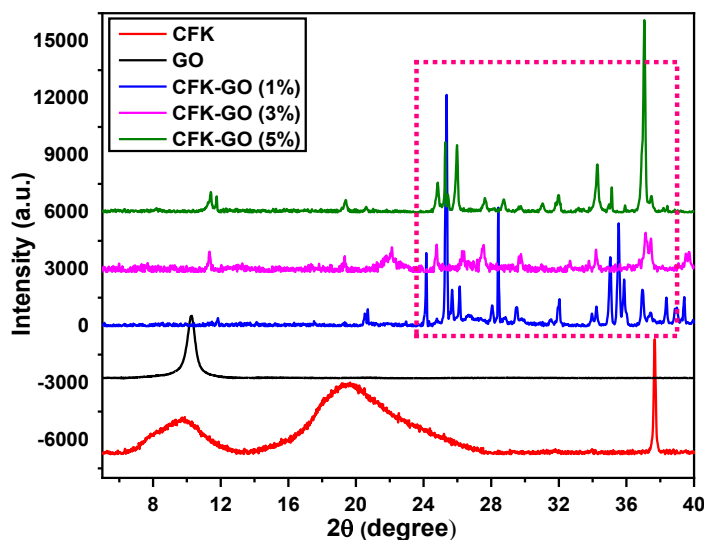


Figure 3.8: XRD patterns of GO, chicken feather keratin (CFK), CFK-GO (1%), CFK-GO (3%) and CFK-GO (5%)

It is recognized that keratin proteins are semi-crystalline in nature and established by their XRD profile which shows that the amorphous region in the keratin is increased after the incorporation of GO. The modification of chicken feather keratin with GO reduced its crystallinity from 60.2 to 22.5% (**Table 3.2**). Both the reducing agents and GO have affected the original crystal

structure of the keratin protein. However, the concentration of GO has a profound effect on the structural regeneration of keratin.

Table 3.2: % Crystallinity of chicken feather keratin and derived biosorbents

Sample codes	CFK	CFK-GO (1%)	CFK-GO (3%)	CFK-GO (5%)
Crystallinity (%)	60.2	51.6	44.7	22.5

It is well known that reducing agents destroy the secondary structure of the proteins during dissolution. Through modification of keratin with GO, the GO sheet structure and physical interactions with keratin can assist keratin biopolymeric chains to orient in parallel or folded form, limit their arrangements, and cause more crystalline β -sheet structure. As a result, the biopolymer is more ordered, where nanoparticle is dispersed much more evenly as seen in the case of 1% GO addition. This is consistent with the crystallinity data as CFK-GO (1%) has 51.6% crystallinity as compared to % crystallinity of 44.7 and 22.5 exhibited by CFK-GO 3% and 5%, respectively.

3.3.3. Thermal behavior of biosorbents

Thermal analysis was performed using TGA to obtain the information about the thermal stability and degradation pattern of the chicken feather keratin and its derived biosorbents. The TGA and derivative thermogravimetry (DTG) curves of CFK and its derived biosorbents shows the two and three-stage pattern of weight loss (**Fig. 3.9 a & b**). The first weight loss (6-7%) around 60 °C belongs to water evaporation present on the surface of the chicken feather keratin biopolymer.

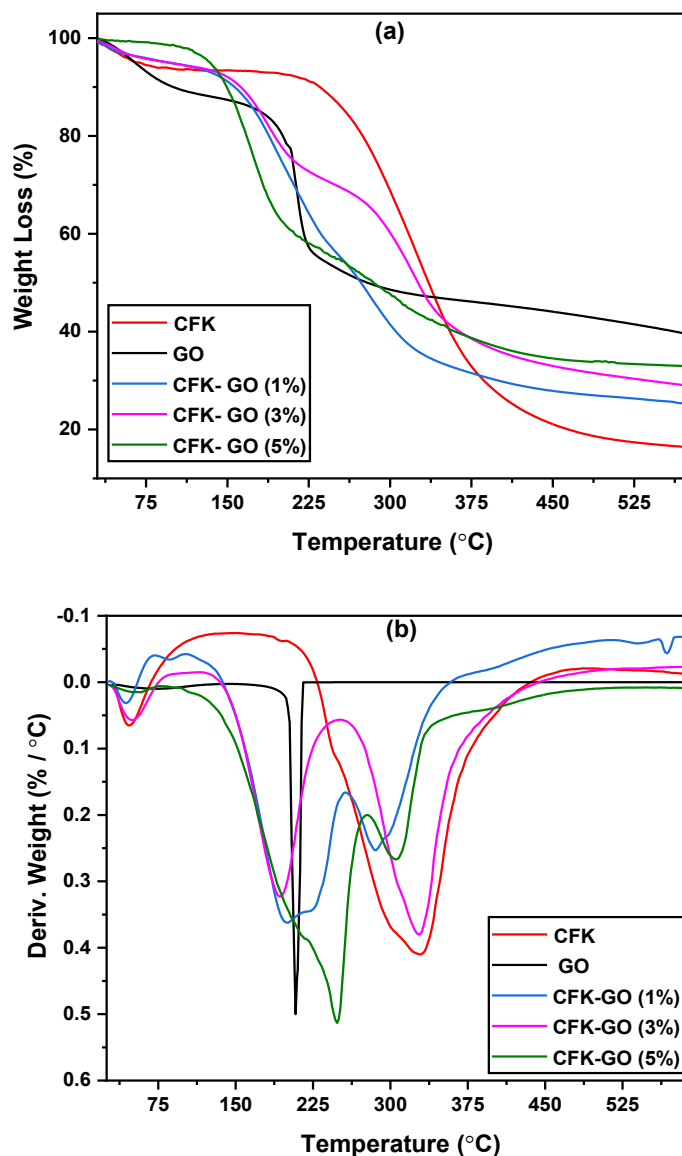


Figure 3.9: (a) TGA & (b) DTG curves GO, chicken feather keratin (CFK), CFK-GO (1%), CFK-GO (3%) and CFK-GO (5%)

For up to 200°C, CFK was thermally stable, following a sharp weight loss from 228 to 396 °C with a decrease reached up to 73%, ascribed to the helix structure denaturation, chain linkages, peptide bridges destruction, and degradation of skeletal structure. During this time, keratin was also decomposed into smaller products and several gaseous molecules. TGA curves of modified keratin with GO showed that the stability of keratin was increased tremendously by the addition

of graphene oxide (1,3 and 5%) into the polymer matrix of keratin proteins. The second stage weight loss of biosorbents belongs to decomposition of hydroxyl and carboxyl groups present on the graphene oxide rings and release as CO and CO₂. At 600 °C derived biosorbents has smaller weight loss and greater stability as compared to chicken feathers keratin. Among the biosorbents, CFK-GO (5%) showed maximum stability while CFK-GO (1%) is least stable among derived biosorbents. This reveals the modification of keratin with graphene oxide have impact on the thermal stability of keratin proteins.

The minimum of DTG profile displays the maximum weight loss at a specific temperature. The DTG curve (**Fig. 3.9b**) of chicken feathers keratin represents maximum weight loss at 326 °C up to 55% ascribed to decomposition of proteins. However, chicken feathers keratin derived biosorbents with graphene oxide exhibited two main weight losses, first between 195-248.35 °C which is absent in unmodified chicken feathers keratin. This confirms that thermal behavior of chicken feathers keratin was altered by the incorporation of graphene oxide. In case of CFK-GO (5%) displayed maximum weight loss in this temperature range as it comprises maximum concentration (%) of graphene oxide as compared to other biosorbents. The second DTG minimum is between 284 - 327.02°C belongs to degradation of chicken feather keratin but weight loss at this temperature is less for biosorbents CFK-GO (1 and 5%) as compared to CFK-GO (3%).

Differential Scanning Calorimetry (DSC) was used to study the phase behaviour of the CFK and derived biosorbents as shown in **Fig. 3.10**. DSC thermograms of the CFK shows 3 major peaks, first around 95 °C, corresponding to the evaporation of moisture, 2nd peak around 226 °C belongs to disordering or destruction of the secondary structure between protein macromolecules i.e., α -helix structure and this also designates as transition of melt. The third peak at 270–290 °C is characterized to the thermal degradation of the keratin macromolecular chains. In the case of

the keratin derived biosorbents, moisture loss was occurring at lower temperatures because of the presence of free water on protein surface, as the addition of GO into the polymer matrix replaces water. Besides, peak size is not broader in biosorbents, that was consistent with the XRD data, where loss in crystallinity was observed. The incorporation of GO partially disrupted the macromolecular keratin protein chains. It is well known that interactive forces are stronger in proteins β -sheets than helical structures, a similar pattern was observed here as CFK required more heat for thermal decomposition as compared to its derived biosorbents.

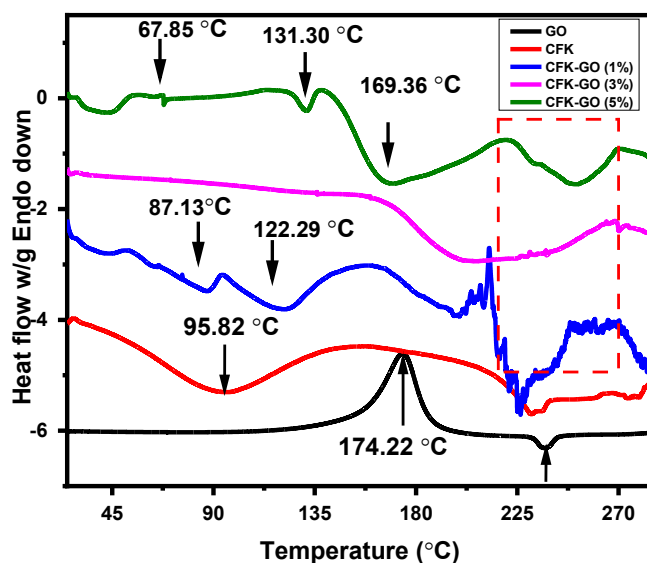


Figure 3.10: DSC heat flow signals GO, chicken feather keratin (CFK), CFK-GO (1%), CFK-GO (3%) and CFK-GO (5%)

3.3.4. Morphology and internal structure of biosorbents

Surface morphology and internal structure of the biosorbents are of utmost importance as they determine their biosorption performance. The variation in these features by the incorporation of GO into the feather keratin proteins were studied using scanning electron microscopy (SEM) and transmission electron microscopy (TEM).

Fig. 3.11 (a-d) shows the SEM images of the neat CFK proteins and its derived biosorbents. Neat CFK proteins exhibited long shafts, barbs as presented with arrow and smooth surface indicated with circle (**Fig. 3.11 a**). The addition of GO into the feather keratin resulted in ruptured/damaged surface as evident in **Fig. 3.11 b**. In addition, they have either rough surface morphology (**Fig. 3.11 c**) or shiny patches (encircled), which is ascribed to the presence of GO on the surface of the CFK. The incorporation of GO leads to intercalation and/or exfoliation of the native keratin biopolymer. Most interestingly, the original structure of CFK was lost, and the shaft were no longer identical (**Fig 3.11 d**); more amorphous regions were formed as corroborated with XRD data in which the crystallinity of CFK was reduced due to the dissolution and GO addition. From these images, it clearly shows that in some cases, GO caused the surface modification and feathers remained intact, while in others, they cracked their surfaces and penetrated the biopolymeric matrix of the keratin. In addition, **Fig. 3.11 e** clearly shows that biosorbents have many vacant pores and cavities after modification with graphene oxide. These structural variations may increase the contact area and activated sites for the metals biosorption.

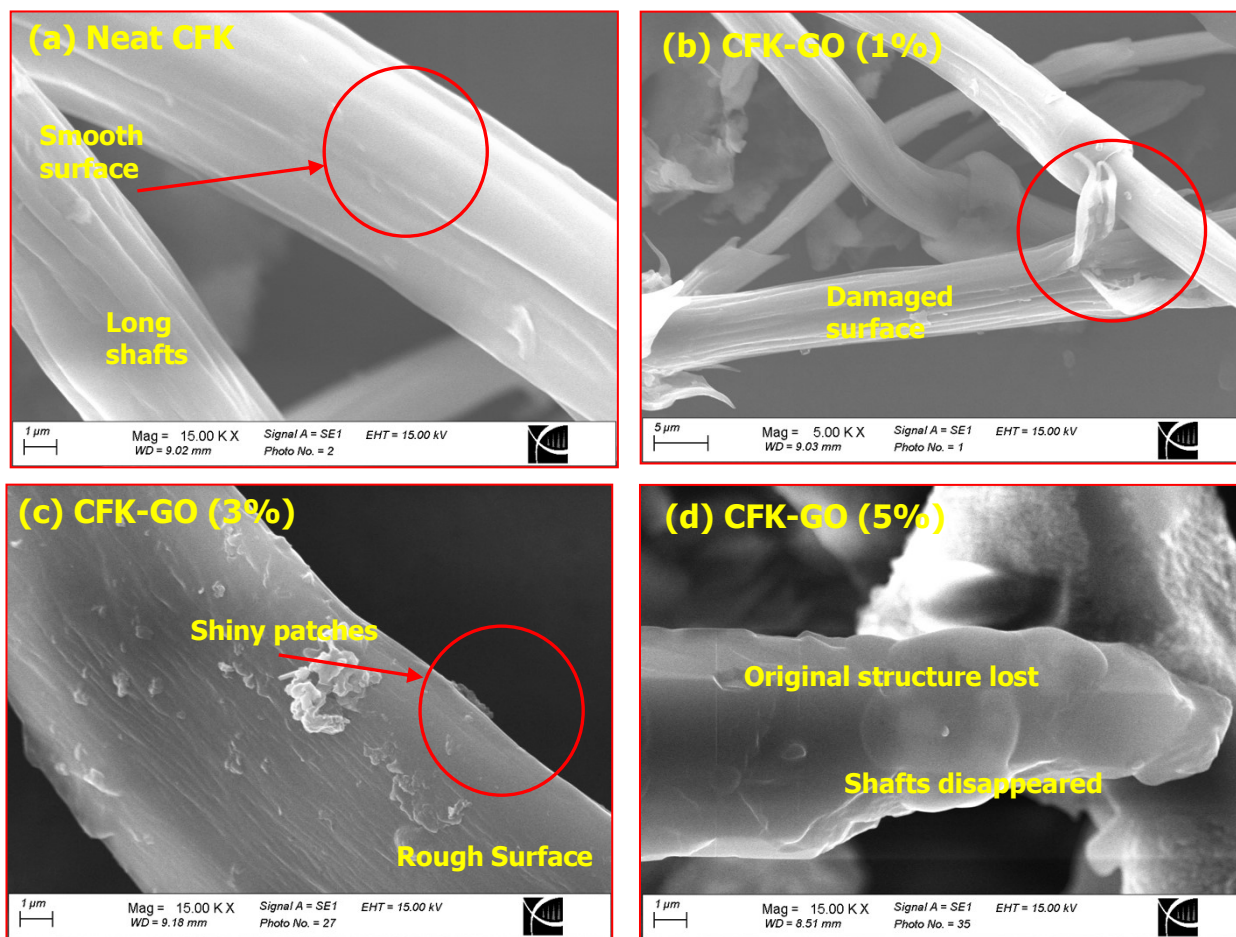


Figure 3.11: SEM images of (a) chicken feather keratin (CFK), (b) CFK-GO (1%), (c) CFK-GO (3%) and (d) CFK-GO (5%)

Fig. 3.12 shows the TEM micrograph of neat CFK proteins and GO derived biosorbents. The images (**Fig. 3.12 a-e**) of CFK/GO based biosorbents clearly show that GO was inserted into the keratin biopolymer layers which changed its internal structure. The dispersion of 1% GO into CFK was better than the other two biosorbents with 3 and 5% GO.

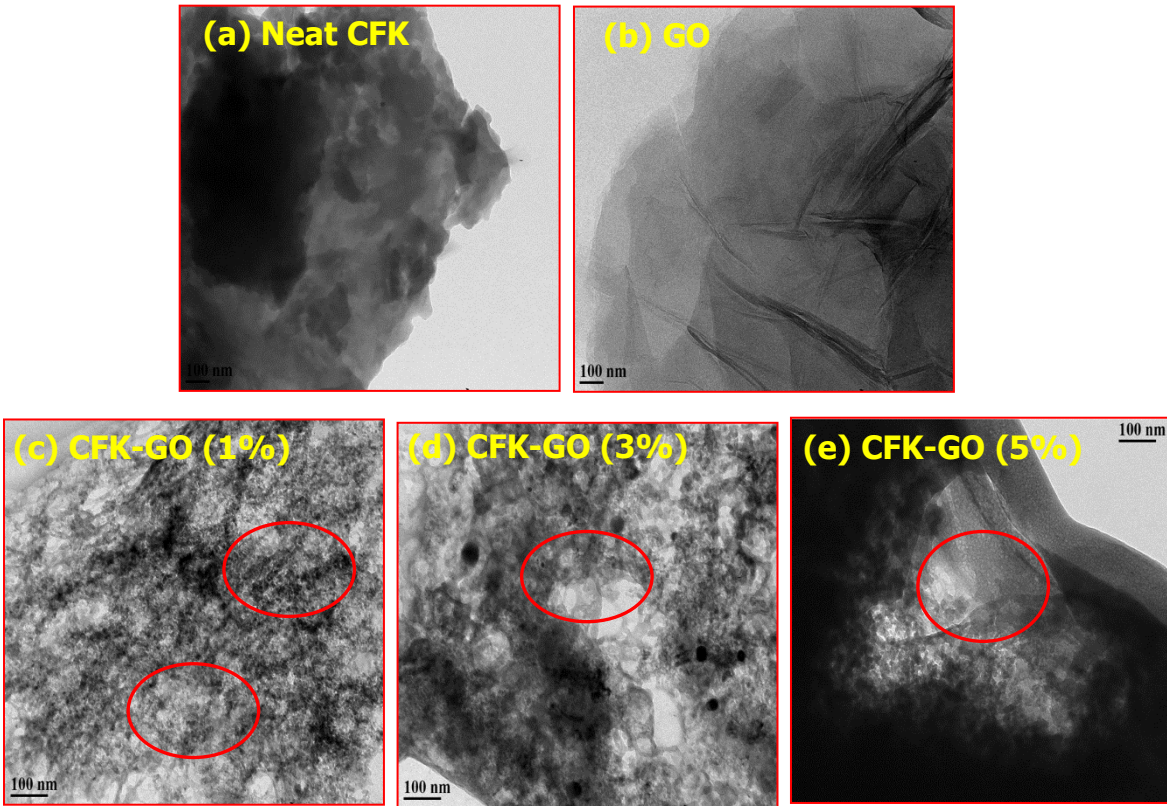


Figure 3.12: TEM micrographs of (a) graphene oxide (b) chicken feather keratin (CFK), (c) CFK-GO (1%), (d) CFK-GO (3%) and (e) CFK-GO (5%)

3.3.5. Surface area and pore size determination of biosorbents

The three critical parameters to determine the biosorption capacity of porous materials are pore size distribution (PSD), pore volume and surface area. These characteristics were measured using BET analysis and non-local density functional theory method (NLDFT) which are shown in **Fig. 3.13-3.14** and summarized in **Table 3.3**.

The polymeric material can be classified into microporous (widths < 2 nm) mesoporous (widths 2-50 nm) and macroporous (widths > 50 nm) materials, defined by the International Union of Pure and Applied Chemistry (IUPAC) (Thommes et al., 2015).

Table 3.3: BET and NLDFT results

Characteristics	CFK	CFK-GO (1%)	CFK-GO (3%)	CFK-GO (5%)
S_{BET} (m ² /g)	1.06	19.50	1.23	5.26
NLDFT Data				
Cumulative Pore Volume (cc/g)	3.60×10^{-4}	8.32×10^{-3}	7.50×10^{-4}	4.02×10^{-2}

Chicken feathers keratin and its derived biosorbents pore size distribution was measured by NLDFT and shown in **Fig. 3.13 (a-d)**. PSD of Chicken feathers keratin (**Fig. 3.13 a**) reveals that it has mesoporous structure with mostly pores located at 16.07 nm. The second and third maximum are around 28 and 32 nm belonging to larger size mesoporous regions however these PSD are much lesser as compared to primary maximum. **Fig. 3.13 (b-d)** represents the PSD of chicken feathers keratin derived biosorbents with graphene oxide, have primary maximum at 2.71, 3.22 and 6.31 nm for CFK-GO (1%), CFK-GO (3%), and CFK-GO (5%) respectively. The derived biosorbents have also mesoporous regions primarily, however the primary maximum in case of biosorbents is shifted more closer to the microporous region. This tremendous increase in the number of mesopores as compared to chicken feathers keratin ascribed to the presence of graphene oxide into polymeric chains which alter the pore geometries. Among derived biosorbents, primary maximum in CFK-GO (1%) showed least size of 2.71 nm in the mesoporous region and much closer to the microporous region. The other distinct maximum in this case is at 3.50 nm which is also near to the microporous region. While there is no such maximum observed in this region with other biosorbents. These maxima may contribute to better biosorption efficiency of CFK-GO (1%) for metals uptake in contrast to other biosorbents determined with ICP-MS and shown in **Fig. 3.15-3.16**.

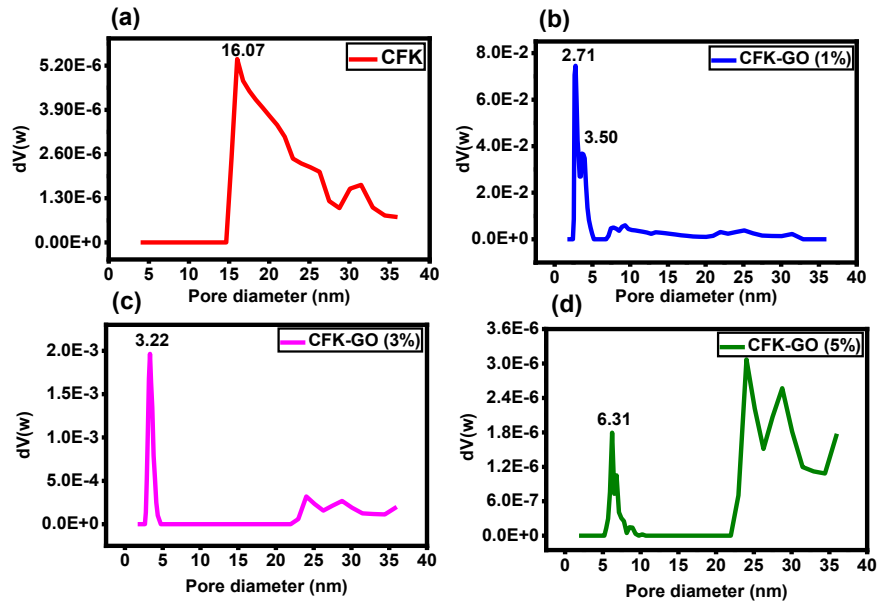


Figure 3.13: Pore size distribution (PSD) of (a) CFK (b) CFK-GO (1%) (c) CFK-GO (3%) (d) CFK-GO (5%) using non-linear density functional theory method (NLDFT)

From the graphs (Fig. 3.14), it is evident that the pore volume increases with an increase in relative pressure for chicken feathers keratin and its graphene oxide derived biosorbents. However, rise in CFK pore volume is rapid with an increase in relative pressure in comparison with its biosorbents. The other obvious difference of CFK graph is a decrease in pore volume after a maximum. While in case of biosorbents, no such decline in pore volume is observed. As can be seen from the biosorption performance graph, the biosorption efficiency of CFK is minimum as compared to its biosorbents. In the PSD graphs, chicken feather keratin derived biosorbents pore size distribution is more ranging from 2.71- 38 nm while in CFK pore size ranges from 16.07-38 nm. As the pore sizes increases, the contact points between the porous material and adsorbates increase and interactive forces on the surface overlap (Tagliavini et al., 2017) which possibly blocks the spaces within the material and the biosorption drops as seen in CFK.

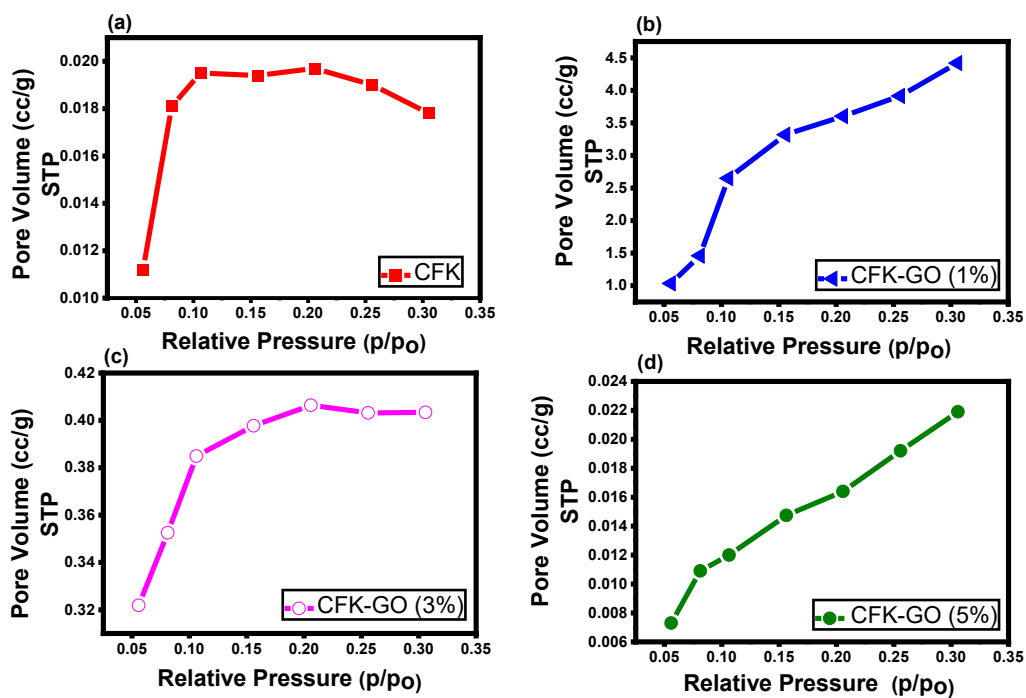


Figure 3.14: Pore volume calculated from nitrogen uptake at the given relative pressure (a) CFK (b) CFK-GO (1%) (c) CFK-GO (3%) (d) CFK-GO (5%) using multipoint BET

Another critical factor to assess adsorption performance of porous materials is their specific surface area. Commonly, BET method is employed to evaluate the specific surface area of the porous materials (assumes multilayer formation) based on nitrogen adsorption isotherm at 77 K. The specific surface area (amount of adsorbate per gram of adsorbent) of the porous materials is directly associated with their maximum sorption capacity (Tagliavini et al., 2017). Specific surface areas of the neat chicken feathers keratin and its derived biosorbents was measured using BET method and results are shown in **Table 3.3**. The specific surface area (amount of adsorbate per gram of adsorbent) of the porous materials is directly associated with their maximum sorption capacity (Mokhatab et al., 2019). The multi point BET surface area of chicken feathers keratin was (**Table 3.3**) 1.06 m²/g, however after modification with graphene oxide BET surface area of the chicken feather keratin was tremendously enhanced up to 19.50 m²/g. This increase in surface area

influenced the biosorption efficiency of the biosorbents in comparison with neat chicken feathers keratin as supported by their biosorption performance shown in **Fig. 3.13-3.14**. The CFK modified with 1% graphene oxide showed best biosorption efficiency among all 3 biosorbents which can be ascribed to its largest surface area ($19.50 \text{ m}^2/\text{g}$) among all. While CFK-GO (3%) and CFK-GO (5%) has surface area of 1.23 and $5.26 \text{ m}^2/\text{g}$ respectively.

Overall, compared to neat chicken feathers keratin, an increase in surface area and pore volume of the biosorbents were observed because of the incorporation of graphene oxide into chicken feathers keratin. This is corroborated with the % crystallinity data provide in **Table 3.1** of the chicken feathers keratin and its derived biosorbents. The crystallinity decreased by the graphene oxide addition into chicken feathers keratin and consequently crystallinity lost, leading to increase surface area and pore volume in case of biosorbents.

3.3.6. Biosorption performance

The biosorption affinities of synthesized biosorbents were tested for the removal of multi-metals having different speciation including oxy-anions (Cr, As, Se) and cations (Cd, Co, Ni, Pb, Zn) simultaneously from the synthetic contaminated water using ICP-MS. (**Fig. 3.15-3.16**). The biosorption capacities of CFK modified with GO were remarkably altered compared to neat chicken feather keratin. The better biosorption performance showed by the derived biosorbents for divalent cations (Co, Ni, Zn, Pb and Cd) and oxyanions (Cr, As, Se) is attributed to the structural changes, when CFK is modified with GO which are validated with ATR-FTIR, XPS, XRD, TGA results and surface characterization of CFK using SEM, TEM and BET.

The **Fig. 3.15** clearly shows that unmodified CFK exhibited lower biosorption capacities for the metals with the lowest removal efficiency of $\geq 16 \%$ for Cr (VI) and maximum of $\geq 70 \%$ for Se (VI). While the neat GO exhibited minimum ($\geq 25\%$) for As (III) and the highest ($\geq 70\%$)

for Co (II). All the modified CFK based biosorbents exhibited better removal efficiency than the neat CFK and GO. The modification of CFK with 1% graphene oxide presented the best biosorption efficiency for all metals oxy- anions and cations. However, overall biosorption efficiencies for the oxy-anions and metal cation are improved and better than the neat chicken feather keratin. This is ascribed to the presence of GO which interacted with the keratin polymer matrix and form ester linkages leading to intercalation or exfoliation of keratin biopolymer. As a result, molecular structure of keratin altered and may expose more anionic groups for biosorption. This is evident from increase in the biosorption efficiency of Cr (VI) from $\geq 16\%$ to $\geq 86\%$ by the addition of GO. Similarly, biosorption efficiency of As (III) and Se (VI) went up to $\geq 97\%$ and $\geq 99\%$, respectively.

In case of metal cations, CFK with 1% GO exhibited $\geq 99\%$, $\geq 92\%$, $\geq 91\%$, $\geq 88\%$ and $\geq 82\%$ for Ni (II), Co (II), Pb (II), Cd (II) and Zn (II) respectively. In comparison between CFK modified with 3 and 5% GO, the biosorbent with 5% exhibited better biosorption ability for the contaminants than the 3% GO. However, presence of more GO in the polymeric matrix of keratin in case of CFK-GO (5%). CFK contains multiple amino acids, and they have mainly amino, carboxylic, hydroxyl and thiol groups which are the active sites. The biosorption of the metal ions is determined by the complexation with these active sites. This can be explained with the Lewis acid and base concepts, where base provides electron pairs and acid take up the electrons. The metal cations are classified into hard and soft “Lewis” acids. Among analyzed cationic species, Pb^{2+} and Cd^{2+} are the soft acids while Ni^{2+} , Zn^{2+} and Co^{2+} have properties between hard and soft “Lewis” acids. Oxygen containing functional groups and aliphatic nitrogen groups present in keratin proteins are known as hard bases, aromatic nitrogen at border and sulfur containing groups as soft Lewis bases. This explains the binding of Ni^{2+} to aromatic nitrogen such as tryptophan, and Cd^{2+}

to thiol groups of the keratin proteins (KOCATÜRK & Bornova, 2008; Zahara et al., 2021). However, the selectivity order in aqueous media for Ni (II) > Co (II) is in accordance with the reducing order of ionic radii of these ions. However, sulfhydryl (-SH) groups have natural affinity to combine with the Se (VI) and As (III) (Shen et al., 2013), which makes competition in biosorption with the Pb^{2+} and Cd^{2+} ions.

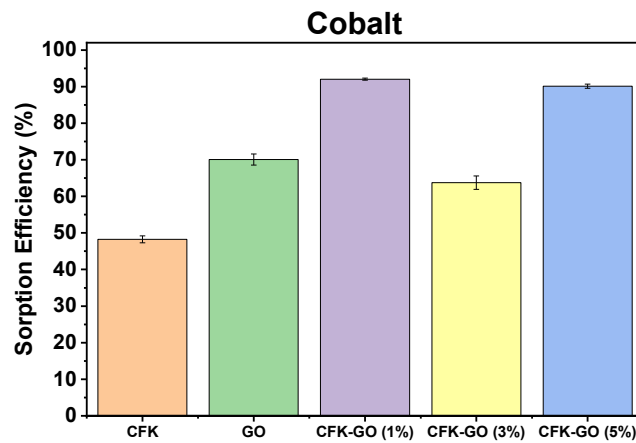
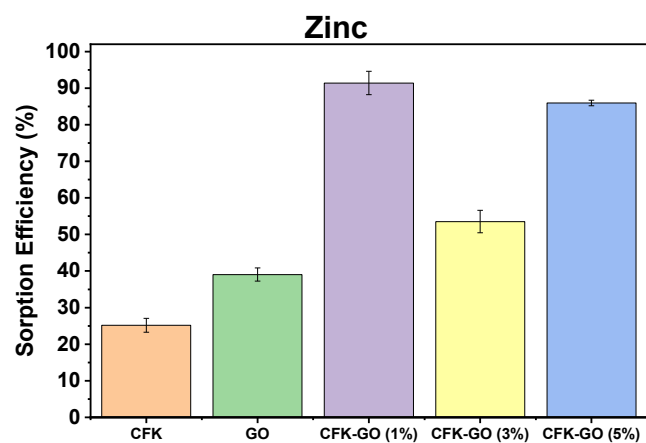
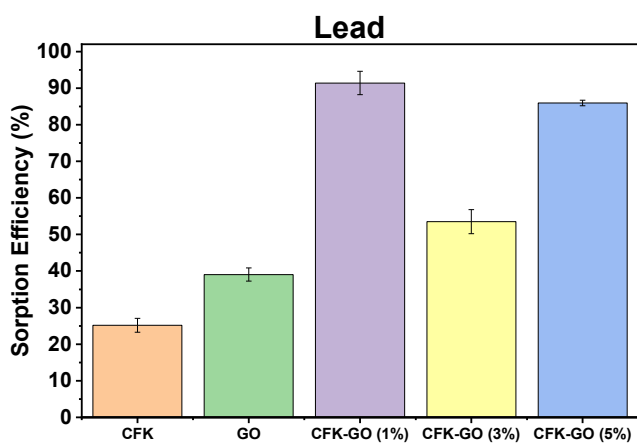
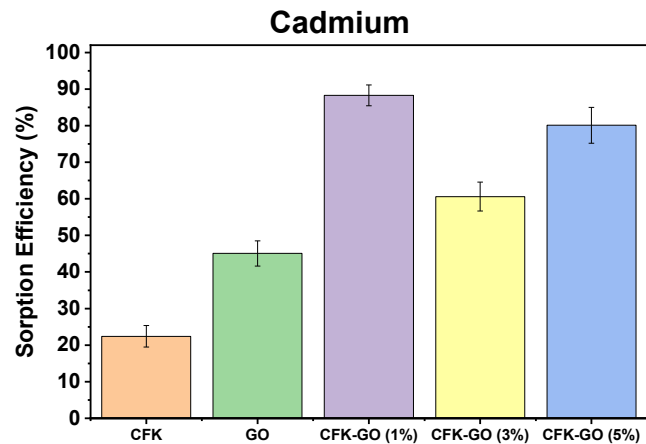
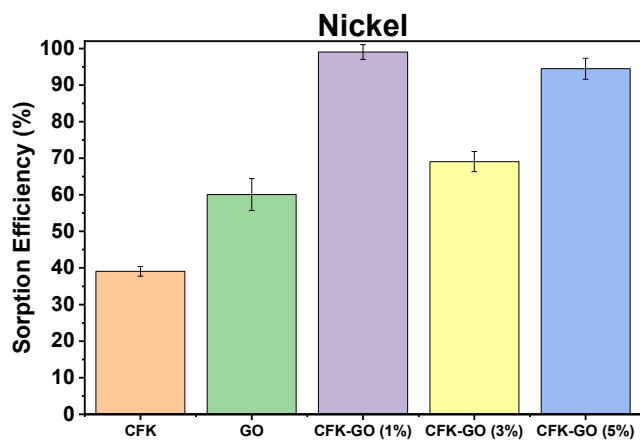


Figure 3.15: Biosorption efficiency of chicken feather keratin (CFK), graphene oxide (GO), CFK-GO (1%), CFK-GO (3%) and CFK-GO (5%) for metal cations (Ni, Cd, Pd, Zn, Co)

All biosorbents showed removal efficiency $\geq 99\%$ for Se, 95-97 % for As and 68-86 % for Cr. It is important to mention that all the biosorbent with 1 % GO incorporation exhibited better removal efficiency for the oxyanions Se and As, however biosorbent with 5% GO showed better biosorption than biosorbent having 3% GO. The biosorbent having 1% of GO exhibited the best results for the removal of metals among the developed biosorbents and showed ≥ 99 and 91% removal efficiency for Ni and Pb respectively.

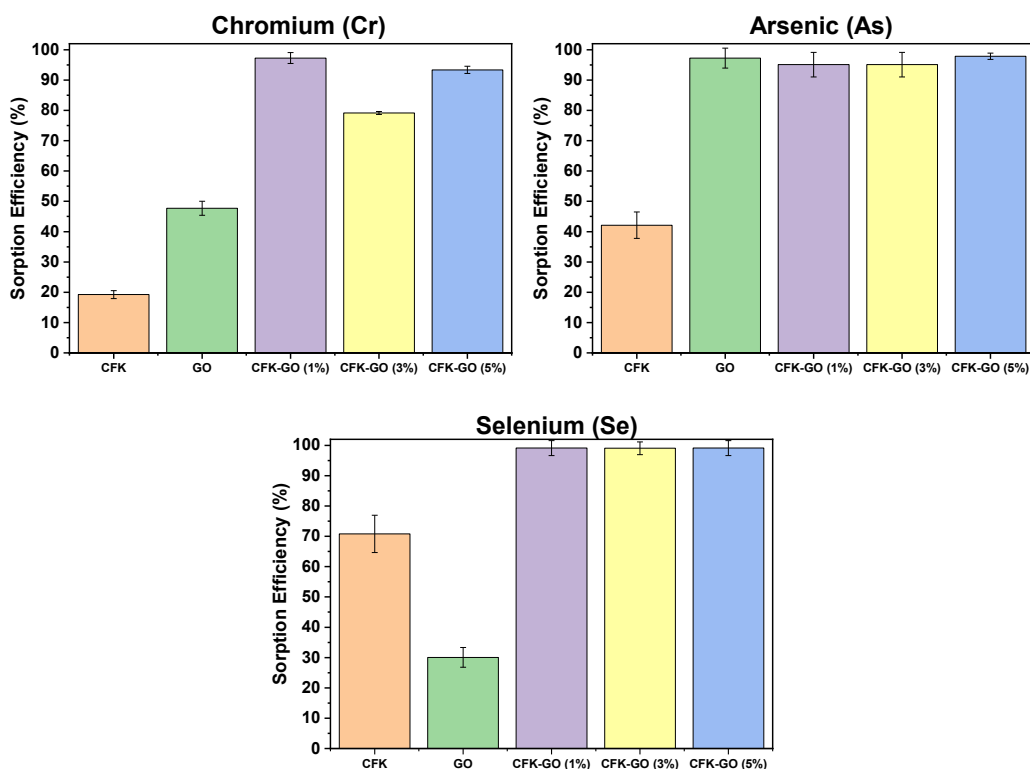


Figure 3.16: Biosorption efficiency of chicken feather keratin (CFK), graphene oxide (GO), CFK-GO (1%), CFK-GO (3%) and CFK-GO (5%) for oxyanions (Cr, As, Se)

The removal of Cr (VI) oxyanionic species (CrO_4^{2-}) at neutral pH from water using CFK is ascribed to biosorption on the proteins via electrostatic interaction, followed by reduction due to the presence thiol, amine, and carboxyl groups on the protein exposed surface and converted

into Cr (III) hydroxide form and chelation with the free amino groups. These phenomena explain the biosorption mechanism for chromium on the keratin protein surface (Misra et al., 2001; Park et al., 2007). All CFK derived biosorbents exhibited excellent affinity for the removal of As^{III} and Se^{VI}. It is generally believed that arsenic biosorption through keratin biopolymer involves an ion-exchange phenomenon in which arsenic oxyanions have a tendency to approach positively charged active sites of the biosorbent (Khosa et al., 2013).

These claims are corroborated with the variations observed by FTIR and XRD analysis. The XRD data showed that GO greatly changed the α -helix and β -sheet structures as well as degree of crystallinity of the derived biosorbents, which caused the changes in the surface morphology of the keratin proteins. These structural changes may attribute to the greater biosorption properties of biosorbents in this study. Overall, the surface structure of the chicken feather keratin was substantially altered as it turned into bright, rough, and heterogeneous. All these changes observed in SEM images shows the characteristics of increased surface activity of CFK, which may have contributed to the greater biosorption efficiency of the biosorbents. Hence, modification of CFK with GO attributed to the increased biopolymer-GO interactions and decreased protein-proteins biopolymer chain interactions. As a result, more biosorption sites on the keratin protein matrix were exposed resulting in greater biosorption towards heavy metal ions.

3.3.7. Mechanistic insights of biosorption

Mechanistic insights of metal biosorption plays vital role to tune the biosorption properties of the biosorbents. To investigate the possible mechanisms for the uptake of metals, we characterized the CFK and its biosorbent with the highest biosorption performance using SEM, XRD, TGA, XPS and FTIR.

The process for heavy metal biosorption through biopolymeric materials is a complex phenomenon. The interaction mechanism of keratin with metals depends on the nature of various functional groups present in the backbone and side chains. Amino and carboxyl groups are mostly considered as the most reactive sites for metal biosorption. At a neutral or weakly acidic pH, lone pairs of nitrogen behave as a binding site for metal cations. In the case of highly acidic atmosphere, protonation of protein amino groups occurs, making them cations, which then interact with the metal anions. Generally, proteins adsorb the metals through electrostatic forces or chelation/complexation, hydrogen bonding, ion exchange, and Van der Waals forces (Peydayesh & Mezzenga, 2021; Rodzik et al., 2020; Saha, Zubair, et al., 2019).

SEM images of the neat chicken feathers keratin and its derived biosorbent surfaces were taken to see the changes after metals biosorption. Rough, coarse, and uneven surfaces were observed for CFK (**Fig. 3.17 a-d**) and its biosorbents (**Fig. 3.17 e-h**) after biosorption. Irregular cluster of metals are attached on the CFK surface (**Fig. 3.16 a-c**) and entangled around the protein's layers (**Fig. 3.17 a**). In addition, caves, pores, and surfaces of the CFK (**Fig. 3.17 b**) as well as biosorbents (**Fig. 3.17 e**) are covered with the (bright spots encircled in red) metal cations and anions. The structural changes were observed in the chicken feather keratin after biosorption and its long shafts (**Fig. 3.17 a-d**) were transformed into spindle fiber (**Fig. 3.17 e**) and in the form of stacked layers (**Fig. 3.17 f-g**).

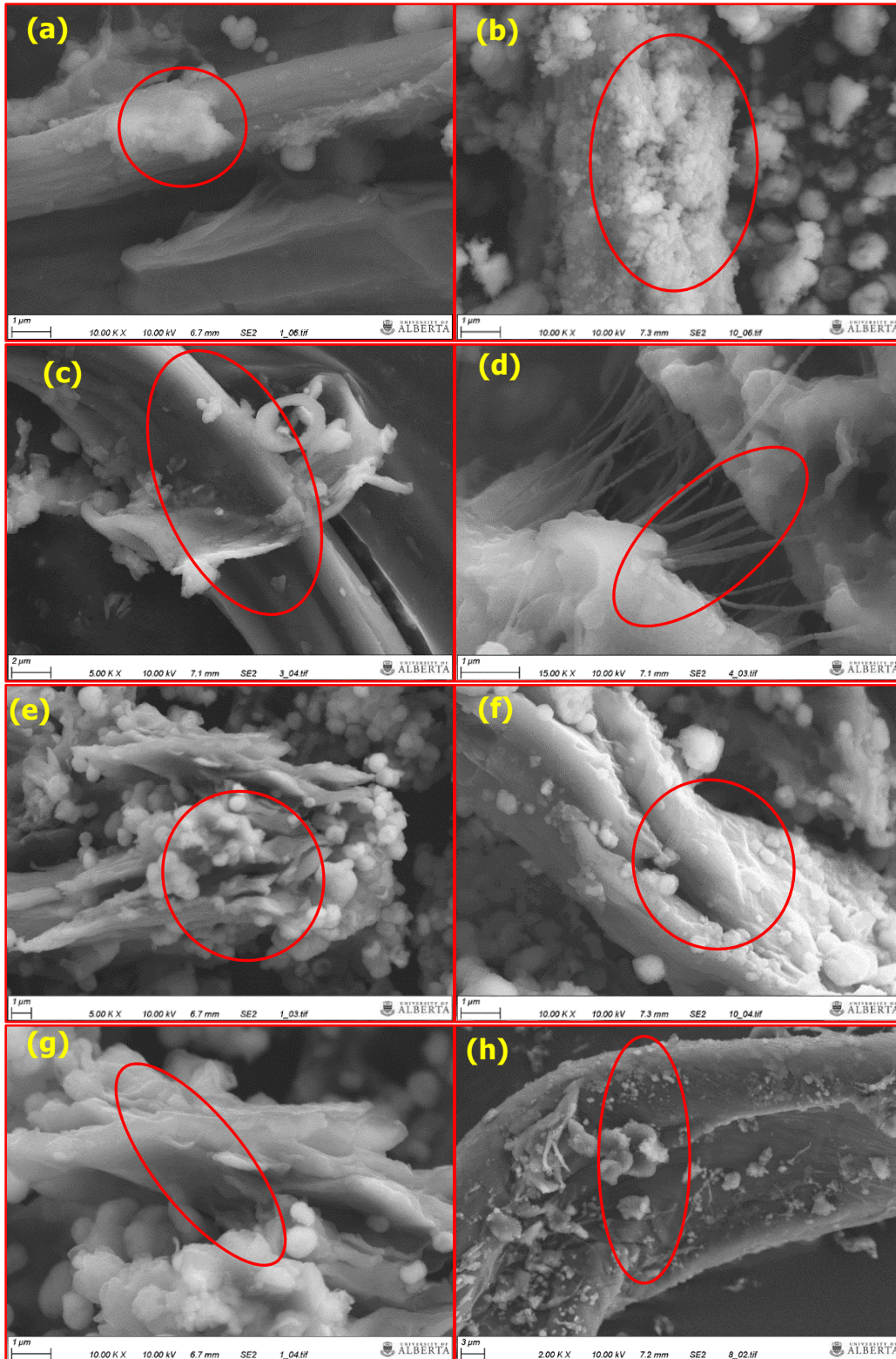


Figure 3.17: SEM images of (a-d) chicken feather keratin (CFK) and (e-h) biosorbents after biosorption

After biosorption, thermal stability of CFK and biosorbents were improved and showed lower decomposition rate, indicated a complexation between metals and proteins, as displayed in **Fig. 3.18** TG curves. The XRD patterns of the CFK and derived biosorbents after the biosorption showed broad peaks and shifting towards lower 2θ revealed an amorphous structure (**Fig. 3.19**). This is attributed to the dominant mechanism of chelation and electrostatic interactions (Kyzas et al., 2014). It is also evident that no new diffraction peaks were observed after the metal biosorption indicating more of a physisorption phenomenon compared to chemisorption.

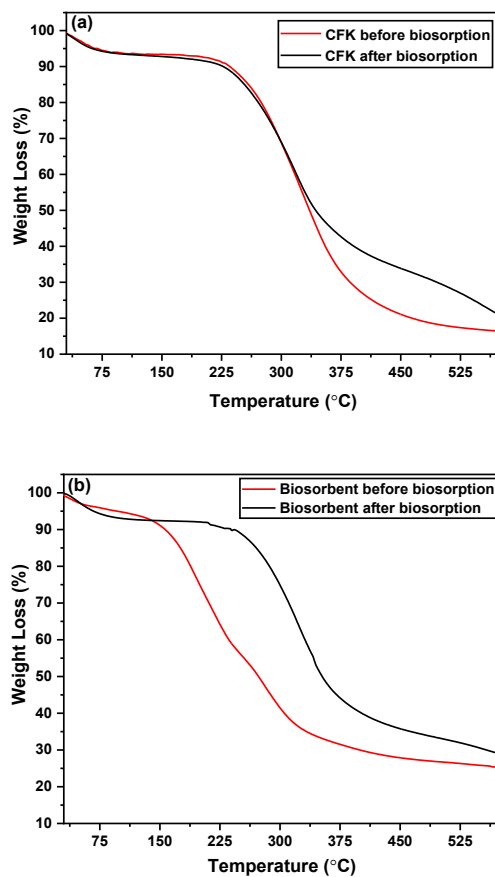


Figure 3.18: TGA curves of (a) chicken feather keratin (CFK) before biosorption (red) and after biosorption (black) (b) chicken feather keratin derived biosorbent before biosorption (red) and after biosorption (black)

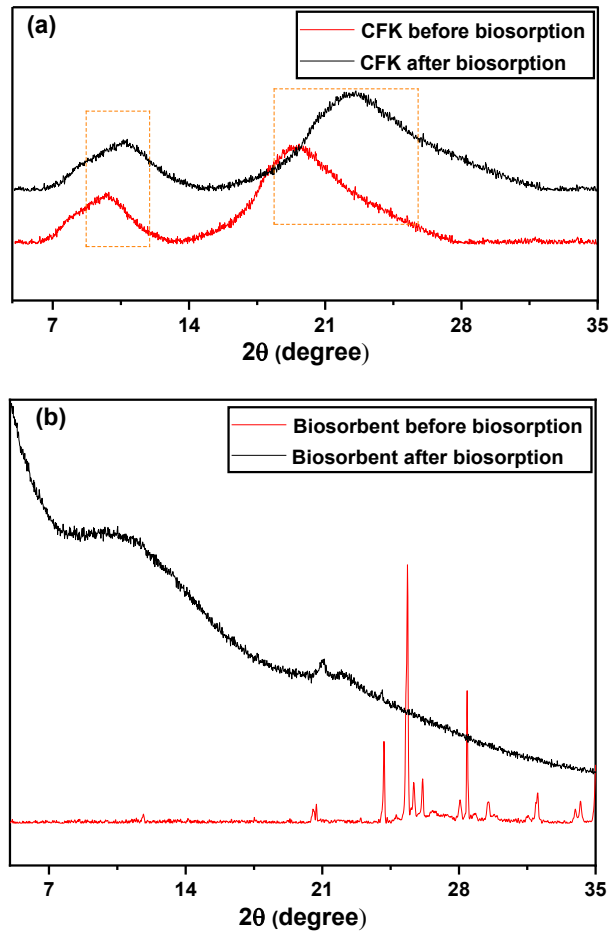


Figure 3.19: XRD patterns of (a) chicken feather keratin (CFK) before biosorption (red) and after biosorption (black) (b) chicken feather keratin derived biosorbent before biosorption (red) and after biosorption (black)

FTIR spectra (as shown in **Fig. 3.20**) were normalized to see the intensity differences of peaks before and after metal's biosorption. It clearly shows that peak in the $3200\text{-}3400\text{ cm}^{-1}$ region was broad after biosorption, that reveals the -NH_2 and -OH groups may involve in the metal removal process. There is possibility of protonation of both groups, which can remove anionic species via electrostatic interactions. (Jiang et al., 2013) On the other hand, this can be contributed

by the bond formation between lone pair of nitrogen and metal cations (Kyzas et al., 2014). The amide band II band (N-H bending and C-H stretching) shifted to 1526 cm^{-1} from 1509 cm^{-1} along with tremendous increase in the intensity. This region is very sensitive to the environment of N-H group ascribed to metals biosorption at the proteins side chains which in turn altered the surrounding environment of N-H group (Barth, 2007).

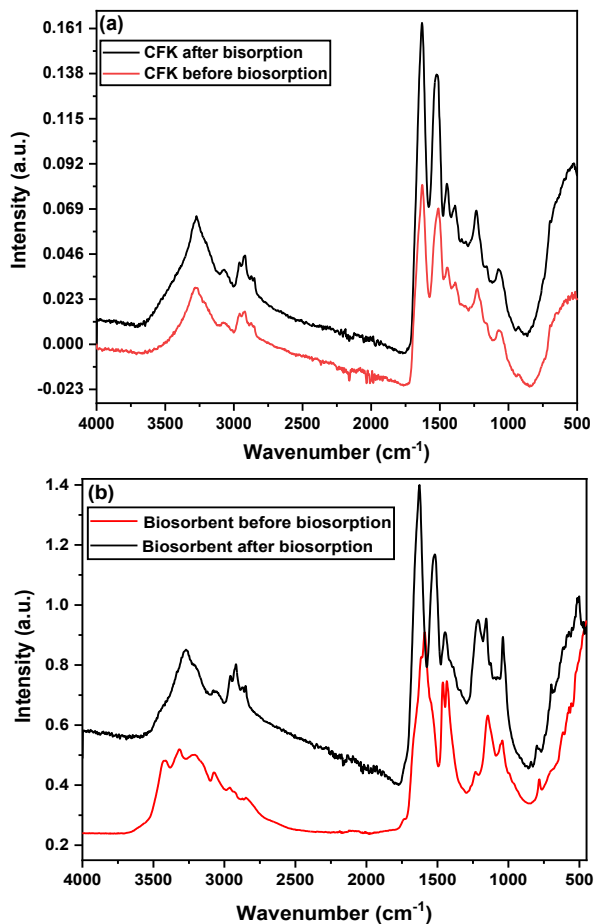


Figure 3.20: ATR-FTIR of (a) chicken feather keratin (CFK) before biosorption (red) and after biosorption (black) (b) chicken feather keratin derived biosorbent before biosorption (red) and after biosorption (black)

XPS were performed to observe the changes in N 1s before and after the biosorption. XPS graphs of neat chicken feathers keratin and its derived biosorbents showed two peaks before and after biosorption as showed in **Fig. 3.21**. The first peak at 399.65 eV belongs to N atoms of -NH_2 or -NH , while second peak at 400.04 eV identified as NH_3^+ groups of the chicken feathers keratin protein due to their zwitterionic nature as presented in **Fig. 3.21 (a)**. These groups may serve as the coordination sites for the metal's biosorption. After biosorption, these peaks shifted towards higher binding energies i.e., 400.11 and 401.44 eV respectively. The decrease in electron cloud density of the nitrogen atom may result in shift towards higher binding energy (Yu et al., 2013). There is possibility of formation of $\text{CFK-NH}_2\text{-M}^{2+}$ or CFK-NH-M . This shift in binding energies of the bonds determines the complex formation between chicken feather keratin protein surface functional groups and the metal ions during which lone pair on the nitrogen were shared with metal ions. In addition, biosorption of oxyanions might be due to the electrostatic interactions with the protonated amino groups of the CFK. Similar patterns were obtained in XPS N1s of the biosorbent. The slight shift in binding energy values was observed in the biosorbent after biosorption from 399.57 to 399.96 eV, attributed to amine and 2nd peak from 400.01 to 400.59 eV ammonium ion. In summary, the biosorption of metals through chicken feathers keratin occurs through phenomena such as complexion, hydrogen bonding, electrostatic interactions, and chelation.

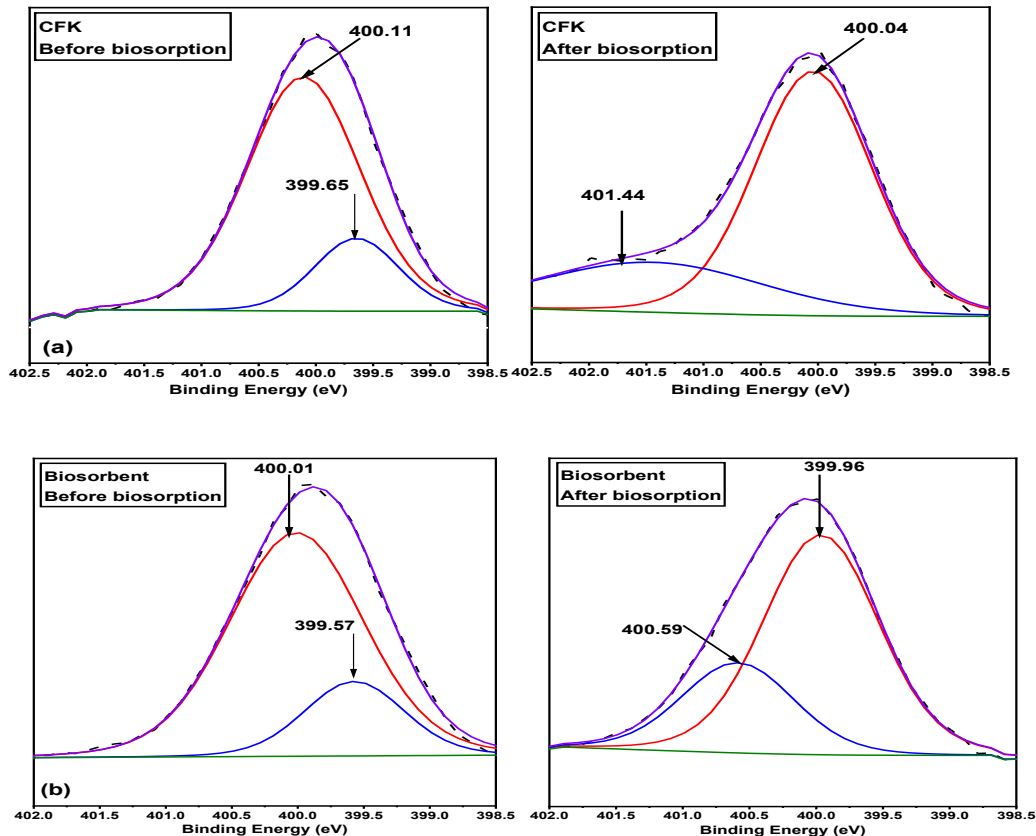


Figure 3.21: XPS N1s spectra of the (a) chicken feathers keratin and (b) biosorbent before and after biosorption

3.4. Conclusions

The facile modification of chicken feathers keratin with water dispersed graphene oxide can improve its biosorption efficiency for the simultaneous removal of metal cationic and oxyanion species from contaminated water. The developed biosorbents exhibited biosorption capacities of ≥ 99 and 95-97 % for Se and As oxyanions respectively. This excellent efficiency of biosorption is ascribed to the incorporation of graphene oxide which altered the keratin structure by forming ester linkage and electrostatic interactions. As a result, more functional groups were exposed on their surfaces that improved the affinity for oxyanions. Moreover, keratin has inherent ability to

combine with these oxyanions. Among metals cations, maximum removal of ≥ 99 was observed for Ni (II), while for Co (II) and Pb (II), the removal efficiencies were ≥ 92 and $\geq 91\%$ respectively. This study highlights that hybrid biosorbents with remarkably high removal efficiency can be developed by intercalation/exfoliation of keratin biopolymer with GO for effective removal of different species of metals (oxyanions & cations) from wastewater. This work will help to develop a low-cost technology for water remediation from heavy metals with potential for reuse and encourages the utilization of chicken feathers rather than landfilling to avoid environmental concerns.

3.5. References

- Al-Asheh, S., Banat, F., & Al-Rousan, D. (2002). Adsorption of copper, zinc and nickel ions from single and binary metal ion mixtures on to chicken feathers. *Adsorption Science & Technology*, 20(9), 849-864.
- Aluigi, A., Tonetti, C., Rombaldoni, F., Puglia, D., Fortunati, E., Armentano, I., Santulli, C., Torre, L., & Kenny, J. M. (2014). Keratins extracted from Merino wool and Brown Alpaca fibres as potential fillers for PLLA-based biocomposites. *Journal of materials science*, 49(18), 6257-6269.
- Aluigi, A., Zoccola, M., Vineis, C., Tonin, C., Ferrero, F., & Canetti, M. (2007). Study on the structure and properties of wool keratin regenerated from formic acid. *International journal of biological macromolecules*, 41(3), 266-273.
- Arshad, M., Kaur, M., & Ullah, A. (2016). Green biocomposites from nanoengineered hybrid natural fiber and biopolymer. *ACS sustainable chemistry & engineering*, 4(3), 1785-1793.
- Badrelzaman, M., Khamis, M. I., Ibrahim, T. H., & Jumean, F. H. (2020). Scale-Up of self-regenerating semi-batch adsorption cycles through concurrent adsorption and reduction of Cr (VI) on sheep wool. *Processes*, 8(9), 1092.
- Barth, A. (2007). Infrared spectroscopy of proteins. *Biochimica et Biophysica Acta (BBA)-Bioenergetics*, 1767(9), 1073-1101.
- Dodson, J. R., Parker, H. L., García, A. M., Hicken, A., Asemave, K., Farmer, T. J., He, H., Clark, J. H., & Hunt, A. J. (2015). Bio-derived materials as a green route for precious & critical metal recovery and re-use. *Green Chemistry*, 17(4), 1951-1965.
- Edwards, H., Hunt, D., & Sibley, M. (1998). FT-Raman spectroscopic study of keratotic materials: horn, hoof and tortoiseshell. *Spectrochimica Acta Part A: Molecular and Biomolecular Spectroscopy*, 54(5), 745-757.
- El-Khodary, S. A., El-Enany, G. M., El-Okr, M., & Ibrahim, M. (2014). Preparation and characterization of microwave reduced graphite oxide for high-performance supercapacitors. *Electrochimica Acta*, 150, 269-278.
- Gupta, V. K., Mittal, A., Kurup, L., & Mittal, J. (2006). Adsorption of a hazardous dye, erythrosine, over hen feathers. *Journal of colloid and interface science*, 304(1), 52-57.
- Idris, A., Vijayaraghavan, R., Rana, U. A., Fredericks, D., Patti, A. F., & Macfarlane, D. R. (2013). Dissolution of feather keratin in ionic liquids. *Green Chemistry*, 15(2), 525-534.
- Jeong, H., Jin, M., So, K., Lim, S., & Lee, Y. (2009). Tailoring the characteristics of graphite oxides by different oxidation times. *Journal of Physics D: Applied Physics*, 42(6), 065418.
- Jiang, Y.-J., Yu, X.-Y., Luo, T., Jia, Y., Liu, J.-H., & Huang, X.-J. (2013). γ -Fe₂O₃ nanoparticles encapsulated millimeter-sized magnetic chitosan beads for removal of Cr (VI) from water: thermodynamics, kinetics, regeneration, and uptake mechanisms. *Journal of Chemical & Engineering Data*, 58(11), 3142-3149.
- Kaur, M., Arshad, M., & Ullah, A. (2018). In-situ nanoreinforced green bionanomaterials from natural keratin and montmorillonite (MMT)/cellulose nanocrystals (CNC). *ACS Sustainable Chemistry & Engineering*, 6(2), 1977-1987.
- Khosa, M. A., & Ullah, A. (2014). In-situ modification, regeneration, and application of keratin biopolymer for arsenic removal. *Journal of hazardous materials*, 278, 360-371.
- Khosa, M. A., Wu, J., & Ullah, A. (2013). Chemical modification, characterization, and application of chicken feathers as novel biosorbents. *RSC advances*, 3(43), 20800-20810.

- KOCATÜRK, S., & Bornova, I. (2008). REMOVAL OF HEAVY METAL IONS FROM AQUEOUS SOLUTIONS BY KERATIN. *Chemical Engineering*, 603, 00.
- Kumar, S., & Parekh, S. H. (2020). Linking graphene-based material physicochemical properties with molecular adsorption, structure and cell fate. *Communications Chemistry*, 3(1), 1-11.
- Kyzas, G. Z., Sifaka, P. I., Lambropoulou, D. A., Lazaridis, N. K., & Bikiaris, D. N. (2014). Poly (itaconic acid)-grafted chitosan adsorbents with different cross-linking for Pb (II) and Cd (II) uptake. *Langmuir*, 30(1), 120-131.
- Liu, B., & Huang, Y. (2011). Polyethyleneimine modified eggshell membrane as a novel biosorbent for adsorption and detoxification of Cr (VI) from water. *Journal of Materials Chemistry*, 21(43), 17413-17418.
- Ma, B., Qiao, X., Hou, X., & Yang, Y. (2016). Pure keratin membrane and fibers from chicken feather. *International journal of biological macromolecules*, 89, 614-621.
- Marcano, D. C., Kosynkin, D. V., Berlin, J. M., Sinitskii, A., Sun, Z., Slesarev, A., Alemany, L. B., Lu, W., & Tour, J. M. (2010). Improved synthesis of graphene oxide. *ACS nano*, 4(8), 4806-4814.
- McGovern, V. (2000). Recycling poultry feathers: more bang for the cluck. *Environmental Health Perspectives*, 108(8), A366-A369.
- Misra, M., Kar, P., Priyadarshan, G., & Licata, C. (2001). Keratin protein nano-fiber for removal of heavy metals and contaminants. *MRS Online Proceedings Library (OPL)*, 702.
- Mittal, A. (2006). Adsorption kinetics of removal of a toxic dye, Malachite Green, from wastewater by using hen feathers. *Journal of hazardous materials*, 133(1-3), 196-202.
- Mokhatab, S., Poe, W. A., & Mak, J. Y. (2019). Natural gas dehydration and mercaptans removal. *Handbook of Natural Gas Transmission and Processing*, 4.
- Motarjemi, Y., Moy, G., & Todd, E. (2013). *Encyclopedia of food safety*. Academic Press.
- Paredes, J., Villar-Rodil, S., Martínez-Alonso, A., & Tascon, J. (2008). Graphene oxide dispersions in organic solvents. *Langmuir*, 24(19), 10560-10564.
- Park, D., Lim, S.-R., Yun, Y.-S., & Park, J. M. (2007). Reliable evidences that the removal mechanism of hexavalent chromium by natural biomaterials is adsorption-coupled reduction. *Chemosphere*, 70(2), 298-305.
- Park, S., An, J., Potts, J. R., Velamakanni, A., Murali, S., & Ruoff, R. S. (2011). Hydrazine-reduction of graphite-and graphene oxide. *Carbon*, 49(9), 3019-3023.
- Peydayesh, M., & Mezzenga, R. (2021). Protein nanofibrils for next generation sustainable water purification. *Nature communications*, 12(1), 1-17.
- Rodzik, A., Pomastowski, P., Sagandykova, G. N., & Buszewski, B. (2020). Interactions of whey proteins with metal ions. *International journal of molecular sciences*, 21(6), 2156.
- Rojas, S., & Horcajada, P. (2020). Metal-organic frameworks for the removal of emerging organic contaminants in water. *Chemical reviews*, 120(16), 8378-8415.
- Saha, S., Arshad, M., Zubair, M., & Ullah, A. (2019). Keratin as a Biopolymer. In *Keratin as a protein biopolymer* (pp. 163-185). Springer.
- Saha, S., Zubair, M., Khosa, M., Song, S., & Ullah, A. (2019). Keratin and chitosan biosorbents for wastewater treatment: a review. *Journal of Polymers and the Environment*, 27(7), 1389-1403.
- Shannon, M. A., Bohn, P. W., Elimelech, M., Georgiadis, J. G., Marinas, B. J., & Mayes, A. M. (2010). Science and technology for water purification in the coming decades. *Nanoscience and technology: a collection of reviews from nature Journals*, 337-346.

- Shen, S., Li, X.-F., Cullen, W. R., Weinfeld, M., & Le, X. C. (2013). Arsenic binding to proteins. *Chemical reviews*, 113(10), 7769-7792.
- Tagliavini, M., Engel, F., Weidler, P. G., Scherer, T., & Schäfer, A. I. (2017). Adsorption of steroid micropollutants on polymer-based spherical activated carbon (PBSAC). *Journal of hazardous materials*, 337, 126-137.
- Tesfaye, T., Sithole, B., & Ramjugernath, D. (2017). Valorisation of chicken feathers: a review on recycling and recovery route—current status and future prospects. *Clean Technologies and Environmental Policy*, 19(10), 2363-2378.
- Thamer, B. M., Aldabahi, A., Moydeen A, M., Rahaman, M., & El-Newehy, M. H. (2021). Modified electrospun polymeric nanofibers and their nanocomposites as nanoadsorbents for toxic dye removal from contaminated waters: A review. *Polymers*, 13(1), 20.
- Thommes, M., Kaneko, K., Neimark, A. V., Olivier, J. P., Rodriguez-Reinoso, F., Rouquerol, J., & Sing, K. S. (2015). Physisorption of gases, with special reference to the evaluation of surface area and pore size distribution (IUPAC Technical Report). *Pure and applied chemistry*, 87(9-10), 1051-1069.
- Ullah, A., & Wu, J. (2013). Feather fiber-based thermoplastics: effects of different plasticizers on material properties. *Macromolecular Materials and Engineering*, 298(2), 153-162.
- Yu, Z., Zhang, X., & Huang, Y. (2013). Magnetic chitosan–iron (III) hydrogel as a fast and reusable adsorbent for chromium (VI) removal. *Industrial & engineering chemistry research*, 52(34), 11956-11966.
- Zahara, I., Arshad, M., Naeth, M. A., Siddique, T., & Ullah, A. (2021). Feather keratin derived sorbents for the treatment of wastewater produced during energy generation processes. *Chemosphere*, 273, 128545.
- Zangmeister, C. D. (2010). Preparation and evaluation of graphite oxide reduced at 220 C. *Chemistry of Materials*, 22(19), 5625-5629.
- Zhang, H., Carrillo-Navarrete, F., López-Mesas, M., & Palet, C. (2020). Use of chemically treated human hair wastes for the removal of heavy metal ions from water. *Water*, 12(5), 1263.
- Zhao, J., Liu, L., & Li, F. (2015). *Graphene oxide: physics and applications*. Springer.
- Zhu, Y., Murali, S., Cai, W., Li, X., Suk, J. W., Potts, J. R., & Ruoff, R. S. (2010). Graphene and graphene oxide: synthesis, properties, and applications. *Advanced materials*, 22(35), 3906-3924.
- Zsirai, T., Qiblawey, H., A-Marri, M. J., & Judd, S. (2016). The impact of mechanical shear on membrane flux and energy demand. *Journal of Membrane Science*, 516, 56-63. <https://doi.org/10.1016/j.memsci.2016.06.010>
- Zubair, M., & Ullah, A. (2021). Biopolymers in environmental applications: industrial wastewater treatment. *Biopolymers and their industrial applications*, 331-349.

CHAPTER 4: Green Biosorbents Prepared from Chemically Cross-link Keratin Biopolymer using Nanochitosan for Heavy Metals Remediation from Water

4.1. Introduction

Currently, access to clean water is one of the most significant challenges, and it is becoming extremely scarce and polluted. Rapid industrialization, including metals, mining, paper pesticide and fertilizer, leather and batteries, is expanding the stress on water resources and aggravating the global clean water needs (Fu & Wang, 2011; Werber et al., 2016). Most of the industrial wastewater is discharged into freshwater bodies without adequate treatment and severely pollutes the water resources. Industrial wastewater contains many heavy metals and affects terrestrial and marine life. Mainly, industrial wastewater contains heavy metals such as arsenic, lead, copper, zinc, chromium, nickel etc. Heavy metals are non-degradable and tend to accumulate in living organisms, having a pivotal role in harming populations around the globe, particularly in countries with limited resources (Sharma et al., 2022; Yasmeen et al., 2022).

Various conventional methods have been used for the remediation of industrial effluents before releasing them into the environment. These methods include membrane, electrochemical or chemical precipitation, ion exchange, flocculation, evaporation, coagulation, filtration and adsorption through activated carbon (Dodson et al., 2015; Lo et al., 2014; Wang & Chen, 2009). However, these techniques are not viable in areas with limited resources because of the high cost, poor heavy metal adsorption performance and high energy or chemical needs (Arshad et al., 2020; Chai et al., 2021; Zubair et al., 2021). Hence, there is an urgent need to develop green, sustainable, and economical alternatives with excellent removal efficiency for industrial wastewater treatment.

Recently, bio-derived materials have become the limelight in developing sorbent materials for contaminants removal from contaminated water. Various biobased materials have been studied as potential biosorbents including polysaccharides (chitosan, starch cellulose, alginates, lignin), fungi, and proteins (soy, gelatin, zein, keratin, silk, albumin), bacteria and algae (Zubair & Ullah, 2021). Among biopolymers, proteins are the favourable choice due to their natural abundance, biodegradable nature and excellent biosorption capacity. Within proteins, keratin has a unique diverse chemical structure and offers exciting opportunities for modification with advanced biosorption properties (Saha et al., 2019; Witus & Francis, 2011).

Keratin can be extracted from low-cost biomass sources such as hairs, nails, claws, hooves, wool, horns and feathers (Feroz et al., 2020). Feathers, a significant poultry industry by-product considered waste for a long time and poses serious ecological and commercial issues. Globally, 8-9 million tonnes of chicken feathers are produced yearly. However, keratin biopolymer (>90) from chicken feathers is one of the viable options due to its natural abundance, easy availability and environment-friendly nature (Šafarič et al., 2020). Nonetheless, using keratin in its native form for biosorption has several drawbacks, including separation from the reaction mixture, low biosorption capacity and mass loss after regeneration. Keratin proteins have multiple functional groups in the side chains and auxiliary groups that can be transformed chemically into desired properties to facilitate the biosorption of contaminants. Especially, breaking di-sulphide linkage can open the keratin biopolymer, which can be chemically cross-linked using nanoparticles to modify its biosorption ability.

Herein, we report the keratin derived biosorbents using nanochitosan to biosorb the heavy metals from contaminated water. Nanochitosan (NC) is polycationic in nature and contains amino and primary/secondary hydroxyl groups. Nanochitosan can make chemical or electrostatic

interactions with keratin polymeric networks to improve their biosorption efficiency (Zubair et al., 2020). The core piece of this work is to find an alternative way to use chicken feathers keratin to produce affordable, renewable and sustainable keratin-nanochitosan based biosorbents for industrial wastewater treatment.

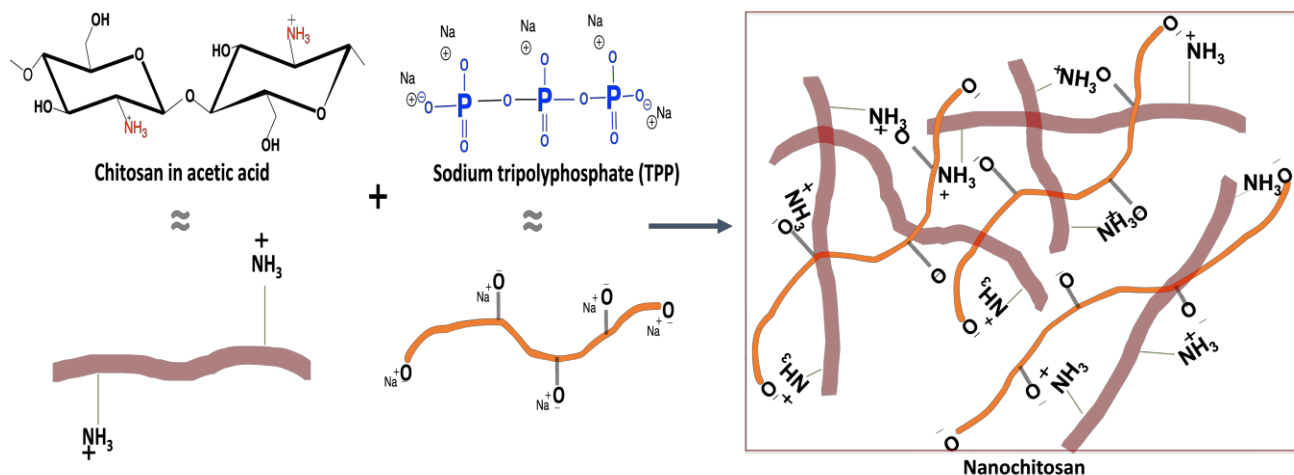
4.2. Experimental strategy

The chemical modification of keratin biopolymer with bio-derived nanoparticles can be feasible and sustainable to increase its surface affinity for metal biosorption in large-scale applications such as water remediation. Keratin has a dense structure due to disulphide bonds that cross-link the keratin strongly. To achieve high biosorption performance of keratin, first, keratin was dissolved by breaking their di-sulphide bonds using a reducing agent **Scheme II (a)**. In the 2nd step, nanochitosan was introduced into the dissolved keratin solution to maximize its biosorption efficiency for metals **Scheme II (b)**.

The nano-chitosan has polar functional groups such as the hydroxyl group, which can interact with the keratin's side chains, enhancing the polar and charged side chains on the keratin surfaces and making them more effective for metals removal. Chitosan can be converted into nano-size particles by the ionic gelation method where tripolyphosphate (TPP) is used.

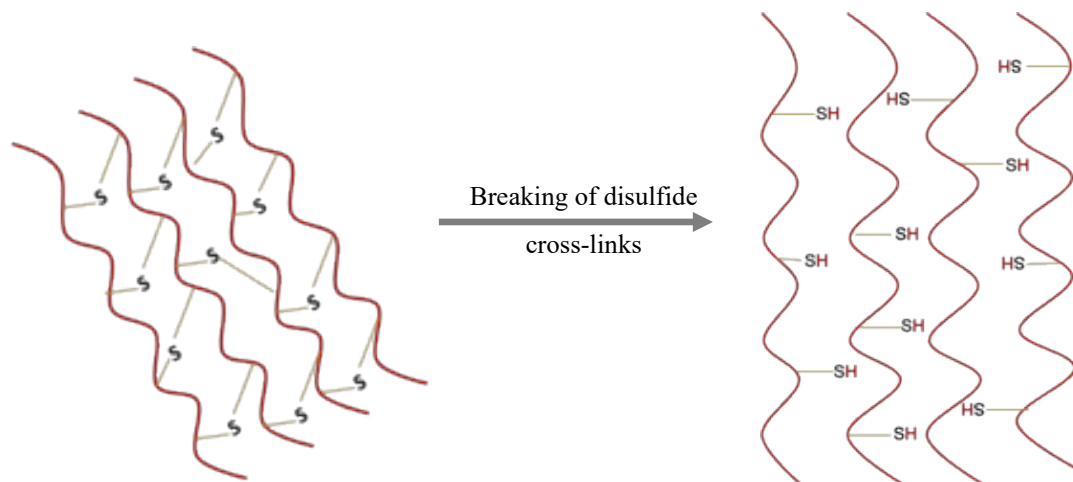
The chitosan has a positively charged amino group (NH_3^+) and tripolyphosphate (TPP) has $\text{P}_3\text{O}_{10}^{5-}$ anions which result in ionic interaction between them. Chitosan has weak polybasic nature and ionization of the amino group increases as the solution pH decreases. In addition, TPP is dissociated into $\text{P}_3\text{O}_{10}^{5-}$ anions at low pH (Kahdestani et al., 2021; Yang et al., 2009). Therefore, nanosized chitosan prepared in the acidic TPP solutions is completely ionic cross-linked. This method has two advantages, chitosan will not only convert into nanoparticles but also $-\text{NH}_2$ group of the chitosan will be protected for further reaction **Scheme I**. Hence, cross-linking between the

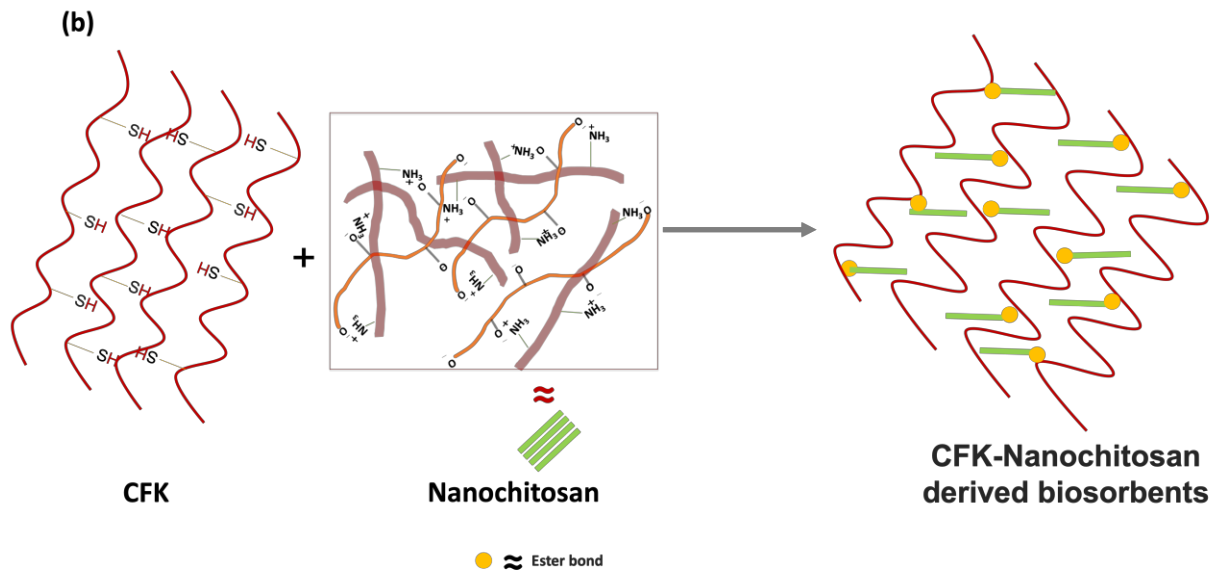
hydroxyl group of the nanochitosan and the carboxyl group of the keratin biopolymer forms an ester ($O = C - O$) linkage between them as shown in **Scheme II (b)**.



Scheme I: Synthesis of nanochitosan and protection of amino group at the C2 position

(a)





Scheme II: preparation of chicken feather keratin-nanochitosan (CFK-NC) (a) Breaking of di-sulfide bonds (b) Cross-linking between CFK-NC

4.3. Results & Discussions

4.3.1. Characterization of nanochitosan

To develop the biosorbents chitosan was converted into nanochitosan using sodium tripoly phosphate and confirmed by ATR-FITR and XRD as shown in **Fig 4.1** and **4.2**.

4.3.1.1. Structural analysis

ATR-FTIR of chitosan and synthesized nanochitosan was measured and shown in **Fig. 4.1**. FTIR spectra of chitosan exhibited peaks at around 3400 cm^{-1} that can be ascribed to hydroxyl while peaks at 2870 cm^{-1} assigned to C–H stretching vibration. [30,31]. The peak observed at 1703 cm^{-1} shows the C=O stretching of the amide bond. On the other hand, a peak at 1430 cm^{-1} presented the presence of N-H bending and C-H deformation (Vijayalakshmi et al., 2016; Wang et al., 2011). The FTIR spectrum of the nanochitosan chitosan displayed a peak at 1156 cm^{-1} that confirmed the existence of anti-symmetric stretching vibration of COC as well as CN stretching

vibration that corroborated the formation of chitosan nanoparticles as shown in **Fig. 4.1**. In the chitosan/TPP spectrum, 2 new peaks at 1630 and 1560 cm^{-1} emerge, i.e., N–O asymmetric stretching showed the phosphoric and ammonium ions linkage. Also, a 1080 cm^{-1} peak can be assigned to P–O stretching appeared due to the cross-linked chitosan nanoparticles (Kahdestani et al., 2021).

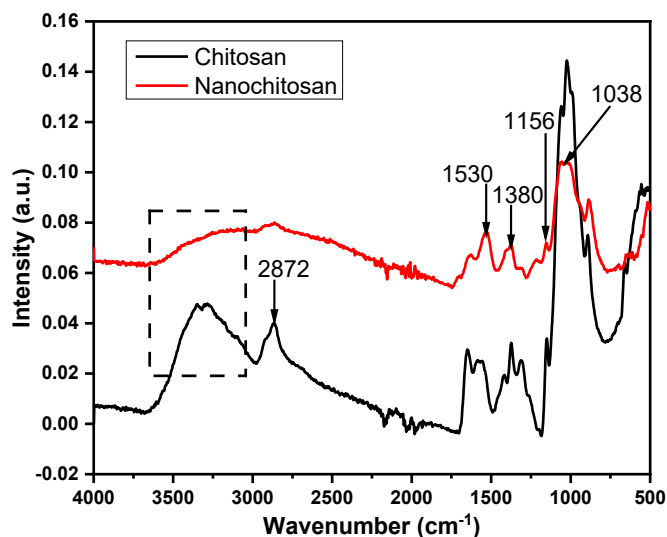


Figure 4.1: ATR-FTIR of chitosan and nanochitosan

4.3.1.2. Crystallinity analysis

Fig. 4.2 displays the XRD patterns of chitosan and nanochitosan respectively. The chitosan possesses a semi-crystalline structure and showed two distinctive diffraction peaks at 2θ of 11.59 and 23.28 relating to the plane of (020) and (110) correspondingly (Zhang et al., 2011).

When the size of chitosan nanoparticles was reduced, the position of the peaks did not shift considerably, which corroborates the nanochitosan phase purity. Moreover, the peak intensities declined due to the influence on the physical properties of the chitosan nanoparticles, i.e., the molecular weight was reduced, and the acetylation degree was increased. As a result, it

destroyed the crystallinity and led to the more amorphous character in the chitosan (Zhang et al., 2012). The typical peaks peak for nanochitosan declines and are broad, ascribed to the cross-linking and is consistent with the previous studies (Bhumkar & Pokharkar, 2006; Kahdestani et al., 2021; Wan et al., 2003). The degree of crystallinity corroborated this claim as chitosan showed a degree of crystallinity of 22.46 while nanochitosan had 9.13.

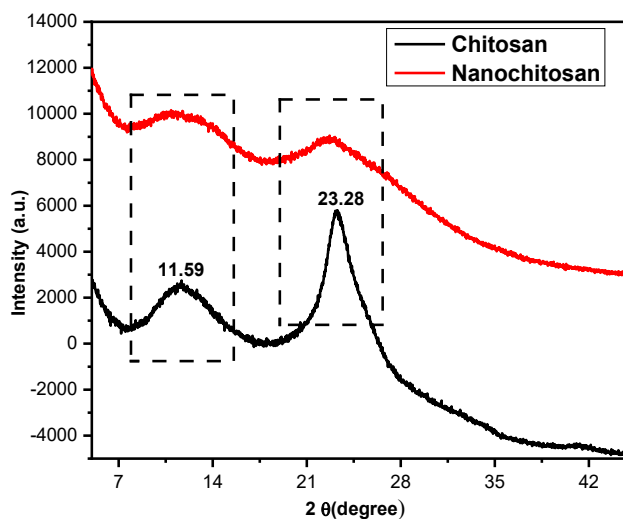


Figure 4.2: XRD patterns of chitosan and nanochitosan

4.3.2. Structure characterization of the biosorbents

The changes in functional groups, chemical bonding status and crystallinity of neat chicken feather keratin and its derived biosorbents were determined by ATR-FTIR, XPS and XRD respectively. **Fig. 4.3** shows the ATR-FTIR of neat chicken feathers keratin and its derived biosorbents containing nanochitosan. The FTIR spectra of all samples reveal that their characteristic peaks are similar. The typical peaks are in accordance with the keratin indicating a high content of keratin is present in all samples. Four major regions were identified for peptide linkage ($-\text{CONH}$) i.e., 3270 cm^{-1} , 1630 cm^{-1} , 1515 cm^{-1} and 1230 cm^{-1} which are identified as

amide A, amide I, II and III regions respectively (Ma et al., 2016; Zhang et al., 2015). The absorption band at 3274 cm^{-1} is ascribed to the O-H and N-H stretching vibrations and labelled as Amide A. However, this band is shifted towards the lower wavenumber after incorporating nanochitosan due to the disruption in hydrogen bonding within the keratin polymeric matrix (Idris et al., 2014). The absorption band at 2917 cm^{-1} belongs to the CH_3 symmetrical stretching vibration. While the strong absorption bands at 1630 and 1515 cm^{-1} belong to C-O stretching (Amide I) and N-H bending and C-H stretching of the amide bonds (Amide II). The weak absorption band around 1230 cm^{-1} is shown due to the stretching of C-N and in-plane bending of N-H, and a minor influence owing to the bending vibration of C-O and C-C stretching (Idris et al., 2013). The bands I-III provide evidence about the conformation and backbone structure of proteins.

From the literature, the peak at 3274 cm^{-1} (amide A region) belongs to the α - helix and amide II region around 1515 cm^{-1} ascribed to the β -sheets. In contrast, the peak at 1630 cm^{-1} (amide I region) is related to the combination of α - helix and β -sheets. Thus, neat chicken feathers keratin in addition to keratin-nanochitosan derived biosorbents have both α - helix and β -sheets microstructures (Martinez-Hernandez et al., 2005; Senoz & Wool, 2010). The most prominent peaks in the biosorbents are around 1050 and 1150 cm^{-1} which confirms the presence of nanochitosan in the keratin biopolymer. These peaks are due to the presence of tripolyphosphate (P=O and P-O stretching) in the nanochitosan introduced at the chitosan to transform into nanoparticles (Huang & Yang, 2004; Vijayalakshmi et al., 2016). There were not additional bands observed in the ATR-FTIR of the developed biosorbents. The XPS results reveal that some chemical transformation has occurred which is described below.

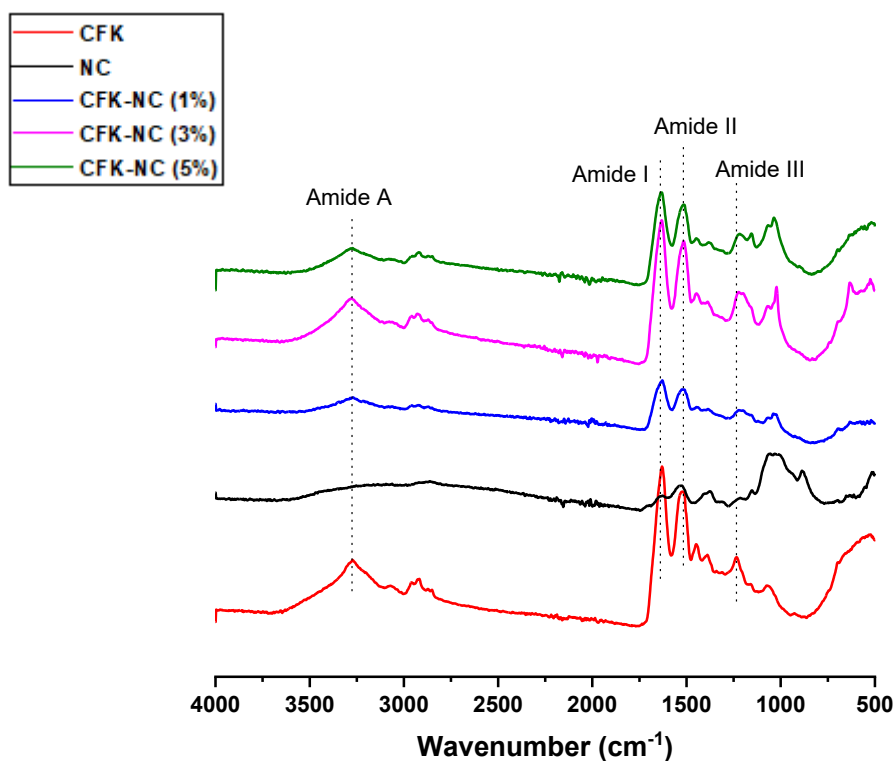


Figure 4.3: ATR- FTIR signals of neat chicken feather keratin and prepared keratin biosorbents.

XPS spectra of neat chicken feather keratin and nanochitosan derived biosorbents are presented. Three distinct peaks can be seen in the chicken feather keratin XPS at bonding energy of 284.99 285.99 and 288.29 eV which can be assigned to C-C/C-H, C-O / C-N and C = O / C-O-C bonds, respectively Kaur et al. observed similar peaks for chicken feather keratin modification with cellulose nanocrystals (Kaur et al., 2018). However, the modification of chicken feather keratin with chitosan nanoparticles presents one additional peak at around 289 eV which can be ascribed to the ester bond developed between the hydroxyl group of the nanochitosan and the carboxyl group of the keratin biopolymer (Arshad et al., 2016).

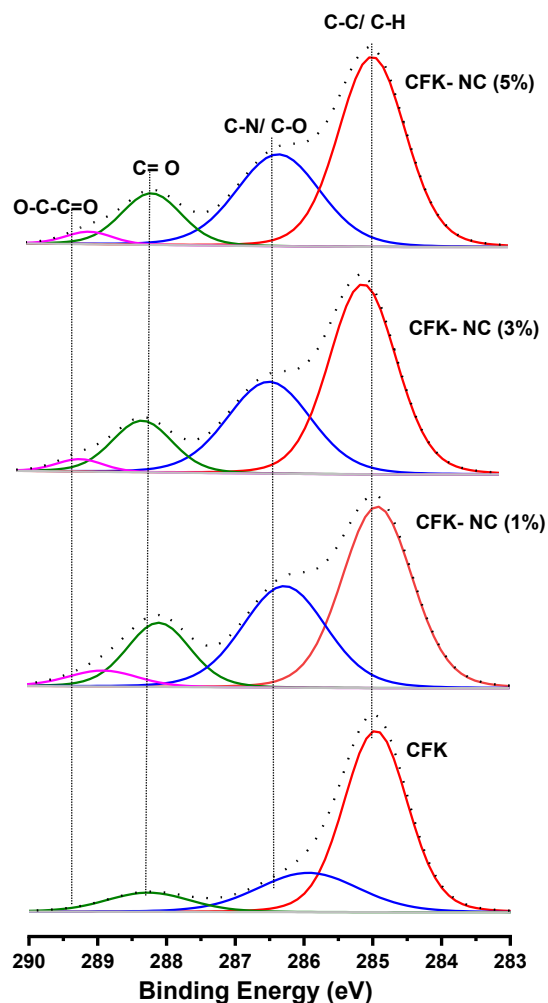


Figure 4.4: XPS peaks of neat chicken feather keratin and prepared keratin biosorbents.

XRD of neat chicken feathers keratin and keratin-nanochitosan derived biosorbents exhibited two characteristic diffraction patterns 2θ peaks at 19° and 11° indicating the interlayer spacings of around 4 and 9 Å, respectively (Idris et al., 2013; Tsukada et al., 1995) as shown in **Figure 4.5**. These 2θ peaks correspond to the α - helix and β -sheets which is consistent with ATR-FTIR results. The peaks are broader in the neat chicken feather keratin; however, these peaks are sharp after the introduction of nanochitosan into the keratin biopolymer attributed to the cross-linking of nanochitosan with the keratin biopolymer. In addition, these peaks are shifted toward high 2θ i.e., 11.42 and 19.36. As a result, interlayer spacing between the protein layers is decreased

due to the strong interaction between the nanochitosan and functional groups present within the polymeric matrix of keratin. The peak width is related to the crystal size in the protein biopolymer, the wider the peak smaller the crystals are. So, keratin-nanochitosan derived biosorbents possess a relatively larger crystal size than the neat CFK for the α - helix and β -sheets structures. As a result, more compact molecular structures were obtained in case of keratin-nanochitosan biosorbents.

Table 4.1: % Crystallinity of chicken feather keratin and CFK-NC biosorbents

Sample codes	CFK	CFK-NC (1%)	CFK-NC (3%)	CFK-NC (5%)
Crystallinity (%)	60.2	27.94	13.80	31.76

It is recognized that keratin proteins have semi-crystalline natural biomacromolecular structure (Idris et al., 2014) as exhibited in XRD peaks of the keratin and its nanochitosan derived biosorbents. The % crystallinity of 60.2 was observed for neat chicken feather keratin. While the % crystallinity of neat chicken feathers with nanochitosan addition was changed tremendously and decreased to 27.94, 13.80 and 31.76 for CFK-NC (1,3 and 5%), respectively (**Table 4.1**), and implies the development of disordered/amorphous regions (Carr & Gerasimowicz, 1988). With the incorporation of nanochitosan, the % crystallinity of keratin is lost, and the amorphous phase may be extended which corresponds with the biosorption of the keratin-nanochitosan derived biosorbents increases with the increase in nanochitosan content. However, this reduction was maximum in the case of CFK-NC (3%), which may contribute to better biosorption compared to other developed biosorbents with 1 and 5% nanochitosan. Nanochitosan contains many hydroxyl groups which can interact with keratin in two ways: intermolecular hydrogen bonding and chemical bonding between hydroxyl of nanochitosan and carboxyl group of the keratin proteins.

This is corroborated with XPS analysis (**Fig. 4.4**) that exhibited a new bond formation between keratin and nanochitosan i.e., ester linkage. In addition, many peak crystallinity peaks were observed in the keratin- nanochitosan derived biosorbents. These peaks may appear due to the loss of the original crystal domain in neat chicken feathers and rebuild a new crystallinity region because of the new interactions developed between keratin and nanochitosan.

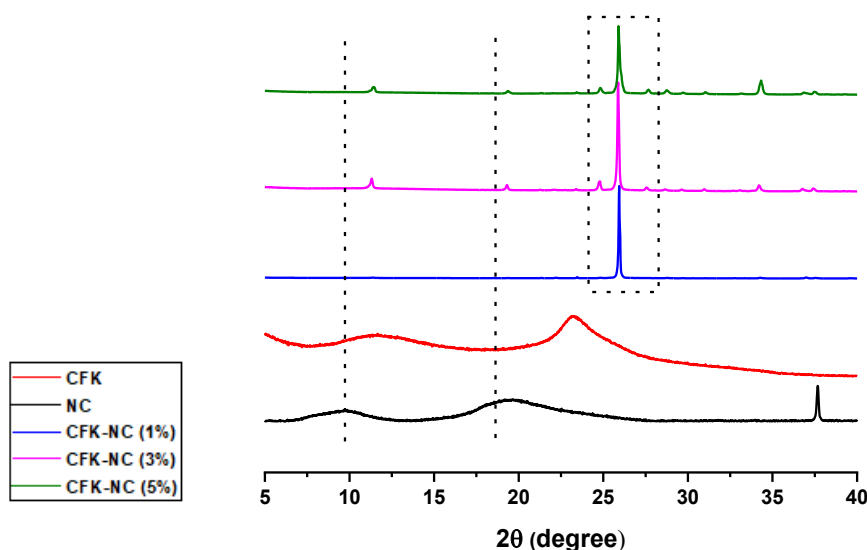
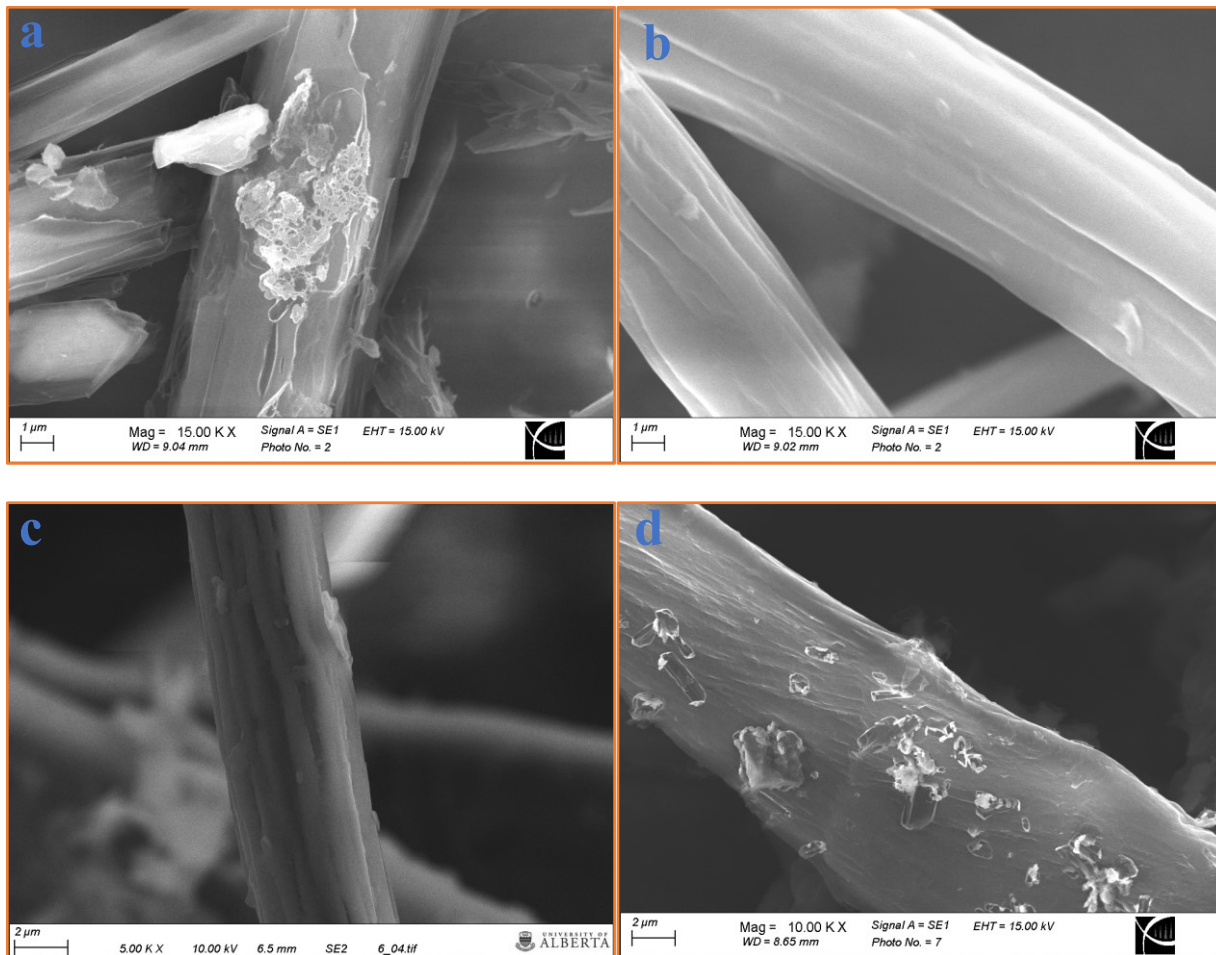


Figure 4.5: XRD patterns of neat chicken feather keratin and prepared keratin biosorbents.

4.3.3. Surface characterization of the biosorbents

The surface morphology of the neat chicken feather keratin proteins was examined with scanning electron microscopy and compared with the surface variations after modification with nanochitosan. SEM images of the keratin-nanochitosan derived biosorbents clearly show substantial differences in the surface morphology in contrast with the neat keratin surface. The neat chicken feather keratin has a fibrous smooth and homogeneous surface and long shafts. However, the incorporation of nanochitosan turned the surface of keratin into a coarse or rough

surface as seen in SEM images (**Figure 4.6 c-h**). The breaking of disulfide linkage in keratin biopolymer followed by the cross-linking with nanochitosan may disrupt the ordered alignment of biopolymers, resulting in an uneven surface. In addition, bright spots are clearly visible in images **d** and **f** that confirm the presence of chitosan nanoparticles on the surface of keratin biopolymer. All variations mentioned above due to nanochitosan addition into the polymeric matrix alter the microstructures of the resultant biosorbents significantly as seen in SEM images of biosorbents. SEM images (**g & h**) of CFK-NC (5%) exhibit a surface with cracked structure that seems to reflect the highest contents of nanochitosan which alter the surface more significant in comparison with biosorbents containing low contents (1,3%) of nanochitosan.



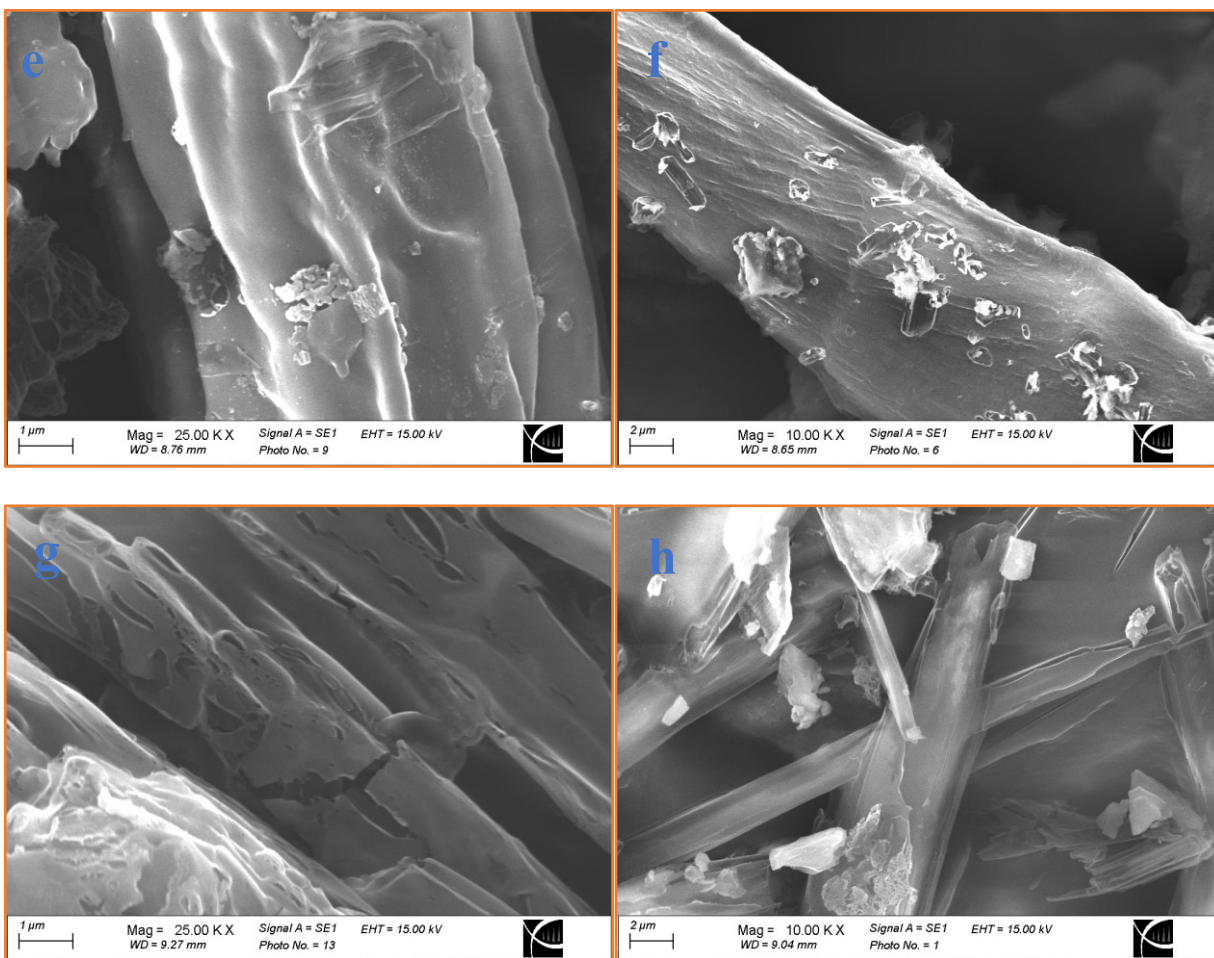


Figure 4.6: SEM images of (a, b) neat chicken feather keratin (c, d) CFK-NC (1%) (e,f) CFK-NC (3%) (g, h) CFK-NC (5%)

The incorporation of nanochitosan in the keratin matrix results in the keratin-nanochitosan biosorbents with no indication for phase separation as shown in **Figure 4.7**. This suggests that NC is compatible with keratin and dispersed through the polymeric matrix. However, dispersion is better in cases of 1 and 3% compared to the 5%, as clearly depicted in the TEM images. As a result, internal structure of chicken feather keratin is changed dramatically in CFK-NC biosorbents.

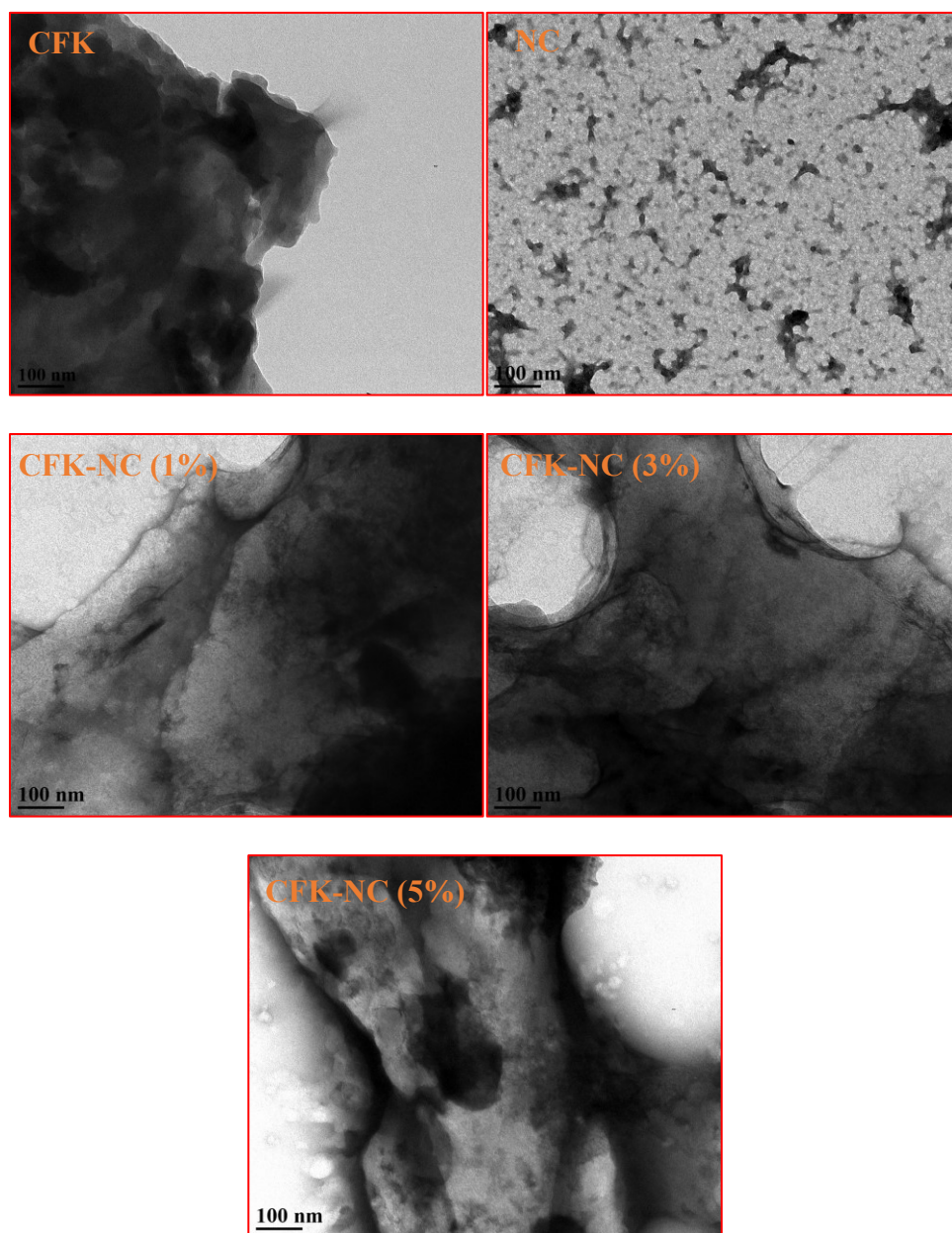


Figure 4.7: TEM images of chicken feather keratin (CFK), NC, CFK-NC (1%), CFK-NC (3%) and CFK-NC (5%)

4.3.4. Thermal stability and phase behavior of the biosorbents

Thermal analysis was performed using TGA to obtain information about the thermal stability and degradation pattern of the chicken feather keratin and keratin-chitosan based biosorbents. TGA curves clearly show that CFK and derived biosorbents have three-stage weight loss, as shown in **Fig. 4.8**. At the first stage around 100 °C, the weight loss in neat chicken feather keratin is up to 7% while in the case of keratin-chitosan based biosorbents the loss is between 1.88-5.8 %. This weight loss corresponds to moisture loss present in the keratin biopolymer. In the second stage, sharp weight loss occurs between 250-375 °C and drops to 67.02 for keratin biopolymer. However, in this stage, weight loss for keratin-chitosan reduced to 62.72 %, 56.83 and 55.72% for CFK-NC 1,3, 5% respectively. During this step, volatile compounds such as H₂S and SO₂ are discharged from keratin as it has disulphide bonds which break at this temperature (Idris et al., 2014; Menefee & Yee, 1965).

A similar trend was observed at 575 °C where CFK leftover is 16.34% and CFK- NC 1,3,5% were 21.85, 27.87 and 29.33% respectively. In case of CFK-NC (5%) displayed minimum weight loss at the end as it contains maximum contents (5%) of nanochitosan as compared to other biosorbents. This last stage loss is attributed to thermo-oxidative degradation where the helix structure denaturation, chain linkages, peptide bridge destruction, and degradation of the skeletal structure occur. Keratin biopolymer was also decomposed into smaller products and several gaseous molecules (Dinu et al., 2021). This confirms that the thermal behavior of chicken feathers keratin was altered by the incorporation of nanochitosan.

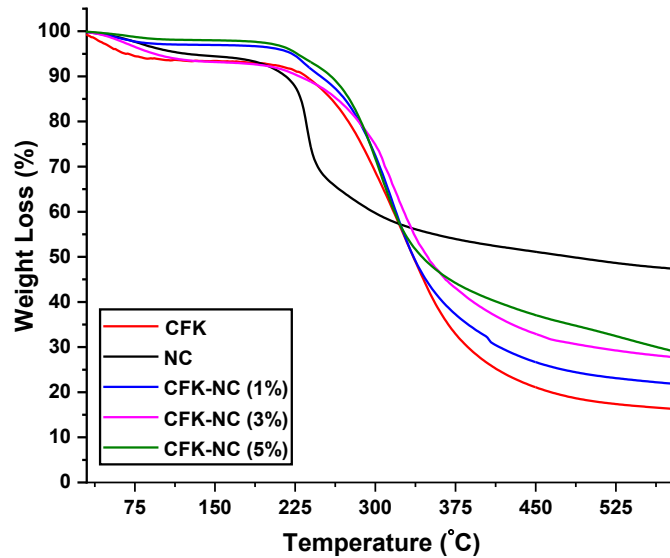


Figure 4.8: TGA curves of chicken feather keratin (CFK), NC, CFK-NC (1%), CFK-NC (3%) and CFK-NC (5%)

Differential Scanning Calorimetry (DSC) was used to analyze the phase behaviour of the neat CFK, and derived biosorbents as shown in **Fig. 4.9**. A broad peak at around 100 °C was observed related to water loss. However, in the case of biosorbents especially CFK-NC 1 and 3% showed a sharp shift towards higher temperature because of delayed moisture i.e., bound water. The neat chicken feather keratin showed a peak between 230 and 235 °C ascribed to the β -form crystallites melting and cysteine-rich matrix degradation (Tonin et al., 2006). However, after modification with nanochitosan, the keratin biopolymer exhibited a peak that appeared at higher temperatures along with an increase in the underlying area, representing the chemical or physical interactions that are developed between keratin and nanochitosan. Here, peaks are sharp in biosorbents containing 1 and 3% nanochitosan and consistent with the XRD data, where % crystallinity loss was observed.

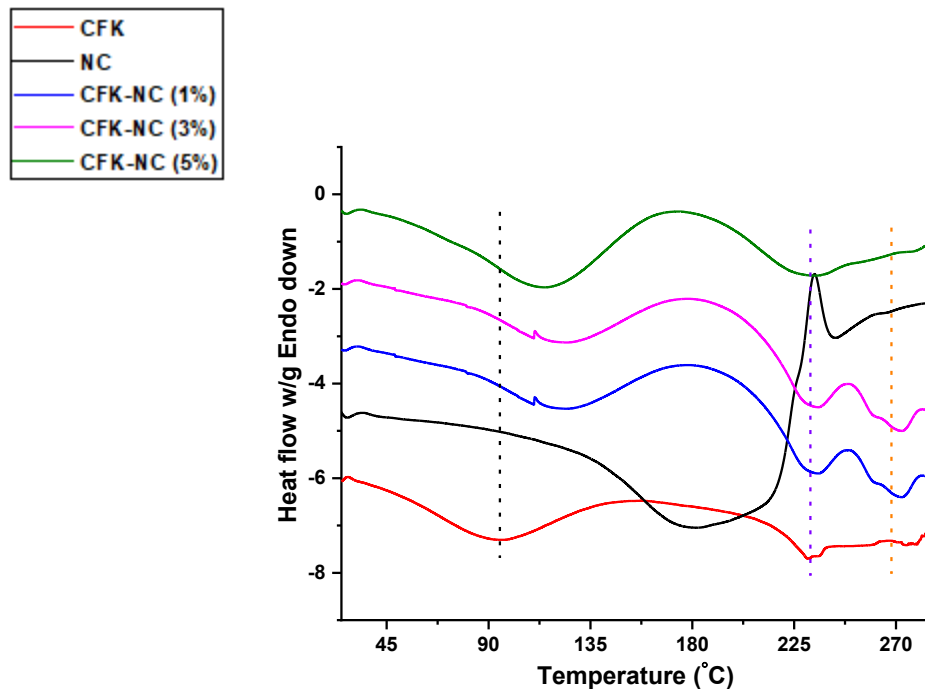


Figure 4.9: DSC curves of chicken feather keratin (CFK), NC, CFK-NC (1%), CFK-NC (3%) and CFK-NC (5%)

4.3.5. Biosorption performance and mechanism

The process of heavy metal biosorption through biopolymeric materials is a complex phenomenon. The interaction mechanism of keratin with metals depends on the nature of various functional groups present in the backbone and side chains. Amino and carboxyl groups are the most reactive sites for metal biosorption. At a neutral or weakly acidic pH, lone pairs of nitrogen behave as a binding site for metal cations. In the case of a highly acidic atmosphere, protonation of protein amino groups occurs, making them cations, which then interact with the metal anions. Generally, proteins adsorb the metals through electrostatic forces or chelation/complexation, hydrogen bonding, ion exchange, and Van der Waals forces (Peydayesh & Mezzenga, 2021; Rodzik et al., 2020; Saha et al., 2019).

Biosorption of biosorbents was tested for the simultaneous removal of 8 metals arsenic (As), selenium (Se), chromium (Cr), nickel (Ni), cobalt (Co), lead (Pb), cadmium (Cd) and zinc (Zn). The prepared biosorbents were effective for the simultaneous removal of both anionic species (As, Se, Cr) and cations species ((Ni, Co, Pb, Cd, Zn). The modification of chicken feather keratin with nanochitosan altered the biosorption efficiency of CFK significantly and enhanced many folds, as shown in **Fig. 4.10 - 4.11**. Among chicken feather keratin-nanochitosan biosorbents, CFK-NC (3%) showed the highest biosorption efficiency for the metal anions of As ($\geq 98\%$) and Se ($\geq 92\%$), and cations Co, Cd and Pb ($\geq 92\%$) from the $600 \mu\text{g L}^{-1}$ laboratory simulated water. However, CFK-NC (5%) exhibited maximum biosorption efficiency for Zn i.e., $\geq 78\%$ among biosorbents. Nickel was the metal cation has the least biosorption efficiency for the biosorbents among all test metal cations and anions. All CFK-NC biosorbents show metal biosorption from the contaminated water, as SEM images (**Fig. 4.6**) were taken after metal biosorption which clearly indicates the removal of the contaminant on the surface of the prepared biosorbents. BET analysis revealed that the surface area of the biosorbents was increased after the incorporation of nanochitosan in keratin biopolymer compared with neat chicken feather keratin and contributed to the improved removal efficiency of the biosorbents.

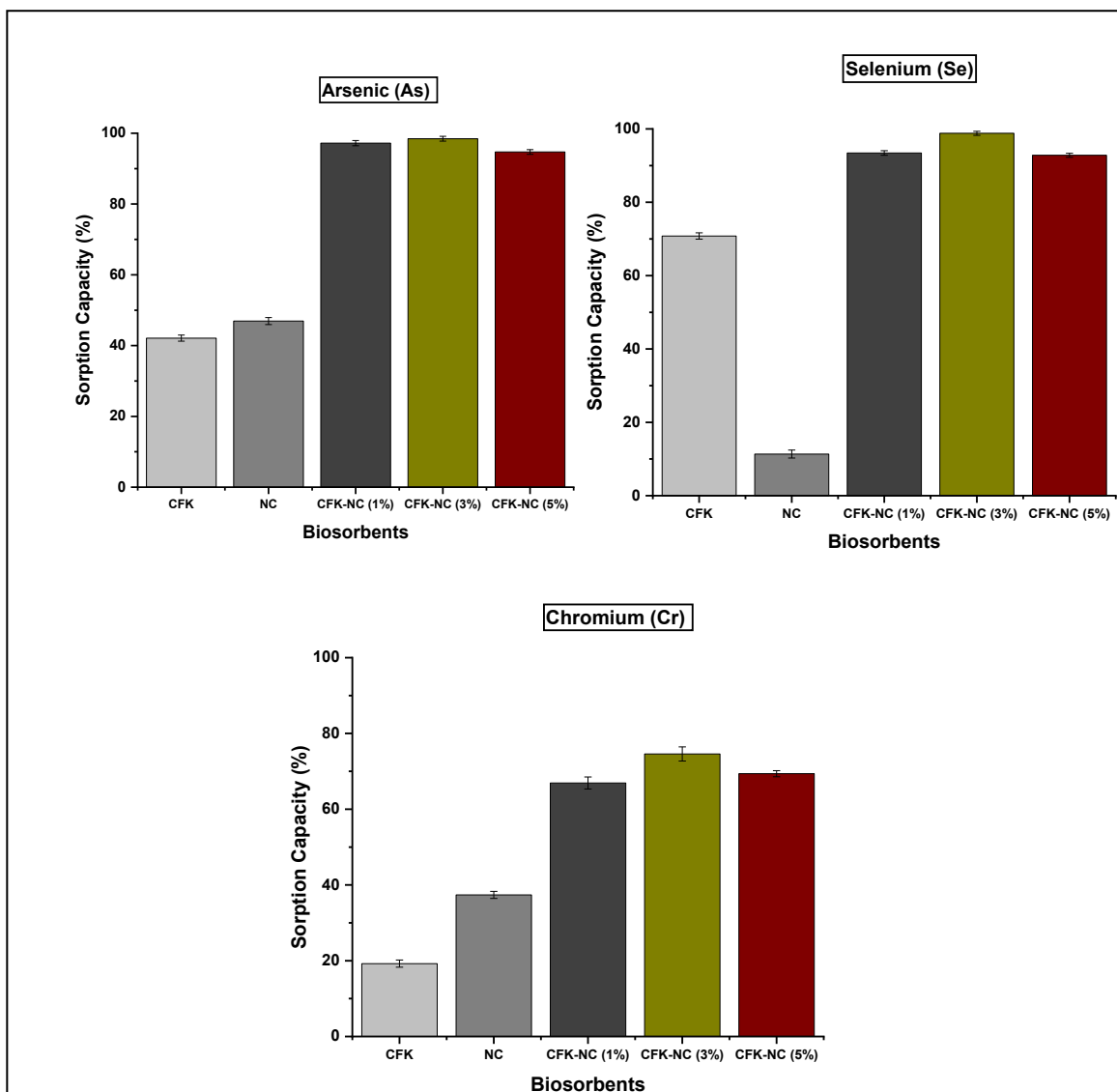


Figure 4.10: Biosorption performance of the keratin-nanochitosan derived biosorbents for anionic species (As, Se, Cr).

Surface area (S_{BET}) of chicken feather keratin modified with 3% nanochitosan was 5.62 m^2/g which is better than the other two biosorbents as the surface is one of the factors that influence the biosorption efficiency of the materials. So, the larger surface area of CFK-NC (3%) may be attributed to its better biosorption efficiency for certain metal cations and anions than other biosorbents. Pore size distribution (PSD) is another factor from BET analysis that determines the

sorption efficiency of polymeric materials. PDS of the prepared chicken feather keratin-nanochitosan (Fig. 4.12) depicts the maxima in towards mesoporous region and much closer to the microporous area while CFK has in the microporous region. Studies reported that a small porous material has better sorption of the species than those with sizeable porous size. A similar trend is observed here as CFK-NC (3%) has porous size maxima at 2.89 which falls almost in the microporous region, the lowest among all prepared biosorbents and has better biosorption efficiency.

The CFK modified with nanochitosan gave the better biosorption efficiency for all metals oxy- anions and cations than neat CFK. This is attributed to the presence of nanochitsoan which interacted with the keratin polymer matrix through ester linkages and electrostatic interactions. In addition, surface characterization is evident that nanochitosan is intercalated/exfoliated within the keratin biopolymer.

Consequently, the structure of keratin was changed at the molecular level keratin and uncovered more active sites for biosorption. Overall, biosorption efficiency (≥ 74 - ≥ 98 %) for anionic species was better than cationic species which may result in the more cationic groups being exposed during the modification process of keratin with nanochitosan.

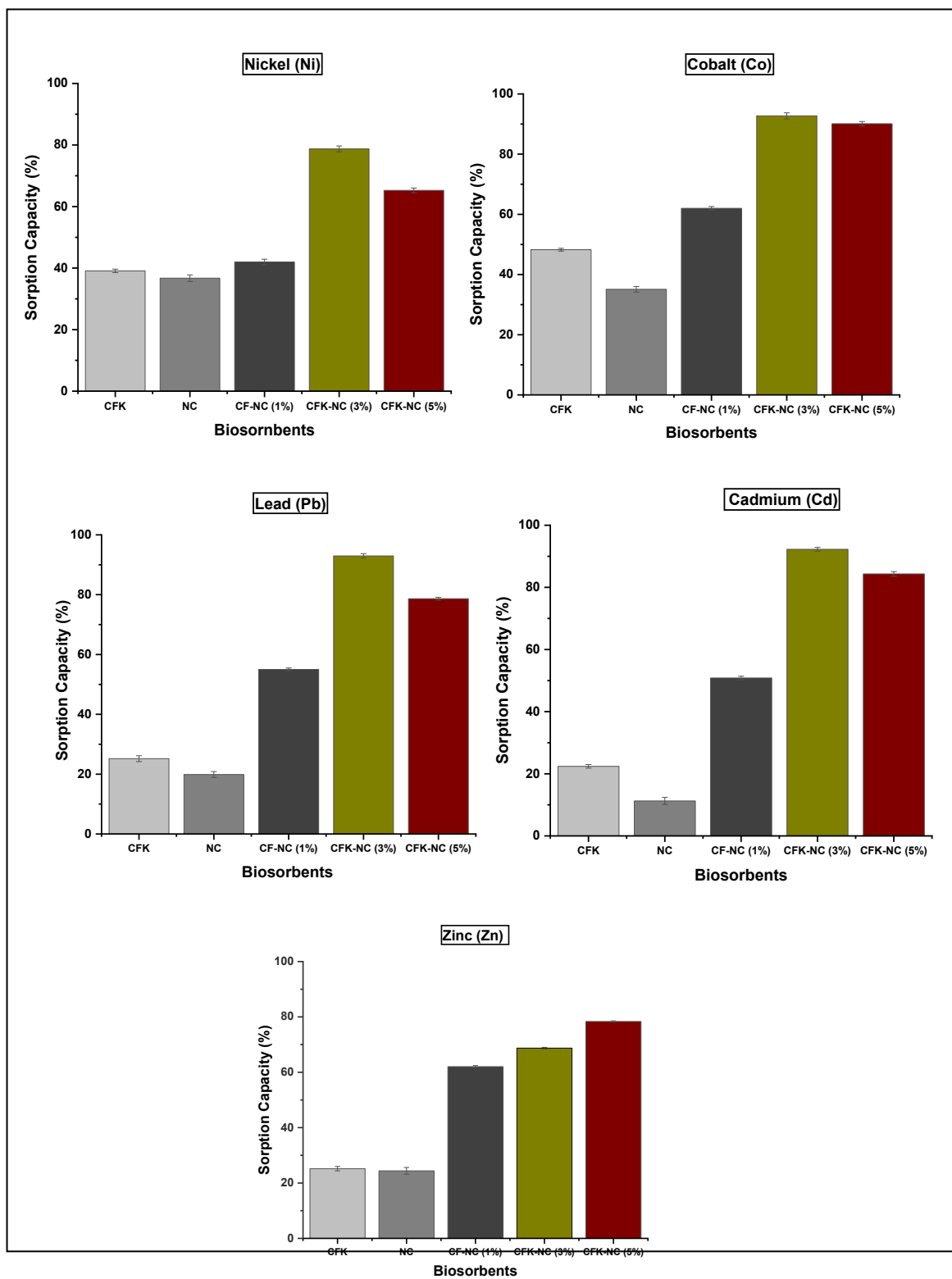


Figure 4.11: Biosorption performance of the keratin-nanochitosan derived biosorbents for cations species ((Ni, Co, Pb, Cd, Zn).

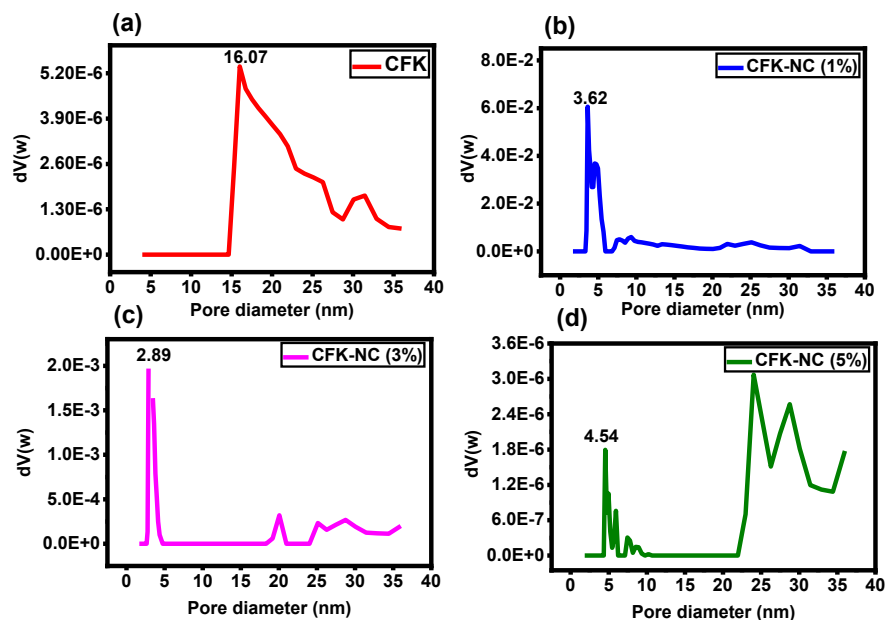


Figure 4.12: Pore size distribution of (a) chicken feather keratin (CFK) (b) CFK contains 1% nanochitosan (c) CFK contains 3% nanochitosan (d) CFK contains 5% nanochitosan using non-linear density functional theory method (NLDFT)

Also, keratin has the inherent ability to adsorb the oxyanions such as arsenic and selenium through the thiol group and can compete with the divalent metal cations biosorption (Khosa & Ullah, 2014; Shen et al., 2013). Biosorption of oxy anion chromium, Cr (VI) (CrO_4^{2-}) at pH 7.5 occurs through electrostatic interaction and reduction with groups such as thiol, amine, and carboxyl groups (KOCATÜRK & Bornova, 2008; Zahara et al., 2021) and exchanges into Cr (III) hydroxide form and can chelate with the free amino groups. (Misra et al., 2001; Park et al., 2007).

Table 4.2: BET surface area of the biosorbents

Characteristics	CFK	CFK-NC (1%)	CFK-NC (3%)	CFK-NC (5%)
S _{BET} (m ² /g)	1.231	2.54	5.62	3.261

Keratin biopolymer possess contains 14 different amino acids and rich with cysteine. The amino acid profile of keratin mainly shows that it has amino, carboxylic, hydroxyl and thiol groups as active sites for the metal biosorption (Alahyaribeik & Ullah, 2020; Khosa & Ullah, 2014). The biosorption efficiency of the material can be determined by the various interaction developed between the metal and biosorbent such as complexion, electrostatic and hydrogen bonding with these active sites. After metal biosorption, SEM images of the biosorbents indicated a rough and glistening surface. Metal sorbed biosorbent has irregular grooves and ridges layers (**Fig. 4.13**) in fibrous networks which are considered essential for the biosorption of heavy metal ions to the biosorbents surface and ultimately to the active sites. Image **4.13 b** presents agglomerates on the biosorbent surface due to the presence of metals biosorption. Overall, surface morphology of the biosorbent turned into coarse, have holes, cracked or damaged (**Fig. 4.13 e**) and were not present in the original biosorbent before the biosorption of metal ions. Similar changes were observed in the previous studies during the metal biosorption process. **Fig. 3.14 c** shows the FTIR spectra of biosorbent after biosorption process of metal-containing polluted water showing that peaks at amide I, II and II (1638, 1509, and 1250 cm⁻¹) have distinct changes in their signal intensities and wavenumbers. Keratin proteins are involved in metal biosorption so their intramolecular interaction between the layers is altered. These suggested that -OH, -COOH and -NH₂ are directly involved in the biosorption process (Chakraborty et al., 2020). After biosorption, the amide A (around 3200 cm⁻¹, circled blue,) region band is broad and shifted to a higher wavenumber, demonstrating that hydroxyl groups are involved in the biosorption process and bonded with

metals through hydrogen bonding. A similar phenomenon is observed in a previous study reported by Liu et al (Liu et al., 2015) where proteins were involved in the biosorption of Pb, Cd and Zn.

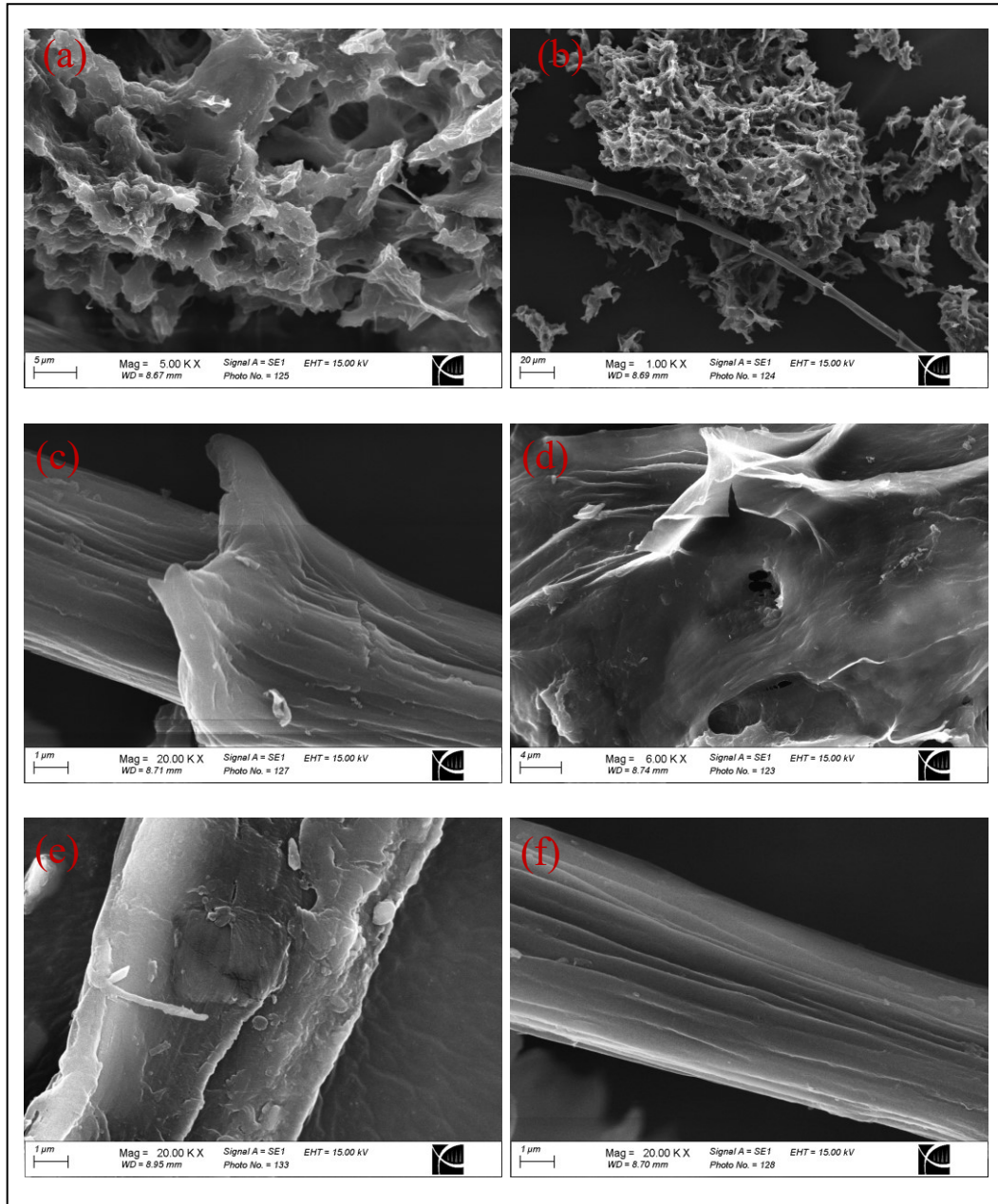


Figure 4.13: SEM images of biosorbent after biosorption from metal-contaminated water

Another type of interaction that may contribute to metal biosorption is through complexation. TGA graph (Fig. 4.14 b) of the biosorbent clearly shows higher stability (29% as

compared to 27%) due to the presence of metal complexes with the keratin biopolymer. Chelation and electrostatic interactions also play important role to metal biosorption. XRD patterns of the metal sorbed biosorbent presented broader peaks compared to sharp peaks in the original biosorbent. Furthermore, peaks shifting towards lower 2θ (10.4 from 11.42) and indication chelation and electrostatic forces developed between the metals and the biosorbent. Kyzas et reported a similar type of interaction between the chitosan derived materials for the heavy metals biosorption (Kyzas et al., 2014).

XPS analysis of the biosorbent indicated three peaks at binding energies of 399.27 and 399.86 eV belong to N atoms of $-\text{NH}_2$ or $-\text{NH}$ eV of keratin biopolymer and nanochitosan, while the third peak at 400.83 eV belongs to NH^{3+} groups of the CFK (**Fig. 4.14 d**) and provides coordination sites for the metal's biosorption. However, after the metal biosorption process, peaks moved to higher 400.55 and 401.85 eV. The decrease in electron cloud density on the nitrogen shift towards a higher binding energy (Yu et al., 2013) because of CFK-NC-NH-M^{2+} or CFK-NC-NH-M formation.

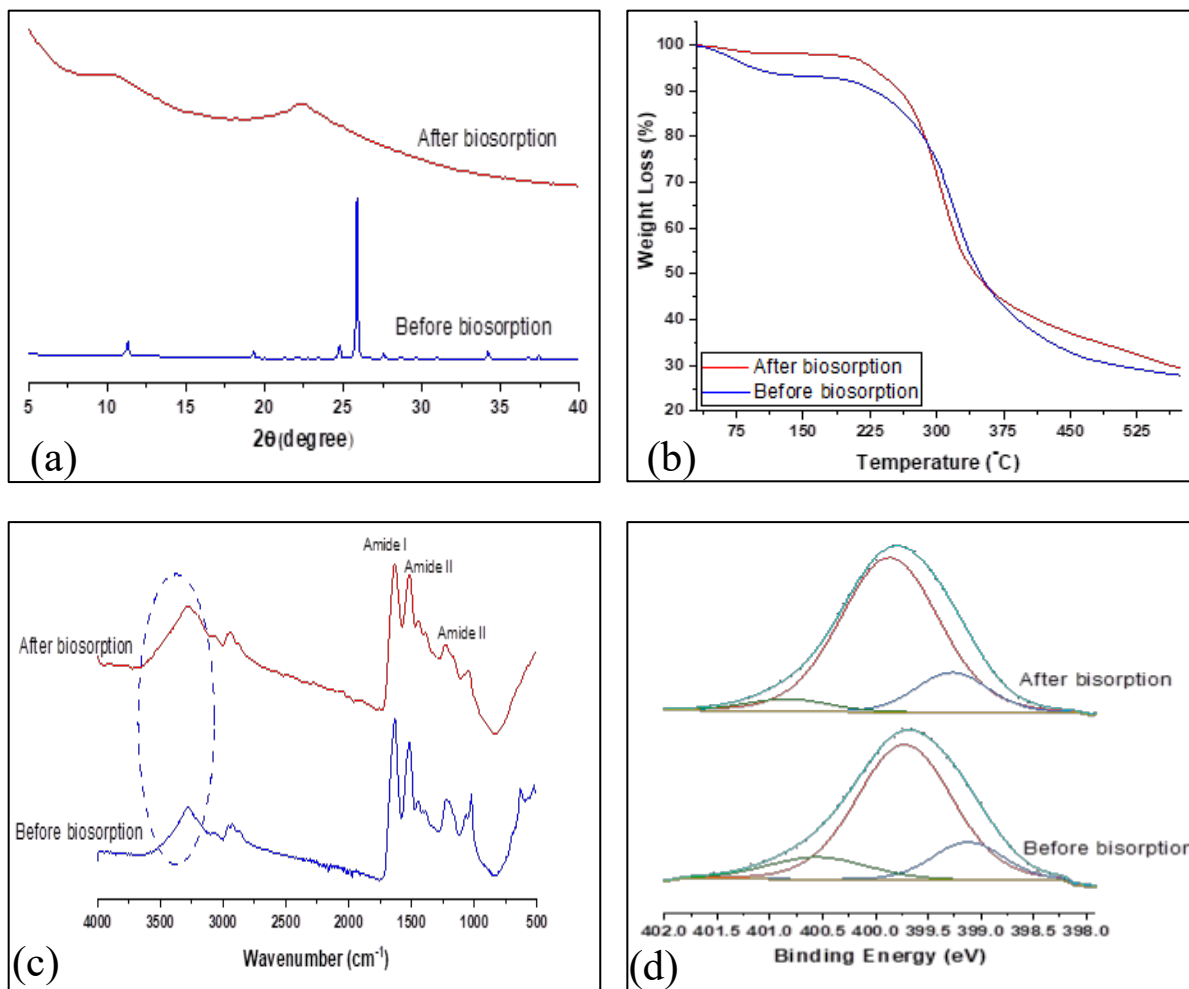


Figure 4.14: Structural elucidation of biosorbent to determine the biosorption mechanism with (a) XRD (b) TGA (c) ATR- FTIR (d) XPS

Overall, we predicted that developed biosorbents sorbed the metals from the contaminated water via complexation, hydrogen bonding, electrostatic interactions, and chelation as shown in **Fig 4.15**.

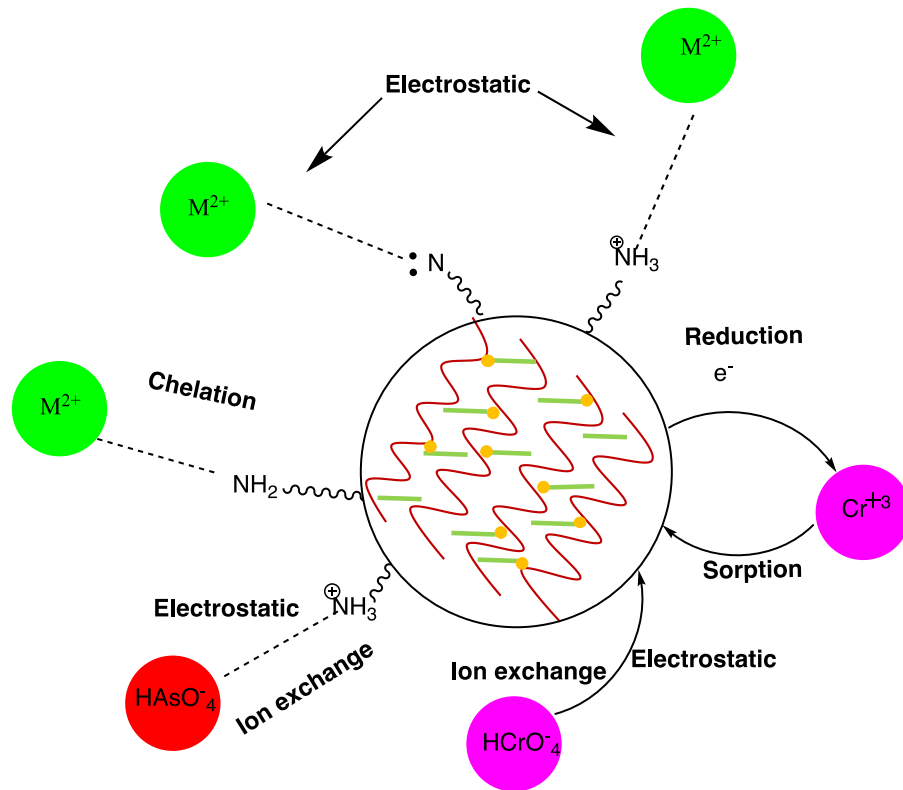


Figure 4.15: Plausible mechanism of metal ions removal from the keratin derived biosorbents

4.4. Conclusions

In this study, we prepared chicken feather keratin derived biosorbents with nanochitosan to improve its biosorption efficiency for metal removal from contaminated water. The nanochitosan was incorporated successfully into the keratin biopolymer through electrostatic and ester bond linkage. ICP-MS analysis showed that chicken feather keratin-nanochitosan based biosorbents have excellent biosorption efficiency for the metals as compared to the unmodified chicken feather keratin. Among biosorbent, CFK-NC containing 3% nanochitosan showed maximum biosorption for As and Se upto 98%, ascribed to its better interactions with the CFK, large surface area and pore size distribution as compared to other biosorbents. The biosorption process is confirmed and a plausible biosorption mechanism is revealed through FT-IR, TGA,

XRD and XPS analysis. It is proposed that keratin-nanochitosan structures capture metal cations and anions through a combination of complexation, hydrogen bonding, electrostatic interactions and chelation. Based on the study findings, demonstrate the excellent biosorption of heavy metal ions by CFK-NC derived biosorbents. This study concluded that chicken feather keratin as a renewable carbon resource is promising biosorbent in large-scale applications for the remediation of industrial wastewater containing multiple heavy metal cations and anions.

4.5. References

- Alahyaribeik, S., & Ullah, A. (2020). Methods of keratin extraction from poultry feathers and their effects on antioxidant activity of extracted keratin. *International Journal of Biological Macromolecules*, 148, 449-456.
- Arshad, M., Kaur, M., & Ullah, A. (2016). Green biocomposites from nanoengineered hybrid natural fiber and biopolymer. *ACS sustainable chemistry & engineering*, 4(3), 1785-1793.
- Arshad, M., Zubair, M., Rahman, S. S., & Ullah, A. (2020). Polymers for advanced applications. In *Polymer Science and Nanotechnology* (pp. 325-340). Elsevier.
- Bhumkar, D. R., & Pokharkar, V. B. (2006). Studies on effect of pH on cross-linking of chitosan with sodium tripolyphosphate: a technical note. *Aaps Pharmscitech*, 7(2), E138-E143.
- Carr, C. M., & Gerasimowicz, W. V. (1988). A carbon-13 CPMAS solid state NMR spectroscopic study of wool: effects of heat and chrome mordanting. *Textile Research Journal*, 58(7), 418-421.
- Chai, W. S., Cheun, J. Y., Kumar, P. S., Mubashir, M., Majeed, Z., Banat, F., Ho, S.-H., & Show, P. L. (2021). A review on conventional and novel materials towards heavy metal adsorption in wastewater treatment application. *Journal of Cleaner Production*, 296, 126589.
- Chakraborty, R., Asthana, A., Singh, A. K., Yadav, S., Susan, M. A. B. H., & Carabineiro, S. A. (2020). Intensified elimination of aqueous heavy metal ions using chicken feathers chemically modified by a batch method. *Journal of Molecular Liquids*, 312, 113475.
- Dinu, R., Briand, N., & Mija, A. (2021). Influence of Keratin on Epoxidized Linseed Oil Curing and Thermoset Performances. *ACS Sustainable Chemistry & Engineering*, 9(46), 15641-15652.
- Dodson, J. R., Parker, H. L., García, A. M., Hicken, A., Asemave, K., Farmer, T. J., He, H., Clark, J. H., & Hunt, A. J. (2015). Bio-derived materials as a green route for precious & critical metal recovery and re-use. *Green Chemistry*, 17(4), 1951-1965.
- Feroz, S., Muhammad, N., Ratnayake, J., & Dias, G. (2020). Keratin-Based materials for biomedical applications. *Bioactive materials*, 5(3), 496-509.
- Fu, F., & Wang, Q. (2011). Removal of heavy metal ions from wastewaters: a review. *Journal of environmental management*, 92(3), 407-418.
- Huang, H., & Yang, X. (2004). Synthesis of chitosan-stabilized gold nanoparticles in the absence/presence of tripolyphosphate. *Biomacromolecules*, 5(6), 2340-2346.
- Idris, A., Vijayaraghavan, R., Rana, U. A., Fredericks, D., Patti, A. F., & Macfarlane, D. R. (2013). Dissolution of feather keratin in ionic liquids. *Green Chemistry*, 15(2), 525-534.
- Idris, A., Vijayaraghavan, R., Rana, U. A., Patti, A. F., & Macfarlane, D. R. (2014). Dissolution and regeneration of wool keratin in ionic liquids. *Green Chemistry*, 16(5), 2857-2864.
- Kahdestani, S. A., Shahriari, M. H., & Abdouss, M. (2021). Synthesis and characterization of chitosan nanoparticles containing teicoplanin using sol-gel. *Polymer Bulletin*, 78(2), 1133-1148.
- Kaur, M., Arshad, M., & Ullah, A. (2018). In-situ nanoreinforced green bionanomaterials from natural keratin and montmorillonite (MMT)/cellulose nanocrystals (CNC). *ACS Sustainable Chemistry & Engineering*, 6(2), 1977-1987.
- Khosa, M. A., & Ullah, A. (2014). In-situ modification, regeneration, and application of keratin biopolymer for arsenic removal. *Journal of hazardous materials*, 278, 360-371.

- KOCATÜRK, S., & Bornova, I. (2008). REMOVAL OF HEAVY METAL IONS FROM AQUEOUS SOLUTIONS BY KERATIN. *Chemical Engineering*, 603, 00.
- Kyzas, G. Z., Siafaka, P. I., Lambropoulou, D. A., Lazaridis, N. K., & Bikiaris, D. N. (2014). Poly (itaconic acid)-grafted chitosan adsorbents with different cross-linking for Pb (II) and Cd (II) uptake. *Langmuir*, 30(1), 120-131.
- Liu, W., Zhang, J., Jin, Y., Zhao, X., & Cai, Z. (2015). Adsorption of Pb (II), Cd (II) and Zn (II) by extracellular polymeric substances extracted from aerobic granular sludge: efficiency of protein. *Journal of Environmental Chemical Engineering*, 3(2), 1223-1232.
- Lo, Y.-C., Cheng, C.-L., Han, Y.-L., Chen, B.-Y., & Chang, J.-S. (2014). Recovery of high-value metals from geothermal sites by biosorption and bioaccumulation. *Bioresource technology*, 160, 182-190.
- Ma, B., Qiao, X., Hou, X., & Yang, Y. (2016). Pure keratin membrane and fibers from chicken feather. *International journal of biological macromolecules*, 89, 614-621.
- Martinez-Hernandez, A. L., Velasco-Santos, C., De Icaza, M., & Castano, V. M. (2005). Microstructural characterisation of keratin fibres from chicken feathers. *International journal of environment and pollution*, 23(2), 162-178.
- Menefee, E., & Yee, G. (1965). Thermally-induced structural changes in wool. *Textile Research Journal*, 35(9), 801-812.
- Misra, M., Kar, P., Priyadarshan, G., & Licata, C. (2001). Keratin protein nano-fiber for removal of heavy metals and contaminants. *MRS Online Proceedings Library (OPL)*, 702.
- Park, D., Lim, S.-R., Yun, Y.-S., & Park, J. M. (2007). Reliable evidences that the removal mechanism of hexavalent chromium by natural biomaterials is adsorption-coupled reduction. *Chemosphere*, 70(2), 298-305.
- Peydayesh, M., & Mezzenga, R. (2021). Protein nanofibrils for next generation sustainable water purification. *Nature communications*, 12(1), 1-17.
- Rodzic, A., Pomastowski, P., Sagandykova, G. N., & Buszewski, B. (2020). Interactions of whey proteins with metal ions. *International journal of molecular sciences*, 21(6), 2156.
- Šafarič, R., Fras Zemljič, L., Novak, M., Dugonik, B., Bratina, B., Gubeljak, N., Bolka, S., & Strnad, S. (2020). Preparation and characterisation of waste poultry feathers composite fibreboards. *Materials*, 13(21), 4964.
- Saha, S., Zubair, M., Khosa, M., Song, S., & Ullah, A. (2019). Keratin and chitosan biosorbents for wastewater treatment: a review. *Journal of Polymers and the Environment*, 27(7), 1389-1403.
- Senoz, E., & Wool, R. P. (2010). Microporous carbon–nitrogen fibers from keratin fibers by pyrolysis. *Journal of applied polymer science*, 118(3), 1752-1765.
- Sharma, P., Singh, S. P., Parakh, S. K., & Tong, Y. W. (2022). Health hazards of hexavalent chromium (Cr (VI)) and its microbial reduction. *Bioengineered*, 13(3), 4923-4938.
- Shen, S., Li, X.-F., Cullen, W. R., Weinfeld, M., & Le, X. C. (2013). Arsenic binding to proteins. *Chemical reviews*, 113(10), 7769-7792.
- Tonin, C., Zoccola, M., Aluigi, A., Varesano, A., Montarsolo, A., Vineis, C., & Zimbardi, F. (2006). Study on the conversion of wool keratin by steam explosion. *Biomacromolecules*, 7(12), 3499-3504.
- Tsukada, M., Freddi, G., Monti, P., Bertoluzza, A., & Kasai, N. (1995). Structure and molecular conformation of tussah silk fibroin films: Effect of methanol. *Journal of Polymer Science Part B: Polymer Physics*, 33(14), 1995-2001.

- Vijayalakshmi, K., Devi, B., Sudha, P., Venkatesan, J., & Anil, S. (2016). Synthesis, characterization and applications of nanochitosan/sodium alginate/microcrystalline cellulose film. *J. Nanomed. Nanotechnol*, 7(6).
- Wan, Y., Creber, K. A., Peppley, B., & Bui, V. T. (2003). Synthesis, characterization and ionic conductive properties of phosphorylated chitosan membranes. *Macromolecular Chemistry and Physics*, 204(5-6), 850-858.
- Wang, J., & Chen, C. (2009). Biosorbents for heavy metals removal and their future. *Biotechnology advances*, 27(2), 195-226.
- Wang, X., Xi, Z., Liu, Z., Yang, L., & Cao, Y. (2011). The fabrication and property of hydrophilic and hydrophobic double functional bionic chitosan film. *Journal of Nanoscience and Nanotechnology*, 11(11), 9737-9740.
- Werber, J. R., Osuji, C. O., & Elimelech, M. (2016). Materials for next-generation desalination and water purification membranes. *Nature Reviews Materials*, 1(5), 1-15.
- Witus, L. S., & Francis, M. B. (2011). Using synthetically modified proteins to make new materials. *Accounts of chemical research*, 44(9), 774-783.
- Yang, C.-H., Lin, Y.-S., Huang, K.-S., Huang, Y.-C., Wang, E.-C., Jhong, J.-Y., & Kuo, C.-Y. (2009). Microfluidic emulsification and sorting assisted preparation of monodisperse chitosan microparticles. *Lab on a Chip*, 9(1), 145-150.
- Yasmeen, K., Saeed, I., & Zubair, M. (2022). Estimations of Potential Risk of Carcinogenic Arsenic in Smokeless Tobacco Products. *New Journal of Chemistry*.
- Yu, Z., Zhang, X., & Huang, Y. (2013). Magnetic chitosan–iron (III) hydrogel as a fast and reusable adsorbent for chromium (VI) removal. *Industrial & engineering chemistry research*, 52(34), 11956-11966.
- Zahara, I., Arshad, M., Naeth, M. A., Siddique, T., & Ullah, A. (2021). Feather keratin derived sorbents for the treatment of wastewater produced during energy generation processes. *Chemosphere*, 273, 128545.
- Zhang, W., Zhang, J., Jiang, Q., & Xia, W. (2012). Physicochemical and structural characteristics of chitosan nanopowders prepared by ultrafine milling. *Carbohydrate Polymers*, 87(1), 309-313.
- Zhang, Y., Zhang, X., Ding, R., Zhang, J., & Liu, J. (2011). Determination of the degree of deacetylation of chitosan by potentiometric titration preceded by enzymatic pretreatment. *Carbohydrate Polymers*, 83(2), 813-817.
<https://doi.org/https://doi.org/10.1016/j.carbpol.2010.08.058>
- Zhang, Y., Zhao, W., & Yang, R. (2015). Steam flash explosion assisted dissolution of keratin from feathers. *ACS Sustainable Chemistry & Engineering*, 3(9), 2036-2042.
- Zubair, M., Arshad, M., & Ullah, A. (2020). Chitosan-based materials for water and wastewater treatment. In *Handbook of chitin and chitosan* (pp. 773-809). Elsevier.
- Zubair, M., Arshad, M., & Ullah, A. (2021). Nanocellulose: A sustainable and renewable material for water and wastewater treatment. In *Natural Polymers-Based Green Adsorbents for Water Treatment* (pp. 93-109). Elsevier.
- Zubair, M., & Ullah, A. (2021). Biopolymers in environmental applications: industrial wastewater treatment. *Biopolymers and their industrial applications*, 331-349.

CHAPTER 5: Green Nanoengineered Keratin Derived Biosorbents with Acryl Amide Modified Graphene Oxide for Heavy Metal Ions Removal from Synthetic Wastewater

5.1. Introduction

Water is considered one of the fundamental human rights. However, one in every three humans does not have access to clean drinking water around the globe (Ahmed et al., 2022; Goswami & Bisht, 2017; Peydayesh & Mezzenga, 2021). Due to water shortage, availability of clean Water was included as a 6th sustainable development goal at the 2015 UN Sustainable Development Summit for 2030 to ensure access to and sustainable management of water and sanitation for everyone. Besides, clean and safe water is the prime factor in achieving individual sustainable development goals (Dagerskog & Olsson, 2020).

Environmental calamities, ever-growing population and urbanization are worsening aspects of maintaining a safe and sustainable water supply (Organization, 2019). There are various sources of water contamination including the industrial and agricultural sectors, mining, urban activities and landfills which are directly released into the world's water bodies (Ahmed et al., 2022; Krishnan et al., 2021). These activities heavily pollute the water resources and contribute to toxic compounds such as organics, metal ions and micropollutants (Liu et al., 2021; Walker et al., 2019). Worldwide, nearly 2 million tons of wastewater are discharged daily into water bodies from industrial, sewage and agricultural sectors (Connor, 2015). As a result, millions of people are sick and 14000 people die every day (Bolisetty et al., 2019).

Several water remediation techniques such as nanofiltration, reverse osmosis distillation and adsorption have been used to alleviate this dreadful situation (Ahmed et al., 2022;

Bhattacharya et al., 2018; Bi et al., 2021). Though these approaches may have high removal efficiency for pollutants, they rarely can be considered green and sustainable fields (Qasem et al., 2021; Wang et al., 2021). Among these, contaminants removal using adsorption is an exciting technology because of its low investment and operational costs, the least energy needs and most significantly, adsorbing materials can be extracted from waste or by-products. Therefore, utilizing these waste resources as adsorbing material having low environmental footprints is prudent (Bolisetty et al., 2019). Green chemistry provides the solution to this challenge where efficient use of renewable raw materials is urging for the production and application of chemical products (Anastas & Warner, 1998).

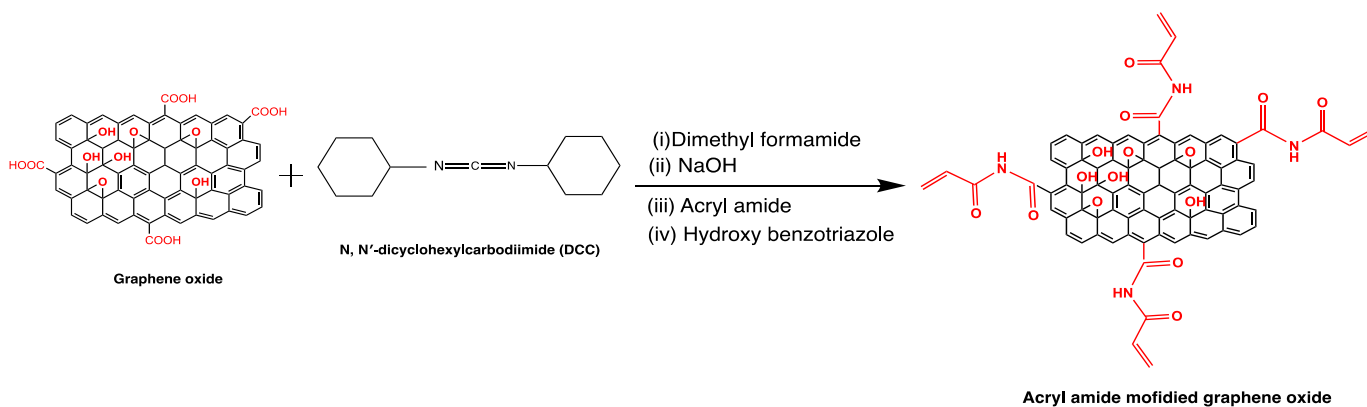
Keratin is an omnipresent polymer in mammals, avians and reptilians including nails, hair, skin, feathers, gecko pads, horns, claws, scales, hagfish slime, hooves, whale baleen and beaks (Feroz et al., 2020; Lazarus et al., 2021; Saha, Arshad, et al., 2019; Saha, Zubair, et al., 2019). Keratin has a broad range of architectures with multifaced functions that have led to developing various keratin derived materials with tailored properties for water remediation. Consequently, keratin's structural diversity serves as a design template for the next generation of nanoengineered adsorbing materials for heavy metals removal from the aqueous media (Lazarus et al., 2021). The keratinous materials' ability enables them to perform diverse functions due to their structural ingeniousness and tunability (Saha, Arshad, et al., 2019; Saha, Zubair, et al., 2019). Thus, they have become an excellent candidate for the biosorption process and have been applied as a functional material for water remediation from inorganic ions as environmentally sustainable and green materials (Chilakamarry et al., 2021; Dodson et al., 2015). However, keratin derived biosorbents have low biosorption efficiency or are very selective towards a specific pollutant.

Herein, we aimed to improve the keratin's performance as a multifunctional polymeric material to be used in developing biosorbents for heavy metals removal from contaminated water. The active sites of the chicken feather keratin (CFK) can be exposed by the chemical modification with surface modified graphene oxide to improve the removal efficiency of the inorganic contaminants from the contaminated water. To achieve this, graphene oxide (GO) was modified with acryl amide to introduce the acryl amide group on the graphene oxide surface. The purpose of introducing an acrylic group on the graphene oxide is to facilitate the polymerization with the CFK which can give a more organized, compact structure to protein and makes them more effective for inorganic contaminants removal from polluted water.

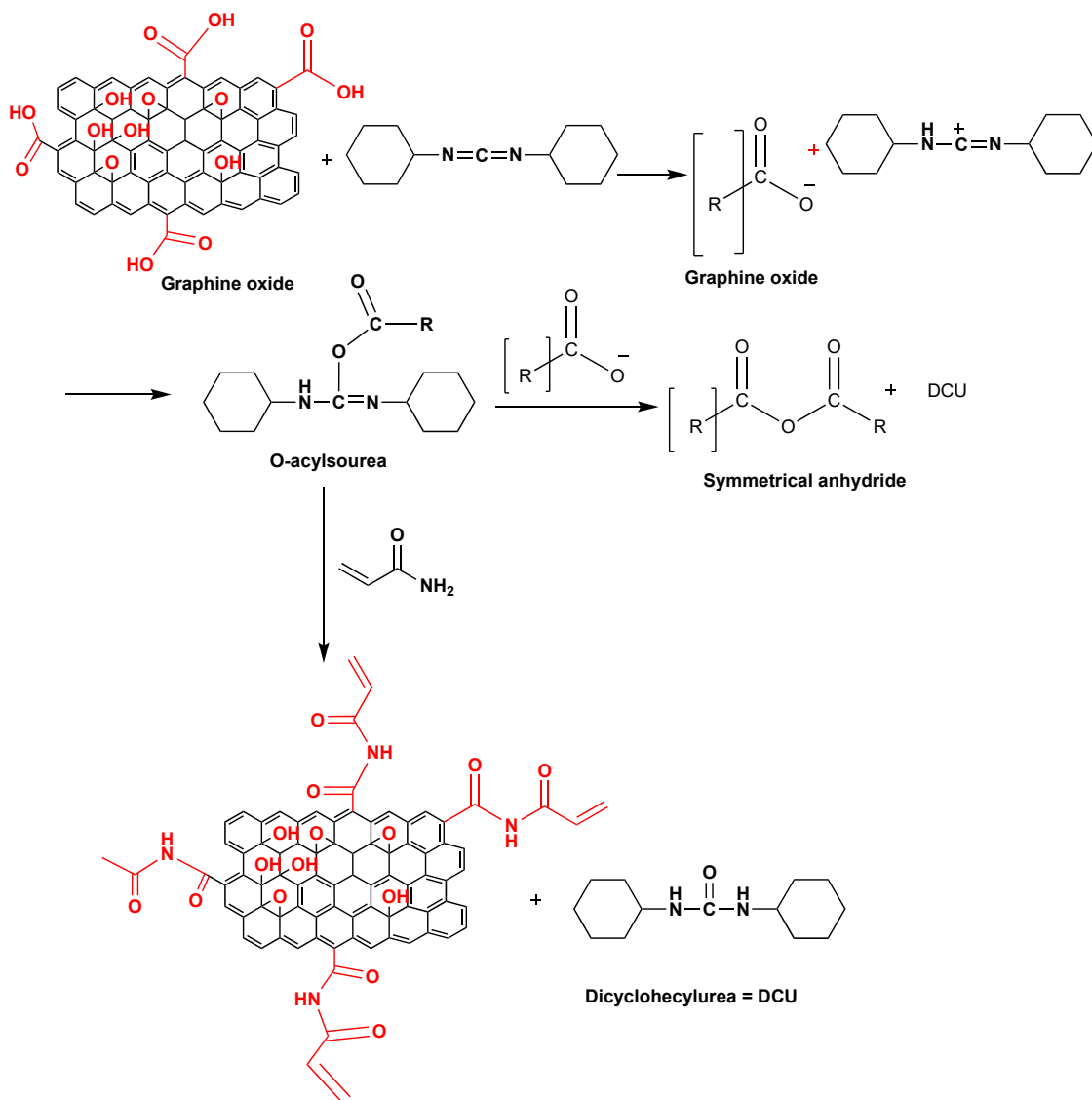
5.2. Experimental strategy

N, N'-dicyclohexylcarbodiimide (DCC) is often used an additive and most used methods of coupling segment with hydroxy benzotriazole (HoBt) as the most efficient additives. The additive is essential to reduce isomerization to acceptable levels.

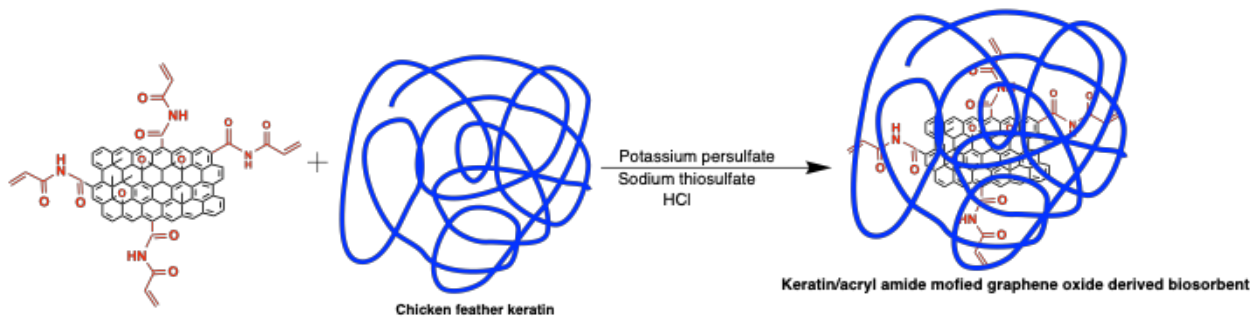
(a) Synthesis of acryl modified graphene oxide



Mechanism:



(b) Preparation of keratin/acryl modified graphene oxide derived biosorbent



5.3. Results & Discussions

5.3.1. Structural analysis

ATR-FTIR spectra of graphene oxide and modified graphene oxide with acryl amide are shown in **Fig. 5.1**. Graphene oxide modified with the acryl amide exhibited several new peaks. The carboxylic carbonyl signal (1738 cm^{-1}) of the graphene oxide was disappeared after acryl amide was incorporated into the graphene oxide and a new transmission band at 1624 cm^{-1} was appeared which can be ascribed to the -C=O of the amide group. In addition, two new transmissions at 1566 and 3317 cm^{-1} belonged to the -NH bending and stretching respectively. All these changes confirmed the modification of graphene oxide with the acryl amide.

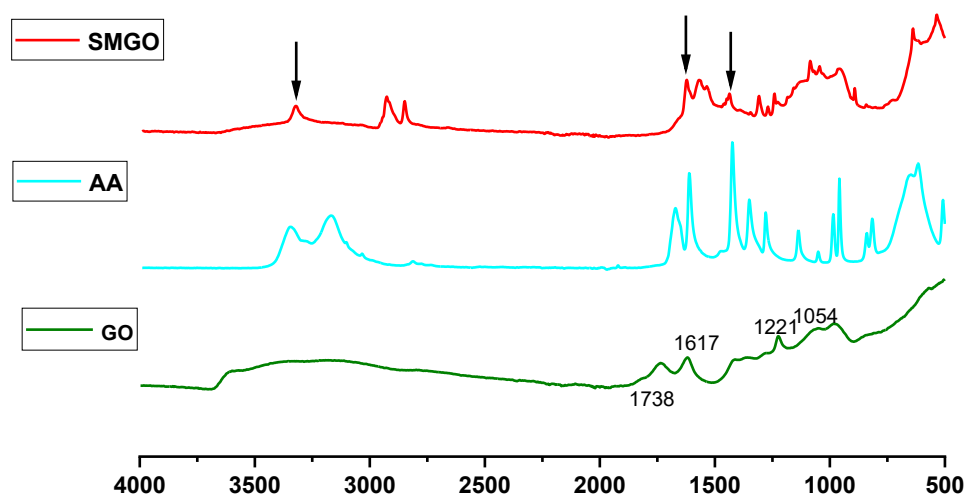


Figure 5.1: ATR-FTIR spectra of GO, AA and SMGO

The surface modified graphene oxide (SMGO) was further polymerized with the chicken feather keratin and ATR-FTIR as shown in **Fig. 5.2(a)**. The transmission band of the CFK at 3274 cm^{-1} was shifted to the higher wavenumber and a new sharp peak at 3325 cm^{-1} was observed which clearly indicated the modification of CFK with surface modified graphene oxide. Furthermore,

two strong transmission band at 2927 and 2850 cm^{-1} corresponds to the C-H and =C-H, respectively. These characteristics differences in peaks confirmed the presence of surface modified graphene oxide into the CFK.

In XPS spectra (**Fig. 5.2 b**), three peaks were observed in CFK at 284.99, 285.99 and 288.29 eV bonding energies and assigned to C-C/C-H, C-O / C-N and C = O / C-O-C bonds, respectively. On the other hand, grafting of acrylamide modified graphene oxide on the CFK gave peaks at bonding energies of 285.76, 286.44, 287.54 and 289.51 eV. The shift of peaks towards higher bonding energies in the case of C-C/C-H, C-O / C-N and towards lower for C = O / C-O-C bonds is ascribed to the interaction of SMGO with the CFK. One new peak was also observed in the XPS spectra of CFK-SMGO at 289.51 and assigned to ester linkage (-O-C=O), which confirms the successful grafting of SMGO on the CFK surface. A similar phenomenon was observed by Arshad and coworkers while grafting acryl POSS on the surface of the keratin fiber (Arshad et al., 2016).

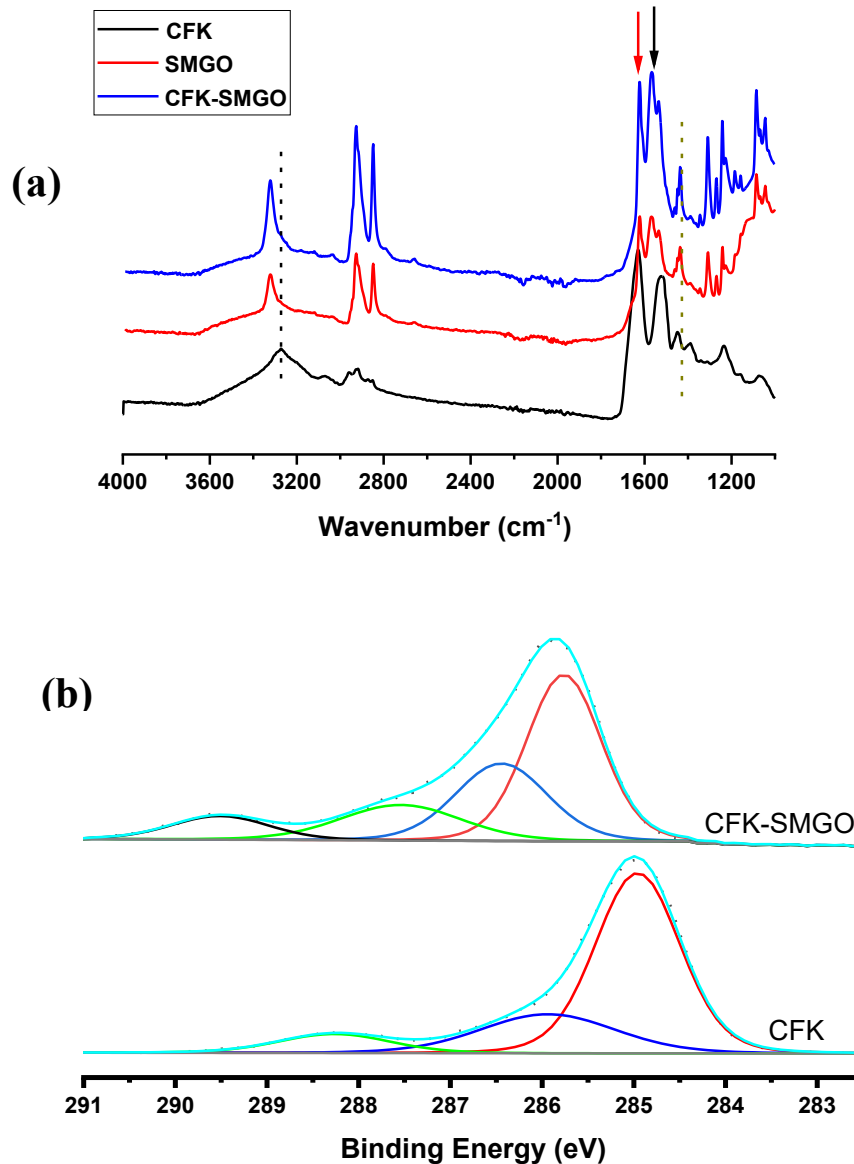


Figure 5.2: ATR-FTIR (a) and XPS spectra of CFK and CFK-SMGO biosorbent

The synthesized GO exhibited a sharp peak at 2θ of 10.30° with a d-spacing of around 8.80°A which was increased due to the presence of oxygenated (hydroxyl, epoxy and carbonyl) functional groups during the chemical exfoliation of graphite. Upon acrylamide functionalization on the GO surface, d-spacing was further enlarged to around 10°A at 2θ of 8.98° as shown in **Fig. 5.3**. which revealed that the surface of the graphene oxide is functionalized with the acryl amide

group. A similar phenomenon was observed when the amine group was introduced onto the GO surface (Pravin & Gnanamani, 2018). The interaction of the acryl amide with the GO may reduce the crystallinity of the graphite sheets which causes the main diffraction peak towards a 2θ at lower angle (Chen et al., 2015). These variations support the successful functionalization of GO with acrylamide.

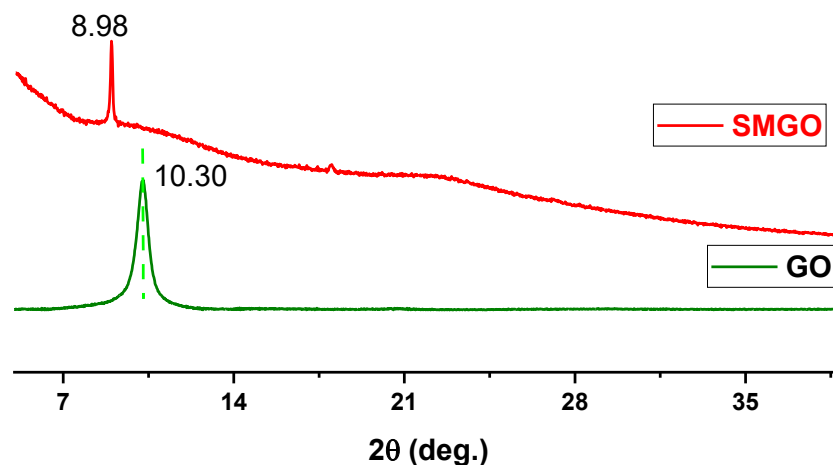


Figure 5.3: XRD patterns of GO and SMGO

The neat chicken feather keratin had two broad peaks belonging to α -helix and β -sheet structure at about $2\theta = 9.66^\circ$ and 19.50° , respectively (Idris et al., 2013; Khosa & Ullah, 2014). However, XRD patterns of CFK changed after incorporating surface modified (acrylamide functionalized) graphene oxide a clearly visible in **Fig. 5.4**. The CFK-SMGO derived biosorbent had no clear α -helix and β -sheet structure peaks which overlapped and one broad peak appeared instead. This change clearly depicts the disruption in the crystallinity pattern of the CFK due to the addition or polymerization of SMGO with the polymeric matrix.

Table 5.1: % Crystallinity of CFK and CFK-SMGO biosorbent

Sample codes	CFK	CFK-SMGO
Crystallinity (%)	60.2	15.59

The % crystallinity of the CFK was reduced to 15.59 from 60.2% after the addition of SMGO. In addition, new crystallinity peaks appeared at 2θ around 21, 22, 28, 30, and 32 which confirms the presence of new crystallinity regions due to the new interaction developed between the chicken feather keratin and surface modified graphene oxide (Arshad et al., 2016).

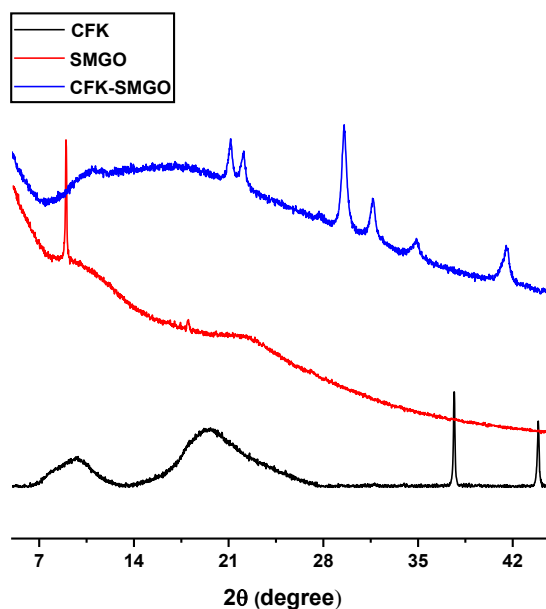


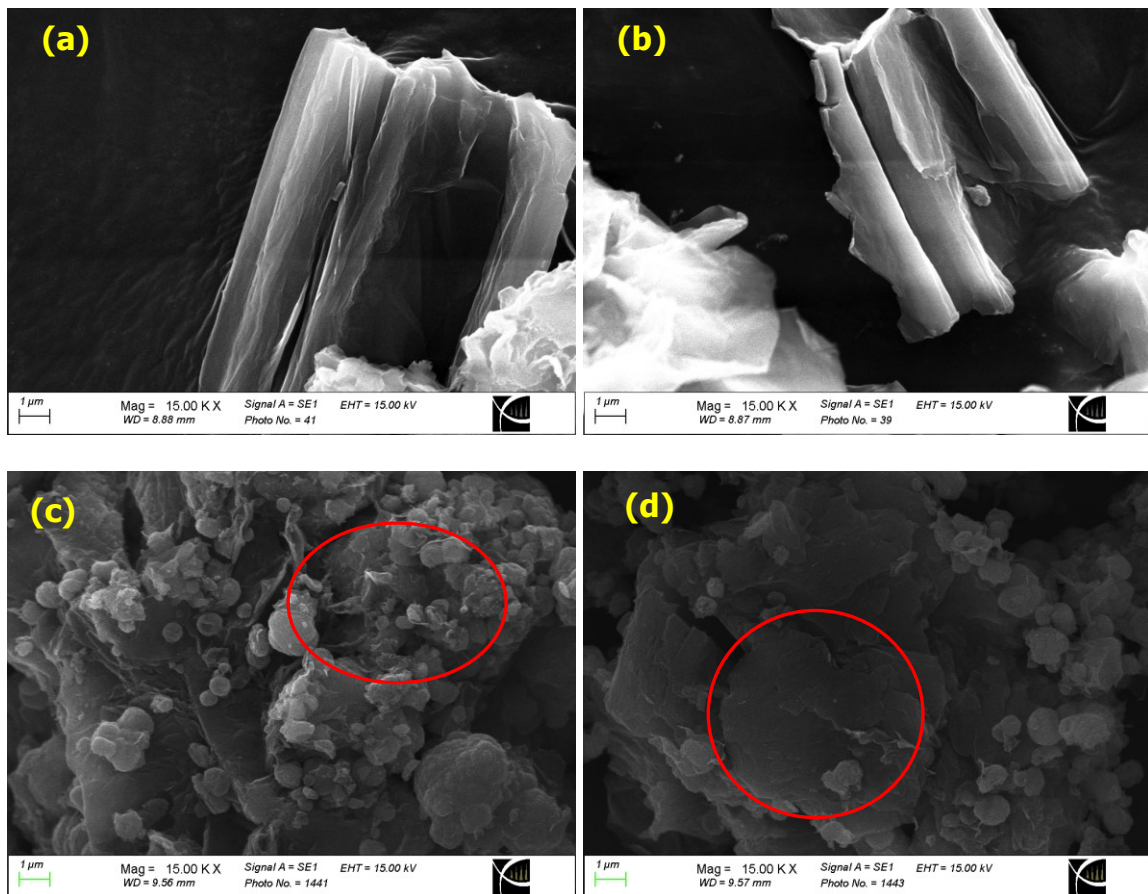
Figure 5.4: XRD patterns of CFK, SMGO and CFK-SMGO biosorbents

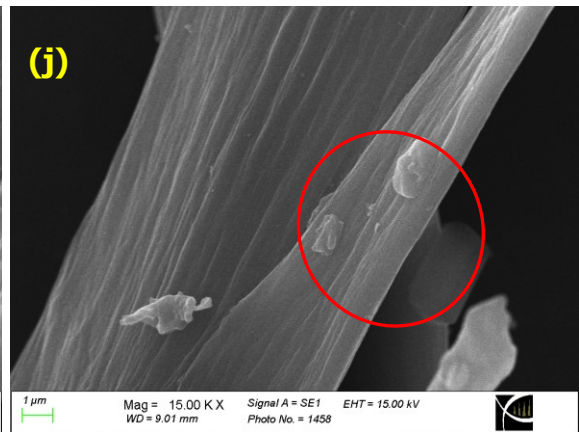
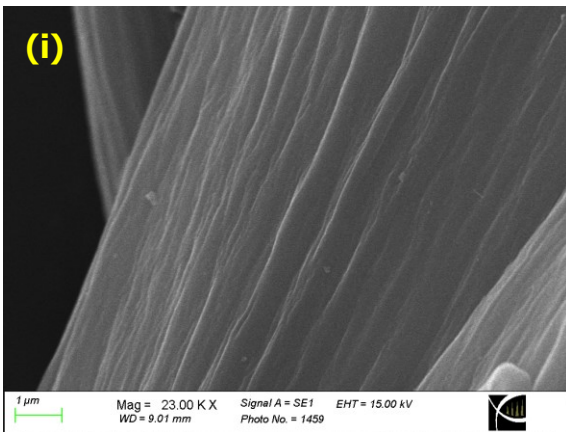
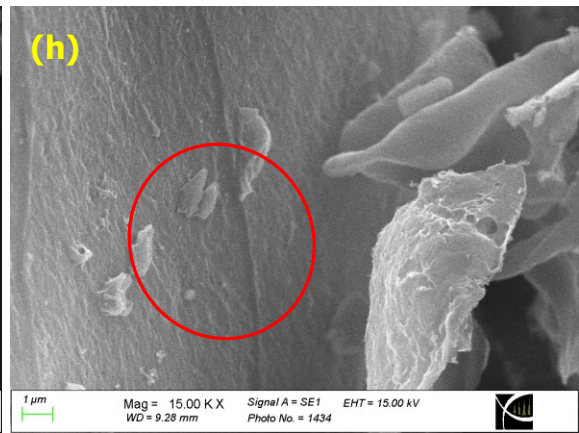
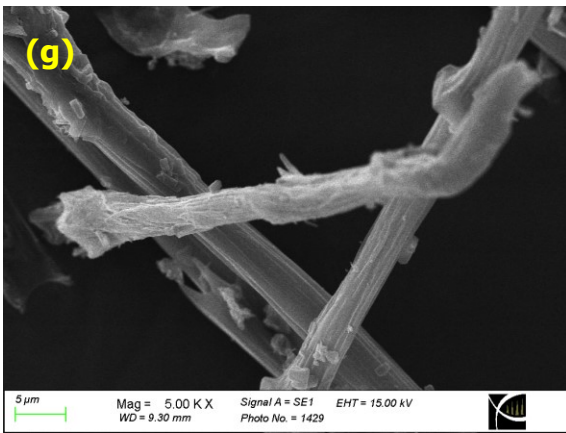
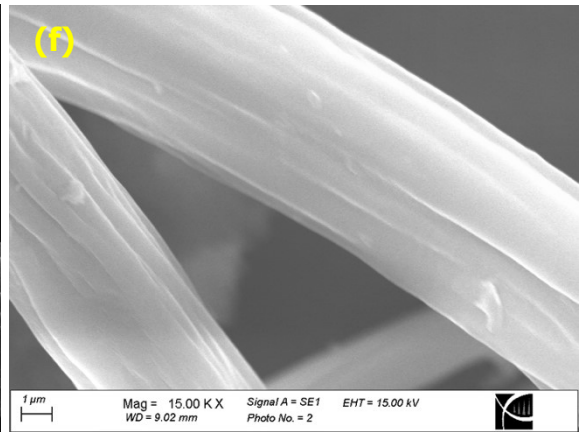
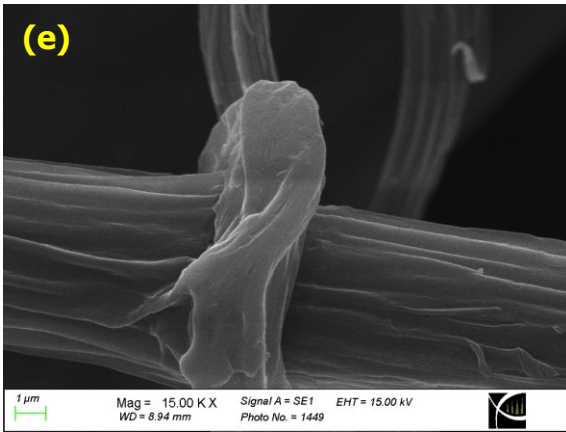
5.3.2. Surface morphology and internal structure

Scanning electron microscope images of the graphene oxide (**Fig. 5.5 a-b**) revealed wrinkled nano buds of a paper-like structure which resembles a jasmine flower. However, the morphology of the graphene oxide was changed tremendously as exhibited in images **Fig. 5.5 c-d**, indicating the surface modification of GO with acryl amide. The surface modified graphene

oxide displayed small spherical structures on the GO surface that contributed due to the acrylamide modification. In addition, surface roughness was increased after the modification with acrylamide.

The surface modified graphene oxide was introduced into the chicken feather keratin which altered its surface morphology as clearly seen in SEM images from **Fig. 5.5 g-l**. The original innate structure of the CFK disappeared due to SMGO on the surface of the polymeric protein matrix. The surface of the keratin turned porous, as seen in **Fig. 5.5 h**. The small blocks or spots (**Fig. 5.5 j-k**) can be observed on the surface of CFK which can be ascribed to the presence of SMGO on the keratin surface.





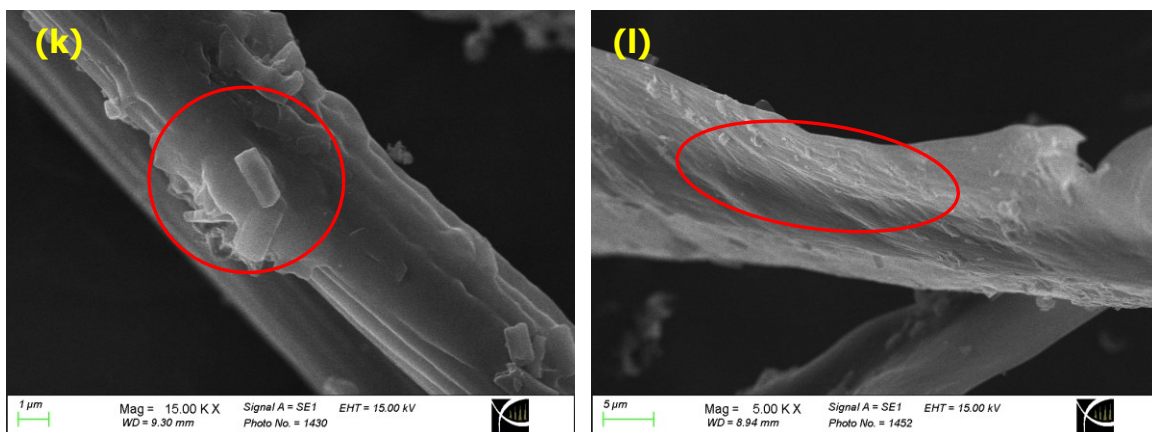


Figure 5.5: SEM images of (a-b) GO (c-d) SMGO (e-f) CFK (g-l) CFK-SMGO biosorbent

The inner structural changes were observed using TEM and exhibited many flat layers of sheets as shown in **Fig. 5.6**. TEM images of SMGO have darker contrast as compared to GO. These dark regions can be ascribed to the presence of acrylamide ground demonstrating the successful introduction on the GO surface (**Fig. 5.6 b**).

The surface modified GO was incorporated into the CFK, changing its internal structure. The neat chicken feather keratin typically indicated dark regions however the addition of SMGO altered the inner structure which showed darker and lighter regions which confirmed the presence of SMGO in the polymeric matrix.

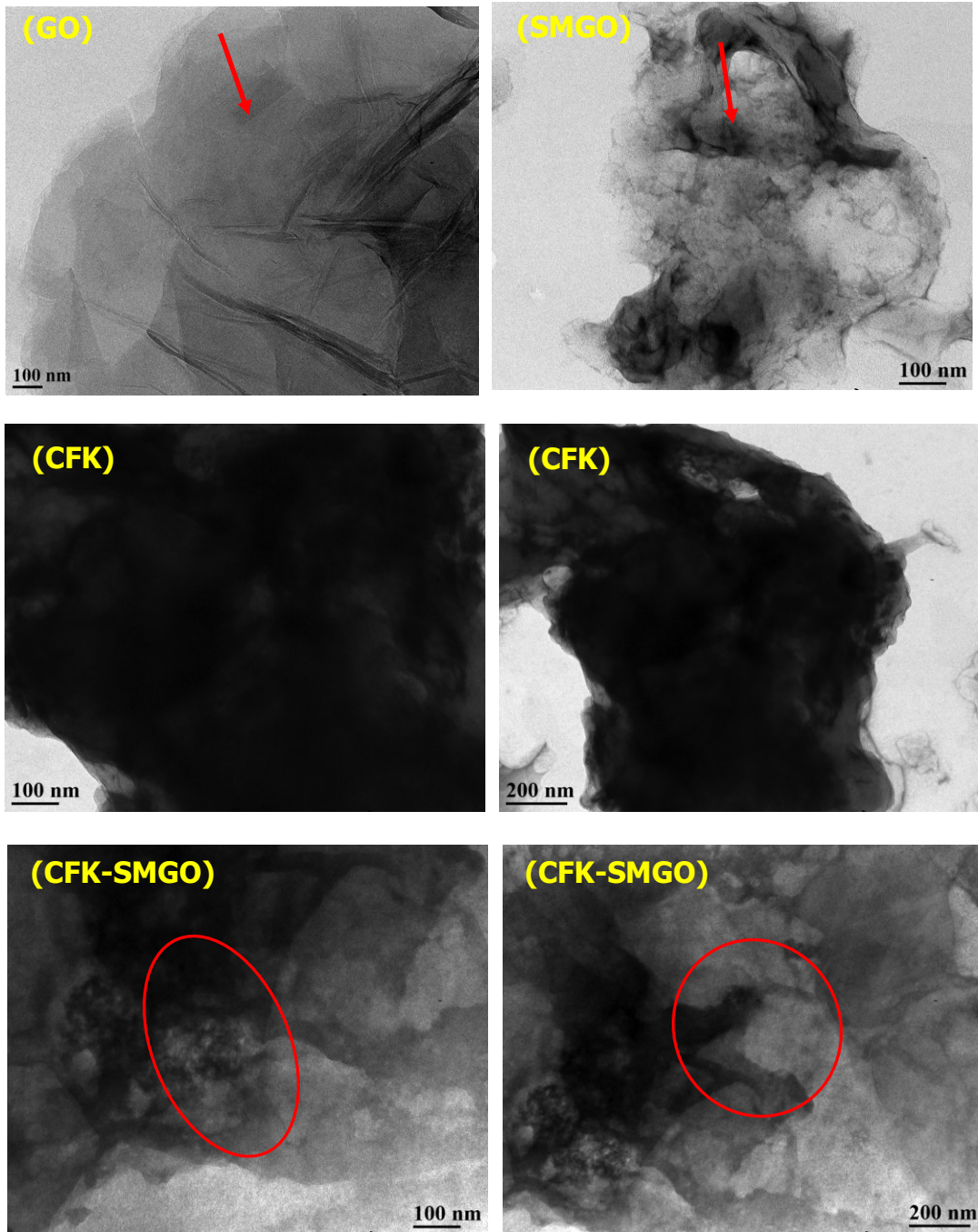


Figure 5.6: TEM images of GO, SMGO) CFK and CFK-SMGO derived biosorbent

5.3.3. Thermal properties

Fig. 5.7 depicts the thermogravimetric (TG) and derivative thermogravimetric (DTG) thermograms of graphene oxide (GO) and surface modified graphene oxide (SMGO). Graphene oxide (GO) is thermally unstable and loses weight in three steps. The 1st loss starts at around 100 °C. The second stage is a major loss, around 229 °C and the final stage starts after 350 °C. Oxygenated groups such as hydroxyl and carboxyl groups and intercalated water, are released in the form of CO, CO₂ and steam during this stage (Jeong et al., 2009; Marcano et al., 2010). The third stage loss is slow and starts from 350 °C to 900 °C. Graphene oxide exhibited a major weight loss of about 55% in the temperature range of 90-228 °C related to the breakdown of labile oxygen containing functionalities and demonstrating a lower thermal stability (Zangmeister, 2010). This weight loss can be attributed to decomposing the most stable oxygen functionalities such as the carbonyl (Park et al., 2011).

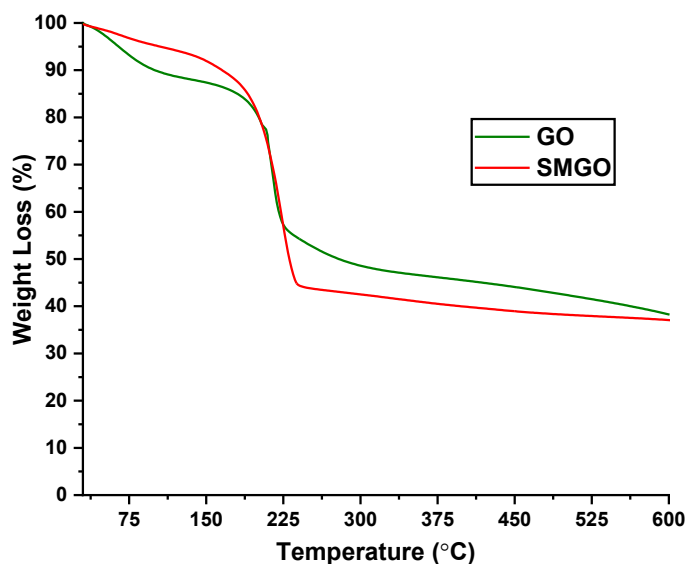


Figure 5.7: Thermo-gravimetric analysis (TGA) of GO and SMGO

The acryl amide functionalized GO presented less weight (~5%) loss below 100 °C which was designated to the acryl amide group attachment which replaced the carboxylic group that

lessened the amount of adsorbed water (Shanmugharaj et al., 2013). The graphene oxide GO indicated a weight loss of about ~12% related to the evaporation of the attached water molecules in the GO (Choudhary et al., 2012). The significant weight loss of the acryl amide modified GO of about ~41% from 200–225 °C, was ascribed to the thermal decomposition of acrylamide groups on the graphene oxide. The DTG curves of the GO and SMGO are shown in **Fig. 5.8**, clearly showing higher degradation temperature for SMGO reinforced by the degradation of the chemical grafting of acryl amide inserted between the GO sheets. The DTG curve of graphene oxide showed maximum weight loss at 208.14 °C. However, this weight loss is shifted to 226.20 °C in surface modified graphene oxide due to the decomposition of acryl amide groups.

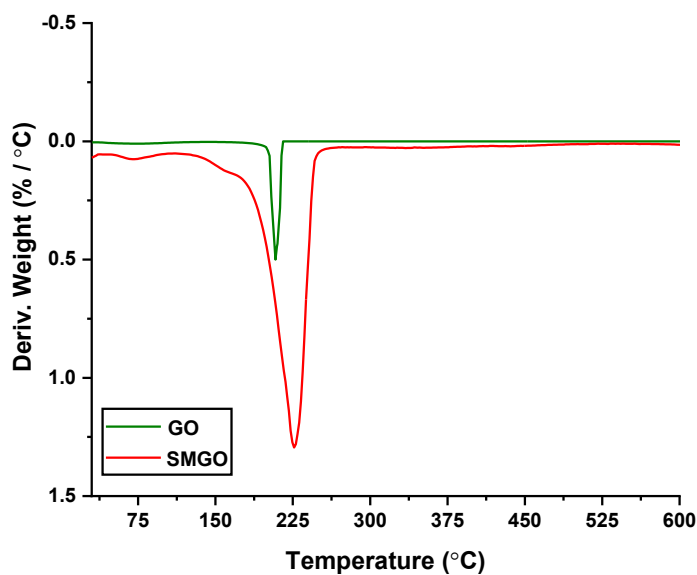


Figure 5.8: DTG of GO and SMGO

Fig. 5.9 represents the thermogravimetric (TG) of chicken feather keratin and derived biosorbent after introducing SMGO into the keratin polymeric matrix. The thermal stability of the SMGO grafted keratin biopolymer was better as is apparent from the TGA curves. The neat CFK was decomposed upto 84% at around 600 °C. On the other hand, grafting of SMGO decreased the

decomposition upto 74%. The thermal stability of the CFK was increased, attributed to the grafting of the surface modified graphene oxide to the keratin biopolymer. The TGA curve displays degradation of keratin biopolymer consists of 3 distinct stages. In the first stage, mass loss at around 90 °C depicts moisture removal from the keratin. The second stage decomposition was sharp and ranged from 230- 376 °C in the chicken feather keratin (10-68% weight loss) nonetheless, SMGO grafted chicken feather keratin this sharp loss was not observed after 355 °C and loss reached upto 54%. This difference in behavior is contributed by the grating of SGMO on the CFK.

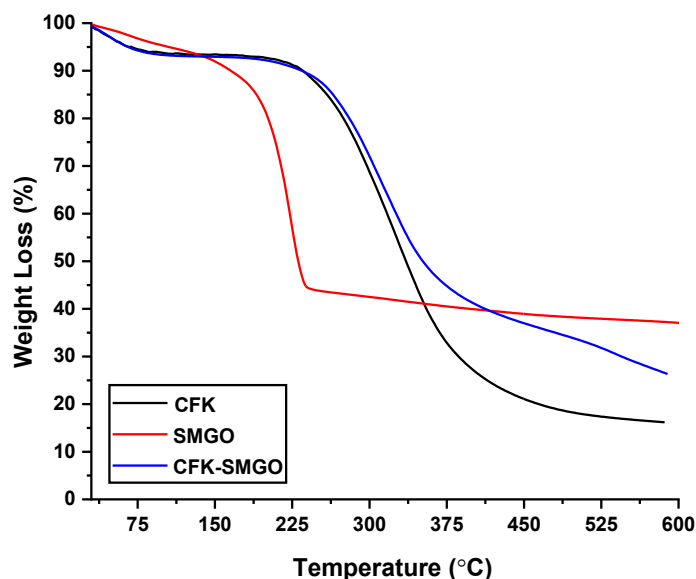


Figure 5.9: TGA curves of CFK, SMGO and CFK-SMGO derived biosorbent

The third weight loss follows after 350 °C is the polypeptides breakdown and continued up to 575 °C, nearly 84 and 74% to neat chicken feather keratin and chicken feather keratin/surface modified graphene oxide (CFK-SMGO). From all this showed that CFK-SMGO derived biosorbent had thermal stability than the pure CFK. The total weight loss of the neat chicken

feather was higher than the CFK-SMGO. The DTG curve results (**Fig. 5.10**) suggested maximum weight loss at around 325 °C in both CFK and CFK-SMGO. The weight loss in SMGO grafted CFK started 4-5 °C early due to the presence of surface modified graphene oxide with acryl amide.

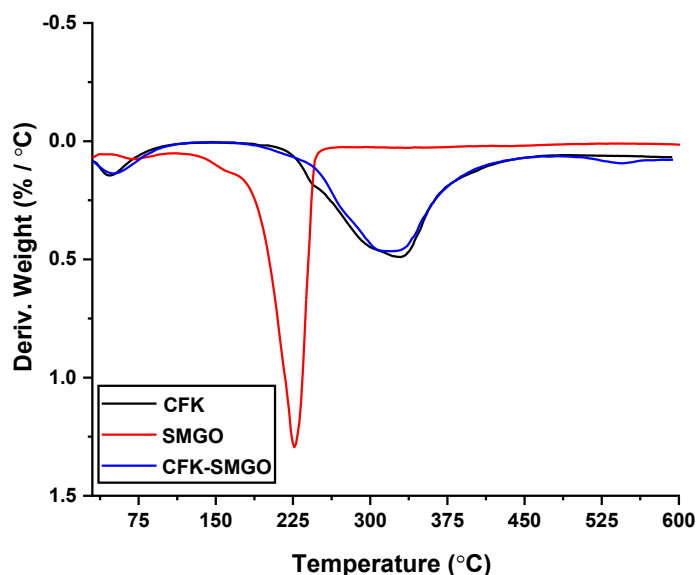


Figure 5.10: DTG curves of CFK, (SMGO), CFK-SMGO derived biosorbent

The DSC thermograms of graphene oxide and surface modified graphene oxide are shown in **Fig. 5.11**. DSC of GO nitrogen exhibited a strong exothermic peak at 173.37 °C attributed to GO's thermal reduction, i.e., deoxygenation of the graphene oxide (Xu et al., 2016). However, one small endothermic peak was also observed around 237.04 °C. SMGO exhibited a broad exothermic peak at 167.15 °C due to substitution of carbonyl groups and three endothermic peaks at 218.90 and 233.14, 277.37 °C due to presence of acryl amide groups on the graphene oxide surface.

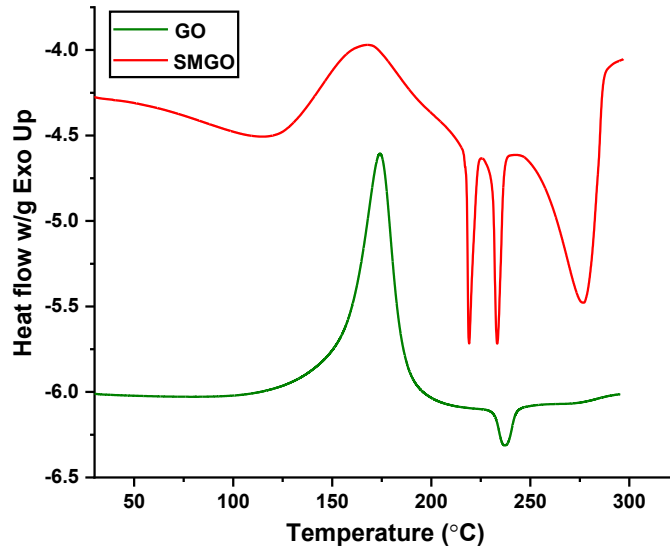


Figure 5.11: DSC curves of GO and SMGO

DSC thermograms of CFK and its derived biosorbent with surface modified graphene oxide is shown in **Fig 5.12**. Three thermal signals were observed for the neat keratin biopolymers temperature range of 25-300 °C. In case of CFK, the peak around 100 °C temperature is related to the moisture. However, the addition of surface modified graphene oxide into the CFK, the moisture loss is delayed, or no free water was available on the polymeric surface and the temperature shifted to 130.47 °C. The presence of low moisture contents and delayed moisture loss in the case of CFK-SMGO is due to the presence of surface modified graphene oxide molecules on the surface of keratin biopolymer. The grafting of SMGO with the polar groups on keratin surface reduced the availability of polar groups for the biosorption of moisture via hydrogen bonding. Arshad and coworkers observed a similar phenomenon, they used POSS (Polyhedral Oligomeric Silsesquioxanes) molecules to graft on the keratin surface and its moisture loss was delayed (Arshad et al., 2016). While a second endothermic peak was observed at about 231.42 °C, ascribed to the helix denaturation in keratin biopolymer (Kakkar et al., 2014). The denaturation temperature of surface modified graphene oxide grafted chicken feather keratin polymer had higher than neat

keratin biopolymer. The second endothermic peak of the grafted keratin polymers was exhibited at around 237.18 °C. These results showed evidence of the enhanced thermal properties of grafted keratin biopolymer compared to CFK. The shift in the crystalline melting peak was due to a change in the amorphous region of the keratin biopolymer (Ye & Feng, 2013; Zubair et al., 2022).

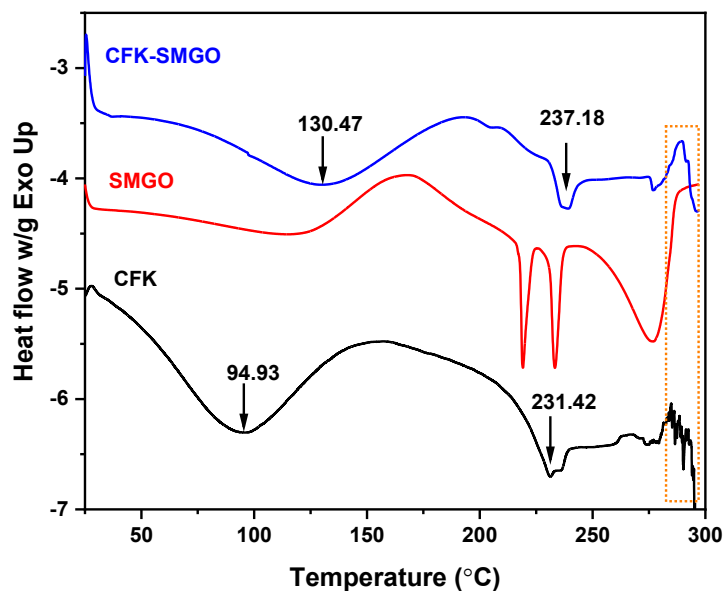


Figure 5.12: DSC curves of CFK, SMGO and CFK-SMGO derived biosorbent

5.3.4. Biosorption Performance

The prepared chicken feather keratin derived biosorbent modified with acryl amide modified graphene was tested for the biosorption of heavy metals ions biosorption. The biosorption was examined at 7.5 pH for the simultaneous removal of metal oxyanions including As, Se, Cr and cations including Ni, Co, Pb, cd Zn from polluted synthetic water containing 600 μgL^{-1} of each metal concentration in 24 hours. It can be seen from the biosorption graphs (**Fig. 5.13**) that the biosorption of As (II), Cr (VI) and Se (IV) onto the biosorbent were ≥ 91.10 , ≥ 89.55 and $\geq 74.33\%$, respectively.

At pH 7.5, M^{2+} exhibited the maximum biosorption capability of 96.34, 97.36, 99.03, 99.21 and 59.06 % for Co (II), Ni (II), Cd (II), Pb (II) and Zn (II) respectively as shown in **Fig. 5.14**. The

biosorption of the CFK depends on the presence of functional groups such as $-\text{COOH}$, $-\text{COO}^-$, $-\text{NH}_2$, $-\text{NH}_3^+$ and $-\text{SH}$ which are ultimately determined by the solution pH (Amieva et al., 2015; Kong et al., 2016). The biosorption of divalent cations was observed better than oxyanions because the protonated groups such as $-\text{COOH}$ and $-\text{SH}$ were deprotonated, and the large electrostatic attraction favoured the interaction between Mn^{2+} and CFK/SMGO, leading to an increase in the biosorption activity and efficiency of the biosorbent (Bao et al., 2011). On the other hand, divalent cations and H_3O^+ competed for the biosorption sites on the CFK/SMGO surface at pH 7.5, influencing metal cations' biosorption. These biosorption capacities are better than both neat chicken feather keratin and surface modified graphene oxide. This improvement in the biosorption efficiency of the chicken feather keratin may result from the uneven or increased exposure of biosorption sites on the surface of CFK-SMGO. Divalent cations showed higher affinity towards CFK/SMGO for biosorption as compared to oxyanions (As, Cr and Se) since their positive charges led to stronger electrostatic attraction at 7.5 pH.

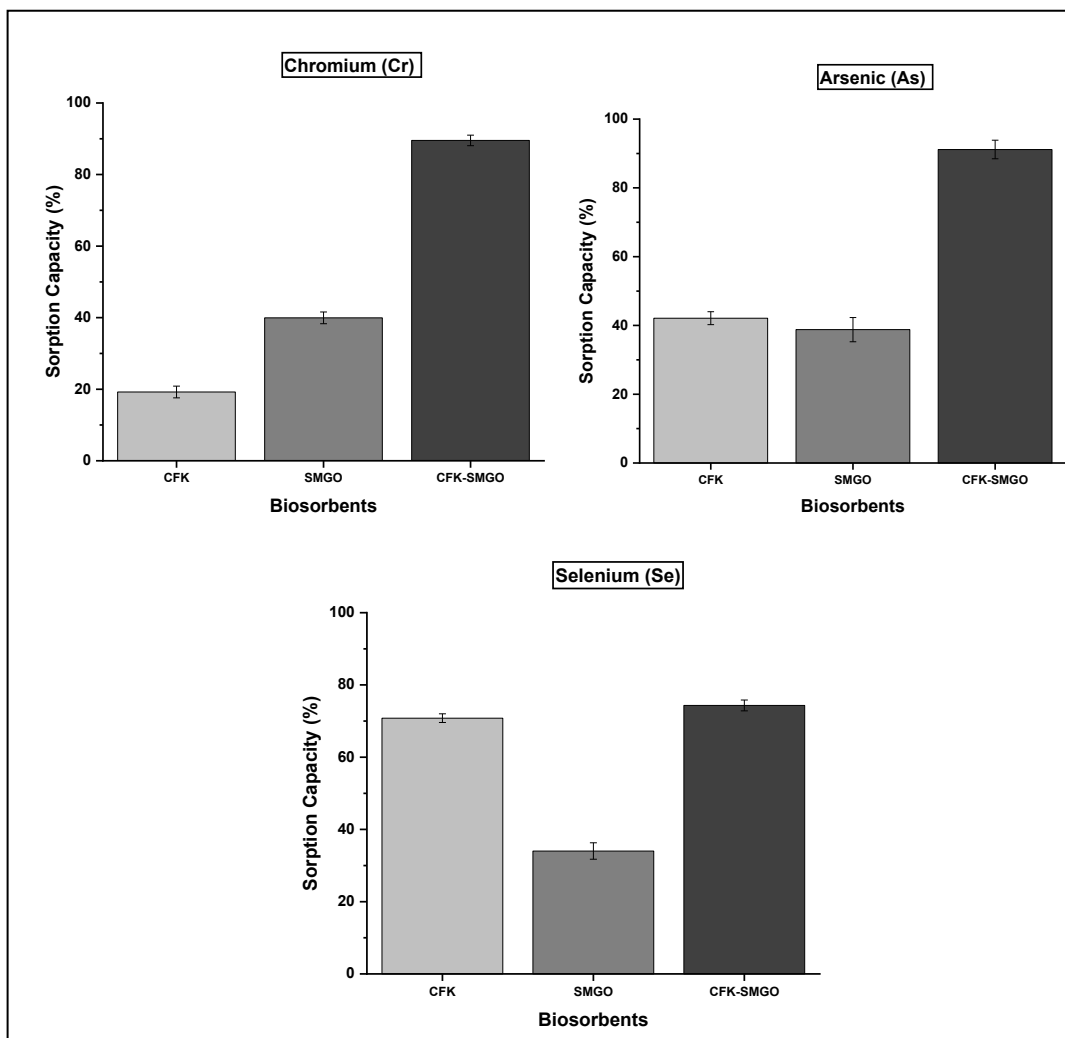


Figure 5.13: Biosorption performance of the CFK, SMGO, CFK-SMGO for anionic species (As, Se, Cr)

The charge densities and ionic radii of the metal cations determine their affinities for the biosorption sites of the polymers. At 7.5 pH, the biosorption efficiency of the metal cations is demonstrated in the following order: Pb^{2+} (1.19 \AA°) > Cd^{2+} (1.58°) > Ni^{2+} (0.69 \AA°) > Co^{2+} (0.72 \AA°) > and Zn^{2+} (0.74 \AA°). The affinity of cations with the same valence is proportionally connected to their ionic radii (Chen et al., 2018).

The prepared biosorbent showed higher biosorption for Ni^{2+} than Co^{2+} . Both belong to 3d transition metals; Ni (II) has smaller ionic radii than the Co (II). This contributed to the better

attraction between biosorbent and Ni^{2+} as the electrostatic attraction is proportional to the square distance between these two species. The stronger the attraction, the greater is the biosorption efficiency as the ligand approaches closer to the metal ions, increasing the bonding force with the biosorbent (Tansel et al., 2006).

However, in comparing the biosorption of metal cations with oxyanions, this concept theory was not applicable since they are present mainly in the form of negatively charged anions such as CrO_4^{-2} , AsO_3^{-3} , HSeO_3^{-2} (IV), SeO_3^{-2} (IV), and SeO_4^{-2} (VI) (Ayub & Raza, 2021; Dima et al., 2015; Ishikawa et al., 2004) which made their bonding difficult with the carboxylate anion. Consequently, the biosorption efficiency of the CFK/SMGO biosorbent was observed to be less as compared to the metal cations. On the other hand, the selectivity of the cations with different valence shells also depends on their ionic radii which can describe the better biosorption of Pb (II) among all sorbed metal cations. Smaller metal cations attached to water molecules more than larger cations (Tansel et al., 2006). As a result, a larger hydrated radius is created, which decreases the electrostatic interaction between biosorbent and metal cations. A study reported by Chen and coworkers observed the same trend for the affinity of anionic species using surfactant micelles (cationic ion exchange material) in an ultrafiltration separation (Chen & Jafvert, 2017).

Among the oxoanionic species, the order of selectivity was Arsenic (II) > Chromium (VI) > Selenium Se (IV). The presence of three hydroxyl groups in the arsenite creates hydrogen bonding with the chicken feather keratin proteins and water molecules which provides better surface biosorption compared to CrO_4^{2-} and SeO_4^{2-} (Asiabi et al., 2017). In SeO_4^{2-} , the absence of hydroxyl groups leads to poor surface biosorption with electrostatic interaction.

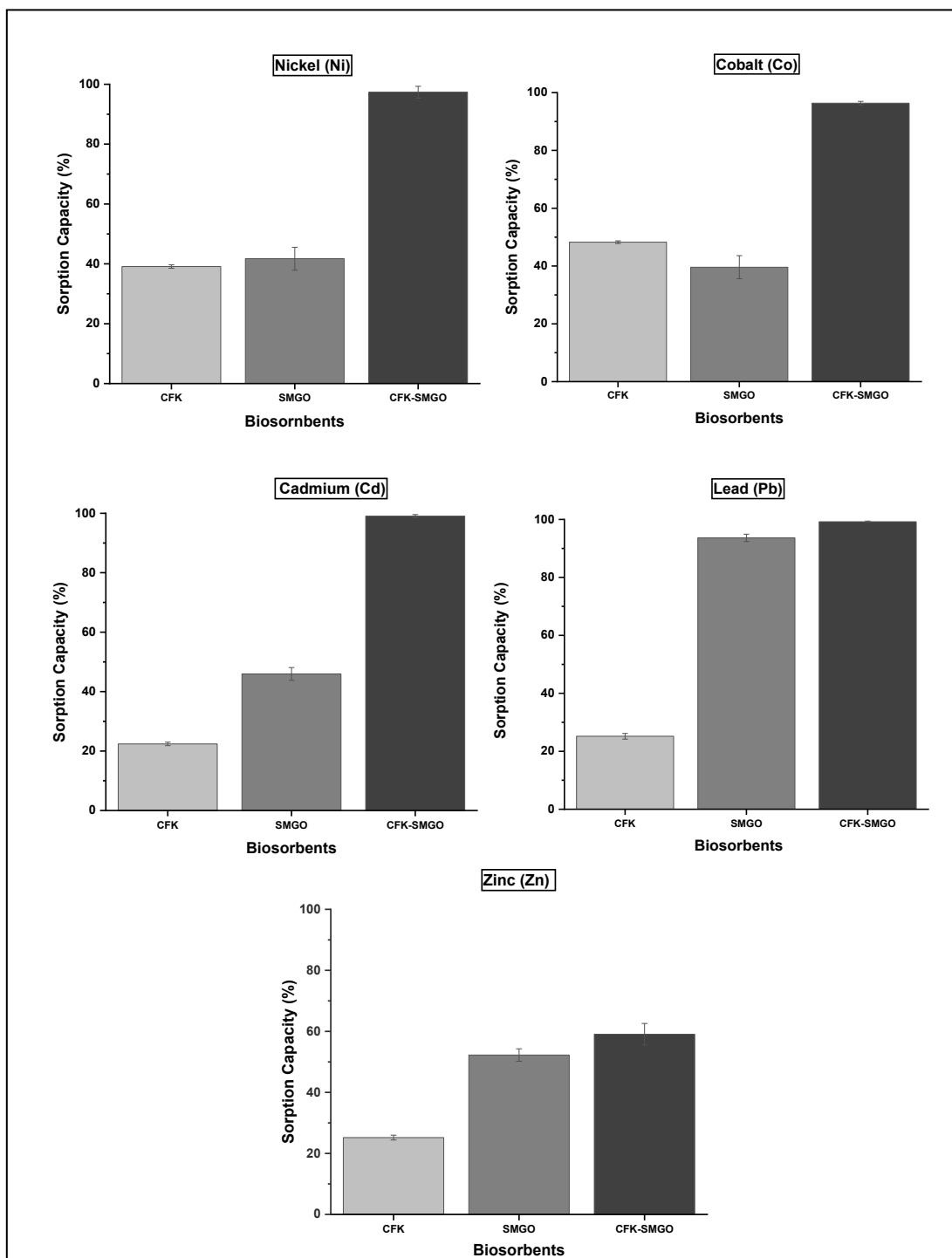


Figure 5.14: Biosorption performance of the CFK, SMGO, CFK-SMGO for cationic species ((Ni, Co, Pb, Cd, Zn)

5.4. Conclusions

The surface modified graphene oxide with acryl amide greatly improved the biosorption performance of chicken feather keratin protein. This improved performance was contributed due to the development of chemical interaction between CKF and SMGO. As a result, biosorption efficiency of CKF was enhanced as compared to neat CFK. The biosorption efficiency of CFK for metal cations was better than the metal anions except Zn (II). Metal anions are in the form of negatively charged anions such as CrO_4^{-2} , AsO_3^{-3} , HSeO_3^{-2} (IV), SeO_3^{-2} (IV), and SeO_4^{-2} (VI) which made their biosorption hard with the carboxylate anion in comparison with metal cations. The CFK/SMGO showed metal cation biosorption efficiency upto ≥ 99.03 and $\geq 99.21\%$ for Ni (II) and Cd (II) respectively. This behavior of biosorbent towards Ni (II) is due to its smaller ionic radii which increases the bonding force with the biosorbent. On the other hand, Cd belongs to the 4d transition metals and can form stable complexes and stronger interaction with the ligand. Among metal anions, arsenic showed maximum biosorption efficiency which was observed $\geq 91.1\%$ that contributed by the hydrogen bonding with the chicken feather keratin as arsenite has three hydroxyl group. These results indicated that grafting of surface modified graphene oxide on the chicken feather keratin proteins is a tremendous approach to improve its biosorption efficiency for the simultaneous removal of metal cations and anions.

5.5. References

- Ahmed, S. F., Kumar, P. S., Rozbu, M. R., Chowdhury, A. T., Nuzhat, S., Rafa, N., Mahlia, T., Ong, H. C., & Mofijur, M. (2022). Heavy metal toxicity, sources, and remediation techniques for contaminated water and soil. *Environmental Technology & Innovation*, 25, 102114.
- Amieva, E. J.-C., Fuentes-Ramirez, R., Martinez-Hernandez, A., Millan-Chiu, B., Lopez-Marin, L. M., Castaño, V., & Velasco-Santos, C. (2015). Graphene oxide and reduced graphene oxide modification with polypeptide chains from chicken feather keratin. *Journal of Alloys and Compounds*, 643, S137-S143.
- Anastas, P. T., & Warner, J. C. (1998). Green chemistry. *Frontiers*, 640, 1998.
- Arshad, M., Kaur, M., & Ullah, A. (2016). Green biocomposites from nanoengineered hybrid natural fiber and biopolymer. *ACS sustainable chemistry & engineering*, 4(3), 1785-1793.
- Asiabi, H., Yamini, Y., & Shamsayei, M. (2017). Highly selective and efficient removal of arsenic (V), chromium (VI) and selenium (VI) oxyanions by layered double hydroxide intercalated with zwitterionic glycine. *Journal of hazardous materials*, 339, 239-247.
- Ayub, A., & Raza, Z. A. (2021). Arsenic removal approaches: A focus on chitosan biosorption to conserve the water sources. *International Journal of Biological Macromolecules*, 192, 1196-1216.
- Bao, Y., Ma, J., & Li, N. (2011). Synthesis and swelling behaviors of sodium carboxymethyl cellulose-g-poly (AA-co-AM-co-AMPS)/MMT superabsorbent hydrogel. *Carbohydrate Polymers*, 84(1), 76-82.
- Bhattacharya, S., Gupta, A. B., Gupta, A., & Pandey, A. (2018). Introduction to water remediation: importance and methods. In *Water remediation* (pp. 3-8). Springer.
- Bi, J., Tao, Q., Huang, X., Wang, J., Wang, T., & Hao, H. (2021). Simultaneous decontamination of multi-pollutants: A promising approach for water remediation. *Chemosphere*, 284, 131270.
- Bolisetty, S., Peydayesh, M., & Mezzenga, R. (2019). Sustainable technologies for water purification from heavy metals: review and analysis. *Chemical Society Reviews*, 48(2), 463-487.
- Chen, M., & Jafvert, C. T. (2017). Anion exchange on cationic surfactant micelles, and a speciation model for estimating anion removal on micelles during ultrafiltration of water. *Langmuir*, 33(26), 6540-6549.
- Chen, M., Shafer-Peltier, K., Randtke, S. J., & Peltier, E. (2018). Competitive association of cations with poly (sodium 4-styrenesulfonate)(PSS) and heavy metal removal from water by PSS-assisted ultrafiltration. *Chemical Engineering Journal*, 344, 155-164.
- Chen, Y., Tao, J., Ezzeddine, A., Mahfouz, R., Al-Shahrani, A., Alabedi, G., & Khashab, N. M. (2015). Superior performance nanocomposites from uniformly dispersed octadecylamine functionalized multi-walled carbon nanotubes. *C*, 1(1), 58-76.
- Chilakamarry, C. R., Mahmood, S., Saffe, S. N. B. M., Arifin, M. A. B., Gupta, A., Sikkandar, M. Y., Begum, S. S., & Narasaiah, B. (2021). Extraction and application of keratin from natural resources: a review. *3 Biotech*, 11(5), 1-12.
- Choudhary, S., Mungse, H. P., & Khatri, O. P. (2012). Dispersion of alkylated graphene in organic solvents and its potential for lubrication applications. *Journal of Materials Chemistry*, 22(39), 21032-21039.

- Connor, R. (2015). *The United Nations world water development report 2015: water for a sustainable world* (Vol. 1). UNESCO publishing.
- Dagerskog, L., & Olsson, O. (2020). *Swedish sludge management at the crossroads*. JSTOR.
- Dima, J. B., Sequeiros, C., & Zaritzky, N. E. (2015). Hexavalent chromium removal in contaminated water using reticulated chitosan micro/nanoparticles from seafood processing wastes. *Chemosphere*, *141*, 100-111.
- Dodson, J. R., Parker, H. L., García, A. M., Hicken, A., Asemave, K., Farmer, T. J., He, H., Clark, J. H., & Hunt, A. J. (2015). Bio-derived materials as a green route for precious & critical metal recovery and re-use. *Green Chemistry*, *17*(4), 1951-1965.
- Feroz, S., Muhammad, N., Ratnayake, J., & Dias, G. (2020). Keratin-Based materials for biomedical applications. *Bioactive materials*, *5*(3), 496-509.
- Goswami, K. B., & Bisht, P. S. (2017). The Role of water resources in socio-economic development. *Int. J. Res. Appl. Sci. Eng. Technol*, *5*, 1669-1674.
- Idris, A., Vijayaraghavan, R., Rana, U. A., Fredericks, D., Patti, A. F., & Macfarlane, D. R. (2013). Dissolution of feather keratin in ionic liquids. *Green Chemistry*, *15*(2), 525-534.
- Ishikawa, S.-I., Sekine, S., Miura, N., Suyama, K., Arihara, K., & Itoh, M. (2004). Removal of selenium and arsenic by animal biopolymers. *Biological Trace Element Research*, *102*(1), 113-127.
- Jeong, H., Jin, M., So, K., Lim, S., & Lee, Y. (2009). Tailoring the characteristics of graphite oxides by different oxidation times. *Journal of Physics D: Applied Physics*, *42*(6), 065418.
- Kakkar, P., Madhan, B., & Shanmugam, G. (2014). Extraction and characterization of keratin from bovine hoof: A potential material for biomedical applications. *SpringerPlus*, *3*(1), 1-9.
- Khosa, M. A., & Ullah, A. (2014). In-situ modification, regeneration, and application of keratin biopolymer for arsenic removal. *Journal of hazardous materials*, *278*, 360-371.
- Kong, W., Li, Q., Liu, J., Li, X., Zhao, L., Su, Y., Yue, Q., & Gao, B. (2016). Adsorption behavior and mechanism of heavy metal ions by chicken feather protein-based semi-interpenetrating polymer networks super absorbent resin. *RSC advances*, *6*(86), 83234-83243.
- Krishnan, S., Zulkapli, N. S., Kamyab, H., Taib, S. M., Din, M. F. B. M., Abd Majid, Z., Chaiprapat, S., Kenzo, I., Ichikawa, Y., & Nasrullah, M. (2021). Current technologies for recovery of metals from industrial wastes: An overview. *Environmental Technology & Innovation*, *22*, 101525.
- Lazarus, B. S., Chadha, C., Velasco-Hogan, A., Barbosa, J. D., Jasiuk, I., & Meyers, M. A. (2021). Engineering with keratin: A functional material and a source of bioinspiration. *Isience*, *24*(8), 102798.
- Liu, Y., Wang, P., Gojenko, B., Yu, J., Wei, L., Luo, D., & Xiao, T. (2021). A review of water pollution arising from agriculture and mining activities in Central Asia: Facts, causes and effects. *Environmental Pollution*, *291*, 118209.
- Marcano, D. C., Kosynkin, D. V., Berlin, J. M., Sinitskii, A., Sun, Z., Slesarev, A., Alemany, L. B., Lu, W., & Tour, J. M. (2010). Improved synthesis of graphene oxide. *ACS nano*, *4*(8), 4806-4814.
- Organization, W. H. (2019). *Progress on household drinking water, sanitation and hygiene 2000-2017: special focus on inequalities*. World Health Organization.

- Park, S., An, J., Potts, J. R., Velamakanni, A., Murali, S., & Ruoff, R. S. (2011). Hydrazine-reduction of graphite-and graphene oxide. *Carbon*, 49(9), 3019-3023.
- Peydayesh, M., & Mezzenga, R. (2021). Protein nanofibrils for next generation sustainable water purification. *Nature communications*, 12(1), 1-17.
- Pravin, M., & Gnanamani, A. (2018). Preparation, characterization and reusability efficacy of amine-functionalized graphene oxide-polyphenol oxidase complex for removal of phenol from aqueous phase. *RSC advances*, 8(67), 38416-38424.
- Qasem, N. A., Mohammed, R. H., & Lawal, D. U. (2021). Removal of heavy metal ions from wastewater: A comprehensive and critical review. *Npj Clean Water*, 4(1), 1-15.
- Saha, S., Arshad, M., Zubair, M., & Ullah, A. (2019). Keratin as a Biopolymer. In *Keratin as a protein biopolymer* (pp. 163-185). Springer.
- Saha, S., Zubair, M., Khosa, M., Song, S., & Ullah, A. (2019). Keratin and chitosan biosorbents for wastewater treatment: a review. *Journal of Polymers and the Environment*, 27(7), 1389-1403.
- Shanmugaraj, A., Yoon, J., Yang, W., & Ryu, S. H. (2013). Synthesis, characterization, and surface wettability properties of amine functionalized graphene oxide films with varying amine chain lengths. *Journal of colloid and interface science*, 401, 148-154.
- Tansel, B., Sager, J., Rector, T., Garland, J., Strayer, R. F., Levine, L., Roberts, M., Hummerick, M., & Bauer, J. (2006). Significance of hydrated radius and hydration shells on ionic permeability during nanofiltration in dead end and cross flow modes. *Separation and Purification Technology*, 51(1), 40-47.
- Walker, D., Baumgartner, D., Gerba, C., & Fitzsimmons, K. (2019). Surface water pollution. In *Environmental and pollution science* (pp. 261-292). Elsevier.
- Wang, L., Rinklebe, J., Tack, F. M., & Hou, D. (2021). A review of green remediation strategies for heavy metal contaminated soil. *Soil Use and Management*, 37(4), 936-963.
- Xu, Q., Zeng, M., Feng, Z., Yin, D., Huang, Y., Chen, Y., Yan, C., Li, R., & Gu, Y. (2016). Understanding the effects of carboxylated groups of functionalized graphene oxide on the curing behavior and intermolecular interactions of benzoxazine nanocomposites. *RSC advances*, 6(37), 31484-31496.
- Ye, S., & Feng, J. (2013). A new insight into the in situ thermal reduction of graphene oxide dispersed in a polymer matrix. *Polymer Chemistry*, 4(6), 1765-1768.
- Zubair, M., Wu, J., & Ullah, A. (2022). Bionanocomposites from spent hen proteins reinforced with polyhedral oligomeric silsesquioxane (POSS)/cellulose nanocrystals (CNCs). *Biocatalysis and Agricultural Biotechnology*, 43, 102434.

CHAPTER 6: Summary and Future Perspectives

The chicken feather keratin is an unexploited renewable carbon biomass resource of proteins for developing a variety of proteins derived bio-based materials. Annually, almost 40×10^9 kg of chicken feathers are generated by the poultry industry around the globe, and most of them are either burnt or landfilled and create environmental pollution (Tesfaye et al., 2017; Uzun et al., 2011). Chicken feather contains around 92-94% of keratin proteins (Zubair et al., 2022); hence $36 - 37 \times 10^9$ kg of keratin proteins can be extracted from this waste which is a huge bioresource and can be utilized to make material for various applications including water remediation.

The main objective of this Ph.D. research work was aimed on the utilization of this huge bioresource. For this purpose, first, the proteins were extracted from chicken feathers using reducing agents and second, value addition to extracted keratin proteins in the form of biosorbents production.

As the biosorbent preparation and increasing the biosorption efficiency of CFK are the real challenges restricting its industrial applications, it is necessary to develop a facile method that keratin proteins can be easily transformed into biosorbent with improved biosorption efficiency. Different nano reinforcements can be used to study their effect on the biosorption efficiency of CFK. The concentration of the nanoparticles can have an impact on their biosorption efficiency.

In the first study, graphene oxide with the concentration of 1,3 and 5% of CFK were used to study its effect on the biosorption efficiency of CFK. The results indicated that 1% of the graphene oxide profoundly impacts the biosorption performance of the keratin biopolymer. This is ascribed to the better interaction of graphene oxide with 1%, while more concentration negatively affects its performance. The biosorption efficiency of As (III) and Se (VI) went up to \geq

97 and $\geq 99\%$, respectively. In case of metal cations, CFK with 1% GO exhibited ≥ 99 , ≥ 92 , ≥ 91 , ≥ 88 and $\geq 82\%$ for Ni (II), Co (II), Pb (II), Cd (II) and Zn (II) respectively.

In the second study, nanochitosan (1,3 and 5%) was used to increase the biosorption performance of the chicken feather keratin. The study concluded that 3 weight % of nanochitosan with CFK showed the best results compared to other concentrations. Overall, the biosorption efficiency ($\geq 74 - \geq 98\%$) for anionic species was better than cationic species while As (III) showed the best biosorption efficiency of $\geq 98\%$.

In the third study, surface modified graphene oxide improved the CFK biosorption efficiency. This approach of modifying the sorption efficiency of chicken feather keratin showed promising results with the biosorption of As (II), Cr (VI) and Se (IV) of ≥ 91.1 , ≥ 89.55 , $\geq 74.336\%$ respectively. While CFK/SMGO exhibited the maximum biosorption capability of ≥ 96.34 , ≥ 97.363 , and $\geq 99.03\%$ for Co (II), Ni (II), and Cd (II), respectively.

Understanding the mechanisms of metal biosorption by the CFK is of utmost importance and plays a critical role in modifying the biosorption properties of the biosorbents. The possible mechanisms for the uptake of metal anions and cations were characterized using SEM, XRD, TGA, XPS and FTIR. The results indicated that the biosorption of metals through CFK occurs through phenomena such as complexation, hydrogen bonding, electrostatic interactions and chelation.

Overall, the biosorption efficiency of the CFK modified with GO, NC and SMGO improved tremendously for the simultaneous removal of metal cations and anions in a single treatment. Statistical analysis among three studies was conducted, which indicated that CFK containing 1% GO exhibited the best removal efficiency among all prepared biosorbents for the simultaneous treatment of metal cations and anions from 600 ppb simulated synthetic wastewater. The CFK-GO (1%) showed the best removal efficiency for Ni^{II} (99.04%), Zn^{II} (82.02667%), Se^{VI}

(99.11%) and Cr^{VI} (97.26%). While CFK-SMGO derived biosorbent exhibited the highest removal efficiencies for Co^{II}, Cd^{II}, Pb^{II}, i.e., 96.34, 99.03 and 99.21%, respectively. On the other hand, the best As^{III} removal efficiency (97.26%) was shown by CFK derived biosorbent modified with 3% NC. CFK-SMGO showed greater efficiency for metal cations removal as compared to other prepared biosorbents and CFK-GO (1%) found best for metal anions removal.

The biosorption of the heavy metal ions mainly depends on the availability of functional groups on the surface of keratin proteins (Zahara et al., 2021), which can further improve by mixing different nanoparticles such as cellulose nanocrystals or cellulose nanofibres. The controlled synthesis of keratin biopolymer using a range of nanoparticle concentrations can help reduce water pollution with other contaminants of inorganic and organic nature.

Furthermore, structural studies of the biosorbents and their mechanism of interaction with heavy metal ions by using other techniques such as surface extended X-ray absorption fine structure (SEXAFS), near edge X-ray absorption fine structure (NEXAFS), auger electron spectroscopy (AES), can tune their efficiency and broaden the scope for the removal of other pollutants such as organic contaminants, salts and radionuclides, naphthenic acids and lithium.

The chemical crosslinking or physical interaction of nanochitosan, graphene oxide and surface modified graphene oxide into the keratin biopolymer matrix leads to significant changes in the charge transport and charge distribution because of the interfacial effects. Therefore, understanding surface charge distribution in biosorbents is essential in designing sorbing materials with desirable properties. The use of an electrostatic voltmeter and Kelvin probe is highly recommended to study these attributes.

Moreover, it is highly suggested to conduct biodegradability tests on the developed biosorbents. To prepare biosorbents from CFK proteins, a comprehensive study is proposed on

their biosorption capacities at various concentrations of pollutants and developing isotherms for their feasibility at a larger scale. The properties of biosorbents are mainly dominated by the interfacial interactions between nanoparticles of graphene oxide, nanochitosan and surface modified graphene oxide with keratin biopolymer, so it will be worthwhile to analyze these properties in detail with techniques such as zeta potential analyzer.

The reuse or regeneration studies are recommended to recover the metals and biosorbent, which can cut the overall cost, and a detailed understanding of the biosorption selectivity of multiple pollutants on each other during the biosorption process is required.

The rising apprehensions related to water pollution have led the public and governments to become quite serious about dealing with this burning issue. So, the responsibilities of the researchers have also increased enormously. In future, the mandate for biobased sorbents particularly from waste biomasses with better biosorption capacities and economical designs for water purification technologies will undoubtedly be at its highest.

In summary, the keratin derived biosorbents have shown promising potential in utilization for water remediation in the coming year. In the future, it would be worthwhile to study the removal of organics such as phenol, naphthenic acids etc., from industrial wastewater. Most importantly, simultaneous removal of inorganic and organic ions is proposed because commercially available adsorbents show relatively poor biosorption efficiency for multielement or can be used only for specific pollutants. At first, cost analysis of keratin-graphene oxide/nanochitosan/SMGO derived biosorbents used in this research is recommended. Based on their cost-effective efficiency, the GO and NC can be used to scale up for keratin based green and sustainable biosorbents production at the industrial scale.

The 12 principles of green chemistry specify the foundations of green chemistry and outlines the pathways of improving materials products or raw materials, operations and system. This study follows the green chemistry 7th principle of " use of renewable feedstocks" (Anastas & Beach, 2007) to transform renewable chicken feathers keratin biomass into biosorbent for water remediation from heavy metal ions. The development of novel green and sustainable biosorbents, i.e., chicken feather keratin with low cost and superior performance for water remediation has opened new prospects for water scientists and provided collaborative opportunities to unravel the water pollution problem with a better approach. The expansion of keratin based materials at a larger scale can contribute as a sustainable and renewable material for water remediation at the industrial level. The development of biosorbents using chicken feathers keratin will be beneficial for heavy metals decontamination and reduce the potential health and environmental impacts of chicken feather disposal.

6.1. References

- Anastas, P. T., & Beach, E. S. (2007). Green chemistry: the emergence of a transformative framework. *Green Chemistry Letters and Reviews*, 1(1), 9-24.
- Tesfaye, T., Sithole, B., & Ramjugernath, D. (2017). Valorisation of chicken feathers: a review on recycling and recovery route—current status and future prospects. *Clean Technologies and Environmental Policy*, 19(10), 2363-2378.
- Uzun, M., Sancak, E., Patel, I., Usta, I., Akalın, M., & Yuksek, M. (2011). Mechanical behaviour of chicken quills and chicken feather fibres reinforced polymeric composites. *Archives of Materials Science and Engineering*, 52(2), 82-86.
- Zahara, I., Arshad, M., Naeth, M. A., Siddique, T., & Ullah, A. (2021). Feather keratin derived sorbents for the treatment of wastewater produced during energy generation processes. *Chemosphere*, 273, 128545.
- Zubair, M., Roopesh, M., & Ullah, A. (2022). Nano-modified feather keratin derived green and sustainable biosorbents for the remediation of heavy metals from synthetic wastewater. *Chemosphere*, 308, 136339.

Bibliography

- Abdellatif, M. M., Abdellatif, F. H. H., & Ibrahim, S. (2022). The utilization of cross-linked gelatin/PAMAM aerogels as heavy metal ions bio-adsorbents from aqueous solutions. *Polymer Bulletin*, 1-18.
- Ahamad, T., Naushad, M., Al-Maswari, B. M., & Alshehri, S. M. (2019). Fabrication of highly porous adsorbent derived from bio-based polymer metal complex for the remediation of water pollutants. *Journal of cleaner production*, 208, 1317-1326.
- Ahamad, T., Naushad, M., Eldesoky, G. E., Alqadami, A. A., & Khan, A. (2019). Synthesis and characterization of egg-albumen-formaldehyde based magnetic polymeric resin (MPR): Highly efficient adsorbent for Cd (II) ion removal from aqueous medium. *Journal of Molecular Liquids*, 286, 110951.
- Ahmed, S. F., Kumar, P. S., Rozbu, M. R., Chowdhury, A. T., Nuzhat, S., Rafa, N., Mahlia, T., Ong, H. C., & Mofijur, M. (2022). Heavy metal toxicity, sources, and remediation techniques for contaminated water and soil. *Environmental Technology & Innovation*, 25, 102114.
- Al-Asheh, S., & Banat, F. (2003). Beneficial reuse of chicken feathers in removal of heavy metals from wastewater. *Journal of cleaner production*, 11(3), 321-326.
- Al-Asheh, S., Banat, F., & Al-Rousan, D. (2002). Adsorption of copper, zinc and nickel ions from single and binary metal ion mixtures on to chicken feathers. *Adsorption Science & Technology*, 20(9), 849-864.
- Al-Khaldi, F. A., Abusharkh, B., Khaled, M., Atieh, M. A., Nasser, M., Saleh, T. A., Agarwal, S., Tyagi, I., & Gupta, V. K. (2015). Adsorptive removal of cadmium (II) ions from liquid phase using acid modified carbon-based adsorbents. *Journal of Molecular Liquids*, 204, 255-263.
- Alahyaribeik, S., & Ullah, A. (2020). Methods of keratin extraction from poultry feathers and their effects on antioxidant activity of extracted keratin. *International Journal of Biological Macromolecules*, 148, 449-456.
- Ali, H., Khan, E., & Ilahi, I. (2019). Environmental chemistry and ecotoxicology of hazardous heavy metals: environmental persistence, toxicity, and bioaccumulation. *Journal of chemistry*, 2019.
- Aluigi, A., Tonetti, C., Rombaldoni, F., Puglia, D., Fortunati, E., Armentano, I., Santulli, C., Torre, L., & Kenny, J. M. (2014). Keratins extracted from Merino wool and Brown Alpaca fibres as potential fillers for PLLA-based biocomposites. *Journal of materials science*, 49(18), 6257-6269.
- Aluigi, A., Zoccola, M., Vineis, C., Tonin, C., Ferrero, F., & Canetti, M. (2007). Study on the structure and properties of wool keratin regenerated from formic acid. *International journal of biological macromolecules*, 41(3), 266-273.
- Amieva, E. J.-C., Fuentes-Ramirez, R., Martinez-Hernandez, A., Millan-Chiu, B., Lopez-Marin, L. M., Castaño, V., & Velasco-Santos, C. (2015). Graphene oxide and reduced graphene oxide modification with polypeptide chains from chicken feather keratin. *Journal of Alloys and Compounds*, 643, S137-S143.
- Anastas, P. T., & Beach, E. S. (2007). Green chemistry: the emergence of a transformative framework. *Green Chemistry Letters and Reviews*, 1(1), 9-24.
- Anastas, P. T., & Warner, J. C. (1998). Green chemistry. *Frontiers*, 640, 1998.

- Ansari, S., Ahmed, N., Mahar, R. B., Khatri, Z., & Khatri, M. (2022). Fabrication and characterization of electrospun zein/nylon-6 (ZN6) nanofiber membrane for hexavalent chromium removal. *Environmental Science and Pollution Research*, 29(1), 653-662.
- Arshad, M., Kaur, M., & Ullah, A. (2016). Green biocomposites from nanoengineered hybrid natural fiber and biopolymer. *ACS sustainable chemistry & engineering*, 4(3), 1785-1793.
- Arshad, M., Zubair, M., Rahman, S. S., & Ullah, A. (2020). Polymers for advanced applications. In *Polymer Science and Nanotechnology* (pp. 325-340). Elsevier.
- Asiabi, H., Yamini, Y., & Shamsayei, M. (2017). Highly selective and efficient removal of arsenic (V), chromium (VI) and selenium (VI) oxyanions by layered double hydroxide intercalated with zwitterionic glycine. *Journal of hazardous materials*, 339, 239-247.
- Ayub, A., & Raza, Z. A. (2021). Arsenic removal approaches: A focus on chitosan biosorption to conserve the water sources. *International Journal of Biological Macromolecules*, 192, 1196-1216.
- Babel, S., & Kurniawan, T. (2005). Various treatment technologies to remove arsenic and mercury from contaminated groundwater: an overview. *Southeast Asian Water Environment*, 1.
- Babel, S., & Kurniawan, T. A. (2004). Cr (VI) removal from synthetic wastewater using coconut shell charcoal and commercial activated carbon modified with oxidizing agents and/or chitosan. *Chemosphere*, 54(7), 951-967.
- Badrelzaman, M., Khamis, M. I., Ibrahim, T. H., & Jumean, F. H. (2020). Scale-Up of self-regenerating semi-batch adsorption cycles through concurrent adsorption and reduction of Cr (VI) on sheep wool. *Processes*, 8(9), 1092.
- Bao, Y., Ma, J., & Li, N. (2011). Synthesis and swelling behaviors of sodium carboxymethyl cellulose-g-poly (AA-co-AM-co-AMPS)/MMT superabsorbent hydrogel. *Carbohydrate Polymers*, 84(1), 76-82.
- Barth, A. (2007). Infrared spectroscopy of proteins. *Biochimica et Biophysica Acta (BBA)-Bioenergetics*, 1767(9), 1073-1101.
- Bashir, A., Malik, L. A., Ahad, S., Manzoor, T., Bhat, M. A., Dar, G., & Pandith, A. H. (2019). Removal of heavy metal ions from aqueous system by ion-exchange and biosorption methods. *Environmental Chemistry Letters*, 17(2), 729-754.
- Bhari, R., Kaur, M., & Sarup Singh, R. (2021). Chicken feather waste hydrolysate as a superior biofertilizer in agroindustry. *Current Microbiology*, 78(6), 2212-2230.
- Bhattacharya, S., Gupta, A. B., Gupta, A., & Pandey, A. (2018). Introduction to water remediation: importance and methods. In *Water remediation* (pp. 3-8). Springer.
- Bhumkar, D. R., & Pokharkar, V. B. (2006). Studies on effect of pH on cross-linking of chitosan with sodium tripolyphosphate: a technical note. *Aaps Pharmscitech*, 7(2), E138-E143.
- Bi, J., Tao, Q., Huang, X., Wang, J., Wang, T., & Hao, H. (2021). Simultaneous decontamination of multi-pollutants: A promising approach for water remediation. *Chemosphere*, 284, 131270.
- Bilal, M., Ihsanullah, I., Younas, M., & Shah, M. U. H. (2021). Recent advances in applications of low-cost adsorbents for the removal of heavy metals from water: A critical review. *Separation and Purification Technology*, 278, 119510.
- Bolisetty, S., Peydayesh, M., & Mezzenga, R. (2019). Sustainable technologies for water purification from heavy metals: review and analysis. *Chemical Society Reviews*, 48(2), 463-487.

- Calvo, P., Remunan-Lopez, C., Vila-Jato, J. L., & Alonso, M. (1997). Novel hydrophilic chitosan-polyethylene oxide nanoparticles as protein carriers. *Journal of applied polymer science*, 63(1), 125-132.
- Carlos, L., Einschlag, F. S. G., González, M. C., & Mártire, D. O. (2013). Applications of magnetite nanoparticles for heavy metal removal from wastewater. *Waste Water-Treatment Technologies and Recent Analytical Developments*, 3, 64-73.
- Carr, C. M., & Gerasimowicz, W. V. (1988). A carbon-13 CPMAS solid state NMR spectroscopic study of wool: effects of heat and chrome mordanting. *Textile Research Journal*, 58(7), 418-421.
- Chai, W. S., Cheun, J. Y., Kumar, P. S., Mubashir, M., Majeed, Z., Banat, F., Ho, S.-H., & Show, P. L. (2021). A review on conventional and novel materials towards heavy metal adsorption in wastewater treatment application. *Journal of Cleaner Production*, 296, 126589.
- Chakraborty, R., Asthana, A., Singh, A. K., Yadav, S., Susan, M. A. B. H., & Carabineiro, S. A. (2020). Intensified elimination of aqueous heavy metal ions using chicken feathers chemically modified by a batch method. *Journal of Molecular Liquids*, 312, 113475.
- Chen, M., & Jafvert, C. T. (2017). Anion exchange on cationic surfactant micelles, and a speciation model for estimating anion removal on micelles during ultrafiltration of water. *Langmuir*, 33(26), 6540-6549.
- Chen, M., Shafer-Peltier, K., Randtke, S. J., & Peltier, E. (2018). Competitive association of cations with poly (sodium 4-styrenesulfonate)(PSS) and heavy metal removal from water by PSS-assisted ultrafiltration. *Chemical Engineering Journal*, 344, 155-164.
- Chen, Y., Tao, J., Ezzeddine, A., Mahfouz, R., Al-Shahrani, A., Alabedi, G., & Khashab, N. M. (2015). Superior performance nanocomposites from uniformly dispersed octadecylamine functionalized multi-walled carbon nanotubes. *C*, 1(1), 58-76.
- Chilakamarry, C. R., Mahmood, S., Saffe, S. N. B. M., Arifin, M. A. B., Gupta, A., Sikkandar, M. Y., Begum, S. S., & Narasaiah, B. (2021). Extraction and application of keratin from natural resources: a review. *3 Biotech*, 11(5), 1-12.
- Choudhary, S., Mungse, H. P., & Khatri, O. P. (2012). Dispersion of alkylated graphene in organic solvents and its potential for lubrication applications. *Journal of Materials Chemistry*, 22(39), 21032-21039.
- Connor, R. (2015). *The United Nations world water development report 2015: water for a sustainable world* (Vol. 1). UNESCO publishing.
- Coward-Kelly, G., Chang, V. S., Agbogbo, F. K., & Holtzapfle, M. T. (2006). Lime treatment of keratinous materials for the generation of highly digestible animal feed: 1. Chicken feathers. *Bioresource technology*, 97(11), 1337-1343.
- Dagerskog, L., & Olsson, O. (2020). *Swedish sludge management at the crossroads*. JSTOR.
- Demirbas, A. (2008). Heavy metal adsorption onto agro-based waste materials: a review. *Journal of hazardous materials*, 157(2-3), 220-229.
- Dima, J. B., Sequeiros, C., & Zaritzky, N. E. (2015). Hexavalent chromium removal in contaminated water using reticulated chitosan micro/nanoparticles from seafood processing wastes. *Chemosphere*, 141, 100-111.
- Dinu, R., Briand, N., & Mija, A. (2021). Influence of Keratin on Epoxidized Linseed Oil Curing and Thermoset Performances. *ACS Sustainable Chemistry & Engineering*, 9(46), 15641-15652.

- Dodson, J. R., Parker, H. L., García, A. M., Hicken, A., Asemave, K., Farmer, T. J., He, H., Clark, J. H., & Hunt, A. J. (2015). Bio-derived materials as a green route for precious & critical metal recovery and re-use. *Green Chemistry*, *17*(4), 1951-1965.
- Donner, M. W., Arshad, M., Ullah, A., & Siddique, T. (2019). Unravelling keratin-derived biopolymers as novel biosorbents for the simultaneous removal of multiple trace metals from industrial wastewater. *Science of The Total Environment*, *647*, 1539-1546.
- Duan, C., Ma, T., Wang, J., & Zhou, Y. (2020). Removal of heavy metals from aqueous solution using carbon-based adsorbents: A review. *Journal of Water Process Engineering*, *37*, 101339.
- Duruibe, J. (2007). Ogwuegbu MOC Egwurugwu JN Int. *J. Phys. Sci*, *2*, 112-118.
- Edwards, H., Hunt, D., & Sibley, M. (1998). FT-Raman spectroscopic study of keratotic materials: horn, hoof and tortoiseshell. *Spectrochimica Acta Part A: Molecular and Biomolecular Spectroscopy*, *54*(5), 745-757.
- Eichner, R., Bonitz, P., & Sun, T.-T. (1984). Classification of epidermal keratins according to their immunoreactivity, isoelectric point, and mode of expression. *The Journal of cell biology*, *98*(4), 1388-1396.
- El-Khodary, S. A., El-Enany, G. M., El-Okri, M., & Ibrahim, M. (2014). Preparation and characterization of microwave reduced graphite oxide for high-performance supercapacitors. *Electrochimica Acta*, *150*, 269-278.
- Elgamal, A. M., Abd El-Ghany, N. A., & Saad, G. R. (2023). Synthesis and characterization of hydrogel-based magnetite nanocomposite adsorbents for the potential removal of Acid Orange 10 dye and Cr (VI) ions from aqueous solution. *International Journal of Biological Macromolecules*, *227*, 27-44.
- Esfarili, L., Safarifard, V., Tahmasebi, E., Esfarili, M., & Morsali, A. (2018). Functional group effect of isoreticular metal-organic frameworks on heavy metal ion adsorption. *New Journal of Chemistry*, *42*(11), 8864-8873.
- Fei, Y., & Hu, Y. H. (2022). Design, synthesis, and performance of adsorbents for heavy metal removal from wastewater: a review. *Journal of Materials Chemistry A*.
- Feroz, S., Muhammad, N., Ratnayake, J., & Dias, G. (2020). Keratin-Based materials for biomedical applications. *Bioactive materials*, *5*(3), 496-509.
- Feughelman, M., Lyman, D., Menefee, E., & Willis, B. (2003). The orientation of the α -helices in α -keratin fibres. *International journal of biological macromolecules*, *33*(1-3), 149-152.
- Fu, F., & Wang, Q. (2011). Removal of heavy metal ions from wastewaters: a review. *Journal of environmental management*, *92*(3), 407-418.
- Gao, W. (2015). The chemistry of graphene oxide. In *Graphene oxide* (pp. 61-95). Springer.
- Gendy, E. A., Ifthikar, J., Ali, J., Oyekunle, D. T., Elkhelifia, Z., Shahib, I. I., Khodair, A. I., & Chen, Z. (2021). Removal of heavy metals by covalent organic frameworks (COFs): A review on its mechanism and adsorption properties. *Journal of Environmental Chemical Engineering*, *9*(4), 105687.
- Gómez-Navarro, C., Meyer, J. C., Sundaram, R. S., Chuvilin, A., Kurasch, S., Burghard, M., Kern, K., & Kaiser, U. (2010). Atomic structure of reduced graphene oxide. *Nano letters*, *10*(4), 1144-1148.
- González, A. G., Pokrovsky, O. S., Santana-Casiano, J. M., & González-Dávila, M. (2017). Bioadsorption of heavy metals. In *Prospects and challenges in algal biotechnology* (pp. 233-255). Springer.

- Goswami, K. B., & Bisht, P. S. (2017). The Role of water resources in socio-economic development. *Int. J. Res. Appl. Sci. Eng. Technol*, 5, 1669-1674.
- Gregg, K., & Rogers, G. E. (1986). Feather keratin: composition, structure and biogenesis. In *Biology of the integument* (pp. 666-694). Springer.
- Gupta, V. K., Mittal, A., Kurup, L., & Mittal, J. (2006). Adsorption of a hazardous dye, erythrosine, over hen feathers. *Journal of colloid and interface science*, 304(1), 52-57.
- Hassan, M. M., & Davies-McConchie, J. F. (2012). Removal of arsenic and heavy metals from potable water by bauxsol immobilized onto wool fibers. *Industrial & engineering chemistry research*, 51(28), 9634-9641.
- Hematizad, I., Khanjari, A., Basti, A. A., Karabagias, I. K., Noori, N., Ghadami, F., Gholami, F., & Teimourifard, R. (2021). In vitro antibacterial activity of gelatin-nanochitosan films incorporated with Zataria multiflora Boiss essential oil and its influence on microbial, chemical, and sensorial properties of chicken breast meat during refrigerated storage. *Food Packaging and Shelf Life*, 30, 100751.
- Hoekstra, A. Y. (2015). The water footprint: The relation between human consumption and water use. In *The Water We Eat* (pp. 35-48). Springer.
- Homagai, P. L., Ghimire, K. N., & Inoue, K. (2010). Adsorption behavior of heavy metals onto chemically modified sugarcane bagasse. *Bioresource technology*, 101(6), 2067-2069.
- Huang, H., & Yang, X. (2004). Synthesis of chitosan-stabilized gold nanoparticles in the absence/presence of tripolyphosphate. *Biomacromolecules*, 5(6), 2340-2346.
- Idris, A., Vijayaraghavan, R., Rana, U. A., Fredericks, D., Patti, A. F., & Macfarlane, D. R. (2013). Dissolution of feather keratin in ionic liquids. *Green Chemistry*, 15(2), 525-534.
- Idris, A., Vijayaraghavan, R., Rana, U. A., Patti, A. F., & Macfarlane, D. R. (2014). Dissolution and regeneration of wool keratin in ionic liquids. *Green Chemistry*, 16(5), 2857-2864.
- Ishikawa, S.-I., Sekine, S., Miura, N., Suyama, K., Arihara, K., & Itoh, M. (2004). Removal of selenium and arsenic by animal biopolymers. *Biological Trace Element Research*, 102(1), 113-127.
- Järup, L. (2003). Hazards of heavy metal contamination. *British medical bulletin*, 68(1), 167-182.
- Jayaraj, K., Suriya, M., & Pius, A. (2019). Application of Bio-Waste Materials in The Green Synthesis Of Composites For Water Purification. *Advance Scientific Research*, 7.
- Jeong, H., Jin, M., So, K., Lim, S., & Lee, Y. (2009). Tailoring the characteristics of graphite oxides by different oxidation times. *Journal of Physics D: Applied Physics*, 42(6), 065418.
- Jia, X., Yang, N., Qi, X., Chen, L., & Zhao, Y. (2020). Adsorptive removal of cholesterol by biodegradable zein-graft- β -cyclodextrin film. *International Journal of Biological Macromolecules*, 155, 293-304.
- Jiang, Y., Liu, C., & Huang, A. (2019). EDTA-functionalized covalent organic framework for the removal of heavy-metal ions. *ACS applied materials & interfaces*, 11(35), 32186-32191.
- Jiang, Y.-J., Yu, X.-Y., Luo, T., Jia, Y., Liu, J.-H., & Huang, X.-J. (2013). γ -Fe₂O₃ nanoparticles encapsulated millimeter-sized magnetic chitosan beads for removal of Cr (VI) from water: thermodynamics, kinetics, regeneration, and uptake mechanisms. *Journal of Chemical & Engineering Data*, 58(11), 3142-3149.

- Kadirvelu, K., & Namasivayam, C. (2000). Agricultural by-product as metal adsorbent: sorption of lead (II) from aqueous solution onto coirpith carbon. *Environmental technology*, 21(10), 1091-1097.
- Kahdestani, S. A., Shahriari, M. H., & Abdouss, M. (2021). Synthesis and characterization of chitosan nanoparticles containing teicoplanin using sol-gel. *Polymer Bulletin*, 78(2), 1133-1148.
- Kakkar, P., Madhan, B., & Shanmugam, G. (2014). Extraction and characterization of keratin from bovine hoof: A potential material for biomedical applications. *SpringerPlus*, 3(1), 1-9.
- Kar, P., & Misra, M. (2004). Use of keratin fiber for separation of heavy metals from water. *Journal of Chemical Technology & Biotechnology: International Research in Process, Environmental & Clean Technology*, 79(11), 1313-1319.
- Kaur, M., Arshad, M., & Ullah, A. (2018). In-situ nanoreinforced green bionanomaterials from natural keratin and montmorillonite (MMT)/cellulose nanocrystals (CNC). *ACS Sustainable Chemistry & Engineering*, 6(2), 1977-1987.
- Khaskheli, M. A., Abro, M. I., Chand, R., Elahi, E., Khokhar, F. M., Majidano, A. A., Aaoud, E., Hassan, E., & Rekik, N. (2021). Evaluating the effectiveness of eggshells to remove heavy metals from wastewater. *Desalination and Water Treatment*, 216, 239-245.
- Khosa, M. A., & Ullah, A. (2014). In-situ modification, regeneration, and application of keratin biopolymer for arsenic removal. *Journal of hazardous materials*, 278, 360-371.
- Khosa, M. A., Wu, J., & Ullah, A. (2013). Chemical modification, characterization, and application of chicken feathers as novel biosorbents. *RSC advances*, 3(43), 20800-20810.
- KOCATÜRK, S., & Bornova, I. (2008). REMOVAL OF HEAVY METAL IONS FROM AQUEOUS SOLUTIONS BY KERATIN. *Chemical Engineering*, 603, 00.
- Koley, P., Sakurai, M., & Aono, M. (2016). Controlled fabrication of silk protein sericin mediated hierarchical hybrid flowers and their excellent adsorption capability of heavy metal ions of Pb (II), Cd (II) and Hg (II). *ACS applied materials & interfaces*, 8(3), 2380-2392.
- Kong, J., Yue, Q., Sun, S., Gao, B., Kan, Y., Li, Q., & Wang, Y. (2014). Adsorption of Pb (II) from aqueous solution using keratin waste-hide waste: equilibrium, kinetic and thermodynamic modeling studies. *Chemical Engineering Journal*, 241, 393-400.
- Kong, W., Li, Q., Liu, J., Li, X., Zhao, L., Su, Y., Yue, Q., & Gao, B. (2016). Adsorption behavior and mechanism of heavy metal ions by chicken feather protein-based semi-interpenetrating polymer networks super absorbent resin. *RSC advances*, 6(86), 83234-83243.
- Kreplak, L., Doucet, J., Dumas, P., & Briki, F. (2004). New aspects of the α -helix to β -sheet transition in stretched hard α -keratin fibers. *Biophysical journal*, 87(1), 640-647.
- Krishnan, S., Zulkapli, N. S., Kamyab, H., Taib, S. M., Din, M. F. B. M., Abd Majid, Z., Chairapat, S., Kenzo, I., Ichikawa, Y., & Nasrullah, M. (2021). Current technologies for recovery of metals from industrial wastes: An overview. *Environmental Technology & Innovation*, 22, 101525.
- Kumar, D., & Rani, S. (2015). Synthesis of amide functionalized graphene oxide for humidity sensing application. Proceedings of the 6th International Conference on Sensor Device Technologies and Applications (SENSORDEVICES'15),

- Kumar, S., & Parekh, S. H. (2020). Linking graphene-based material physicochemical properties with molecular adsorption, structure and cell fate. *Communications Chemistry*, 3(1), 1-11.
- Kumari, D., Goswami, R., Kumar, M., Katakai, R., & Shim, J. (2018). Removal of Cr (VI) ions from the aqueous solution through nanoscale zero-valent iron (nZVI) Magnetite Corn Cob Silica (MCCS): a bio-waste based water purification perspective. *Groundwater for Sustainable Development*, 7, 470-476.
- Kyzas, G. Z., Siafaka, P. I., Lambropoulou, D. A., Lazaridis, N. K., & Bikiaris, D. N. (2014). Poly (itaconic acid)-grafted chitosan adsorbents with different cross-linking for Pb (II) and Cd (II) uptake. *Langmuir*, 30(1), 120-131.
- Lazarus, B. S., Chadha, C., Velasco-Hogan, A., Barbosa, J. D., Jasiuk, I., & Meyers, M. A. (2021). Engineering with keratin: A functional material and a source of bioinspiration. *Isience*, 24(8), 102798.
- Li, Y., Liu, J., Yuan, Q., Tang, H., Yu, F., & Lv, X. (2016). A green adsorbent derived from banana peel for highly effective removal of heavy metal ions from water. *RSC advances*, 6(51), 45041-45048.
- Liu, B., & Huang, Y. (2011). Polyethyleneimine modified eggshell membrane as a novel biosorbent for adsorption and detoxification of Cr (VI) from water. *Journal of Materials Chemistry*, 21(43), 17413-17418.
- Liu, D., Li, Z., Li, W., Zhong, Z., Xu, J., Ren, J., & Ma, Z. (2013). Adsorption behavior of heavy metal ions from aqueous solution by soy protein hollow microspheres. *Industrial & engineering chemistry research*, 52(32), 11036-11044.
- Liu, F., Zou, H., Peng, J., Hu, J., Liu, H., Chen, Y., & Lu, F. (2016). Removal of copper (II) using deacetylated konjac glucomannan conjugated soy protein isolate. *International journal of biological macromolecules*, 86, 338-344.
- Liu, J., Su, D., Yao, J., Huang, Y., Shao, Z., & Chen, X. (2017). Soy protein-based polyethylenimine hydrogel and its high selectivity for copper ion removal in wastewater treatment. *Journal of Materials Chemistry A*, 5(8), 4163-4171.
- Liu, L., Liu, Q., Ma, J., Wu, H., Qu, Y., Gong, Y., Yang, S., An, Y., & Zhou, Y. (2020). Heavy metal (loid) s in the topsoil of urban parks in Beijing, China: Concentrations, potential sources, and risk assessment. *Environmental Pollution*, 260, 114083.
- Liu, W., Zhang, J., Jin, Y., Zhao, X., & Cai, Z. (2015). Adsorption of Pb (II), Cd (II) and Zn (II) by extracellular polymeric substances extracted from aerobic granular sludge: efficiency of protein. *Journal of Environmental Chemical Engineering*, 3(2), 1223-1232.
- Liu, Y., Wang, P., Gojenko, B., Yu, J., Wei, L., Luo, D., & Xiao, T. (2021). A review of water pollution arising from agriculture and mining activities in Central Asia: Facts, causes and effects. *Environmental Pollution*, 291, 118209.
- Lo, Y.-C., Cheng, C.-L., Han, Y.-L., Chen, B.-Y., & Chang, J.-S. (2014). Recovery of high-value metals from geothermal sites by biosorption and bioaccumulation. *Bioresource technology*, 160, 182-190.
- Lohri, C. R., Diener, S., Zabaleta, I., Mertenat, A., & Zurbrügg, C. (2017). Treatment technologies for urban solid biowaste to create value products: a review with focus on low-and middle-income settings. *Reviews in Environmental Science and Bio/Technology*, 16(1), 81-130.
- Ma, B., Qiao, X., Hou, X., & Yang, Y. (2016). Pure keratin membrane and fibers from chicken feather. *International journal of biological macromolecules*, 89, 614-621.

- Mahdavian, A. R., & Mirrahimi, M. A.-S. (2010). Efficient separation of heavy metal cations by anchoring polyacrylic acid on superparamagnetic magnetite nanoparticles through surface modification. *Chemical Engineering Journal*, 159(1-3), 264-271.
- Mahmoud, M. E., & Mohamed, R. H. A. (2014). Biosorption and removal of Cr (VI)–Cr (III) from water by eco-friendly gelatin biosorbent. *Journal of Environmental Chemical Engineering*, 2(1), 715-722.
- Marcano, D. C., Kosynkin, D. V., Berlin, J. M., Sinitskii, A., Sun, Z., Slesarev, A., Alemany, L. B., Lu, W., & Tour, J. M. (2010). Improved synthesis of graphene oxide. *ACS nano*, 4(8), 4806-4814.
- Martinez-Hernandez, A. L., Velasco-Santos, C., De Icaza, M., & Castano, V. M. (2005). Microstructural characterisation of keratin fibres from chicken feathers. *International journal of environment and pollution*, 23(2), 162-178.
- Mateo-Sagasta, J., Raschid-Sally, L., & Thebo, A. (2015). Global Wastewater and Sludge Production, Treatment and Use. In P. Drechsel, M. Qadir, & D. Wichelns (Eds.), *Wastewater: Economic Asset in an Urbanizing World* (pp. 15-38). Springer Netherlands. https://doi.org/10.1007/978-94-017-9545-6_2
- McGovern, V. (2000). Recycling poultry feathers: more bang for the cluck. *Environmental Health Perspectives*, 108(8), A366-A369.
- McKittrick, J., Chen, P.-Y., Bodde, S., Yang, W., Novitskaya, E., & Meyers, M. (2012). The structure, functions, and mechanical properties of keratin. *Jom*, 64(4), 449-468.
- Menefee, E., & Yee, G. (1965). Thermally-induced structural changes in wool. *Textile Research Journal*, 35(9), 801-812.
- Misra, M., Kar, P., Priyadarshan, G., & Licata, C. (2001). Keratin protein nano-fiber for removal of heavy metals and contaminants. *MRS Online Proceedings Library (OPL)*, 702.
- Mittal, A. (2006). Adsorption kinetics of removal of a toxic dye, Malachite Green, from wastewater by using hen feathers. *Journal of hazardous materials*, 133(1-3), 196-202.
- Mkhoyan, K. A., Contryman, A. W., Silcox, J., Stewart, D. A., Eda, G., Mattevi, C., Miller, S., & Chhowalla, M. (2009). Atomic and electronic structure of graphene-oxide. *Nano letters*, 9(3), 1058-1063.
- Mohammed, A., Alobaidi, Y., & Abdullah, H. (2022). Synthesis of nanochitosan membranes from shrimp shells. *Egyptian Journal of Chemistry*.
- Mokhatab, S., Poe, W. A., & Mak, J. Y. (2019). Natural gas dehydration and mercaptans removal. *Handbook of Natural Gas Transmission and Processing*, 4.
- Mondal, N. K., & Basu, S. (2019). Potentiality of waste human hair towards removal of chromium (VI) from solution: kinetic and equilibrium studies. *Applied Water Science*, 9(3), 1-8.
- Morais, S., Costa, F. G., & Pereira, M. d. L. (2012). Heavy metals and human health. *Environmental health—emerging issues and practice*, 10(1), 227-245.
- Motarjemi, Y., Moy, G., & Todd, E. (2013). *Encyclopedia of food safety*. Academic Press.
- Naik, R. L., Kumar, M. R., & Narsaiah, T. B. (2022). Removal of heavy metals (Cu & Ni) from wastewater using rice husk and orange peel as adsorbents. *Materials Today: Proceedings*.
- Negroiu, M., Țurcanu, A. A., Matei, E., Râpă, M., Covaliu, C. I., Predescu, A. M., Pantilimon, C. M., Coman, G., & Predescu, C. (2021). Novel adsorbent based on banana peel waste for removal of heavy metal ions from synthetic solutions. *Materials*, 14(14), 3946.
- Nematidil, N., & Sadeghi, M. (2019). Fabrication and characterization of a novel biosorbent and its evaluation as adsorbent for heavy metal ions. *Polymer Bulletin*, 76(10), 5103-5127.

- Ni, N., Zhang, D., & Dumont, M.-J. (2018). Synthesis and characterization of zein-based superabsorbent hydrogels and their potential as heavy metal ion chelators. *Polymer Bulletin*, 75(1), 31-45.
- Nuithitikul, K., Phromrak, R., & Saengngoen, W. (2020). Utilization of chemically treated cashew-nut shell as potential adsorbent for removal of Pb (II) ions from aqueous solution. *Scientific Reports*, 10(1), 1-14.
- Oliveira, J. A., Cunha, F. A., & Ruotolo, L. A. (2019). Synthesis of zeolite from sugarcane bagasse fly ash and its application as a low-cost adsorbent to remove heavy metals. *Journal of cleaner production*, 229, 956-963.
- Organization, W. H. (2019). *Progress on household drinking water, sanitation and hygiene 2000-2017: special focus on inequalities*. World Health Organization.
- Osasona, I., Ojo Adebayo, A., & Ajayi, O. O. (2013). Adsorptive Removal of Chromium (VI) from Aqueous Solution Using Cow Hooves. *Adsorptive Removal of Chromium (VI) from Aqueous Solution Using Cow Hooves.*, 2(1), 1-16.
- Pal, P., Syed, S. S., & Banat, F. (2017). Gelatin-bentonite composite as reusable adsorbent for the removal of lead from aqueous solutions: Kinetic and equilibrium studies. *Journal of Water Process Engineering*, 20, 40-50.
- Paredes, J., Villar-Rodil, S., Martínez-Alonso, A., & Tascon, J. (2008). Graphene oxide dispersions in organic solvents. *Langmuir*, 24(19), 10560-10564.
- Park, D., Lim, S.-R., Yun, Y.-S., & Park, J. M. (2007). Reliable evidences that the removal mechanism of hexavalent chromium by natural biomaterials is adsorption-coupled reduction. *Chemosphere*, 70(2), 298-305.
- Park, H. J., Jeong, S. W., Yang, J. K., Kim, B. G., & Lee, S. M. (2007). Removal of heavy metals using waste eggshell. *Journal of Environmental Sciences*, 19(12), 1436-1441.
- Park, S., An, J., Potts, J. R., Velamakanni, A., Murali, S., & Ruoff, R. S. (2011). Hydrazine-reduction of graphite-and graphene oxide. *Carbon*, 49(9), 3019-3023.
- Parker, D. B., & Brown, M. S. (2003). Water consumption for livestock and poultry production. *Encyclopedia of Water Science, 1st Ed.; Stewart, BA, Howell, TA, Eds.*
- Pérez-Palacios, T., Ruiz, J., Martín, D., Muriel, E., & Antequera, T. (2008). Comparison of different methods for total lipid quantification in meat and meat products. *Food chemistry*, 110(4), 1025-1029.
- Peydayesh, M., & Mezzenga, R. (2021). Protein nanofibrils for next generation sustainable water purification. *Nature communications*, 12(1), 1-17.
- Pravin, M., & Gnanamani, A. (2018). Preparation, characterization and reusability efficacy of amine-functionalized graphene oxide-polyphenol oxidase complex for removal of phenol from aqueous phase. *RSC advances*, 8(67), 38416-38424.
- Qamar, M. A., Javed, M., Shahid, S., Shariq, M., Fadhali, M. M., Ali, S. K., & Khan, M. S. (2023). Synthesis and applications of graphitic carbon nitride (g-C₃N₄) based membranes for wastewater treatment: A critical review. *Heliyon*, e12685.
- Qasem, N. A., Mohammed, R. H., & Lawal, D. U. (2021). Removal of heavy metal ions from wastewater: A comprehensive and critical review. *Npj Clean Water*, 4(1), 1-15.
- Rampino, A., Borgogna, M., Blasi, P., Bellich, B., & Cesàro, A. (2013). Chitosan nanoparticles: Preparation, size evolution and stability. *International journal of pharmaceutics*, 455(1-2), 219-228.
- Rodzic, A., Pomastowski, P., Sagandykova, G. N., & Buszewski, B. (2020). Interactions of whey proteins with metal ions. *International journal of molecular sciences*, 21(6), 2156.

- Rojas, S., & Horcajada, P. (2020). Metal–organic frameworks for the removal of emerging organic contaminants in water. *Chemical reviews*, *120*(16), 8378-8415.
- Šafarič, R., Fras Zemljič, L., Novak, M., Dugonik, B., Bratina, B., Gubelj, N., Bolka, S., & Strnad, S. (2020). Preparation and characterisation of waste poultry feathers composite fibreboards. *Materials*, *13*(21), 4964.
- Saha, S., Arshad, M., Zubair, M., & Ullah, A. (2019). Keratin as a Biopolymer. In *Keratin as a protein biopolymer* (pp. 163-185). Springer.
- Saha, S., Zubair, M., Khosa, M., Song, S., & Ullah, A. (2019). Keratin and chitosan biosorbents for wastewater treatment: a review. *Journal of Polymers and the Environment*, *27*(7), 1389-1403.
- Sangeetha, K., Vidhya, G., Vasugi, G., & Girija, E. (2018). Lead and cadmium removal from single and binary metal ion solution by novel hydroxyapatite/alginate/gelatin nanocomposites. *Journal of Environmental Chemical Engineering*, *6*(1), 1118-1126.
- Sato, T., Qadir, M., Yamamoto, S., Endo, T., & Zahoor, A. (2013). Global, regional, and country level need for data on wastewater generation, treatment, and use. *Agricultural Water Management*, *130*, 1-13. <https://doi.org/10.1016/j.agwat.2013.08.007>
- Saucedo-Rivalcoba, V., Martínez-Hernández, A., Martínez-Barrera, G., Velasco-Santos, C., Rivera-Armenta, J., & Castaño, V. (2011). Removal of hexavalent chromium from water by polyurethane–keratin hybrid membranes. *Water, Air, & Soil Pollution*, *218*(1), 557-571.
- Sayed, S., Saleh, S., & Hasan, E. (2005). Removal of some polluting metals from industrial water using chicken feathers. *Desalination*, *181*(1-3), 243-255.
- Sekimoto, Y., Okiharu, T., Nakajima, H., Fujii, T., Shirai, K., & Moriwaki, H. (2013). Removal of Pb (II) from water using keratin colloidal solution obtained from wool. *Environmental Science and Pollution Research*, *20*(9), 6531-6538.
- Senoz, E., & Wool, R. P. (2010). Microporous carbon–nitrogen fibers from keratin fibers by pyrolysis. *Journal of applied polymer science*, *118*(3), 1752-1765.
- SenthilKumar, P., Ramalingam, S., Sathyaselvabala, V., Kirupha, S. D., & Sivanesan, S. (2011). Removal of copper (II) ions from aqueous solution by adsorption using cashew nut shell. *Desalination*, *266*(1-3), 63-71.
- Shah, A., Tyagi, S., Bharagava, R. N., Belhaj, D., Kumar, A., Saxena, G., Saratale, G. D., & Mulla, S. I. (2019). Keratin production and its applications: current and future perspective. *Keratin as a protein biopolymer*, 19-34.
- Shanmugaraj, A., Yoon, J., Yang, W., & Ryu, S. H. (2013). Synthesis, characterization, and surface wettability properties of amine functionalized graphene oxide films with varying amine chain lengths. *Journal of colloid and interface science*, *401*, 148-154.
- Shannon, M. A., Bohn, P. W., Elimelech, M., Georgiadis, J. G., Marinas, B. J., & Mayes, A. M. (2010). Science and technology for water purification in the coming decades. *Nanoscience and technology: a collection of reviews from nature Journals*, 337-346.
- Sharma, G., & Naushad, M. (2020). Adsorptive removal of noxious cadmium ions from aqueous medium using activated carbon/zirconium oxide composite: isotherm and kinetic modelling. *Journal of Molecular Liquids*, *310*, 113025.
- Sharma, P., Singh, S. P., Parakh, S. K., & Tong, Y. W. (2022). Health hazards of hexavalent chromium (Cr (VI)) and its microbial reduction. *Bioengineered*, *13*(3), 4923-4938.
- Sharma, S., & Gupta, A. (2016). Sustainable management of keratin waste biomass: applications and future perspectives. *Brazilian Archives of Biology and Technology*, *59*.

- Shavandi, A., Silva, T. H., Bekhit, A. A., & Bekhit, A. E.-D. A. (2017). Keratin: dissolution, extraction and biomedical application. *Biomaterials science*, 5(9), 1699-1735.
- Shen, S., Li, X.-F., Cullen, W. R., Weinfeld, M., & Le, X. C. (2013). Arsenic binding to proteins. *Chemical reviews*, 113(10), 7769-7792.
- Siddiqua, A., Hahladakis, J. N., & Al-Attiya, W. A. K. A. (2022). An overview of the environmental pollution and health effects associated with waste landfilling and open dumping. *Environmental Science and Pollution Research*.
<https://doi.org/10.1007/s11356-022-21578-z>
- Subramaniam, M. N., Goh, P. S., Lau, W. J., & Ismail, A. F. (2019). The roles of nanomaterials in conventional and emerging technologies for heavy metal removal: A state-of-the-art review. *Nanomaterials*, 9(4), 625.
- Sun, P., Liu, Z.-T., & Liu, Z.-W. (2009a). Chemically modified chicken feather as sorbent for removing toxic chromium (VI) ions. *Industrial & engineering chemistry research*, 48(14), 6882-6889.
- Sun, P., Liu, Z.-T., & Liu, Z.-W. (2009b). Particles from bird feather: A novel application of an ionic liquid and waste resource. *Journal of hazardous materials*, 170(2-3), 786-790.
- Tagliavini, M., Engel, F., Weidler, P. G., Scherer, T., & Schäfer, A. I. (2017). Adsorption of steroid micropollutants on polymer-based spherical activated carbon (PBSAC). *Journal of hazardous materials*, 337, 126-137.
- Tansel, B., Sager, J., Rector, T., Garland, J., Strayer, R. F., Levine, L., Roberts, M., Hummerick, M., & Bauer, J. (2006). Significance of hydrated radius and hydration shells on ionic permeability during nanofiltration in dead end and cross flow modes. *Separation and Purification Technology*, 51(1), 40-47.
- Team, R. C. (2019). 2020. *R: A Language and Environment for Statistical Computing*. R Foundation for Statistical Computing, Vienna, Austria: Available at: <https://www.R-project.org/>. [Google Scholar].
- Teng, D., Xu, Y., Zhao, T., Zhang, X., Li, Y., & Zeng, Y. (2022). Zein adsorbents with micro/nanofibrous membrane structure for removal of oils, organic dyes, and heavy metal ions in aqueous solution. *Journal of hazardous materials*, 425, 128004.
- Tesfaye, T., Sithole, B., & Ramjugernath, D. (2017a). Valorisation of chicken feathers: a review on recycling and recovery route—current status and future prospects. *Clean Technologies and Environmental Policy*, 19(10), 2363-2378.
- Tesfaye, T., Sithole, B., & Ramjugernath, D. (2017b). Valorisation of chicken feathers: recycling and recovery routes. Proceedings, Sardinia,
- Tesfaye, T., Sithole, B., Ramjugernath, D., & Chunilall, V. (2017). Valorisation of chicken feathers: Characterisation of chemical properties. *Waste Management*, 68, 626-635.
- Thamer, B. M., Aldalbahi, A., Moydeen A, M., Rahaman, M., & El-Newehy, M. H. (2021). Modified electrospun polymeric nanofibers and their nanocomposites as nanoadsorbents for toxic dye removal from contaminated waters: A review. *Polymers*, 13(1), 20.
- Thanawatpoontawee, S., Imyim, A., & Praphairaksit, N. (2016). Iron-loaded zein beads as a biocompatible adsorbent for arsenic (V) removal. *Journal of Industrial and Engineering Chemistry*, 43, 127-132.
- Thommes, M., Kaneko, K., Neimark, A. V., Olivier, J. P., Rodriguez-Reinoso, F., Rouquerol, J., & Sing, K. S. (2015). Physisorption of gases, with special reference to the evaluation of surface area and pore size distribution (IUPAC Technical Report). *Pure and applied chemistry*, 87(9-10), 1051-1069.

- Timorshina, S., Popova, E., & Osmolovskiy, A. (2022). Sustainable Applications of Animal Waste Proteins. *Polymers*, *14*(8), 1601.
- Tonin, C., Zoccola, M., Aluigi, A., Varesano, A., Montarsolo, A., Vineis, C., & Zimbardi, F. (2006). Study on the conversion of wool keratin by steam explosion. *Biomacromolecules*, *7*(12), 3499-3504.
- Tsukada, M., Freddi, G., Monti, P., Bertoluzza, A., & Kasai, N. (1995). Structure and molecular conformation of tussah silk fibroin films: Effect of methanol. *Journal of Polymer Science Part B: Polymer Physics*, *33*(14), 1995-2001.
- Ullah, A., & Wu, J. (2013). Feather fiber-based thermoplastics: effects of different plasticizers on material properties. *Macromolecular Materials and Engineering*, *298*(2), 153-162.
- UNO. (2020). <https://www.un.org/sustainabledevelopment/water-and-sanitation/>
- Uzun, M., Sancak, E., Patel, I., Usta, I., Akalın, M., & Yuksek, M. (2011). Mechanical behaviour of chicken quills and chicken feather fibres reinforced polymeric composites. *Archives of Materials Science and Engineering*, *52*(2), 82-86.
- Vijayalakshmi, K., Devi, B., Sudha, P., Venkatesan, J., & Anil, S. (2016). Synthesis, characterization and applications of nanochitosan/sodium alginate/microcrystalline cellulose film. *J. Nanomed. Nanotechnol*, *7*(6).
- Vilardi, G., Di Palma, L., & Verdone, N. (2018). Heavy metals adsorption by banana peels micro-powder: Equilibrium modeling by non-linear models. *Chinese Journal of Chemical Engineering*, *26*(3), 455-464.
- Walker, D., Baumgartner, D., Gerba, C., & Fitzsimmons, K. (2019). Surface water pollution. In *Environmental and pollution science* (pp. 261-292). Elsevier.
- Wan, Y., Creber, K. A., Peppley, B., & Bui, V. T. (2003). Synthesis, characterization and ionic conductive properties of phosphorylated chitosan membranes. *Macromolecular Chemistry and Physics*, *204*(5-6), 850-858.
- Wang, B., Yang, W., McKittrick, J., & Meyers, M. A. (2016). Keratin: Structure, mechanical properties, occurrence in biological organisms, and efforts at bioinspiration. *Progress in Materials Science*, *76*, 229-318.
- Wang, F., Wu, P., Shu, L., Huang, D., & Liu, H. (2022). High-efficiency adsorption of Cd (II) and Co (II) by ethylenediaminetetraacetic dianhydride-modified orange peel as a novel synthesized adsorbent. *Environmental Science and Pollution Research*, *29*(17), 25748-25758.
- Wang, H., Jin, X., & Wu, H. (2016). Adsorption and desorption properties of modified feather and feather/polypropylene melt-blown filter cartridge of lead ion (Pb²⁺). *Journal of Industrial Textiles*, *46*(3), 852-867.
- Wang, J., & Chen, C. (2009). Biosorbents for heavy metals removal and their future. *Biotechnology advances*, *27*(2), 195-226.
- Wang, L., Rinklebe, J., Tack, F. M., & Hou, D. (2021). A review of green remediation strategies for heavy metal contaminated soil. *Soil Use and Management*, *37*(4), 936-963.
- Wang, S., Li, X., Liu, Y., Zhang, C., Tan, X., Zeng, G., Song, B., & Jiang, L. (2018). Nitrogen-containing amino compounds functionalized graphene oxide: Synthesis, characterization and application for the removal of pollutants from wastewater: A review. *Journal of hazardous materials*, *342*, 177-191.
<https://doi.org/https://doi.org/10.1016/j.jhazmat.2017.06.071>

- Wang, X., Huang, K., Chen, Y., Liu, J., Chen, S., Cao, J., Mei, S., Zhou, Y., & Jing, T. (2018). Preparation of dumbbell manganese dioxide/gelatin composites and their application in the removal of lead and cadmium ions. *Journal of hazardous materials*, 350, 46-54.
- Wang, X., Shi, Z., Zhao, Q., & Yun, Y. (2021). Study on the structure and properties of biofunctional keratin from rabbit hair. *Materials*, 14(2), 379.
- Wang, X., Xi, Z., Liu, Z., Yang, L., & Cao, Y. (2011). The fabrication and property of hydrophilic and hydrophobic double functional bionic chitosan film. *Journal of Nanoscience and Nanotechnology*, 11(11), 9737-9740.
- Weber, J., Schmidt, J., Thomas, A., & Böhlmann, W. (2010). Micropore analysis of polymer networks by gas sorption and ^{129}Xe NMR spectroscopy: toward a better understanding of intrinsic microporosity. *Langmuir*, 26(19), 15650-15656.
- Wen, H.-F., Yang, C., Yu, D.-G., Li, X.-Y., & Zhang, D.-F. (2016). Electrospun zein nanoribbons for treatment of lead-contained wastewater. *Chemical Engineering Journal*, 290, 263-272.
- Werber, J. R., Osuji, C. O., & Elimelech, M. (2016). Materials for next-generation desalination and water purification membranes. *Nature Reviews Materials*, 1(5), 1-15.
- Wichelns, D., Drechsel, P., & Qadir, M. (2015). Wastewater: Economic Asset in an Urbanizing World. In P. Drechsel, M. Qadir, & D. Wichelns (Eds.), *Wastewater: Economic Asset in an Urbanizing World* (pp. 3-14). Springer Netherlands. https://doi.org/10.1007/978-94-017-9545-6_1
- William Horwitz, G. W. L., Jr. (2005). *Official Methods of Analysis* (18th ed.). AOAC International.
- Witus, L. S., & Francis, M. B. (2011). Using synthetically modified proteins to make new materials. *Accounts of chemical research*, 44(9), 774-783.
- Wojciechowska, P., Cierpiszewski, R., & Maciejewski, H. (2022). Gelatin–Siloxane Hybrid Monoliths as Novel Heavy Metal Adsorbents. *Applied Sciences*, 12(3), 1258.
- Wong, S. S., Jameson, D. M., & Wong, S. (2012). *Chemistry of protein and nucleic acid cross-linking and conjugation*. CRC Press Boca Raton, FL, USA:.
- Xu, H., Zhang, Y., Jiang, Q., Reddy, N., & Yang, Y. (2013). Biodegradable hollow zein nanoparticles for removal of reactive dyes from wastewater. *Journal of environmental management*, 125, 33-40.
- Xu, J., Cao, Z., Zhang, Y., Yuan, Z., Lou, Z., Xu, X., & Wang, X. (2018). A review of functionalized carbon nanotubes and graphene for heavy metal adsorption from water: Preparation, application, and mechanism. *Chemosphere*, 195, 351-364.
- Xu, Q., Zeng, M., Feng, Z., Yin, D., Huang, Y., Chen, Y., Yan, C., Li, R., & Gu, Y. (2016). Understanding the effects of carboxylated groups of functionalized graphene oxide on the curing behavior and intermolecular interactions of benzoxazine nanocomposites. *RSC advances*, 6(37), 31484-31496.
- Xu, X., Zhou, C., Zhang, S., Cheng, Z., Yang, Z., Xian, J., & Yang, Y. (2019). Adsorption of Cr^{6+} and Pb^{2+} on soy sauce residue biochar from aqueous solution. *BioResources*, 14(2), 4653-4669.
- Yamauchi, K., & Khoda, A. (1997). Novel proteinous microcapsules from wool keratins. *Colloids and Surfaces B: Biointerfaces*, 9(1-2), 117-119.
- Yang, C.-H., Lin, Y.-S., Huang, K.-S., Huang, Y.-C., Wang, E.-C., Jhong, J.-Y., & Kuo, C.-Y. (2009). Microfluidic emulsification and sorting assisted preparation of monodisperse chitosan microparticles. *Lab on a Chip*, 9(1), 145-150.

- Yang, R., Li, Z., Huang, B., Luo, N., Huang, M., Wen, J., Zhang, Q., Zhai, X., & Zeng, G. (2018). Effects of Fe (III)-fulvic acid on Cu removal via adsorption versus coprecipitation. *Chemosphere*, *197*, 291-298.
- Yasmeen, K., Saeed, I., & Zubair, M. (2022). Estimations of Potential Risk of Carcinogenic Arsenic in Smokeless Tobacco Products. *New Journal of Chemistry*.
- Ye, S., & Feng, J. (2013). A new insight into the in situ thermal reduction of graphene oxide dispersed in a polymer matrix. *Polymer Chemistry*, *4*(6), 1765-1768.
- Yu, Z., Zhang, X., & Huang, Y. (2013). Magnetic chitosan–iron (III) hydrogel as a fast and reusable adsorbent for chromium (VI) removal. *Industrial & engineering chemistry research*, *52*(34), 11956-11966.
- Zahara, I., Arshad, M., Naeth, M. A., Siddique, T., & Ullah, A. (2021). Feather keratin derived sorbents for the treatment of wastewater produced during energy generation processes. *Chemosphere*, *273*, 128545.
- Zaimee, M. Z. A., Sarjadi, M. S., & Rahman, M. L. (2021). Heavy metals removal from water by efficient adsorbents. *Water*, *13*(19), 2659.
- Zainuddin, N. A., Mamat, T. A. R., Maarof, H. I., Puasa, S. W., & Yatim, S. R. M. (2019). Removal of nickel, zinc and copper from plating process industrial raw effluent via hydroxide precipitation versus sulphide precipitation. IOP Conference Series: Materials Science and Engineering,
- Zangmeister, C. D. (2010). Preparation and evaluation of graphite oxide reduced at 220 C. *Chemistry of Materials*, *22*(19), 5625-5629.
- Zhang, H., Carrillo-Navarrete, F., López-Mesas, M., & Palet, C. (2020). Use of chemically treated human hair wastes for the removal of heavy metal ions from water. *Water*, *12*(5), 1263.
- Zhang, W., Zhang, J., Jiang, Q., & Xia, W. (2012). Physicochemical and structural characteristics of chitosan nanopowders prepared by ultrafine milling. *Carbohydrate Polymers*, *87*(1), 309-313.
- Zhang, Y., Zhang, X., Ding, R., Zhang, J., & Liu, J. (2011). Determination of the degree of deacetylation of chitosan by potentiometric titration preceded by enzymatic pretreatment. *Carbohydrate Polymers*, *83*(2), 813-817.
<https://doi.org/https://doi.org/10.1016/j.carbpol.2010.08.058>
- Zhang, Y., Zhao, W., & Yang, R. (2015). Steam flash explosion assisted dissolution of keratin from feathers. *ACS Sustainable Chemistry & Engineering*, *3*(9), 2036-2042.
- Zhao, J., Liu, L., & Li, F. (2015). *Graphene oxide: physics and applications*. Springer.
- Zhao, W., Yang, R., Zhang, Y., & Wu, L. (2012). Sustainable and practical utilization of feather keratin by an innovative physicochemical pretreatment: high density steam flash-explosion. *Green Chemistry*, *14*(12), 3352-3360.
- Zhao, X., & Liu, C. (2019). Efficient removal of heavy metal ions based on the selective hydrophilic channels. *Chemical Engineering Journal*, *359*, 1644-1651.
- Zhou, Q., Yang, N., Li, Y., Ren, B., Ding, X., Bian, H., & Yao, X. (2020). Total concentrations and sources of heavy metal pollution in global river and lake water bodies from 1972 to 2017. *Global Ecology and Conservation*, *22*, e00925.
- Zhou, Z., Liu, Y.-g., Liu, S.-b., Liu, H.-y., Zeng, G.-m., Tan, X.-f., Yang, C.-p., Ding, Y., Yan, Z.-l., & Cai, X.-x. (2017). Sorption performance and mechanisms of arsenic (V) removal by magnetic gelatin-modified biochar. *Chemical Engineering Journal*, *314*, 223-231.

- Zhu, Y., He, X., Xu, J., Fu, Z., Wu, S., Ni, J., & Hu, B. (2021). Insight into efficient removal of Cr (VI) by magnetite immobilized with *Lysinibacillus* sp. JLT12: Mechanism and performance. *Chemosphere*, 262, 127901.
- Zhu, Y., Murali, S., Cai, W., Li, X., Suk, J. W., Potts, J. R., & Ruoff, R. S. (2010). Graphene and graphene oxide: synthesis, properties, and applications. *Advanced materials*, 22(35), 3906-3924.
- Zsirai, T., Qiblawey, H., A-Marri, M. J., & Judd, S. (2016). The impact of mechanical shear on membrane flux and energy demand. *Journal of Membrane Science*, 516, 56-63.
<https://doi.org/10.1016/j.memsci.2016.06.010>
- Zubair, M., Arshad, M., & Ullah, A. (2020). Chitosan-based materials for water and wastewater treatment. In *Handbook of chitin and chitosan* (pp. 773-809). Elsevier.
- Zubair, M., Arshad, M., & Ullah, A. (2021). Nanocellulose: A sustainable and renewable material for water and wastewater treatment. In *Natural Polymers-Based Green Adsorbents for Water Treatment* (pp. 93-109). Elsevier.
- Zubair, M., Roopesh, M., & Ullah, A. (2022). Nano-modified feather keratin derived green and sustainable biosorbents for the remediation of heavy metals from synthetic wastewater. *Chemosphere*, 308, 136339.
- Zubair, M., & Ullah, A. (2021). Biopolymers in environmental applications: industrial wastewater treatment. *Biopolymers and their industrial applications*, 331-349.
- Zubair, M., Wu, J., & Ullah, A. (2022). Bionanocomposites from spent hen proteins reinforced with polyhedral oligomeric silsesquioxane (POSS)/cellulose nanocrystals (CNCs). *Biocatalysis and Agricultural Biotechnology*, 43, 102434.

Appendices:

Appendix-I: Cumulative surface area, pore volume, micropore pore volume and V-t surface area of the CFK and biosorbents

Characteristics	CFK	CFK-GO (1%)	CFK-GO (3%)	CFK-GO (5%)
NLDFT Data				
Cumulative Surface Area (m²/g)	1.60×10^{-1}	11.62	1.543	6.0×10^{-2}
Pore Volume (cc/g)	8.00×10^{-4}	4.02×10^{-2}	8.80×10^{-3}	4.00×10^{-3}
Micropore (MP) Method Analysis				
MP Pore Volume (cc/g)	3.91×10^{-5}	7.50×10^{-2}	1.78×10^{-4}	9.67×10^{-5}
V-t Surface Area (m²/g)	4.30×10^{-2}	1.17×10^2	2.07×10^{-1}	1.85×10^{-1}

Appendix-II: Metals biosorption efficiency (%) of dissolved CFK

	Co	Ni	Pb	Zn	Cd	As	Se	Cr
Biosorption efficiency (%)	43.68 (3.20)	42.65 (2.55)	22.62 (2.83)	44.61 (4.10)	28.31 (2.615)	42.59 (3.08)	63.68 (5.93)	21.42 (1.36)

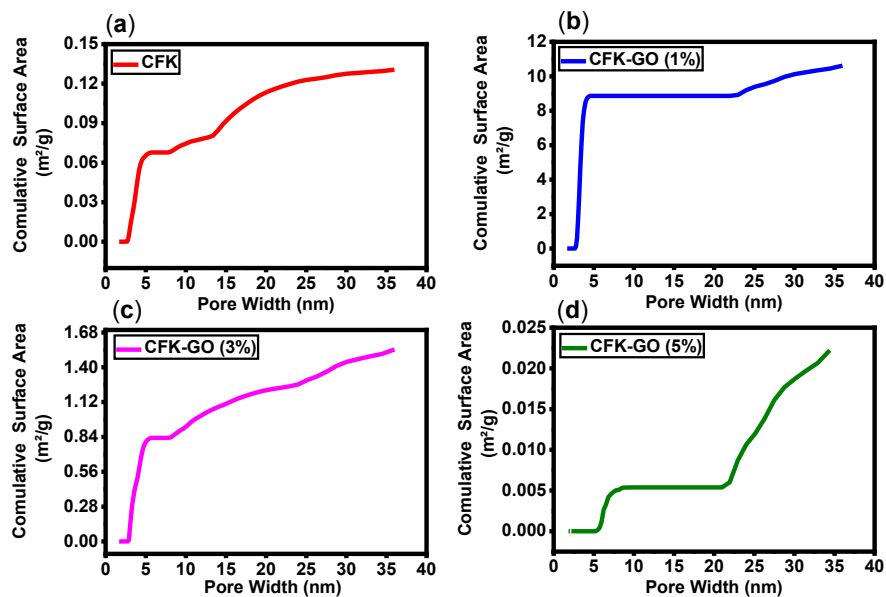
Values given in parenthesis is standard deviation

Appendix-III: Metals biosorption efficiency of CFK-GO (0.5%)

	Co	Ni	Pb	Zn	Cd	As	Se	Cr
Biosorption efficiency (%)	62.92 (2.05)	69.09 (3.60)	54.85 (5.00)	64.05 (3.47)	59.54 (1.66)	92.44 (2.44)	83.79 (2.57)	68.88 (1.14)

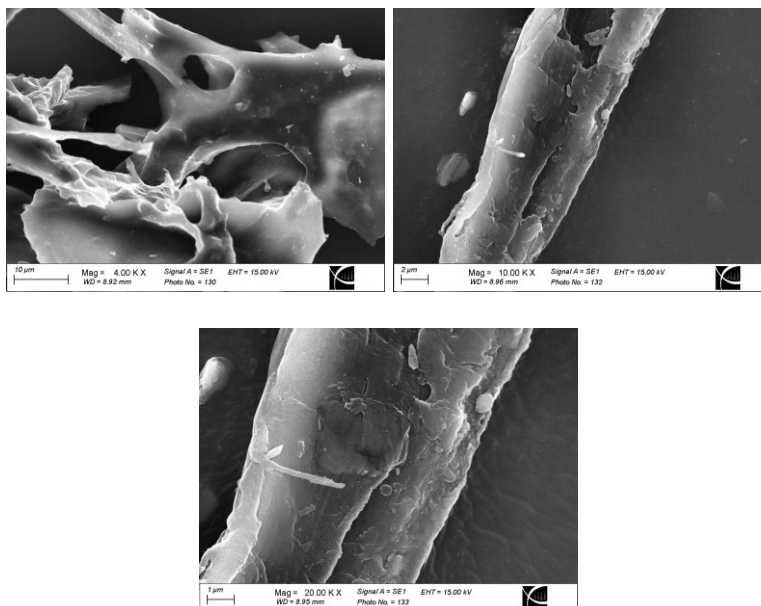
Values given in parenthesis is standard deviation

Appendix-IV: Cumulative surface area of (a) CFK (b) CFK-GO (1%) (c) CFK-GO (3%) (d) CFK-GO (5%) as determined by non-linear DFT

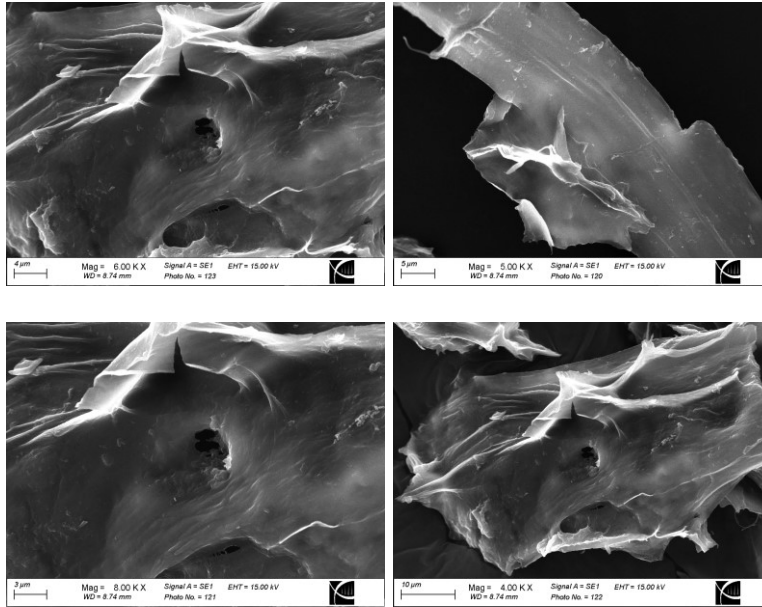


Appendix-V: Scanning electron microscopy images of chicken feather keratin after biosorption

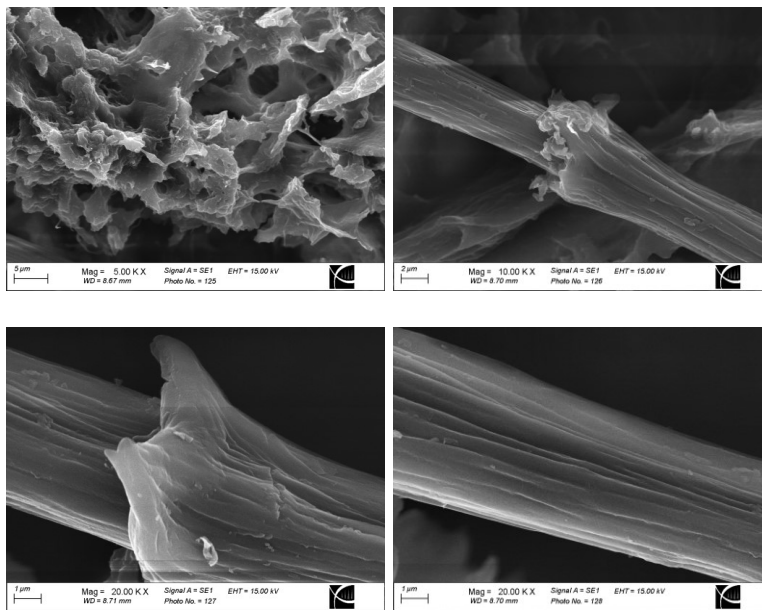
CFK contains 1% nanochitosan



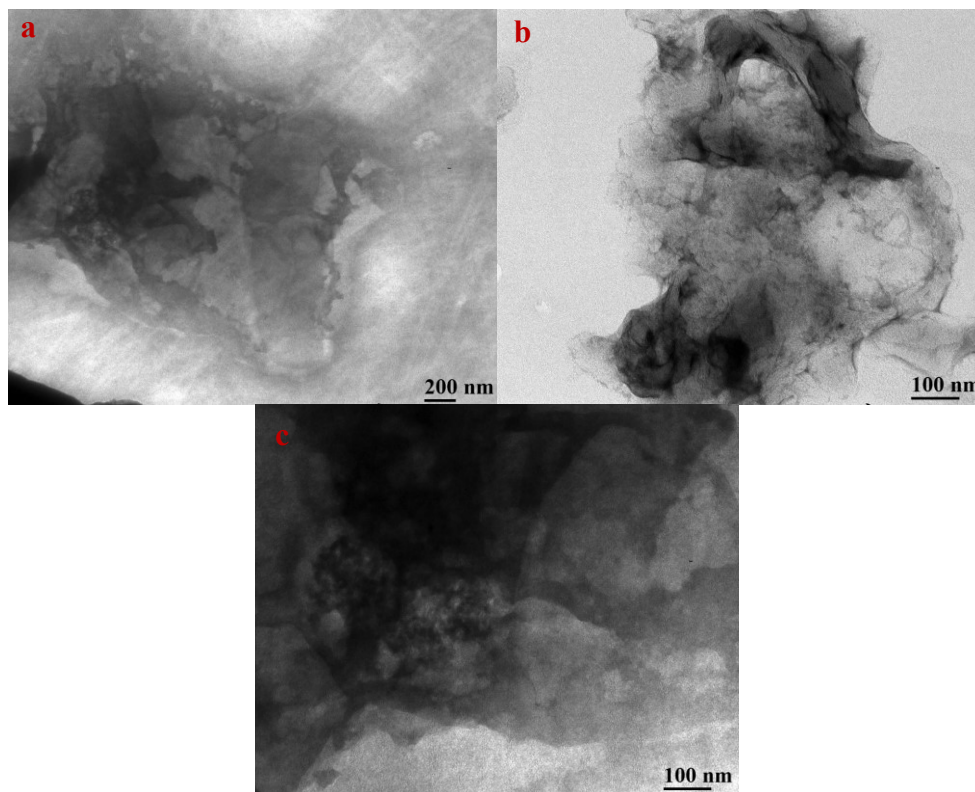
CFK contains 3% nanochitosan



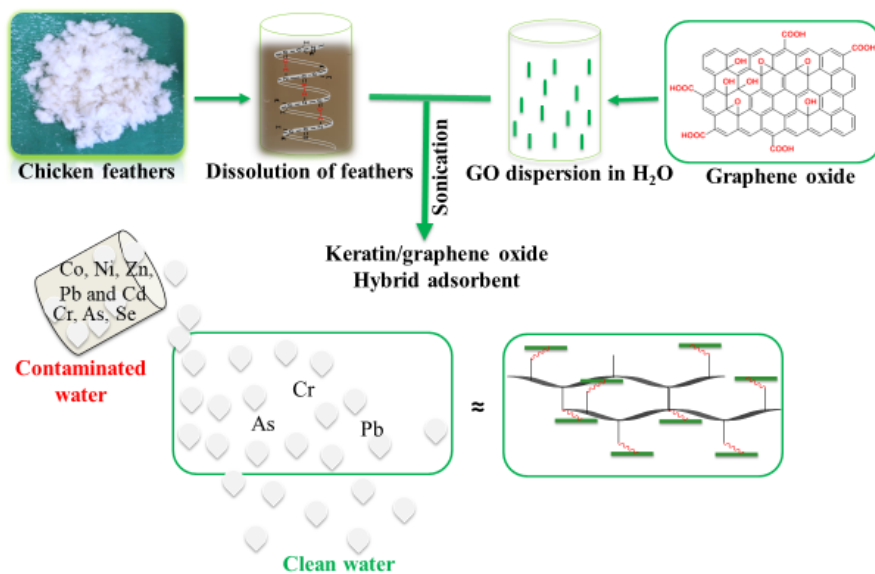
CFK contains 5% nanochitosan



Appendix-VI: Transmission electron microscopy images of SMGO (a & b) and CFK-SMGO (c)

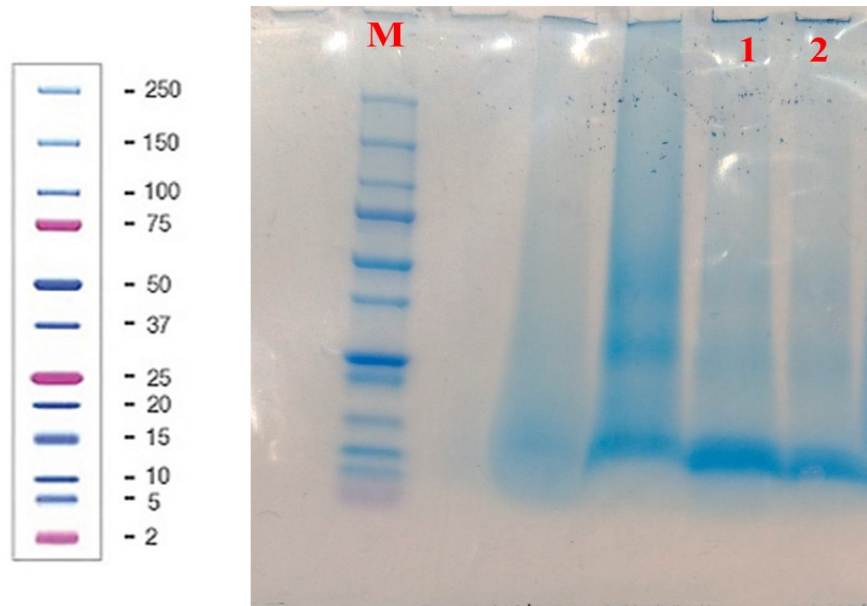


Appendix-VII: Graphical representation of the CFK-GO derived biosorbents



Appendix-VIII: Determination of chicken feathers keratin molecular weight

Sodium dodecyl sulfate polyacrylamide gel electrophoresis (SDS-PAGE) of chicken feather keratin was performed with Bio-Rad Criterion Cell (Bio-Rad Laboratories, Inc., Canada) on a precast (10–20%) Tris–HCl gradient polyacrylamide gel. Before the electrophoresis run, each keratin protein sample was diluted in a loading buffer (Bio-Rad Laboratories, Inc., Canada). The keratin protein bands were stained using Coomassie Brilliant Blue G-250 (Alahyaribeik & Ullah, 2020). A marker of molecular weight (2 to 250 kDa) from a Bio-Rad standard low molecular weight calibration kit was used to identify the M.W. of keratin proteins. The results showed keratin proteins with low molecular weight 10 kDa, which showed no change in the molecular weight of keratin during extraction.



SDS-PAGE of chicken feather keratin (**lanes 1&2**) and marker of standard molecular weight (**lane M**)

Appendix-IX: Comparison of biosorption performance of biosorbents for metal ions among study I, II and III

Ni

Biosorbents	Biosorption efficiency (%)
CFK-GO (1%)	99.04667 ^a
CFK-SMGO	97.36333 ^a
CFK-GO (5%)	94.45667 ^a
CFK-NC (3%)	78.73000 ^b
CFK-GO (3%)	69.06333 ^{bc}
CFK-NC (5%)	65.24700 ^c
CFK-NC (1%)	41.99000 ^d
SMGO	41.72000 ^d

Co

Biosorbents	Biosorption efficiency (%)
CFK-SMGO	96.34333 ^a
CFK-GO (1%)	92.01333 ^a
CFK-NC (3%)	92.01333 ^a
CFK-GO (5%)	90.09333 ^a
CFK-NC (5%)	90.09333 ^a
CFK-GO (3%)	63.72667 ^b
CFK-NC (1%)	63.72667 ^b
SMGO	39.58667 ^c

Cd

Biosorbents	Biosorption efficiency (%)
CFK-SMGO	99.03000 ^a
CFK-NC (5%)	90.32333 ^b
CFK-GO (1%)	88.29333 ^b
CFK-NC (3%)	88.26000 ^b
CFK-GO (5%)	80.11333 ^c
CFK-GO (3%)	60.60000 ^d
CFK-NC (1%)	50.82333 ^e
SMGO	45.94333 ^e

Pb

Biosorbents	Biosorption efficiency (%)
CFK-SMGO	99.21667 ^a
SMGO	93.63333 ^b
CFK-NC (3%)	92.96667 ^{bc}
CFK-GO (1%)	91.40333 ^c
CFK-GO (5%)	85.96333 ^d
CFK-NC (5%)	78.64667 ^e
CFK-NC (1%)	55.00667 ^f
CFK-GO (3%)	53.50000 ^f

Zn

Biosorbents	Biosorption efficiency (%)
CF-GO (1%)	82.02667 ^a
CFK-GO (5%)	78.94000 ^a
CFK-GO (3%)	78.73333 ^a
CFK-NC (5%)	78.35333 ^a
CFK-NC (3%)	68.71667 ^b
CFK-NC (1%)	62.02667 ^c
CFK-SMGO	59.06000 ^c
SMGO	52.24667 ^d

*Values with same superscript are not significantly different

As

Biosorbents	Biosorption efficiency (%)
CFK-NC (3%)	98.44667 ^a
CFK-GO (5%)	97.84667 ^a
CFK-NC (1%)	97.20667 ^a
CFK-GO (1%)	95.10333 ^{ab}
CFK-GO (3%)	95.10333 ^{ab}
CFK-NC (5%)	94.70000 ^{ab}
CFK-SMGO	91.16000 ^b
SMGO	38.78333 ^c

Cr

Biosorbents	Biosorption efficiency (%)
CFK-GO (1%)	97.26000 ^a
CFK-GO (5%)	93.36333 ^b
CFK-SMGO	89.55000 ^c
CFK-GO (3%)	79.15000 ^d
CFK-NC (3%)	74.57667 ^e
CFK-NC (5%)	69.21000 ^f
CFK-NC (1%)	66.93333 ^f
SMGO	39.94667 ^g

Se

Biosorbents	Biosorption efficiency (%)
CFK-GO (5%)	99.12667 ^a
CFK-GO (1%)	99.11333 ^a
CFK-GO (3%)	99.06000 ^a
CFK-NC (3%)	98.80000 ^a
CFK-NC (1%)	93.44667 ^a
CFK-NC (5%)	92.80667 ^a
CFK-SMGO	74.33667 ^b
SMGO	34.02000 ^c

Appendix-X: Comparison of biosorption performance of biosorbents within study I, II and III

Study I: Anionic species

Biosorbents	Cr	Tukey test	As	Tukey test	Se	Tukey test
CFK-GO (1%)	97.22	A	95.15	B	99.01	A
CFK-GO (1%)	97.29		95.15		99.17	
CFK-GO (1%)	97.27		95.01		99.16	
CFK-GO (3%)	79.16	C	95.15	B	99.01	A
CFK-GO (3%)	79.15		95.15		99.17	
CFK-GO (3%)	79.14		95.01		99	
CFK-GO (5%)	93.38	B	97.87	A	99.07	A
CFK-GO (5%)	93.38		97.84		99.16	
CFK-GO (5%)	93.33		97.83		99.15	
P value	P<0.001		P<0.001		P<0.001	
DF	2		2		2	

*Values in the same column with same superscript are not significantly different

Study II: Anionic species

Biosorbents	Cr	Tukey test	As	Tukey test	Se	Tukey test
CFK-NC (1%)	67.22	C	97.36	B	93.01	B
CFK-NC (1%)	67.29		97.15		93.17	
CFK-NC (1%)	66.29		97.11		94.16	
CFK-NC (3%)	74.44	A	98.19	A	99.3	A
CFK-NC (3%)	75.15		98.14		98.2	
CFK-NC (3%)	74.14		99.01		98.9	
CFK-NC (5%)	69.38	B	94.73	C	93.07	B
CFK-NC (5%)	69.37		94.84		92.16	
CFK-NC (5%)	68.88		94.53		93.19	
P value	P<0.001		P<0.001		P<0.001	
DF	2		2		2	

Study III: Anionic species

Biosorbents	Cr	Tukey test	As	Tukey test	Se	Tukey test
SMGO	40.78	B	35.2	B	38.22	B
SMGO	38.05		38.9		38.22	
SMGO	41.01		42.25		25.62	
CFK-SMGO	90.34	A	94.22	A	76	A
CFK-SMGO	90.46		90.15		73.1	
CFK-SMGO	87.85		89.11		73.91	
P value	P<0.001		P<0.001		P<0.001	
DF	1		1		1	

*Values in the same column with same superscript are not significantly different

Study I: Cationic species

Biosorbents	Co		Pb		Ni		Zn		Cd	
CFK-GO (1%)	92.01	A	91.45	A	99.07	A	82.05	A	88.23	A
CFK-GO (1%)	92.01		91.33		99		82.05		88.34	
CFK-GO (1%)	92.02		91.43		99.07		81.98		88.31	
CFK-GO (3%)	64.09	C	53.33	C	69.1	C	78.75	C	60.63	C
CFK-GO (3%)	63.98		53.51		69.09		78.75		60.66	
CFK-GO (3%)	63.11		53.66		69		78.7		60.51	
CFK-GO (5%)	90.1	B	85.96	B	94.49	B	78.98	B	80.17	B
CFK-GO (5%)	90.1		85.98		94.39		78.96		80.17	
CFK-GO (5%)	90.08		85.95		94.49		78.88		80	
P value	P<0.001		P<0.001		P<0.001		P<0.001		P<0.001	
DF	2		2		2		2		2	

Study II: Cationic species

Biosorbents	Co		Ni		Cd		Pb		Zn	
CF-NC (1%)	92.01	A	42.02	C	50.23	C	55.26	C	62.05	C
CFK-NC (1%)	92.01		42.88		50.88		55.33		62.05	
CFK-NC (1%)	92.02		41.07		51.36		54.43		61.98	
CFK-NC (3%)	64.09	C	78.1	A	88.63	B	92.1	A	68.75	B
CFK-NC (3%)	63.98		79.09		88.6		93.51		68.7	
CFK-NC (3%)	63.11		79		87.55		93.29		68.7	
CFK-NC (5%)	90.1	B	65.421	B	91.17	A	78.94	B	78.18	A
CFK-NC (5%)	90.1		65.39		89.8		78.1		78.6	
CFK-NC (5%)	90.08		64.93		90		78.9		78.28	
P value	P<0.001		P<0.001		P<0.001		P<0.001		P<0.001	
DF	2		2		2		2		2	

*Values in the same column with same superscript are not significantly different

Study III: Cationic species

Biosorbents	Co		Pb		Ni		Zn		Cd	
SMGO	31.87	B	95.1	B	33.56	B	50.06	B	41.63	B
SMGO	36.01		93.01		37.58		56.9		54.2	
SMGO	50.88		92.79		54.02		49.78		42	
CFK-SMGO	95.63	A	99.34	A	95.1	A	55.39	A	98.41	A
CFK-SMGO	96.63		99.34		98.42		59.34		99.31	
CFK-SMGO	96.77		98.97		98.57		62.45		99.37	
P value	P<0.001		P<0.001		P<0.001		P<0.001		P<0.001	
DF	1		1		1				1	

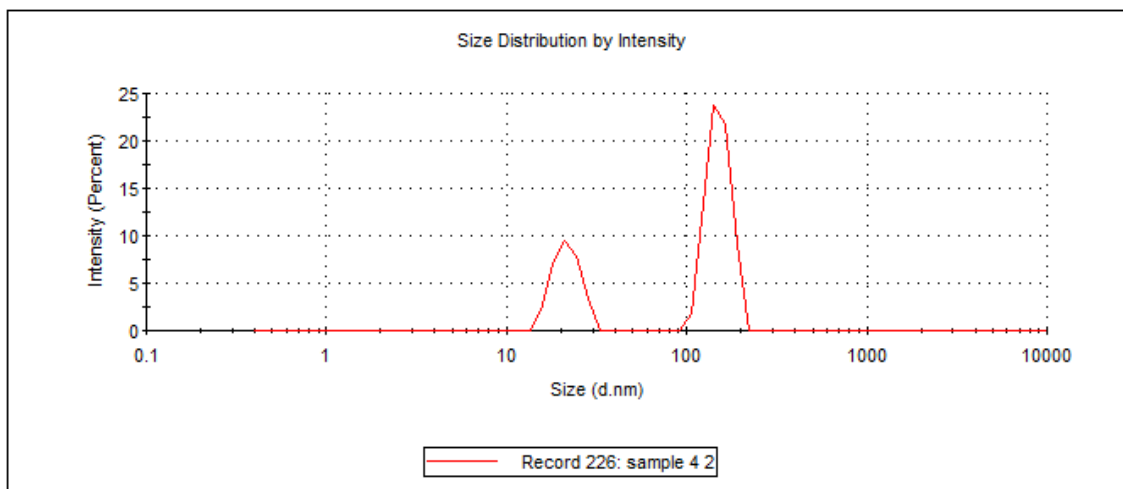
Values in the same column with same superscript are not significantly different

Appendix-XI: Dynamic light scattering (DLS) results of NC

Z-Average (d.nm): 455.6
PdI: 0.503
Intercept: 0.978

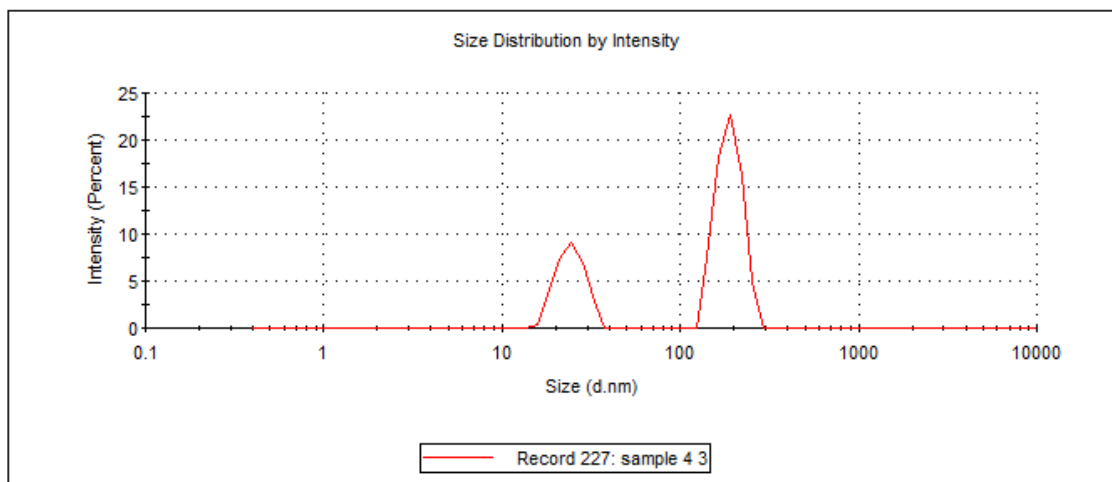
	Size (d.nm):	% Intensity:	St Dev (d.nm):
Peak 1:	150.5	69.7	22.12
Peak 2:	21.56	30.3	3.560
Peak 3:	0.000	0.0	0.000

Result quality : Refer to quality report



	Size (d.nm):	% Intensity:	St Dev (d.nm):
Z-Average (d.nm): 369.7	Peak 1: 189.8	69.7	30.73
Pdl: 0.412	Peak 2: 24.43	30.3	4.261
Intercept: 0.943	Peak 3: 0.000	0.0	0.000

Result quality : Refer to quality report



Appendix-XII: Permission for figure 1.1

Rightslink® by Copyright Clearance Center

2023-01-22, 3:47 PM



Total concentrations and sources of heavy metal pollution in global river and lake water bodies from 1972 to 2017

Author: Qiaoqiao Zhou, Nan Yang, Youzhi Li, Bo Ren, Xiaohui Ding, Hualin Bian, Xin Yao

Publication: Global Ecology and Conservation

Publisher: Elsevier

Date: June 2020

© 2020 The Authors. Published by Elsevier B.V.

Creative Commons Attribution-NonCommercial-No Derivatives License (CC BY NC ND)

This article is published under the terms of the [Creative Commons Attribution-NonCommercial-No Derivatives License \(CC BY NC ND\)](#).

For non-commercial purposes you may copy and distribute the article, use portions or extracts from the article in other works, and text or data mine the article, provided you do not alter or modify the article without permission from Elsevier. You may also create adaptations of the article for your own personal use only, but not distribute these to others. You must give appropriate credit to the original work, together with a link to the formal publication through the relevant DOI, and a link to the Creative Commons user license above. If changes are permitted, you must indicate if any changes are made but not in any way that suggests the licensor endorses you or your use of the work.

Permission is not required for this non-commercial use. For commercial use please continue to request permission via RightsLink.

[BACK](#)

[CLOSE WINDOW](#)

© 2023 Copyright - All Rights Reserved | [Copyright Clearance Center, Inc.](#) | [Privacy statement](#) | [Data Security and Privacy](#)
| [For California Residents](#) | [Terms and Conditions](#) Comments? We would like to hear from you. E-mail us at customercare@copyright.com

Appendix-XIII: References

Alahyaribeik, S., & Ullah, A. (2020). Methods of keratin extraction from poultry feathers and their effects on antioxidant activity of extracted keratin. *International Journal of Biological Macromolecules*, 148, 449-456.